

**EMPG – XVII**

**17th International Symposium on  
Experimental Mineralogy,  
Petrology and Geochemistry**

organised by  
Helmholtz Centre Potsdam  
GFZ German Research Centre for Geosciences  
and  
University of Potsdam

Zoom Meeting, March 1 – 3, 2021

Abstract Xqnpqg

February 2021

**EMPG – XVII****17th International Symposium on  
Experimental Mineralogy,  
Petrology and Geochemistry**

## Abstracts

## Theme 1 “Planetary mantles and cores”

(sorted alphabetically by first author)

## The Effect of Pulsed Laser Heating on the Stability of Ferropericlase at High Pressures

Georgios Aprilis<sup>1</sup>, Anna Pakhomova<sup>2</sup>, Stella Chariton<sup>3</sup>, Saiana Khandarkhaeva<sup>3</sup>, Caterina Melai<sup>3</sup>, Elena Bykova<sup>2</sup>, Maxim Bykov<sup>3</sup>, Timofey Fedotenko<sup>1</sup>, Egor Koemets<sup>3</sup>, Catherine McCammon<sup>3</sup>, Aleksandr I. Chumakov<sup>4</sup>, Michael Hanfland<sup>4</sup>, Natalia Dubrovinskaia<sup>1,5</sup>, Leonid Dubrovinsky<sup>3</sup>

<sup>1</sup> Materials Physics and Technology at Extreme Conditions, Laboratory of Crystallography, Universität Bayreuth, D-95440 Bayreuth, Germany

<sup>2</sup> Deutsches Elektronen-Synchrotron (DESY), D-22607 Hamburg, Germany

<sup>3</sup> Bayerisches Geoinstitut, Universität Bayreuth, D-95440 Bayreuth, Germany

<sup>4</sup> ESRF—The European Synchrotron, CS 40220, CEDEX 9, 38043 Grenoble, France

<sup>5</sup> Department of Physics, Chemistry and Biology (IFM), Linköping University, SE-581 83 Linköping, Sweden

It is widely accepted that the lower mantle consists of mainly three major minerals—ferropericlase, bridgmanite and calcium silicate perovskite. Ferropericlase ((Mg,Fe)O) is the second most abundant of the three, comprising approximately 16–20 wt% of the lower mantle. The stability of ferropericlase at conditions of the lowermost mantle has been highly investigated, with controversial results [1–3]. Amongst other reasons, the experimental conditions during laser heating (such as duration and achieved temperature) have been suggested as a possible explanation for the discrepancy. In this study [4], we investigate the effect of pulsed laser heating on the stability of ferropericlase, with a geochemically relevant composition of  $\text{Mg}_{0.76}\text{Fe}_{0.24}\text{O}$  (Fp24) at pressure conditions corresponding to the depth from 800 km up to 1200 km within the upper part of the lower mantle, and at a temperature range of 1550 K to 3400 K. We report on the decomposition of Fp24 with the formation of a high-pressure (Mg,Fe)<sub>3</sub>O<sub>4</sub> phase with CaTi<sub>2</sub>O<sub>4</sub>-type structure, as well as the dissociation of Fp24 into Fe-rich and Mg-rich phases induced by pulsed laser heating. Our results provide further arguments that the chemical composition of the lower mantle is more complex than initially thought, and that the compositional inhomogeneity is not only a characteristic of the lowermost part, but includes depths as shallow as below the transition zone.

### References:

- [1] Dubrovinsky et al., (2000) *Science*, 289, 430–432
- [2] Lin et al., (2003) *Proc. Natl. Acad. Sci.*, 100, 4405–4408
- [3] Fei et al., (2007) *Geophys. Res. Lett.*, 34, L17307
- [4] Aprilis et al., (2020) *Minerals*, 10(6), 542

## Thermodynamics, elasticity and phase stability of grossite (CaAl<sub>4</sub>O<sub>7</sub>) at HP-HT : implications for solar nebula condensation

Donato Belmonte<sup>1</sup> Fernando Cámara<sup>2</sup> Paolo Lotti<sup>2</sup> Marco Merlini<sup>2</sup> Mattia La Fortezza<sup>1</sup>

<sup>1</sup> Dipartimento di Scienze della Terra, dell'Ambiente e della Vita (DISTAV), University of Genoa, Genoa, Italy

<sup>2</sup> Dipartimento di Scienze della Terra A. Desio, University of Milan, Milan, Italy

Grossite (CaAl<sub>4</sub>O<sub>7</sub>) is an important constituent phase of high alumina cements (HAC) and a common refractory phase in calcium-rich inclusions (CAIs) found in primitive chondritic meteorites, but its thermophysical properties are poorly constrained and its thermodynamic behaviour mostly unknown. In particular, the knowledge of phase stability relations of Ca-aluminates up to high pressure and temperature conditions (HP-HT) is concealed by the lack of a thorough information on the thermodynamics of such phases. Since grossite is thought to be one of the first stable condensates crystallizing from the primitive solar nebula, this knowledge is crucial to predict its condensation temperature and to ultimately understand chemico-physical process in the solar nebula [1]. Thermodynamics, equation of state and elasticity of grossite (space group *C2/c*) have been investigated in this work by first principles theory (using a WC1LYP hybrid functional and CRYSTAL program) and experimental methods (synchrotron radiation high-pressure single crystal X-ray diffraction, using an ETH-type Diamond Anvil Cell and M.E.W. as pressure-transmitting fluid, at Xpress beamline at Elettra, Trieste,  $\lambda = 0.4957 \text{ \AA}$ ) in a broad range of P-T conditions (i.e. 0-10 GPa and 0-2000 K). First principles calculations provide a static bulk modulus [i.e.  $K_{0,Wc1LYP} = 128.8(1) \text{ GPa}$ ], which is in remarkable agreement with our measured value at ambient conditions [i.e.  $K_0 = 123(4) \text{ GPa}$ ]. Furthermore, ab initio calculation of the full elastic tensor (with 13 independent components) permits to define the shear modulus (i.e.  $G_{VRH} = 52.1 \text{ GPa}$ ) and seismic anisotropy of the *C2/c* phase, for which no experimental data exist so far. Our calculations show as both the shear modulus and aggregate shear-wave velocities ( $V_s$ ) decrease with the increasing pressure and how this anomalous behavior is mostly related to the marked pressure dependence displayed by some of the shear elastic constants (i.e.  $C_{12}$ ,  $C_{13}$  and  $C_{23}$ ) and provide the evidence for elastic softening with pressure. Thermodynamic properties and P-V-T EoS have been computed in the framework of quasi-harmonic approximation (QHA) by phonon dispersion calculations on  $2 \times 2 \times 2$  supercells to reach numerical convergence. A very low volume thermal expansion coefficient, which makes grossite a very good non-silicate refractory material, is confirmed both by LT and HT experiments and by ab initio calculations. The calculated thermodynamic properties (e.g. heat capacity and entropy) shows a good agreement with the available calorimetric data in the low-T range (i.e.  $T < 298.15 \text{ K}$ ), but it turns out they are rather different from those assessed in current thermodynamic databases in the HT range [2]. Some possible hypotheses for such discrepancies is provided. Ab initio thermodynamic properties of grossite have been used to constrain its phase stability field in the CaO-Al<sub>2</sub>O<sub>3</sub>-SiO<sub>2</sub> system at HP-HT by means of Gibbs free energy minimization, stressing that: i) the primary phase field of grossite progressively shrinks with pressure up to disappear from the CAS system at  $P > 0.4 \text{ GPa}$ ; ii) a subsolidus disproportionation reaction of grossite to give CaAl<sub>2</sub>O<sub>4</sub> (krotite) + Al<sub>2</sub>O<sub>3</sub> (corundum) occurs at HP-HT conditions. Relevant implications for condensation temperatures of the solar nebula are finally presented and discussed.

[1] Ebel, D.S., and Grossman, L., (2000) *Geochim. Cosmochim. Acta*, 64, 339-366.

[2] Berman, R.G., and Brown, T.H., (1984) *Geochim. Cosmochim. Acta*, 48, 661-678.

## Sound velocity measurements of B2-Fe-Ni-Si alloy under high pressure by inelastic X-ray scattering: Implications for the composition of Earth's core

S. Dominijanni<sup>1</sup>, C. A. McCammon<sup>1</sup>, E. Ohtani<sup>2</sup>, D. Ikuta<sup>2</sup>, T. Sakamaki<sup>2</sup>, T. Ishii<sup>1</sup>, G. Criniti<sup>1</sup>, L. S. Dubrovinsky<sup>1</sup>, S. Khandarkhaeva<sup>1</sup>, T. Fedotenko<sup>3</sup>, K. Glazyrin<sup>4</sup>, H. Uchiyama<sup>5</sup>, H. Fukui<sup>6,7</sup> and A. Q. R. Baron<sup>7</sup>

<sup>1</sup>Bayerisches Geoinstitut, University of Bayreuth, Germany

<sup>2</sup>Department of Earth and Planetary Materials Science, Graduate School of Science, Tohoku University, Sendai, Miyagi, Japan

<sup>3</sup>Material Physics and Technology at Extreme Conditions, Laboratory of Crystallography, University of Bayreuth, 95440 Bayreuth, Germany

<sup>4</sup>Photon Science, Deutsches Elektronen Synchrotron, Hamburg, Germany

<sup>5</sup>Research and Utilization Division, Japan Synchrotron Radiation Research Institute, SPring-8, Sayo-gun, Hyogo 679-5198, Japan

<sup>6</sup>Graduate School of Material Science, University of Hyogo, Kamigori, Hyogo 678-1297, Japan

<sup>7</sup>Materials Dynamics Laboratory, RIKEN SPring-8 Center, Sayo-gun, Hyogo 679-5148, Japan

Knowledge of elastic properties of Fe-Ni alloys at high pressure is crucial for understanding the structure, composition, and dynamics of Earth's core. In this context, particularly relevant is the comparison of density ( $\rho$ ), compressional ( $V_P$ ), and shear ( $V_S$ ) wave velocities of Fe alloys with seismological observations, e.g., PREM (Dziewonski & Anderson, 1981). Since the pioneering work of Birch (1952), it is considered likely that light elements, such as Si, are alloyed with iron in Earth's core to account for the density difference between *hcp* Fe and geophysical observations. However, controversies remain about the effect of light elements on the elastic properties of Fe-Ni alloys and their abundance in Earth's core. Considering that Si is one of the favoured light elements in the inner core, we investigated the elastic properties of *bcc* Fe<sub>0.67</sub>Ni<sub>0.06</sub>Si<sub>0.27</sub> (15 wt. % Si) with B2 structure by combined high resolution inelastic X-ray scattering and powder X-ray diffraction in diamond anvil cells at SPring-8 (BL35XU beamline). Additional X-ray diffraction measurements were conducted at DESY PETRA III (P02.2 beamline) to investigate the compressibility of the same material. Compressional sound velocities and densities were measured up to 100 GPa at room temperature while shear wave velocities were derived from  $V_P$  and  $\rho$  with the adiabatic bulk modulus ( $K_S$ ) from an equation of state. Our results extrapolated to inner core conditions (Alfè et al., 2002) are consistent with inner core PREM values of  $V_P$ ,  $V_S$ , and  $\rho$  based on a linear mixing model with 18(5) vol % *bcc* Fe<sub>0.67</sub>Ni<sub>0.06</sub>Si<sub>0.27</sub> and 82(5) vol % *hcp* Fe, which corresponds to 2-3 wt. % Si.

### References:

Alfè, D., et al. (2002). *Earth planet. Sci. Lett.*, 195(1–2), 91–98.

Birch, F. (1952). *J. Geophys. Res.*, 57(2), 227–286.

Dziewonski, A. M. & Anderson, D. L. (1981). *Phys. Earth Planet. Inter.*, 25, 297–356.

## Dependence of Heat Transport in Solids on Length-scale, Pressure, and Temperature: Implications for Mechanisms, Thermodynamics, and Earth's Interior

Anne M. Hofmeister

Dept. Earth and Planetary Science, Washington University, St Louis MO 63130 USA; hofmeist@wustl.edu; 1-314-935-7440

Laser-flash analysis (LFA) is accurate because contact losses are avoided and spurious, plus boundary-to-boundary radiative effects are removed. Thermal diffusivity ( $D$ ) data from LFA on diverse solids at moderate temperature ( $T$ ) while varying sample thickness  $L$  from  $\sim 0.03$  to 10 mm reveal that  $D(T) = D_{\infty}(T)[1 - \exp(-bL)]$ . When  $L$  is several mm,  $D_{\infty}(T) = FT^{-G} + HT$  for insulators and some metals where  $F$  is constant,  $G$  is  $\sim 1$  or 0, and  $H$  is  $\sim 0.001$ , as ascertained by Hofmeister et al. (2014). Parameters  $F$  and  $G$  are interdependent, so  $D$  at 298 K suffices for models. The attenuation parameter  $b = 6.19D_{\infty}^{-0.477}$  at 298 K for electrical insulators, elements, and alloys. Dimensional analysis confirms that  $D \rightarrow 0$  as  $L \rightarrow 0$ , which is consistent with heat diffusion requiring a medium. Thermal conductivity ( $\kappa$ ) behaves similarly, being proportional to  $D$  times density and specific heat, which are well-known scale-independent material properties. Attenuation describing heat conduction signifies that light is the diffusing entity. Electrons in metals carry negligible heat, but rapidly, as demonstrated theoretically and experimentally (Criss and Hofmeister, 2017). A radiative transfer model with 1 free parameter that represents a simplified absorption coefficient describes the complex form for  $\kappa(T)$  of all types of solids, including the strong peak at cryogenic temperatures. Three parameters describe  $\kappa$  with a secondary peak and/or a high- $T$  increase. The strong length dependence and experimental difficulties in diamond anvil studies yield problematic transport properties. Reliable low-pressure data on diverse thick samples reveal a new identity for specific heat [ $\partial \ln(c_p)/\partial P = -\text{linear compressibility}$ ] and show that  $\partial \ln(\kappa)/\partial P = \partial \ln(\alpha)/\partial P - \partial \ln(c_p)/\partial P$  where  $\alpha$  is thermal expansivity. These relationships confirm that heat conduction in solids equals diffusion of light down the thermal gradient, since changing  $P$  affects the space occupied by matter, but not by light. Regarding Earth's interior, thermal diffusivity and/or thermal conductivity for regions at moderate geologic temperatures can be determined from existing low  $T$ , ambient  $P$  LFA data on  $D$  of minerals or rocks and the above equations. Above  $\sim 2000$ K, the radiative transfer model is essential for partially transparent materials, where measured absorption coefficients, rather than a fitting parameter, are needed for accuracy. For opaque metals, spectra are only needed to explore extremes of many thousands of Kelvins.

### References:

- Hofmeister, A.M., Dong, J.J., and Branlund J.M. (2014) Thermal diffusivity of electrical insulators at high temperatures: evidence for diffusion of phonon-polaritons at infrared frequencies augmenting phonon heat conduction, *J. Applied Phys.* **115**, 163517.
- Criss, E.M. and Hofmeister, A.M. (2017) Isolating lattice from electronic contributions in thermal transport measurements of metals and alloys and a new model. *Int. J. Modern Physics: B* **31** (<http://www.worldscientific.com/doi/pdf/10.1142/S0217979217502058>)

## Synthesis, structural features and isomorphism of oxide phases in the Ca-Al-O system at P-T parameters of the transition zone and lower mantle of the Earth

Anastasiia Iskrina<sup>1,2</sup>, Andrey Bobrov<sup>1,2,3</sup>, Anna Spivak<sup>2</sup>, Nikolai Eremin<sup>1</sup>, Ekaterina Marchenko<sup>1</sup>, Leonid Dubrovinsky<sup>4</sup>

<sup>1</sup> Geological Faculty, Moscow State University, Leninskie Gory, Moscow, Russia 119991

<sup>2</sup> D.S. Korzhinskii Institute of Experimental Mineralogy of Russian Academy of Sciences (IEM RAS), Chernogolovka, Moscow oblast, Russia 142432

<sup>3</sup> Vernadsky Institute of Geochemistry and Analytical Chemistry of Russian Academy of Sciences, Moscow, Russia 119991

<sup>4</sup> Bavarian Research Institute of Experimental Geochemistry and Geophysics (BGI) University of Bayreuth, Bayreuth, Germany 95440

Aluminum takes the first place among metals and the third place among the elements after oxygen and silicon by the prevalence in the Earth's crust. According to various researchers the relative content of Al<sub>2</sub>O<sub>3</sub> in the Earth's mantle ranges within 4.0–4.5 wt% (McDonough et al., 1995) while the concentration of aluminum in the Earth's crust reaches 16.4 wt% (Green et al., 1979). Aluminates may be the hosts of aluminum under the conditions of the transition zone and lower mantle of the Earth (Ringwood, 1975). The CaFe<sub>2</sub>O<sub>4</sub>-type of structure was proposed by Ringwood (Ringwood, 1975) for CaAl<sub>2</sub>O<sub>4</sub> as the most likely at the mantle conditions. To date, several intermediate compounds are known in the CaO-Al<sub>2</sub>O<sub>3</sub> system (e.g. CaAl<sub>2</sub>O<sub>4</sub>; CaAl<sub>4</sub>O<sub>7</sub>; CaAl<sub>12</sub>O<sub>19</sub>) (Ito et al., 1980; Jerebtsov et al., 2001). Also Ca-aluminates may include various cations, such as Fe, Mg, Na, influencing the phase relations in the CaO-Al<sub>2</sub>O<sub>3</sub> system.

Experiments on synthesis of the phases in the CaO-Al<sub>2</sub>O<sub>3</sub> system with addition of Fe were carried out on a 1200-t multi-anvil Sumitomo press at P=15 and 24 GPa, T=1600°C at the Bavarian Research Institute of Experimental Geochemistry and Geophysics (BGI) (Germany). The phases CaAl<sub>2</sub>O<sub>4</sub>, Ca<sub>2</sub>Al<sub>6</sub>O<sub>11</sub> and Ca(Al, Fe)<sub>2</sub>O<sub>4</sub> were synthesized. Orthorhombic phases CaAl<sub>2</sub>O<sub>4</sub> and Ca(Al, Fe)<sub>2</sub>O<sub>4</sub> crystallize in a space group *Pnma* and have the CaFe<sub>2</sub>O<sub>4</sub>-type structure. The tetragonal phase Ca<sub>2</sub>Al<sub>6</sub>O<sub>11</sub> is a new phase, crystallizes in a space group *P4<sub>2</sub>/mnm*. The structures of the synthesized phases were refined by the method of single-crystal X-Ray diffraction using synchrotron radiation. The compressibility of the Ca(Al,Fe)<sub>2</sub>O<sub>4</sub> phase was studied up to ~60 GPa. In this pressure range, no phase transformations were detected, but the spin transition for iron was registered. As one of the results of this study, it was possible to obtain the equation of state for the Ca(Al,Fe)<sub>2</sub>O<sub>4</sub> phase. The data obtained may be applied to construction of a P-T phase diagram in the CaO-Al<sub>2</sub>O<sub>3</sub> system (the current diagrams are limited to a pressure of 16 GPa).

Our results suggest that all studied phases are stable in the transition zone and lower mantle and can be considered as potential aluminum concentrators in the Earth's deep geospheres.

### References:

- McDonough et al., (1995) Chem. Geol., 120, 223-253  
Green et al., (1979), Academic Press, London, 265-299  
Ringwood, (1975), McGraw-Hill, New York - Toronto, 618 p.  
Ito et al., (1980), Mat Res Bull, 15, 925-932  
Jerebtsov et al., (2001), Ceramics Int, 27, 25-28

## Crystal-chemistry and stability of the 3.65 Å phase

Monika Koch-Müller<sup>1</sup>, Richard Wirth<sup>2</sup>, Oona Appelt<sup>1</sup>, Bernd Wunder<sup>1</sup>

<sup>1</sup>Deutsches GeoForschungsZentrum Potsdam, Sektion 3.6 Telegrafenberg, 14473 Potsdam, Germany

<sup>2</sup>Deutsches GeoForschungsZentrum Potsdam, Sektion 3.5 Telegrafenberg, 14473 Potsdam, Germany

Numerous studies have shown that dehydration of serpentine causes intermediate-depth earthquakes. However, earthquakes are also observed at the bottom of the mantle transition zone, possibly caused by dehydration embrittlement. Possible carriers of water to these depths are Dense Hydrous Magnesium Silicates (DHMS) and deep seismicity might be caused by dehydration of the DHMS. An important DHMS is the 10 Å phase,  $\text{Mg}_3\text{Si}_4\text{O}_{10}(\text{OH})_2 \cdot x\text{H}_2\text{O}$ . At pressures above 10 GPa the 10 Å phase transforms to another important DHMS, namely the 3.65 Å phase.

Wunder et al. (2011, 2012) synthesized the 3.65 Å phase and determined the chemical formula as  $\text{MgSi}(\text{OH})_6$ . According to Rietveld refinement of powder XRD pattern, the structure can be considered as a modified A-site defective perovskite with a network of corner-sharing alternating  $\text{Mg}(\text{OH})_6$  and  $\text{Si}(\text{OH})_6$  octahedra. It contains 36 wt. %  $\text{H}_2\text{O}$  distributed as hydroxyl groups over 6 different H-positions.

To study the dehydration mechanism of the 3.65 Å phase we investigated the reaction



We performed reversed experiments in a rotating Multi-Anvil Press at 10 GPa and 470 - 550 °C. We observed the dehydration of the 3.65 Å, thus the formation of CEn, and the hydration of CEn, thus the formation of the 3.65 Å phase. The reactions were very sluggish and not complete even after 96 hours. We investigated the recovered samples by electron microprobe and transmission electron microscopy. In the hydration experiment a few large (30 - 50 μm) remnants of CEn without any cracks could be found surrounded by cracked submicron-sized CEn. In this debris-like areas an amorphous phase (0.85 Mg : 1.05 Si with about 20 wt% of water) was found which further was consumed and finally formed the 3.65 Å phase (1 Mg : 1 Si with 34%  $\text{H}_2\text{O}$ ). Thus, the submicron-sized broken CEn transforms via an amorphous water-bearing precursor phase to the 3.65 Å phase. From the back scattered images of the recovered sample of the dehydration experiment we can clearly see that there is a high porosity due to dehydration and that the 3.65 Å phase is being consumed. There are still some educt CEn as perfect crystals present but the product CEn form the majority as fine grained (submicron-sized) newly formed crystals. Even having a different origin, the textures of the CEn crystals in both, hydration and dehydration experiments are similar, showing perfect large crystals together with submicron-sized grains.

### References:

Wunder et al. (2011) *Am Mineral*, 96, 1207 - 1214.

Wunder et al. (2012) *Am Mineral*, 97, 1043 - 1048.

## Microstructures across phase transitions in SiO<sub>2</sub> investigated by multigrain crystallography (MGC)

Matthias Krug<sup>1</sup>, Estelle Ledoux<sup>2</sup>, Jeffrey P. Gay<sup>2</sup>, Julien Chantel<sup>2</sup>, Sergio Speziale<sup>3</sup>, Anna Pakhomova<sup>4</sup>, Rachel Husband<sup>4</sup>, Hanns-Peter Liermann<sup>4</sup>, Sébastien Merkel<sup>2</sup> and Carmen Sanchez-Valle<sup>1</sup>

<sup>1</sup> Institut für Mineralogie, WWU Münster, Germany

<sup>2</sup> Unité Matériaux et Transformations, CNRS, Université de Lille, France

<sup>3</sup> Deutsches GeoForschungsZentrum Potsdam, Germany

<sup>4</sup> DESY – Deutsches Elektronen-Synchrotron, Hamburg, Germany

Free silica has been shown to form in basaltic crust upon subduction and is presumably stable throughout the pressure range of the whole mantle (Perrillat et al. 2006; Ricolleau et al. 2010). Phase transitions in silica are associated with seismic discontinuities in the mantle, in particular (1) the X-discontinuity in the upper mantle at ~ 300 km depth, which could be caused by the coesite-stishovite transformation (Schmerr et al. 2013; Chen et al. 2015) and (2) seismic scatterers in the mid-mantle between 800 and 1800 km depth, which could be explained by the transformation from stishovite to post-stishovite (Kaneshima and Helffrich 1999; Niu 2014). However, these interpretations are still debated because it is unclear whether a fairly low silica proportion of only ~ 20 vol.% in subducted basaltic crust (Ricolleau et al. 2010) is enough to cause the observed seismic signals. The effect of phase transitions on the microstructure and texture in subducted material, i. e. grain sizes and grain orientations, is still poorly understood, yet might affect the seismic signals in terms of seismic anisotropy and seismic wave reflectivity.

In this study, we performed multigrain crystallography (MGC) analysis (Sørensen et al. 2012) in a laser-heated diamond-anvil cell (LH-DAC) to determine in-situ the microstructures induced by phase transitions in high-pressure silica phases. This method enables monitoring the position, orientation and size of individual grains in a polycrystalline assembly, providing insights in the evolution of these parameters for hundreds of grains across phase transitions. Starting from quartz, we monitored the transitions from quartz to coesite, from coesite to stishovite and finally from stishovite to post-stishovite to pressures above 80 GPa along cold slab and average mantle geotherms. Our results show that the first two transitions are accompanied by a reduction of the average grain size and an increase in the amount of grains. Furthermore, we observed no correlation between the grain orientations across the transitions, which shows that potential crystal-preferred orientations are not inherited from quartz to coesite or from coesite to stishovite. The implications of these results for mantle discontinuities and seismic anomalies will be discussed.

### References:

- Chen et al., (2015) *Earth and Planetary Science Letters*, 412, 42-51.  
Kaneshima & Helffrich, (1999) *Science*, 283(5409), 1888-1892.  
Niu, (2014) *Earth and Planetary Science Letters*, 402, 305-312.  
Perrillat et al. (2006) *Physics of the Earth and Planetary Interiors*, 157(1-2), 139-149.  
Ricolleau et al., (2010) *Journal of Geophysical Research: Solid Earth*, 115(B8).  
Schmerr et al., (2013) *Geophysical Research Letters* 40(5), 841-846.  
Sørensen et al., (2012) *Zeitschrift für Kristallographie Crystalline Materials*, 227(1), 63-78.

## Plasticity of Fe-Si and Fe-Si-C alloys at the conditions of the Earth's core

Ilya Kupenko<sup>1</sup>, Carmen Sanchez-Valle<sup>1</sup>, Melissa Achorner<sup>1</sup>, Matthias Krug<sup>1</sup>, Julien Chantel<sup>2</sup>, Estelle Ledoux<sup>2</sup>, Xenia Ritter<sup>1</sup>, Aaron Rigoni<sup>3</sup>, Hans-Peter Liermann<sup>4</sup>, Sébastien Merkel<sup>2</sup>

<sup>1</sup> Institut für Mineralogie, University of Münster, 48149 Münster, Germany

<sup>2</sup> Unité Matériaux et Transformations, CNRS, Université de Lille 59000 Lille, France

<sup>3</sup> Institut für Materialphysik, University of Münster, 48149 Münster, Germany

<sup>4</sup> Photon Science, DESY, D-22607, Hamburg, Germany

The cores of terrestrial planets are comprised of Fe-Ni alloys, with around 4-7 wt% of the light element(s) that account for the observed core density deficiency and reduced seismic velocity compared to pure Fe-Ni. Carbon and silicon are both considered as major light elements of the core: both have high cosmic abundance and can be efficiently incorporated into iron-nickel metal during core formation. Moreover, the (Mg/Si) ratios of the mantle are inconsistent with those of the chondrites and the 'missing' silicon could be hosted in the core as Fe(Ni)-Si alloys.

Additionally to the average velocities mismatch, there is evidence for prominent anisotropy in the inner core, with the compressional waves traveling faster along the Earth's rotation axis compared to the waves traveling in the equatorial plane (Morelli et al., 1986). The anisotropic structures in the inner core are likely formed by dynamic processes that induce the plastic deformation and development of textures of inner core materials under pressure. However, the deformation should be produced by the typical stresses available to drive flow in the core, which are relatively low. Gleason and Mao, (2013) showed that hcp-iron at core conditions has very low strength and, therefore, small stresses are enough for significant plastic deformation. Yet, the effect of light elements on the plasticity of iron is poorly known, although this information is crucial for understanding how planetary cores deform.

Here we investigate the plastic deformation of hcp-Fe-Si and Fe-Si-C alloys up to 280 GPa and 180 GPa respectively at room temperature employing a technique of radial x-ray diffraction in diamond anvil cells. We utilize the radial diffraction patterns in order to map the development of texture in the sample and the dominant deformation mechanisms of the alloys. We will present the analysis of measured data and discuss their potential application to constrain plastic deformation in the cores of the Earth and other terrestrial planets.

### References:

Morelli et al., (1986) *Geophys. Res. Lett.* 13, 1545–1548

Gleason and Mao, (2013) *Nat. Geosci.* 6, 1–4.

## Experimental investigation of the phase stability in the bridgmanite-magnesite system

Libon, L.<sup>\*1</sup>, Spiekermann, G.<sup>1</sup>, Sieber, M. J.<sup>1,2</sup>, Kaa, J.<sup>3,4</sup>, Dominijanni, S.<sup>5</sup>, Biedermann, N.<sup>3</sup>, Appel, K.<sup>3</sup>, Morgenroth, W.<sup>1,6</sup>, Albers, C.<sup>4</sup>, McCammon, C.<sup>5</sup>, Roddatis, V.<sup>2</sup>, Henet, L.<sup>7</sup>, Wilke, M.<sup>1</sup>

<sup>1</sup>Institute for Geosciences, University of Potsdam, Germany

<sup>2</sup>Deutsches GeoForschungsZentrum, Potsdam, Germany

<sup>3</sup>European XFEL, Schenefeld, Germany

<sup>4</sup>Fakultät Physik/DELTA, TU Dortmund, Germany

<sup>5</sup>Bayerisches Geoinstitut, University of Bayreuth, Germany

<sup>6</sup>European Synchrotron Radiation Facility, France

<sup>7</sup>ICMN, CNRS Orléans, France

Magnesite is observed to be chemically stable at high pressure (>80 GPa) (Binck et al., 2020). However, to constrain its stability in the lower mantle, we have to investigate its interaction with co-existing lower mantle phases. Previous experimental studies on MgCO<sub>3</sub>+SiO<sub>2</sub> imply that at <35 GPa magnesite is stable at mantle geotherm conditions (Litasov & Shatskiy, 2019). In addition to those studies, we are considering a more complex system that involves reaction of magnesite with (Mg,Fe)SiO<sub>3</sub>-glass, a bulk composition closer to that of the lower mantle.

Experiments were conducted using a multi-anvil press and laser-heated diamond anvil cells (LH-DAC) with conditions ranging from 25 to 65 GPa and 1700 to 3000 K. The experiments were designed to test sub-solidus reactions, melting, decarbonation and diamond formation. Multi-anvil press experiments at 25 GPa and T below the mantle geotherm (1700 K) show formation of carbonate-silicate melt. In addition, bridgmanite and stishovite are found, indicating that bridgmanite melts incongruently to form stishovite at the chosen bulk composition, in accordance with Litasov & Shatskiy (2019). LH-DAC experiments were performed associated with in situ X-ray diffraction. Our data show reaction to bridgmanite, ferromagnesite and stishovite. A melt phase could not be detected at high T. However, formation of stishovite could indicate incongruent melting, implying that any traces of melting is erased during cooling.

Our preliminary interpretation indicates that the melting curve in the magnesite-bridgmanite system is situated at T below the mantle geotherm. Therefore, our data suggest that subducted carbonated-bearing silicate lithologies that survive down to the lower mantle would melt at conditions of the top of the lower mantle, implying that carbonates are not stable at these conditions. This process could give a better understanding of carbon storage in the deep Earth.

### References:

Binck, et al., (2020b) *Physical Review Materials*, 4(5), 1-9.

Litasov, K. D. and Shatskiy, A. F. (2019) *Geochemistry International*, 57(9), 1024-1033.

## **Tuite, $\gamma$ -Ca<sub>3</sub>(PO<sub>4</sub>)<sub>2</sub> in peridotitic bulk composition: Phase stability and volatile incorporation in the upper to lower mantle transition zone**

\*Tristan Pausch<sup>1</sup>, Jaseem Vazhakuttiyakam<sup>1</sup>, Anthony C Withers<sup>2</sup>, Bastian Joachim-Mrosko<sup>1</sup>, Jürgen Konzett<sup>1</sup>

<sup>1</sup> Institute for Mineralogy and Petrography, University of Innsbruck, Innrain, 52A-6020, Innsbruck, Austria

<sup>2</sup> Universität Bayreuth, Bayerisches Geoinstitut (BGI), Germany

Apatite is by far the most abundant phosphate in both terrestrial and extraterrestrial rocks, and is also a carrier of incompatible trace elements and halogens of eminent importance. During subduction apatite breaks down at upper mantle conditions to form the anhydrous calcium phosphate tuite [ $\gamma$ -Ca<sub>3</sub>(PO<sub>4</sub>)<sub>2</sub>] (Konzett et al., 2012). Tuite may then take over as the principal phosphorus carrier in the transition zone, and possibly in the lower mantle. Whereas the potential of tuite as a host for incompatible trace elements has been confirmed by previous studies (Zhai et al., 2014), its suitability as a volatile carrier and its upper P-T stability and phase relations in the major lithologies of subducting lithosphere at the upper-to-lower mantle transition remain to be explored.

The aim of this study is to experimentally determine the tuite stability field in the Earth's mantle and evaluate its role as potential trace element carrier mineral. Experiments were performed using a spinel lherzolite starting material (Konzett & Ulmer, 1999), doped with 3% synthetic  $\beta$ -Ca<sub>3</sub>(PO<sub>4</sub>)<sub>2</sub> and a trace element mix, at pressures ranging from 15 to 25 GPa and at 1600°C, 1800°C and 2000°C.

Preliminary results show that tuite breaks down between 1600°C and 1800°C, at pressures between 20 GPa and 25 GPa. At 20 GPa and 1600°C, among others, tuite coexists with partial melt and majoritic garnet, a phase assemblage that infers that tuite is not the major sink for trace elements. However, at 25 GPa and 1600°C, neither garnet nor partial melt is stable any more, implying that the role of tuite as trace element carrier might be particularly relevant at higher pressures.

### References:

- Konzett J. and Ulmer P., (1999) *J Petrol.*, 40,629–652.  
Konzett J. et al., (2012) *Contrib Mineral Petrol.*, 163,277–296  
Zhai S. et al., (2014) *Sci China: Earth Sci.*, 57,2922–2927

## **EMPG – XVII**

### **17th International Symposium on Experimental Mineralogy, Petrology and Geochemistry**

Abstracts

Theme 2 “Melt physics and chemistry”

(sorted alphabetically by first author)

## Nitrogen solubility in silicate melt in equilibrium with N-rich fluid under magmatic condition and reduced $fO_2$

Fabien Bernadou<sup>1</sup>, Fabrice Gaillard<sup>1</sup>, Evelyn Füre<sup>2</sup>, Yves Marrocchi<sup>2</sup>, Aneta Slodczyk<sup>1</sup>, Ida Di Carlo<sup>1</sup>

<sup>1</sup> Institut des Sciences de la Terre d'Orléans, CNRS/Université d'Orléans/BRGM, 1a rue de la Férollerie 45071, Orléans cedex 2, France

<sup>2</sup> Centre de Recherches Pétrographiques et Géochimiques, CNRS-EPR2300, 15 rue Notre Dame des Pauvres, BP20, 54501 Vandoeuvre-les-Nancy, France

Investigation of the nitrogen behaviour during the magmatic degassing process is important in order to improve the understanding of the genesis of our atmosphere. This study addresses the partitioning of nitrogen between silicate melt of basaltic composition and N-rich fluid phase.

Experimental investigations have mainly used Internally Heated Pressure Vessel (IHPV) with conditions between 1200 to 1300°C, 800 to 2400 bar of pressure and  $fO_2$  between IW-4 and NNO while 1 experiment was conducted in Piston Cylinder apparatus (PC) at pressure of 10 kbar, a temperature of 1300°C and a  $fO_2 \approx$  IW-3. The analyses of the nitrogen concentration in the silicate glasses were carried out using the secondary ionization mass spectrometry (CRPG, Nancy); major element abundances in the glasses are determined using the electronic microprobe at ISTO and FTIR spectroscopy was used to determine the water and  $CO_2$  contents in the glasses. Oxygen fugacity of the experimental charges was determined using Co-Ni redox sensors, Fe-Pd alloys and water content of the experimental charges.

The obtained glass nitrogen content are low (1 to 30 ppm of nitrogen in silicate glasses) for the most oxidizing condition and increase drastically toward the  $fO_2$  more reduced than IW-1: more than 1000 ppm of nitrogen in silicate glasses at IW-4. Nitrogen concentrations appear to increase as the conditions becomes more reducing and as pressure increases. Our silicate glasses were also analysed with RAMAN spectrometer in order to try to identify the different N species present. The data obtained in our study could then be compared with fluid saturated data from the literature. A model of nitrogen solubility in silicate melts has been calibrated with our data and some data of low and high pressure (Li et al., 2015; Libourel et al., 2003; Speelmanns et al., 2019):

$$[N_{calc}] = K_{phys} * PN_2 + fO_2^{-3/4} * K_{chim} * PN_2^{1/2}$$

This solubility model depends on the temperature, the  $fO_2$  and the  $N_2$  pressure in fluid. It can be used to calculate the nitrogen content of a silicate melt as a function of redox conditions. We will show some applications that can help us constraining the timing of nitrogen release to the atmosphere.

### References:

- Li, Y. et al., (2015) Earth Planet. Sci. Lett. 411, 218–228.  
 Libourel, G. et al., (2003) Geochim. Cosmochim. Acta 67, 4123–4135.  
 Speelmanns, I.M. et al., (2019) Earth Planet. Sci. Lett. 510, 186–197.

## Vaporisation of group 13 elements from earth-like silicate melts by Knudsen Effusion Mass Spectrometry

Lukas Bischof<sup>1</sup>, Paolo Sossi<sup>1</sup>, Dmitry Sergeev<sup>2</sup>, Michael Müller<sup>2</sup>, Max Schmidt<sup>1</sup>

<sup>1</sup> Institute of Geochemistry and Petrology, ETH Zürich, CH-8092, Zürich, Switzerland

<sup>2</sup> Forschungszentrum Jülich GmbH, Institut für Energie und Klimaforschung (IEK), 52425 Jülich, Germany

Within the framework of former studies (e.g. Braukmüller et al., 2019), bulk silicate Earth (BSE) has been shown to contain an overabundance of the group 13 elements, Ga and In, in comparison to other moderately volatile elements (normalised to CI chondrites, which approximate best the initial composition of the solar nebula). However, the origin of these Ga- and In-anomalies has not yet been explained. Possible explanations include late accretion of a CI-like component, resulting in a 'plateau' of moderately volatile elements (Braukmüller et al., 2019), or conditions that diverged from those of the canonical solar nebula, resulting in different element volatilities by impact events (Sossi et al. 2019). In order to progress on such questions, the vaporisation behaviour of these elements from Earth-like silicate melts has to be quantified and then thermodynamically modelled.

For these purposes, Knudsen Effusion Mass Spectrometry (KEMS), a well-known method in physical chemistry for investigating thermodynamic properties of chemical substances, is applied to determine the *i*) identity and *ii*) vapour pressures of chemical species evaporating from geologically relevant silicate melts. Samples were placed in an iridium Knudsen cell and heated by a tungsten wire furnace *via* electron impact, producing a vapour inside the cell in equilibrium with the condensed phase(s). A small fraction of the vapour effuses out of the orifice to form a molecular beam that was subsequently ionised by electron impact at 60 eV and measured by a Faraday cup in a Finnigan MAT 271 magnetic sector mass spectrometer (Kobertz et al., 2014). Calibration of the temperature of the Knudsen cell and the signal intensity at known partial pressure was performed at the melting point of pure Ag metal.

We detected the ions  $E^+$ ,  $E^{2+}$ ,  $E^{3+}$ ,  $E_2^+$ ,  $EO^+$  and  $E_2O^+$  (where  $E = \text{Ga or In}$ ) above the pure oxides  $\text{Ga}_2\text{O}_3$  and  $\text{In}_2\text{O}_3$ . Following correction for ionisation cross sections, we find  $pE^0 \sim pE_2O \gg pEO$ , in agreement with previous work (Gomez et al. 1982; Shchukarev et al. 1969). An anorthite-diopside eutectic silicate melt composition doped with  $\sim 1000$  and  $\sim 10,000$  ppm of  $\text{Ga}_2\text{O}_3$  and  $\text{In}_2\text{O}_3$  was studied within a temperature range of 1150-1400 °C (the experiments initially contained equal amounts of Thallium, which were however  $>99\%$  evaporated at around 1000 °C). The ions  $E^+$ ,  $EO^+$  and  $E_2O^+$  were observed for both Ga and In above the silicate melt. The partial pressures of monatomic  $\text{Ga}^0$  and  $\text{In}^0$  relative to  $\text{Ga}_2\text{O}$  and  $\text{In}_2\text{O}$  were higher than for pure oxides, reflecting the lower activities of  $\text{GaO}_{1.5}$  and  $\text{InO}_{1.5}$  in the silicate melt. Activities of melt oxide components were calculated *via* LA-ICP-MS analyses of the remaining glass. We show that the relative volatilities of these two elements differ from those predicted from the solar nebula.

### References:

- Braukmüller et al., (2019) *Nature Geosci.* **12**, 564-568;  
Sossi et al., (2019) *GCA*, **260**, 204-231 ;  
Kobertz et al. (2014) *CALPHAD*, **46**, 62-79;  
Gomez et al. (1982) *J. Chem. Thermodynamics*, **14**, 447-459; Shchukarev et al. (1969) *Russian J. Inorg. Chem.* **14**, 1-5

## High-pressure in situ X-ray diffraction and X-ray absorption spectroscopy measurements using the Macquarie D-DIA apparatus at the Australian Synchrotron

Nicholas Farmer<sup>1</sup>, Tracy Rushmer<sup>1</sup>, Jeremy Wykes<sup>2</sup>

<sup>1</sup> Department of Earth and Environmental Sciences, Macquarie University, Macquarie Park, NSW 2109, Australia

<sup>2</sup> Australian Synchrotron, 800 Blackburn Road, Clayton, VIC 3168, Australia

The Macquarie University Deformation-DIA (MQ D-DIA) multi-anvil press enables in situ experimentation at the Australian Synchrotron under high-temperature and high-pressure conditions up to  $\sim 1500$  °C and 6 GPa. The MQ D-DIA can be deployed at suitable beamlines or used ‘offline’ on the experiment floor. Several online experiments have been conducted at the X-ray absorption spectroscopy (XAS) beamline, where we have developed a detector and optical setup at the XAS beamline that allows both XAS and energy-scanning X-ray diffraction (ES-XRD) measurements to be collected during high-pressure and high-temperature experiments.

Sample pressure and temperature in the MQ D-DIA has been calibrated by near-simultaneous diffraction of two dissimilar phases (NaCl and Au), and a new Markov chain Monte Carlo method. We have also measured the thermal profile through the sample region using a new technique for mapping compositional variations in electron probe microanalyzer (EPMA) maps of fine-grained polyphase assemblages.

This characterization of sample conditions in the MQ D-DIA facilitates in situ XAS measurements at precisely known pressure and temperature conditions. Preliminary in situ XAS measurements of the speciation of Zr present as a trace component in silicate melt under conditions corresponding to the Earth’s mantle (Figure 1) shows an increase in coordination number with increasing pressure.

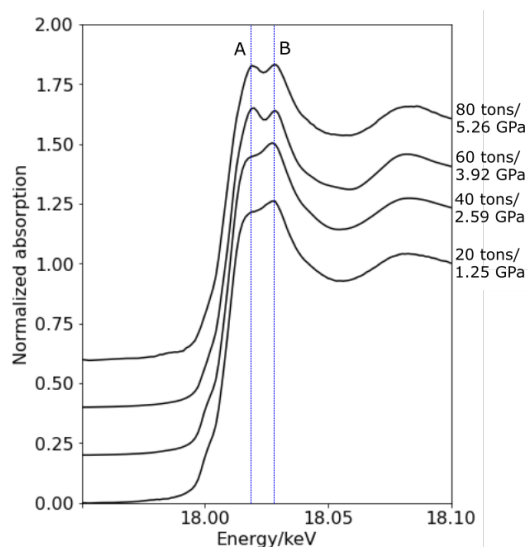


Figure 1: K-edge x-ray absorption spectra of Zr in silicate melt showing variation with pressure.

## Partial melt interconnection in the oceanic low velocity zone

Emmanuel Gardés<sup>1</sup>, Mickael Laumonier<sup>2</sup>, Malcolm Massuyeau<sup>3</sup>, Fabrice Gaillard<sup>4</sup>

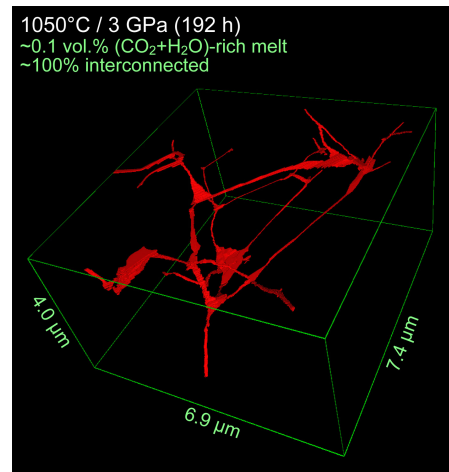
<sup>1</sup> Centre de recherche sur les Ions, les Matériaux et la Photonique (CIMAP), Normandie Université, ENSICAEN, UNICAEN, CEA, CNRS, Caen, France

<sup>2</sup> Laboratoire Magmas et Volcans (LMV), Université Clermont Auvergne, CNRS, IRD, OPGC, Clermont-Ferrand, France

<sup>3</sup> Institute for Mineralogy, University of Münster, Münster, Germany

<sup>4</sup> Institut des Sciences de la Terre d'Orléans (ISTO), Université d'Orléans, CNRS, BRGM, Orléans, France

The origin of the widespread low velocity zone (LVZ) in the shallow oceanic mantle has often been debated in terms of mantle melting. At LVZ depths, volatiles (CO<sub>2</sub> and H<sub>2</sub>O) are present in minute amounts, which implies mantle melting down to below 1000°C with the production of minute amounts of volatile-rich melt, well below 1 vol.%. Those melts have to form intergranular networks to produce any significant effect on mantle properties. However, our knowledge on melt interconnection in the upper mantle remained incomplete as it involves experiments at too large melt fractions, too high temperatures, and simplified petrological systems. Here, we show that melts with mantle-relevant, volatile-rich compositions and fractions do interconnect in mantle rocks down to lithospheric temperatures. This is done by extensive investigations, including high-resolution 3D imaging, on experiments of mantle partial melting where minute amounts of CO<sub>2</sub> and H<sub>2</sub>O generate minute amounts of melt, as in actual mantle. This demonstration reconciles our knowledge about volatile distribution, partial melting and geophysical signals in the upper mantle. The oceanic LVZ is evidenced as a partial melting zone since the distribution of sharp drops in shear wave velocity (Vs) and the domain of (CO<sub>2</sub>+H<sub>2</sub>O)-assisted melting coincide. Moreover, mantle low volatile content and its heterogeneity inferred by geochemistry on surficial samples appear to be imaged *in situ* by geophysics. The weak Vs lowering at global scale is consistent with very small average volatile content in the LVZ, while sharp Vs drops must highlight local volatile enrichments. In-depth deciphering of the dynamics of melt and volatiles in the LVZ calls for investigations on the seismic velocity, permeability and rheology of partially molten mantle rocks covering the diversity of mantle melt compositions, fractions and temperatures.



Interconnection of incipient melt in a (CO<sub>2</sub>+H<sub>2</sub>O)-bearing mantle rock experimentally re-equilibrated at shallow mantle temperature and pressure (3D imaging of melt distribution using serial focused ion beam sectioning-electron imaging)

## Influence of water on the structural and vibrational properties of silica glass

Markus G. Herrmann<sup>1</sup> Sandro Jahn<sup>1</sup>

<sup>1</sup> University of Cologne, Institute of Mineralogy and Geology, Zùlpicher Str. 49b, 50674 Cologne, Germany

Seismic anomalies atop and below the transition zone [1,2] and at the core-mantle boundary [3] have been attributed to the occurrence of hydrous silicate melts. Thus, the structural and physical properties of silicate melts and glasses (as potential structural analogues) are of particular interest for the understanding of the underlying magmatic processes.

The SiO<sub>2</sub>-H<sub>2</sub>O mixture represents the simplest model system of a hydrous silicate melt. At ambient conditions, a phase separation into heterogeneously distributed SiO<sub>2</sub>-rich domains (contain exclusively Si-OH groups) and water-rich districts (formed by molecular water) takes place in hydrous SiO<sub>2</sub> glass [4]. Already small amounts of water (1-2 wt.%) affect the mechanical properties such as the elasticity of SiO<sub>2</sub> glass tremendously [5]. It is therefore surprising that the influence of water on the structure of SiO<sub>2</sub> melt or glass is less investigated, above all at high pressure.

We have investigated the influence of pressures up to 43 GPa and 46 GPa on the structures of anhydrous and hydrous SiO<sub>2</sub> glasses (10.4 wt.% H<sub>2</sub>O) by Raman spectroscopy. As the high-pressure behavior of anhydrous SiO<sub>2</sub> glass was studied intensively in the past, among others by Raman spectroscopy [6], this sample serves as reference material. Our Raman data indicate that the SiO<sub>2</sub> network in both glasses is affected by pressure in a very similar way. Therefore, the additional Si-OH groups seem to have only a minor influence on the high-pressure behavior of SiO<sub>2</sub> glass. For both glasses, a structural phase transition from tetrahedrally coordinated Si into a mixture of a 5/6-fold coordinated Si takes place at around 20 GPa. Moreover, we observed pronounced pressure-induced changes in the OH-modes of the molecular water. At ambient conditions, the shape of these modes is similar to that of liquid water. However, with increasing pressure this feature becomes more ice-like indicating a further structural phase transition. While the pressure-induced changes in the OH-modes are fully reversible, the opposite is true for the modes which are associated with the SiO<sub>2</sub> network. Our Raman spectra suggest that the water-rich domains play a key role on the high-pressure behavior of hydrous SiO<sub>2</sub> glass and thus, they may be also of relevance for the melting processes in the Earth's interior.

### References:

- [1] D. Freitas et al., (2017) *Nature Commun.*, 8, 2186
- [2] W. R. Panero et al., (2020) *Geochem. Geophys. Geosyst.*, 21, e2019GC008712
- [3] Q. Williams et al., (1996) *Science*, 273, 1528-1530
- [4] E. Stopler, (1982) *Contrib. Mineral. Petrol.*, 81, 1-17
- [5] Murakami, (2018) *Sci. Rep.*, 8, 11890
- [6] R. J. Hemley et al., (1986) *Phys. Rev. Lett.*, 57, 747-750

## Influence of CO<sub>2</sub> on the rheology of melts from the Colli Albani Volcanic District (Italy) – foidite to phonolite

Christin Kleest<sup>1</sup>, Sharon L. Webb<sup>1</sup>, Sara Fanara<sup>1</sup>

<sup>1</sup> Georg August Universität Göttingen, Abteilung Experimentelle Mineralogie, Goldschmidtstraße 1, 37077 Göttingen, Germany

This study investigates the influence of CO<sub>2</sub> on the rheology of the ultrapotassic and silica-poor melt compositions from the Colli Albani Volcanic District (CAVD) (Italy). The magma chamber is seated in a thick sedimentary carbonate layer resulting in an interaction between the carbonate wall rock and the magma (i.e. Chiarabba et al. 1997). The assimilation of the wall rock leads to the liberation of a significant amount of a CO<sub>2</sub>-rich fluid and a partial incorporation of the carbonate into the melt (Iacono-Marziano et al. 2007). The solution of CO<sub>2</sub> in the foiditic melts from the CAVD can reach more than 8000 ppm at 300 MPa (Schanofski et al. 2019).

For the present investigations, different amounts of CaCO<sub>3</sub> as the source for CO<sub>2</sub> are added to a series of K-rich melts from foiditic to phonolitic compositions. The studied melt compositions represent the total rock compositions of the two largest eruptions from the CAVD, Pozzolane Rosse and Pozzolane Nere (foiditic and tephri-phonolitic, respectively), the composition of the magma after leucite crystallization and the composition of the magma before carbonate assimilation (tephritic and foiditic, respectively). To represent the K-rich end-member of the central Italian magmatism, a phonolitic composition from the Vesuvius 79 AD eruption is also investigated. The melts are synthesized in an internal heated pressure vessel with  $f_{O_2} = NNO + 3$  and run at approximately 300 MPa at 1250 °C up to 72 hours and are quenched rapidly. The total amount of solved CO<sub>2</sub> is determined by carbon analysis and Fourier transform infrared spectroscopy. To study the rheological features the micropenetration technique is used for viscosity measurements in addition to the differential scanning calorimetry for measurements of the heat capacity.

### References:

- Chiarabba et al (1997) *Crustal structure, evolution and volcanic unrest of the Alban Hills, Central Italy*, Bull Volcanol 59:161-170
- Iacono-Marziano et al (2007) *Limestone assimilation and the origin of CO<sub>2</sub> emissions at the Alban Hills (Central Italy): constraints from experimental petrology*, J Volcanol Geotherm Res 166:91-105
- Schanofski et al (2019) *CO<sub>2</sub>-H<sub>2</sub>O solubility in K-rich phonolitic and leucititic melts*, Contrib Mineral Petrol 174:52

## **A density model for carbonate-rich melts based on high pressure experimental data**

Malcolm Massuyeau<sup>1</sup>, Xenia Ritter<sup>1,2</sup>, Carmen Sanchez-Valle<sup>1</sup>

<sup>1</sup> Institute for Mineralogy, University of Münster, Corrensstraße 24, D - 48149 Münster, Germany

<sup>2</sup> Field Museum, 1400 S Lake Shore Dr, Chicago, IL 60605, United States

Volatiles cycles have a leading place in the evolution and fate of a planet. Depending on its nature, speciation, abundance and mobility, volatiles define the habitability conditions at the surface and greatly affect the physicochemical properties of the inner layers. Conversely, chemical and physical interactions between the inner and outer Earth's layers shape the evolution of the volatiles cycle. Among those various environments, the Earth's mantle constitutes a major actor of this cycle by hosting considerable proportions of carbon, and also hydrogen, both volatiles playing a critical role on melting properties of mantle peridotite, with the highest effects due to CO<sub>2</sub>. Understanding the exchanges and fluxes of carbon (and water) between the upper mantle and exosphere remains a primary goal in the Earth sciences community. Yet, this task is critically prevented by the lack of fundamental constraints on the mobility and migration rates of volatile-bearing melts (i.e., CO<sub>2</sub>-H<sub>2</sub>O-bearing melts) that are important conveyors for the distribution of volatiles. Although the density (and viscosity) data that control the mobility of carbon-rich melts in the mantle is becoming progressively available, density models for multi-component melts at mantle conditions are still lacking. Here we combine recent high pressure density data obtained by the synchrotron X-ray absorption technique with ambient to high pressure density and sound velocity data to propose a model for the density of dry and hydrous carbonate-rich melts to ~4 GPa and 2000 K. The calibration range spans the conditions for incipient melts stabilized in the upper mantle. Further, the applications of this model to quantify the migration/ascent/emplacement of melts through the mantle and the implications for volatile mobility and recycling in the deep Earth are discussed.

## Rare metal concentration in magmas: Insights from partial melting experiments

Julie A-S Michaud<sup>1</sup>, Michel Pichavant<sup>1</sup>, Arnaud Villaros<sup>1</sup>

<sup>1</sup> Université d'Orléans, CNRS, BRGM, ISTO, UMR 7327, F-45071, Orléans, France

Many studies have addressed the behaviour of rare metals during fractional crystallization, fluid exsolution and subsolidus alteration (e.g., Groves and McCarthy, 1978; Hulsbosch et al., 2016; Breiter et al., 2017). In comparison, only little attention has been placed on their behaviour during partial melting. One would expect that partial melting, which allows elements redistribution within the crust, stands as a powerful differentiation process. Therefore, fluid-absent melting experiments were performed using plurimillimetric microcores cut perpendicularly to the natural cleavage of a biotite-rich paragneiss and a muscovite-rich orthogneiss exhibiting different bulk and micas rare metal enrichments. Temperatures of 800 and 850°C, a pressure of 400MPa and a moderately reducing  $fO_2$  around FMQ-0.5 were used. Under the selected conditions, both protoliths produce a rather limited melt fraction (between 8 and 20% vol). Glass major element compositions little differ between the two protoliths although contrasted melt distributions were obtained. Glasses are strictly peraluminous ( $A/CNK > 1.1$ ) and resemble peraluminous two micas/muscovite granite bulk compositions. Dehydration melting of micas results in the formation of peritectic phases in addition to melt (i.e., muscovite: Spl, Ilm, Bt<sub>2</sub>, Mul, Sil; biotite: Spl, Ilm, Opx). Trace element contents of glass and glass-peritectic-mixtures vary significantly depending on the source rock and temperature. Rare metals hosted in micas are selectively partitioned between peritectic phases and melt. In contrast with W, Nb and Ta which are slightly to highly compatible in peritectic phases ( $Kd^{Mix/melt} \sim 1.5-4.5$  for all elements and up to 105 for W at 850°C in the orthogneiss experiment), Li preferentially partitions into the melt ( $Kd^{Mix/melt} < 1$ ). Despite the compatible behaviour of W, Nb and Ta, enriched rare-metal melt concentrations are reached (especially W) in experiments performed with the geochemically fertile orthogneiss. Overall, our experiments show that rare metal granites cannot be produced by a single episode of dehydration melting even at low melt fraction. Alternative solutions for the genesis of rare metal magmas include: (i) entrainment of rare-metal-rich peritectics during melt extraction, (ii) successive melting and extraction events favouring stepwise enrichment of the residual source and, (iii) fractional crystallization of a less enriched parental granite. Muscovite dehydration melting appears as an appealing mechanism to produce W-rich granites in agreement with the close spatial relationships worldwide between muscovite or two micas granites and W mineralization (e.g., Simons et al., 2017; Yang et al., 2019).

### References:

- Breiter et al., (2017) *Lithos*, 292-293, 198-217  
Groves and McCarthy, (1978) *Mineral. Deposita*, 13, 11-26  
Hulsbosch et al., (2016) *Geochim. Cosmochim. Acta*, 175, 299-318  
Simons et al., (2017) *Lithos*, 278-28, 491-512  
Yang et al., (2019) *Ore Geology Reviews*, 111, 102965

## **Al in five fold coordination in silicate glasses and melts: myth or reality?**

Daniel R Neuville

<sup>1</sup> Géomatériaux, CNRS-institut de physique du globe de Paris, Université de Paris, 1 rue Jussieu, 75005 Paris, France

The first human glasses were made 3500 BC. It was essentially sodo-lime silicate glass. To improve the chemical resistance, the thermal properties and increase the viscosity it is interesting to add aluminum in these silicates. And now aluminosilicate melts and glasses are materials widely used in several industrial applications (glass, glass-ceramic and ceramic materials), and implicated in large-scale geological processes. Their properties and structure, imposed by their chemical composition, drive for instance the eruptive dynamics of volcanoes as well as industrial processes of the glass-making industry.

But what is the speciation of the aluminum and how it varies according to the chemical composition and to the temperature?

The aluminum appears essentially in four or five fold coordination in glasses and melts. In alkali aluminosilicate compositions, Al is essentially in four fold coordination whereas the proportion of <sup>[5]</sup>Al increases with earth-alkaline substitution, or with alumina content and with temperature. In the case of alkali aluminosilicate glass and melts, Al is compensated by alkali element and as a function of alkali element (Li, Na, K) a new glass order can be observed.

In a second part, we can observe the presence of <sup>[5]</sup>Al in earth-alkaline aluminosilicate compositions. And its proportion varies as a function of Al and T. In particular, as a function of temperature, <sup>[5]</sup>Al play different roles, close than glass transition temperature <sup>[5]</sup>Al can be a new network former and at more high temperature <sup>[5]</sup>Al can be insure the network dynamics.

In all case, <sup>[4]</sup>Al and <sup>[5]</sup>Al play important role on the structure and properties of silicate glasses and melts and they are the key of network dynamics and nucleation processes.

## Fluorine and chlorine in glass and melt : implication for volcanology and novel-materials

Salomé Pannefieu<sup>1</sup>, Charles Le Losq<sup>1</sup>, Roberto Moretti<sup>1,2</sup> and Daniel R Neuville<sup>1</sup>

<sup>1</sup> CNRS-Institut de Physique du Globe de Paris, Université de Paris, 1 rue Jussieu, 75005 Paris, France

<sup>2</sup> Observatoire volcanologique et sismologique de Guadeloupe, Institut de physique du globe de Paris, F-97113 Gourbeyre, France

Igneous rocks can contain large quantities of halogens, such as fluorine F or chlorine Cl. In glass and ceramic material science, it is well known that the incorporation of halogens in silicate melts drastically affects phase equilibria and transport properties, particularly viscosity. Given this, degassing of halogens may affect the dynamic and progress of a volcanic eruption. Despite such importance, the behavior of F and Cl in magmas remains not clear because of multiple complex interactions with the silicate network that depend on melt composition and of Cl and F relative abundances.

To address this problem, we have prepared several glasses in the diagrams MgO-Al<sub>2</sub>O<sub>3</sub>-SiO<sub>2</sub> (MAS) and K<sub>2</sub>O-Al<sub>2</sub>O<sub>3</sub>-SiO<sub>2</sub> (KAS) containing different concentrations of F and Cl. The structure of the samples and the environment of F and Cl in them were investigated using Raman spectroscopy. Viscosity and heat capacity were measured too. We plan to show our first measurements made and discuss them.

## Phase relations in hydrous REE-bearing carbonatite at 1 GPa, 700-1250°C

Deborah Spartà<sup>1</sup>, Patrizia Fumagalli<sup>1</sup>, Giulio Borghini<sup>1</sup>, Stefano Poli<sup>1</sup>

<sup>1</sup> Dipartimento di Scienze della Terra "Ardito Desio", Università degli Studi di Milano, Italy

REE are known to be concentrated in carbonatites. Due to the difficulties in obtaining quenched glasses, the structure and the role of REE in carbonate-rich melts is currently poorly known (Jones and Wyllie, 1983). The aim of this study is to experimentally investigate the distribution of La in low-silica hydrous carbonate system at lithospheric conditions in order to define the role of La in the melt structure, establish phase relations and the distribution of REE (La). Additionally, experiments will allow to study the glass transition as a function of SiO<sub>2</sub>:CaCO<sub>3</sub> ratio.

Single stage and end-loaded piston cylinder experiments have been performed at 1 GPa in the model system CaO-SiO<sub>2</sub>-La<sub>2</sub>O<sub>3</sub>-H<sub>2</sub>O-CO<sub>2</sub> at temperature between 700-1250°C. Starting materials were prepared as powder mixtures of La<sub>2</sub>(CO<sub>3</sub>)<sub>3</sub> or La<sub>2</sub>O<sub>3</sub>, amorphous SiO<sub>2</sub> and CaCO<sub>3</sub>. Different bulk compositions at fixed La<sub>2</sub>O<sub>3</sub> ~ 10 wt.% with SiO<sub>2</sub>:CaCO<sub>3</sub> = 0.12, 0.2, 0.28, 0.5, 0.7, 1, 1.4 have been considered. Au and AuPd capsules were loaded with starting mixtures, adding ~10-15 wt.% of H<sub>2</sub>O, and sealed while freezing in order to avoid the loss of volatile component. Run products, carefully prepared to avoid any contact with water and polished with diamond paste, have been characterized by BSE images, X-ray diffractometry, Raman spectroscopy and chemically analyzed by electron microprobe.

At subsolidus conditions 700-900°C all bulk compositions contain calcite and quartz coexisting with a Ca,Lu-silicate (~5-40 μm) with an apatite structure and pseudo-hexagonal prismatic shape. At 1000°C wollastonite forms and coexists with Ca,Lu-silicate and calcite or quartz depending on the starting bulk composition. The presence of silica spherules testifies to the coexistence of a high pressure fluid. Melting has been observed in bulk compositions with SiO<sub>2</sub>:CaCO<sub>3</sub> = 1.4, 0.5, 0.28 at 1250°C, 1150°C and 1200°C respectively. Run products quenched to glasses and show evidence of fluid present conditions. In particular, fluid inclusions under the surface of the glass have been identified as molecular H<sub>2</sub>O by Raman spectroscopy. The bulk composition with the lowest SiO<sub>2</sub>:CaCO<sub>3</sub> ratio (0.14), run at 1200°C, does not quench to glass, but show calcite with typical dendritic textures.

Glasses compositions mostly overlap the starting bulks, in agreement with a high degree of melting. They are rather homogeneous and microprobe analyses are in agreement with a significant amount of dissolved volatiles that is proportional to the initial CaCO<sub>3</sub> wt.% of the starting material.

Raman spectroscopy on glasses suggests a low degree of polymerization, and significant solubility of H<sub>2</sub>O and CO<sub>2</sub>. The latter is present mainly as carbonate ion (CO<sub>3</sub><sup>2-</sup>) with a peak at 1080 cm<sup>-1</sup> although molecular CO<sub>2</sub> is also observed. H<sub>2</sub>O Raman signal presents the typical asymmetric band between 2800-3750 cm<sup>-1</sup>. A peak at ~ 850 cm<sup>-1</sup> is preliminarily assigned to LaQ<sup>0</sup> species, in agreement with its role as structure modifier in low viscosity carbonate rich melts.

### References:

Jones AP, Wyllie PJ (1983) *Econ Geol.*, 78:1721-1723

## **EMPG – XVII**

### **17th International Symposium on Experimental Mineralogy, Petrology and Geochemistry**

#### Abstracts Theme 3 “Fluids”

(sorted alphabetically by first author)

## Hydrothermal Alteration and Dissolution of Apatite: Tracing Ore Fluid Evolution Through the Partitioning of Polyvalent Sulfur and Rare Earth Elements

Justin Casaus<sup>1</sup>, Daniel Harlov<sup>2</sup>, Adam Simon<sup>1</sup>

<sup>1</sup> Dept Earth and Environmental Sciences, Univ Michigan, 1100 North University Ave., Ann Arbor, Michigan 48109

<sup>2</sup> Section 3.6, GeoForschungsZentrum GFZ, Telegrafenberg, 14473 Potsdam, Germany

Apatite occurs as an accessory mineral in many geologic environments and is capable of incorporating sulfur ( $S^{6+} > S^{2-} \gg S^{4+}$ ) and REEs via direct and coupled substitution. Published studies have demonstrated the partitioning of REEs and sulfur between apatite and a melt, as well as the role of oxygen fugacity ( $fO_2$ ) in controlling the oxidation state of sulfur. Partitioning of sulfur and REEs, sulfur oxidation states, and their substitution mechanisms for apatite in a sulfur-bearing hydrothermal fluid is not well known.

A series of experiments using cold seal autoclaves were conducted to explore metasomatism of Durango fluorapatite samples at 100 MPa, 600 and 800 °C, with  $fO_2$  buffered at NNO in order to constrain the behavior of sulfur and REEs in fluorapatite for Sulphur-bearing hydrothermal fluids.

The composition of the reacted fluorapatite from each experiment were quantified using electron probe micro-analysis (EPMA). Field emission scanning electron microscope (FE-SEM) element mapping of the fluorapatite for spatial distribution of elements. Analyses revealed sulphur and REE depleted reaction zones. We present first look data from experiment run-products.

Starting and reacted fluorapatite crystal structures will be analyzed using single crystal X-ray diffraction (XRD). Extended X-ray Absorption Fine Structure (EXAFS) spectroscopy and X-ray absorption near edge spectroscopy at the sulfur K-edge (S-XANES) will be performed to measure the in-situ oxidation states of Sulphur in the reacted fluorapatite grains. S-XANES spectra collected will then be used to calculate the  $S^{6+}/\Sigma S$  ratio.

## Fluid pH: Effects on silicate melt-fluid interaction and COH speciation

Dionysis I. Foustoukos<sup>1</sup>, Bjorn O. Mysen<sup>1</sup>

<sup>1</sup> Geophysical Laboratory, Carnegie Institution of Washington, 5251 Broad Branch Rd. NW, Washington DC 20015, USA

A series of hydrothermal diamond anvil experiments was conducted to constrain the role of fluid pH, alkalinity and electrolyte composition on the physical and chemical properties of the coexisting silicate melts. Na-Al bearing silicate glasses were reacted with NaCl-CO<sub>3</sub>-CO<sub>2</sub> enriched aqueous solutions at temperatures ranging from 400 to 800 °C and pressures of ~ 300 to 1200 MPa. The fluid pH ranged from highly acidic (pH = 1, 25 °C) to highly alkaline (pH = 13.2, 25 °C), with bulk ΣCO<sub>2</sub> composition of 0.5 M and salinity of 3.2 wt % NaCl or 0.5 M NaOH<sub>(aq)</sub>. In these experiments, we probed the speciation of carbon in the coexisting melt-fluid phases and assessed the effect of ionic aqueous species (Na<sup>+</sup>, Cl<sup>-</sup>, H<sup>+</sup>) on the solvus of the Na<sub>2</sub>O-Al<sub>2</sub>O<sub>3</sub>-SiO<sub>2</sub>-H<sub>2</sub>O-CO<sub>2</sub>-HCl system. The composition of the silicate glass resembles basaltic andesite with liquidus and glass transition temperatures < 400 °C. Results revealed the dominant presence of CO<sub>3</sub><sup>2-</sup> groups in silicate melts when coexisting with alkaline aqueous solutions. Furthermore, the CO<sub>3</sub>-bearing melts appear to be highly polymerized relative to previous in-situ observations for NA10 melts with HCO<sub>3</sub><sup>-</sup>/CO<sub>3</sub><sup>2-</sup> ~ 0.2 composition. To this end, fluid pH plays a key role in the speciation of oxidized carbon and its solubility in silicate melts. Most importantly, we observed a strong affinity for ionic fluids to suppress the critical point of the melt-fluid immiscibility region to lower temperatures and pressures than those attained in previous studies for the Na<sub>2</sub>O-Al<sub>2</sub>O<sub>3</sub>-SiO<sub>2</sub>-H<sub>2</sub>O system. A supercritical phase was developed at 400 °C and pressures of less than 0.8 MPa. We are in the process of assessing the structure of these low temperature/pressure supercritical phases, however, it appears that the dissolved Na<sup>+</sup> induces critical point suppression effects similar to those observed under elevated Al/(Al+Si) melt compositions. In fact, this might be associated with the elevated SiO<sub>2(aq)</sub> solubility expected in 3.2 wt% NaCl aqueous solutions at high temperatures and pressures (“salting-in” effect). To this end, the extent of SiO<sub>2</sub> solubility governed by the ionic strength and H<sub>2</sub>O activity of crustal fluids may play a key role in phase relationships between fluids and silicate melts.

## The impact of sulfur on the transfer of platinum group elements by hydrothermal fluids

Clément Laskar<sup>1</sup>, Gleb S. Pokrovski<sup>1</sup>, Maria Kokh<sup>1</sup>, Jean-Louis Hazemann<sup>2</sup>,  
Elena Bazarkina<sup>2</sup>, Elsa Desmaele<sup>3</sup>, Rodolphe Vuilleumier<sup>3</sup>

<sup>1</sup> Géosciences Environnement Toulouse, Toulouse, France (clement.laskar@get.omp.eu)

<sup>2</sup> Institut Néel, Université Grenoble Alpes, CNRS, ESRF, Grenoble, France

<sup>3</sup> Ecole Normale Supérieure, UPMC-CNRS-Sorbonne Universités, Paris, France

Knowledge of the mobility of platinum group elements (PGE) in magmatic-hydrothermal fluids is a key to understanding PGE deposit formation. Yet, existing data on aqueous chloride, sulfate, and hydroxide complexes of PGE predict far too small metal contents (<ppt to ppb) in fluids from most geological settings (Bazarkina et al., 2014; Kokh et al., 2017; Tagirov et al., 2019), thus calling upon an important role of the sulfide and, potentially, trisulfur ion ligands in PGE transport (Pokrovski et al., 2015). In an attempt to quantify the effect of sulfur on PGE mobility, we combined solubility measurements, in-situ X-ray absorption spectroscopy (XAS), thermodynamic (TD) and molecular dynamics (MD) modeling, based on recent advances of our knowledge of sulfur speciation in crustal fluids (Pokrovski et al., 2015). Our new data at 300°C and 500 bar suggest formation of two main complexes transporting Pt in the fluid at concentrations of 10s ppm over a wide pH range (4-8): (i)  $\text{Pt}(\text{HS})_4^{2-}$  in hydrogen sulfide  $\text{H}_2\text{S}/\text{HS}^-$  solutions, and (ii)  $\text{Pt}(\text{HS})_2(\text{S}_3)_2^{2-}$  in sulfide-sulfate  $\text{H}_2\text{S}/\text{SO}_4^{2-}/\text{S}_3^-$  solutions (Fig. 1A). Notably, the obtained concentrations of  $\text{Pt}(\text{HS})_4^{2-}$  in  $\text{H}_2\text{S}/\text{HS}^-$  solutions are 1000 times higher than those reported in previous quench-based studies (Gammons and Bloom, 1993), owing to an improved protocol we used for accurate fluid sampling from a flexible-cell reactor (Fig. 1B). TD and MD simulations, based on combined solubility and in-situ XAS data obtained with a hydrothermal cell (Fig. 1C) confirm the large stability of the  $\text{Pt}(\text{HS})_2(\text{S}_3)_2^{2-}$  complex, analogous to that proposed for gold (Pokrovski et al., 2015), with Pt(II) as the major oxidation state. Thus, our new data highlight an important role of previously ignored sulfur complexes that significantly enhance PGE transport by ore-forming fluids in the Earth's crust.

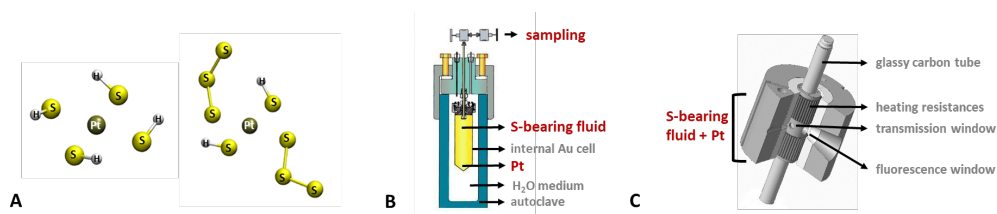


Fig. 1. Optimized MD-simulated geometries of the  $\text{Pt}(\text{HS})_4^{2-}$  and  $\text{Pt}(\text{HS})_2(\text{S}_3)_2^{2-}$  complexes (A), whose solubility and local atomic structure were measured using a flexible-cell reactor (B) and a hydrothermal XAS cell (C), respectively.

### References:

- Bazarkina et al., (2014) *GCA*, 146, 107–131  
 Gammons and Bloom, (1993) *GCA*, 57, 2451–2467  
 Kokh et al., (2017) *GCA*, 197, 433–466  
 Pokrovski and Dubessy, (2015) *EPSL*, 411, 298–309  
 Pokrovski et al., (2015) *PNAS*, 112, 13484–13489  
 Tagirov et al., (2019) *GCA*, 254, 86–101

## The role of CO<sub>2</sub> in molybdenum transporation in magmatic-hydrothermal system

Nuo Li<sup>1</sup>, Francois Holtz<sup>1</sup>, Ingo Horn<sup>1</sup>, Stefan Weyer<sup>1</sup>, Insa Derrey<sup>1</sup>, Wei Xi<sup>1,2</sup>

<sup>1</sup> Institut für Mineralogie, Leibniz Universität Hannover, Hannover 30167, Germany

<sup>2</sup> Xinjiang Research Center for Mineral Resources, Xinjiang Institute of Ecology and Geography, Chinese Academy of Sciences, Urumqi 830011, China

Porphyry deposits is the most important molybdenum source worldwide. A dual classification have been proposed for porphyry Mo deposit based mainly on case studies from Western Cordillera of North America (White et al., 1981; Theodore, 1986). China mainland has a proved Mo metal reserve of >25 Mt, which is more than two times the global total. These deposits, however, are difficult to fit into the dual classification. Compared with counterparts from North America, one of the major differences lies in their CO<sub>2</sub>-rich ore-forming fluids (Chen et al., 2017; Li et al., 2012). However, our knowledge of molybdenum transport in CO<sub>2</sub>-rich geological fluids are still limited.

With this in mind, and as a first step, we report here the results of experiments designed to determine the solubility of molybdenite in CO<sub>2</sub>-bearing H<sub>2</sub>O-NaCl solution. Synthetic fluid inclusions are used to trap the fluid phase for an aqueous solution of 8 wt.% NaCl and variable CO<sub>2</sub>, at 600°C and 2 kbar. Oxygen and sulphur fugacity was buffered by the assemblage magnetite, pyrite plus pyrrhotite. The experiments were conducted in rapid-heat/rapid-quench cold-seal pressure vessels (RH/RQ-CSPVs) at the Leibniz University Hannover. At run conditions with X<sub>CO<sub>2</sub></sub> (=CO<sub>2</sub>/H<sub>2</sub>O, molar fraction) of 0–0.25, the fluid inclusion traps single phase fluid. LA-ICPMS analyses (following Derrey et al., 2017) reveal low Mo concentration, with ca. 80% of them lower than limit of detection. Avalibale data vary slightly from 5 to 86 ppm, mostly between 15 and 60 ppm. No dependence of molybdenite solubility on X<sub>CO<sub>2</sub></sub> is observed, indicating that CO<sub>2</sub> has limited effect on the solubility of molybdenite at run condition.

A fundamental effect of the addition of CO<sub>2</sub> into the H<sub>2</sub>O-NaCl system is enlarging the degree of immiscibility (Duan et al., 1995). In system with X<sub>CO<sub>2</sub></sub> of 0.33, coexisting vapor (salinity = 4.3 wt.%) and brine (salinity = 49 wt.%) inclusions contain 3–36 ppm and 14–89 ppm Mo, respectively. This means, Mo will preferentially partition to the liquid phase during fluid immiscibility, with  $D_{Mo}^{liquid/vapor}$  of 7.6±1.4.

Further implication: using an average concentration of 40 ppm Mo in the fluid, and assuming the felsic magam contained 6 wt.% H<sub>2</sub>O and its density was 2.6 g/cm<sup>3</sup>, at least 160 km<sup>3</sup> magma is required to form a porphyry Mo deposit containg 1 Mt Mo. This confirms that the small granitic porphyry cannot provide the Mo metal itself, but instead, a huge magma chamber is essential.

### References:

- Chen et al., (2017) Ore Geol. Rev., 81,405-430
- Derrey et al., (2017) Am. Miner., 102, 275-283
- Duan et al., (1995) Geochim. Cosmochim. Acta, 59, 14: 2869-2882
- Li et al., (2012) Ore Geol. Rev., 48, 442-459
- Theodore (1986) Mineral deposit models: US Geological Survey Bulletin
- White et al. (1981) Econ. Geol., 75th Annoverary volume, 270-316

## Sulfur speciation in H<sub>2</sub>O-rich fluids based on in situ Raman spectroscopic investigation

Kang Liu, Huaiwei Ni

CAS Key Laboratory of Crust-Mantle Materials and Environments, School of Earth and Space Sciences, University of Science and Technology of China, Hefei 230026, China

Information of sulfur speciation in H<sub>2</sub>O-rich fluids with varied amount of silicate is crucial for understanding sulfur partitioning and isotope fractionation in fluid-mediated processes. We used Raman spectroscopy to determine S speciation in H<sub>2</sub>O-rich fluids at up to 750°C and 2 GPa in hydrothermal diamond anvil cell, for systems including S-H<sub>2</sub>O and Na<sub>2</sub>S<sub>2</sub>O<sub>3</sub>-H<sub>2</sub>O-Na<sub>3</sub>AlSi<sub>5</sub>O<sub>13</sub>. With the S-H<sub>2</sub>O system, we found that the S<sub>3</sub><sup>-</sup> ion, as reported by Pokrovski and Dubrovinsky (2011), could be stabilized to high temperature and pressure in coexistence with SO<sub>2</sub> and H<sub>2</sub>S. For the Na<sub>2</sub>S<sub>2</sub>O<sub>3</sub>-H<sub>2</sub>O-Na<sub>3</sub>AlSi<sub>5</sub>O<sub>13</sub> system, the stability of S<sub>3</sub><sup>-</sup> did not appear to be jeopardized by the presence of silicate component.

These experimental observations prompted us to compute the stability fields of different sulfur species in H<sub>2</sub>O-rich fluids as a function of pH and redox state, using the Deep Water Earth (DEW) model (Sverjensky et al., 2014). At typical redox conditions of subduction zones (from the fayalite-magnetite-quartz buffer to FMQ+2), DEW modeling suggests that S<sub>3</sub><sup>-</sup>, relative to SO<sub>2</sub>, is favored toward higher pH. Because subduction zone fluids saturated by silicate rocks are typically mildly alkaline (Galvez et al., 2016), the modeling result is consistent with our observation of S<sub>3</sub><sup>-</sup> in the silicate-present fluid. We infer that S<sub>3</sub><sup>-</sup> can be an important sulfur species in slab-derived H<sub>2</sub>O-rich fluids, which may be important for mobilizing ore-forming elements from the slab through S<sub>3</sub><sup>-</sup> complexation.

### References:

- Pokrovski and Dubrovinsky (2011) *Science*, 331,1052-1054  
Sverjensky et al., (2014) *GCA*, 129, 125-145  
Galvez et al., (2016) *Nature*, 538, 420-424

## Zirconium and hafnium complexation in fluoride-rich greisen fluids

Anselm Loges<sup>1</sup>, Shilei Qiao<sup>1</sup>, Marion Louvel<sup>2</sup>, Max Wilke<sup>3</sup>, Stephan Klemme<sup>2</sup>, Timm John<sup>1</sup>

<sup>1</sup>Institute of Geological Sciences, Free University Berlin, Germany

<sup>2</sup>Institute of Mineralogy, WWU Münster, Germany

<sup>3</sup>Institute of Geosciences, University Potsdam, Germany

Greisen fluids differ from most other geological fluids in that they are often rich in fluoride and precipitate fluorite and/or topaz. Because fluoride complexation is considerably less well studied than complexation with chloride and other geologically relevant anions, element transport processes leading to greisen related ore deposits are currently not well understood. Fluoride is the hardest naturally occurring Lewis base and therefore is most relevant to the transport of hard Lewis acids, such as the cations of high field strength elements (HFSE). Zirconium (Zr) and Hafnium (Hf) are a pair of elements particularly suited for studies of the influence of fluoride complexation on ore formation because they occur exclusively in tetravalent state in nature. With ionic radii of 590 pm (Zr<sup>4+</sup>) and 580 pm (Hf<sup>4+</sup>), respectively, they are geochemical twins, which are not fractionated by most geological processes other than transport in F-rich fluids.

We report geometries of Zr and Hf fluoride complexes up to 400°C, determined by extended X-Ray absorption fine structure (EXAFS) in a new hydrothermal autoclave, installed at beamline P65, PETRA III, DESY, Hamburg. Existing data sets on the stability of those complexes at lower temperatures were extended to 400°C. Our data show strong temperature dependence of the complex stability for both metals. However, the effect of temperature is not equally strong for Zr and Hf. Fractionation of the twin pair is thus a function of temperature as well as fluoride activity.

We use our experimental data to interpret the occurrence of hydrothermal zircons found in association with fluorite in a greisen alteration zone in rhyolite from Zinnwald, Erzgebirge, Germany. These zircons show extensive zoning in Zr/Hf, and our new experimental data in conjunction with whole rock and mineral chemical data are used to determine if Zr and Hf (and by proxy the other HFSE) are redistributed locally by the greisen fluid or if there is a considerable influx of these elements via the fluid.

## Impact of the S radical ions on the transfer of sulfur and critical metals by fluids and magmas in the lithosphere

Gleb S. Pokrovski<sup>1</sup>, Aurélie Colin<sup>1</sup>, Maria Kokh<sup>1</sup>, Elsa Desmaele<sup>2</sup>, Clément Laskar<sup>1</sup>,  
Anastassia Y. Borisova<sup>1</sup>, Denis Testemale<sup>3</sup>, Jean-Louis Hazemann<sup>3</sup>, Rodolphe Vuilleumier<sup>2</sup>,  
Christian Schmidt<sup>4</sup>, Max Wilke<sup>5</sup>

<sup>1</sup> Fluids at Extremes Group (FLEX), Géosciences Environnement Toulouse, Toulouse, France (gleb.pokrovski@get.omp.eu)

<sup>2</sup> Ecole Normale Supérieure, UPMC-CNRS-Sorbonne Universités, Paris, France

<sup>3</sup> Institut Néel, Université Grenoble Alpes, CNRS, ESRF, Grenoble, France

<sup>4</sup> Deutsches GeoForschungsZentrum (GFZ), Potsdam, Germany

<sup>5</sup> Universität Potsdam, Institut für Geowissenschaften, Potsdam, Germany

Our interpretation of sulfur behavior in aqueous fluids and silicate melts at depth is based on a long-standing paradigm that sulfate, sulfide, and sulfur dioxide are the major sulfur forms. This paradigm was recently challenged by the findings of the disulfur and trisulfur radical ions,  $S_2^{\cdot-}$  and  $S_3^{\cdot-}$ , in hydrothermal fluids (Pokrovski and Dubrovinsky, 2011; Pokrovski and Dubessy, 2015; Schmidt and Seward, 2017). Although both ions have widely been known in non-aqueous chemistry since 1970s (Chivers and Elder, 2013), their impact in Geosciences remains unassessed. This is because, in water-bearing geological environments, they are only stable at elevated temperatures ( $T$ ) and pressures ( $P$ ) and cannot be preserved in quenched products due to fast breakdown to traditional sulfur forms. In this keynote contribution, we overview recent advances of in-situ approaches (Raman and synchrotron X-ray absorption spectroscopy) developed for studying these fascinating but ‘fugitive’ radical species. Our results show that the radical ions are stable and coexist with sulfate and sulfide in ‘aqueous fluid – silicate melt’ systems across a wide  $T$ - $P$  range (to at least 800°C and 30 kbar) and partition 10 to 1000 times more than sulfate and sulfide into the fluid phase. Thus, by enhancing the transfer of sulfur and associated S-loving metals (Au, Pt, Mo, Re) from melt into fluid upon magma degassing,  $S_3^{\cdot-}$  and  $S_2^{\cdot-}$  may be the key players in the formation of economic metal resources within the redox window of the sulfate-sulfide transition typical of magma generation and evolution in subduction zone settings. Furthermore, even in epithermal fluids of moderate  $T$  (<350°C), platinum aqueous complexes with the  $S_3^{\cdot-}$  ligand similar to those known for Au (Pokrovski et al., 2015), are able to transport the metal up to 1000 times more efficiently than the traditional hydrogen sulfide, sulfate or chloride ligands (Laskar et al., 2020). More generally, our data imply an important, but so far largely underestimated, contribution of hydrothermal S-bearing fluids to the transfer and accumulation of platinoids (PGE) and, potentially Mo and Re, in the Earth’s crust. Our results challenge current magmatic models of PGE ore deposit formation, and may offer new routes for selective extraction of critical metals from ore and hydrothermal synthesis of their nanomaterials.

### References:

- Chivers and Elder (2013) Chem. Soc. Rev. 42, 5996  
 Laskar et al. (2020) this volume  
 Pokrovski and Dubrovinsky (2011) Science 331, 1052  
 Pokrovski and Dubessy (2015) Earth Planet. Sci. Lett. 411, 298  
 Pokrovski et al. (2015) Proc. Nat. Acad. Sci. USA 112, 13484  
 Schmidt and Seward (2017) Chem. Geol. 467, 64

## Carbonation of the hydrated forearc mantle by a graphite saturated COH-fluid

Melanie J. Sieber<sup>1,2,3</sup>, Greg M. Yaxley<sup>1</sup>, Jörg Hermann<sup>4</sup>

<sup>1</sup> Research School of Earth Sciences, Australian National University, Canberra, Australia

<sup>2</sup> University of Potsdam, Institute of Geosciences, Potsdam-Golm, Germany

<sup>3</sup> GFZ German Research Centre for Geosciences, Potsdam, Germany

<sup>4</sup> University of Bern, Bern, Switzerland

Significant amounts of carbon are released from the subducting slab into fluids, but less carbon is released from the mantle in arc volcanoes implying the storage of carbon in the mantle wedge. This experimental study shows that carbonation of serpentinites can establish, over time, a significant reservoir for carbon within a partially hydrated mantle wedge and that carbonation of (ultra-) mafic rocks within the subducting slab contributes to the transfer of carbon to greater depths and might supply carbon for arc volcanism or the deep mantle.

Sieber *et al.* (2018) used powdered natural serpentinite in high-pressure experiments establishing the equilibrium phase relations and volatile fluid composition of the CO<sub>2</sub>-H<sub>2</sub>O-antigorite system. We here used cylindrical cores of natural serpentinite as starting material in piston-cylinder experiments to investigate the effectiveness, rate and mechanism of carbonation of serpentinites with natural grain sizes and shapes (Sieber *et al.*, 2020). The interactions between serpentinite and a carbon saturated CO<sub>2</sub>-H<sub>2</sub>O-CH<sub>4</sub>-fluids were investigated between 1.5 and 2.5 GPa and 375 to 700 °C. The results are applied to carbonated high-pressure rocks in the European Alps (Sieber, 2019).

The volatile composition of quenched fluids was analysed by gas chromatography. Solids were examined by Raman-spectroscopy, electron microscopy and Laser-Ablation ICP-MS. Three dimensional high resolution micro X-ray computed tomography of recovered rock-cores visualizes textures and porosity and determines phase abundances.

This study demonstrates that carbonation of the hydrated forearc mantle efficiently sequesters CO<sub>2</sub> from the fluid into newly formed magnesite. Time-series experiments demonstrate that carbonation is completed within ~96 h at 2 GPa and 600 °C. With decreasing CO<sub>2, aq</sub> antigorite is replaced first by magnesite + quartz followed by magnesite + talc + chlorite in distinct, metasomatic fronts. Above antigorite stability magnesite + enstatite + talc + chlorite occur additionally. The formation of fluid permeable reaction zones enhances the reaction rate and efficiency of carbonation. Carbonation likely occurs via an interface-coupled replacement process, whereby interconnected porosity is present within reaction zones after the experiment. Consequently, carbonation of serpentinites is self-promoting and efficient even if fluid flow is channelized into veins. We conclude that significant amounts of carbonates may accumulate, over time, in the hydrated forearc mantle and in carbonated (ultra-) mafic rocks within the subducting slab.

Sieber (2019). thesis, Australian National University, Canberra.

Sieber *et al.*, (2018) Earth and Planetary Science Letters, 496, 177-188

Sieber *et al.*, (2020) Journal of Petrology

## Solubility of magnetite and hematite in slab-derived saline fluids

Carla Tiraboschi<sup>1</sup> & Carmen Sanchez-Valle<sup>1</sup>

<sup>1</sup>University of Münster, Institute of Mineralogy, Corrensstraße 24, D-48149 Münster, Germany

Aqueous fluids have a fundamental role in subduction zones, where fluids derived from devolatilization processes of the oceanic lithosphere and its sedimentary cover, represent a major vectors of mass transfer from the slab to the mantle wedge, and modulate the recycling of elements. In this setting, assessing the mobility of redox sensitive elements, such as iron, can provide useful insights on the oxygen fugacity conditions of slab-derived fluid. However, the amount of iron mobilized by deep aqueous fluids and melts, is still poorly constrained.

We experimentally investigate the solubility of magnetite-hematite assemblages in water-saturated haplogranitic liquids, which represent the felsic melt produced by subducted eclogites. Experiments were conducted at 1–2 GPa and temperature ranging from 700 to 900 °C employing a piston cylinder apparatus. Single gold capsules were loaded with natural hematite, magnetite and synthetic haplogranite ( $\text{Na}_{0.56}\text{K}_{0.38}\text{Al}_{0.95}\text{Si}_{5.19}\text{O}_{12.2}$ ). Two sets of experiments were conducted: a first set with pure  $\text{H}_2\text{O}$  in the experimental charge and a second set with a 1.5 m  $\text{H}_2\text{O}$ -NaCl solution. Capsules were kept frozen during welding to ensure no water loss. Run times from 24 h, for high-temperature experiments, to 72 h for lower temperature runs were considered. The achievement of equilibrium conditions was checked by performing time series experiments at selected  $P$ - $T$  conditions and employing variable grain size dimensions of the starting material.

After quench, the presence of  $\text{H}_2\text{O}$  in the haplogranite glass was checked by Raman spectroscopy, while major elements were determined by electron microprobe analysis.

Results indicate that a significant amount of FeO is released from magnetite and hematite in hydrous melts, even at relatively low-pressure conditions. At 1 GPa the  $\text{FeO}_{\text{tot}}$  quenched in the haplogranite glass ranges from 0.60 wt% at 700 °C, to 1.82 wt% at 900 °C. In the presence of NaCl, we observed an increase in the amount of iron in the glass, e.g., at 800 °C from 1.04 wt% to 1.50 wt% of  $\text{FeO}_{\text{tot}}$ . No significant pressure effect has been observed in the limited pressure range investigated.

Our results suggest that hydrous melts can effectively mobilize iron from Fe-oxides even at low-pressure conditions and that the presence of dissolved salts further enhances their ability to mobilize iron. Slab derived hydrous melts can thus represent a valid agent for mobilizing iron from the subducting slab to the mantle wedge and can strongly influence the geochemical cycles of Fe and the redox conditions of subduction zone fluids.

## Electrical conductivity of H<sub>2</sub>O-KCl fluids up to 4 GPa and 900 °C

Kirill Vlasov<sup>1</sup>, Hans Keppler<sup>1</sup>

<sup>1</sup> Bayerisches Geoinstitut, Universität Bayreuth, 95440 Bayreuth, Germany

Aqueous fluids occur in Earth's crust and in the mantle above subduction zones. KCl is a major solute, particularly in some deep mantle fluids trapped in diamonds (e.g. Kopylova et al., 2010). Electrical conductivity measurements of such fluids therefore have direct geological implications for the interpretation of magnetotelluric data. They may allow the determination of fluid type and fluid fraction in highly conductive zones of the Earth (Pommier, 2014).

To measure electrical conductivity of the KCl-bearing aqueous fluid, we used a piston cylinder cell similar to that described by (Guo and Keppler, 2019). Cells containing 1 M KCl solution inside the pore space of diamond powder were loaded into a piston cylinder apparatus and compressed to 1, 2, 3, and 4 GPa. Resistances were extracted from impedance measurements carried out from 10 MHz to 1 kHz, during several heating and cooling cycles from 28 to 900 °C at constant pressure. After the run, the fluid fraction was calculated according to the Hashin and Shtrikman upper bound model (Hashin and Shtrikman, 1962), based on cell the resistance measured at ambient conditions. Knowing the cell constant, bulk fluid conductivities were then calculated from the resistance values at experimental conditions (Fig. 1).

The data show a strong enhancement of conductivity by pressure and temperature; with increasing temperature, fluid viscosity decreases, while pressure increases the dielectric constant of the fluid and therefore enhances dissociation of KCl into K<sup>+</sup> and Cl<sup>-</sup>. Compared to the NaCl-H<sub>2</sub>O system, the observed conductivities tend to be somewhat lower, due to the reduced mobility of K<sup>+</sup> as compared to Na<sup>+</sup> (Guo and Keppler, 2019).

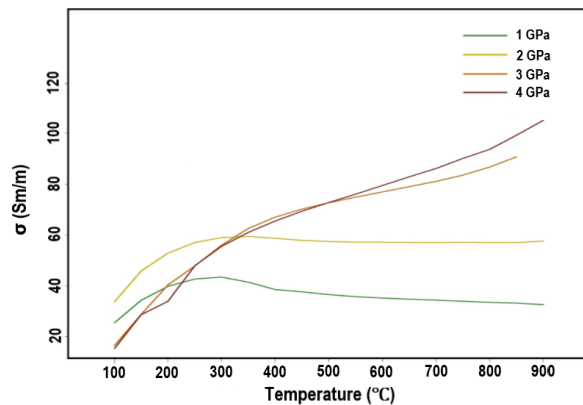


Fig. 1: Measured conductivities of H<sub>2</sub>O-KCl-fluids to 900 °C and 4 GPa. The KCl concentration was equivalent to 1 M = 1 mol/liter at ambient conditions

### References:

- Guo H., Keppler H. (2019) *J. Geophys. Res. Solid Earth*, 124(2) 1397-1411  
 Kopylova M., Navon O., Dubrovinskiy L., Khachatryan, G. (2010) *Earth Planet. Sci. Lett.* 291, 126–137  
 Hashin Z., Shtrikman S., (1962). *J. Appl. Phys.* 33, 3125–3131  
 Pommier A., (2014) *Surv. Geophys.* 35, 41–84

## **Spinodal decomposition of supercritical fluid in a silicate-H<sub>2</sub>O system and the formation and disruption of silicate melt network**

Qinxia Wang<sup>1</sup> Dongyuan Zhou<sup>1</sup> Wan-Cai Li<sup>1,2</sup> Huaiwei Ni<sup>1,2</sup>

<sup>1</sup> CAS Key Laboratory of Crust-Mantle Materials and Environments, School of Earth and Space Sciences, University of Science and Technology of China, Hefei 230026 China

<sup>2</sup> CAS Center for Excellence in Comparative Planetology, Hefei 230026, China

Supercritical fluids, compositionally intermediate between silicate melt and hydrothermal fluid, have distinctive physicochemical properties and can be important agent of mass transfer in Earth's interior. However, reducing temperature and pressure drives supercritical fluid to decompose. Direct observation using a hydrothermal diamond anvil cell reveals that in addition to classical nucleation-growth mechanism, the phase separation of supercritical fluid in a silicate-H<sub>2</sub>O system can proceed also by spinodal decomposition. More importantly, due to contrasting relaxation kinetics of the silicate components and H<sub>2</sub>O, viscoelastic spinodal decomposition of supercritical fluid can give rise to an impressive network, composed of multiple threads and nodes, of silicate melt. Slower cooling decreases network density and increases domain size, but does not seem to fundamentally affect network formation. Further cooling eventually leads to disruption of the melt network and formation of isolated melt droplets to minimize interfacial energy. However, we suggest that this metastable network structure with uneven fluid-melt boundaries could facilitate the genesis of melt/fluid inclusions with a spectrum of silicate to H<sub>2</sub>O ratios, as often observed in pegmatites. Spinodal decomposition and melt network can also increase the efficiency of magma-fluid separation in magmatic-hydrothermal systems.

**EMPG – XVII**

**17th International Symposium on  
Experimental Mineralogy,  
Petrology and Geochemistry**

Abstracts

Theme 4 “Rheology and deformation”

(sorted alphabetically by first author)

## Experimental confirmation of gas percolation threshold in bubble- and crystal-bearing silicic melts under shear

Camille Daffos<sup>1</sup>, Caroline Martel<sup>1</sup>, Laurent Arbaret<sup>1</sup>, Rémi Champallier<sup>1</sup>, Jacques Précigout<sup>1</sup>

<sup>1</sup> Université d'Orléans-CNRS/INSU-BRGM, ISTO, UMR 7327, 45071, Orléans, France

Volcanoes of silica-rich magmas may erupt effusively (lava-dome growth) or explosively (vulcanian and Plinian eruptions), so that understanding their eruptive dynamics is a crucial issue for volcanic risk assessment. The transition from effusive to explosive activity mainly relies on the magma ability to release or retain gases, i.e. on permeability development. Gas percolation threshold in magmas is primarily controlled by intrinsic parameters, such as bubble and crystal fraction and magma viscosity, and by external parameters, such as ascent and strain rates at conduit margins and overlying domes. Our study follows a previous work of in-situ permeability determination in two-phase (bubble and melt) suspensions under magmatic temperatures and confining pressures (Kushnir et al., 2017). In the present work, we added crystals in bubble-bearing melts to investigate the role of a crystalline framework in promoting gas permeability.

We performed torsion experiments in a deformation press of Paterson type, using hydrous haplogranitic (78.6 SiO<sub>2</sub>, 12.5 Al<sub>2</sub>O<sub>3</sub>, 4.6 Na<sub>2</sub>O, 4.2 K<sub>2</sub>O, in wt%, anhydrous basis) melts containing water bubbles and plagioclase (labradorite) crystals. The haplogranitic melts are first hydrated to 10 wt% H<sub>2</sub>O in internally-heated pressure vessels at 950°C and 400 MPa. The hydrated glasses are crushed and manually mixed with different amounts of plagioclase crystals (size fraction between 50 to 90 μm). Crystal fractions,  $\phi_c$ , are of 21 and 50 vol%. The glass-crystal mixtures are sealed in Cu or Au capsules and placed in the Paterson press at 300 MPa and 850°C for rapid isothermal decompression to 50 MPa in order to nucleate water bubbles. SEM and X-ray microtomograph analyses of the starting samples suggest bubble fractions,  $\Phi_b$ , of 30 to 50 vol%, with mean diameters of about 200 μm, and confirm that bubbles are not connected before deformation. Torsion experiments are conducted in the Paterson press, in the wake of the bubble-forming decompression step, at 750 °C and 50 MPa, shear strain rates  $\dot{\gamma}$  from 10<sup>-4</sup> s<sup>-1</sup> to 10<sup>-5</sup> s<sup>-1</sup>, and strains  $\gamma$  up to 4. The results suggest that gas percolation in sheared crystal-bearing magmas develops as tensile fractures or gas channelization, depending on bubble content, crystal framework, and finite deformation.

### References:

Kushnir et al., Earth and Planetary Science Letters 458 (2017) 315-326

## **Deformation of subduction zones multiphase rocks: in situ, high pressure experiments**

Nadege Hilairet<sup>1</sup>, Tommaso Mandolini<sup>1</sup>, Sebastien Merkel<sup>1</sup>, C. Tomé<sup>2</sup>, H. Wang<sup>2</sup>, J. Chantel<sup>1</sup>, J. Guignard<sup>3,\*</sup>, W. Crichton<sup>3</sup>, Y. Le Godec<sup>4</sup>

<sup>1</sup> Univ. Lille, F-59000 Lille, France

<sup>2</sup> Los Alamos National Laboratory, USA

<sup>3</sup> European Synchrotron Radiation Facility, F-38000 Grenoble, France

<sup>4</sup> Sorbonne Université, F-75000 Paris, France

\*now at Univ. Nantes, France

Rocks are polymineralic crystalline aggregates. Quantifying and understanding their mechanical behavior remains a challenge because multiple feedbacks are at play in crystalline aggregates between parameters such as temperature (T), pressure (P) and characteristics such as grain sizes and microstructure. In addition, natural observations and many works emphasize that in polymineralic rocks, heterogeneities in minerals' mechanical properties induce stress and strain partitioning with dramatic consequences for the global mechanical behaviour.

A common approach in rheological studies under high pressures is to investigate monomineralic aggregates as a proxy, and the mineralogical diversity of deep subduction zones aggregates seldom has been considered. Here, I will present how HP deformation experiments with in-situ x-ray measurements and mean field models of polymineralic aggregates can help us with this problem.

Questions that can be answered include sorting out which phases are susceptible to control the aggregate behavior and for which mineralogy. To that extent, we investigate the strain (rate) or stress ranges in the rock that can exist due to different elastic and plastic properties of minerals. The microstructural characteristics, part of which can be monitored in-situ, remain crucial when considering these questions.

I will illustrate the presentation with high-pressure experiments using in-situ X-Ray measurements, mean field models of aggregates, and our current effort using HP tomography on deformed subduction zones rocks.

## Experimental study of the K-richterite formation at 3 GPa

Limanov E.V., Butvina V.G., Safonov O.G., Van K.V.

Korzhinskii Institute of Experimental Mineralogy, Russian Academy of Sciences, Chernogolovka, 142432 Russia

The reaction  $8\text{En} + \text{Di} + [1/2\text{K}_2\text{O} + 1/2\text{Na}_2\text{O} + \text{H}_2\text{O}] = \text{KRich} + 2\text{Fo}$  determines the formation of K-richterite, an important mineral indicator of the highest degree of metasomatism of upper mantle peridotites. This reaction was studied experimentally the presence of a  $\text{K}_2\text{CO}_3\text{-Na}_2\text{CO}_3\text{-CO}_2\text{-H}_2\text{O}$  fluid a temperature of  $1000^\circ\text{C}$  and a pressure of 3 GPa. At a weight ratio  $\text{Na}_2\text{CO}_3/\text{K}_2\text{CO}_3 = 1/1$ , amphibole forms at a weight ratio  $(\text{K}_2\text{CO}_3 + \text{Na}_2\text{CO}_3) / (\text{CO}_2 + \text{H}_2\text{O}) = 3/7$ . The reaction is evidenced by the presence of newly formed olivine along with amphibole (Fig. 1b). The content of the tremolite component in amphibole decreases. Composition of amphibole shifts towards richterite with an increase in the alkaline component in the fluid. Clinopyroxene occurs mainly in the form of inclusions in olivine at a high content of alkaline components in the fluid (Fig. 1c). With the predominance of  $\text{Na}_2\text{CO}_3$  over  $\text{K}_2\text{CO}_3$  ( $7/3$ ), the formation of amphibole was also possible if the ratio  $(\text{K}_2\text{CO}_3 + \text{Na}_2\text{CO}_3) / (\text{CO}_2 + \text{H}_2\text{O}) = 3/7$ . Amphibole is unstable at higher concentration of alkaline components being replaced by a melt. At the ratio  $\text{Na}_2\text{CO}_3 / \text{K}_2\text{CO}_3 = 3/7$ , amphibole was formed only at the ratio  $(\text{K}_2\text{CO}_3 + \text{Na}_2\text{CO}_3) / (\text{CO}_2 + \text{H}_2\text{O}) = 1/9$ . Amphibole occurred as thin needles up to 2 microns in size showing that it as a quenching phase with an increase in the content of  $\text{K}_2\text{CO}_3 + \text{Na}_2\text{CO}_3$  in the fluid. Preliminary experiments have shown that the formation of K-bearing richterite is determined not only by the amount of alkaline components in the fluid, but also depends on the Na / K ratio in the fluid.

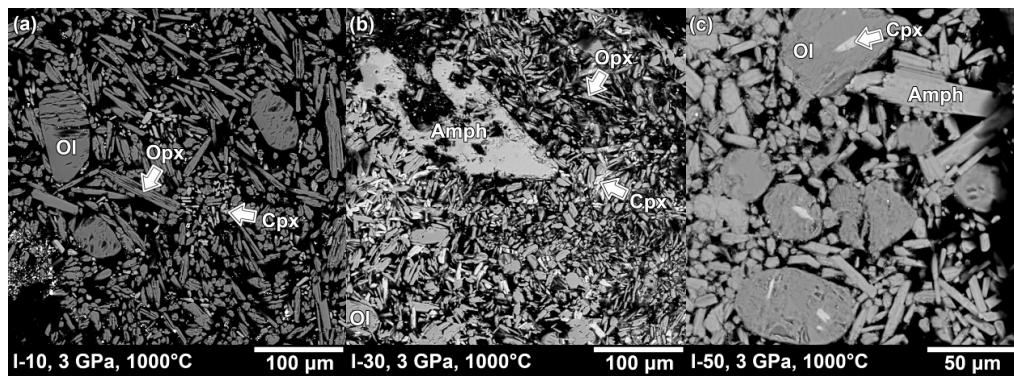


Fig.1 Run products of experiments at the ratio  $\text{Na}_2\text{CO}_3 / \text{K}_2\text{CO}_3 = 1/1$ .

## Microstructural evolution in deforming olivine-serpentine aggregates at subduction zones conditions using *in-situ* X-ray tomography

Tommaso Mandolini<sup>1</sup>, Nadege Hilairet<sup>1</sup>, Julien Chantel<sup>1</sup>, Sébastien Merkel<sup>1</sup>, Yann Le Godec<sup>2</sup>, Nicolas Guignot<sup>3</sup>, Andrew King<sup>3</sup>

<sup>1</sup> Department of Earth and Planetary Materials, Université de Lille, France

<sup>2</sup> Institut de Minéralogie, de Physique des Matériaux et de Cosmochimie (IMPMC), Sorbonne Université, France

<sup>3</sup> SOLEIL Synchrotron, France

Rheology and deformation of serpentinized peridotite play an important role in the flow and dynamics of the subducting slab. Antigorite, the high-temperature variety mineral of serpentine group, coexists with olivine in serpentinized peridotite at conditions of subduction zones. It is generally accepted that antigorite mechanical strength is lower than olivine at geological strain rates. Therefore, in a biminerale rock comprising olivine and antigorite, deformation localization is expected to occur in the weaker antigorite rather than in olivine. Based on polymineralic rocks mechanical and microstructural behaviours (e.g., Handy, 1990), two main end-member configurations are possible: the strong olivine crystals form a loadbearing framework (LBF) that contains spaces filled with antigorite; or the antigorite governs the bulk rheology of the aggregate by forming an interconnected weak layer (IWL), while the olivine crystals behave as clasts.

The aim of this study is to observe at which conditions an IWL stage may be achieved under simple shear deformation in serpentinized peridotite at subduction zones conditions. We carried out torsion experiments at high pressures (HP, > 2 GPa) and high temperatures (HT, 400-600°C) on antigorite + olivine aggregates as a proxy for partially serpentinized peridotite. The experiments are coupled with *in-situ* X-ray tomography on the PSICHE beamline at SOLEIL synchrotron. We retrieve and quantify 2-D and 3-D information on fabrics and/or microstructure evolutions under HP-HT, extent of interconnection (or connectivity), preferred microstructural directions and morphology of the weak antigorite phase. We also perform *post-mortem* electron microscopy analysis on recovered samples of interest to link our X-ray tomography observations to the plastic properties and/or deformation mechanism of the phases. Our results suggest that the total connectivity of the weak antigorite increases with the strain extent transferred to the samples, with antigorite minerals forming, in some cases, clear interconnected weak layers in agreement with IWL behaviour. The stronger olivine then shows localized lattice bending/rotation in clasts indicating local deformation accommodated by intracrystalline low-temperature plasticity.

Reference:

Handy, M., R., 1990. The solid-state flow of polymineralic rocks. *Journal of Geophysical Research* 95, 8647–8661.

## Al, Si interdiffusion in iron-free majoritic garnet: TEM of a polycrystalline diffusion couple

Nobuyoshi Miyajima<sup>1</sup>

<sup>1</sup> Bayerisches Geoinstitut, University of Bayreuth, 95440 Bayreuth, Germany

Atomic diffusion by vacancies of minerals at high pressures are important for the rheology of the Earth's mantle. Because those processes are controlled by moving of two agents (line and point defects) in deformations at high temperature, the post-mortem examination by analytical transmission electron microscope (TEM) is indispensable for evaluating those agents (carriers). Majoritic garnet (MajGt) and bridgmanite are major constituents in the mantle transition zone and the lower mantle, respectively. Diffusivity differences in these mantle minerals are very important to understand the changes of the nature of chemical heterogeneity, viscosity through those creep law, and other various transport properties across the upper and lower mantle boundary.

Here I report an Al = Si + Mg interdiffusion in iron-free MajGt, in comparison to those of Nishi et al. (2013) and van Mierlo et al. (2013) with iron and the other elements such as calcium and chromium. The diffusion couples in multi-anvil experiments are made of pre-synthetic polycrystalline  $\text{Mg}_3\text{Al}_2\text{Si}_3\text{O}_{12}$  pyrope (Prp) and majoritic garnet (Maj76Prp26). The  $2\text{Al} = \text{Mg} + \text{Si}$  interdiffusion between MajGt and Prp has been performed at 18.5 GPa and 1750 °C using a Kawai-type high pressure apparatus. The Al diffusion profiles were measured across the chemical interface by a scanning TEM equipped with energy-dispersive X-ray spectrometer (EDXS).

The effect of grain-boundary diffusion was visible in the EDXS chemical maps. The rate of the interdiffusion (volume diffusion) was determined to be a  $D_{\text{Al-Si}} = 6.2(4) \times 10^{-19}$  ( $\text{m}^2/\text{s}$ ) at 18.5 GPa and 1750 °C, which is almost the same as those of van Mierlo et al. (2013) but one order of magnitude higher than Nishi et al. (2013). The rate at 1750 °C is also comparable with those of Mg and Si self-diffusion coefficients in bridgmanite under lower mantle conditions (Xu et al., 2011).

### References:

- Nishi et al. (2013) *Earth. Planet. Sci. Lett.*, 361, 44
- van Mierlo et al. (2013) *Nat. Geosci.*, 6, 400
- Xu et al. (2011) *J. Geophys. Res.*, 116, B12205

## **A combined Raman spectroscopy and DSC study on the nanocrystal-free viscosity of volcanic melts.**

Paola Stabile<sup>1</sup>, Stefania Sicola<sup>2</sup>, Gabriele Giuli<sup>1</sup>, Eleonora Paris<sup>1</sup>, Michael R. Carroll<sup>1</sup>,  
Joachim Deubener<sup>3</sup>, Danilo Di Genova<sup>4</sup>

<sup>1</sup> School of Science and Technology, Geology Division, Camerino, Italy

<sup>2</sup> Department of Science, Roma Tre University, Rome, Italy

<sup>3</sup> Institute of Non-Metallic Materials, Clausthal University of Technology, Clausthal-Zellerfeld, Germany

<sup>4</sup> Bayerisches Geoinstitut, University of Bayreuth, 95440 Bayreuth, Germany

This study presents Raman spectroscopic and differential scanning calorimetry (DSC) data on nanocrystal-free peralkaline rhyolites with different  $\text{Fe}^{2+}/\text{Fe}_{\text{tot}}$  (0.15 – 0.84) and  $\text{Na}/(\text{Na}+\text{K})$  (0 – 1) (Stabile et al., 2021). Inspection of the low-wavenumber region and deconvolution of the high-wavenumber region of Raman spectra allows us to infer the structural changes occurring with varying iron oxidation state and molar alkali content, while the combination of Raman spectroscopy and DSC measurements allow the characterization of the anhydrous nanocrystal-free viscosity as a function of temperature.

A substantial increase of viscosity is observed with the increase of  $\text{Fe}_2\text{O}_3$  and  $\text{K}_2\text{O}$  content. For instance, we estimate that viscosity of anhydrous peralkaline rhyolites at the eruptive temperature of 750 °C (e.g., Di Carlo et al. 2010) can increase by 3.5 log units when  $\text{Fe}^{2+}/\text{Fe}_{\text{tot}}$  and  $\text{Na}/(\text{Na}+\text{K})$  ratios decrease contemporaneously from 0.84 to 0.15 and from 1 to 0, respectively.

The viscosity variation can be fully ascribed to changes in the amorphous structure of our samples, since we demonstrate that none of our samples changed iron oxidation state, nor underwent nano- crystallization during DSC measurements. Moreover, comparison between our viscosity data and literature suggests that the DSC-approach presented and adopted in this study (Di Genova et al. 2020) is independent of chemical composition and thus it can be used also to retrieve viscosity of nanocrystal-free melts.

This study has relevant implications for magma transport and for the quantification of nanostructure formation for magma viscosity modelling.

### References:

Di Carlo et al. (2010) *J. Petrol.*, 51, 2245–2276

Di Genova et al. (2020) *J. Non. Cryst. Solids* 545, 120248

Stabile et al., (2021) *Chem. Geol.*, 559, 119991

**EMPG – XVII****17th International Symposium on  
Experimental Mineralogy,  
Petrology and Geochemistry**

Abstracts

Theme 5 “Igneous petrology”

(sorted alphabetically by first author)

## A new Zr-Hf geothermometer for magmatic Zircon

Leonid Aranovich

Institute of Geology of Ore Deposits, Petrography, Mineralogy and Geochemistry RAS

Numerous geochemical data on granitoid magmatic series point to a systematic decrease in the whole rock Zr/Hf ratio from the least evolved to the most evolved members. Individual Zircon (*Zrn*) grains also often exhibit regular zoning with decreasing Zr/Hf from cores to rims, as well as grain-to-grain variations. New experimental data on the Zrn and Hafnon ( $\text{HfSiO}_4$ , *Hfn*) solubility in model silicate melts (*m*) in the temperature (*T*) range 1400-1200°C at 1 atm have been collected to address a problem of Zr-Hf partitioning between *Zrn* and melt. It was found that for each studied melt the solubility of both minerals decreases with decreasing *T* and for the melts with the same major elements composition the difference between the *Zrn* and *Hfn* solubility remains almost constant. The new data along with the experimental data on the partitioning of Zr and Hf between felsic melts and *Zrn*, and on the solubility of *Zrn* and *Hfn* in melts with variable *ASI* index have been used to derive an

equation of the Zr-Hf geothermometer:  $T = \frac{1614}{\ln K_d + 1.663}$ , with  $K_d = \frac{X_{Zr}^s X_{Hf}^m}{X_{Zr}^m X_{Hf}^s}$ , where  $X_j^i$  –

concentration of Zr and Hf in *Zrn* (*s*) and melt (*m*), ppm, and *T* – temperature, K. Constant concentration of Zr in *Zrn* of 480000 ppm is applied for temperature calculations. It is shown that the increase in the Hf content from cores to rims often documented in magmatic *Zrn* results from fractional crystallization of *Zrn* with preferential consumption of Zr from the melt. For differentiated granitoid series the temperature corresponding to the beginning of *Zrn* crystallization in the early (least evolved) cumulates should be estimated based on the composition of the central parts of large grains with the highest values of the Zr/Hf ratio. Application of the thermometer to mafic and intermediate rocks may be hampered due to co-crystallization of *Zrn* with oxides and Fe-Mg silicates with elevated Zr and Hf content. The new geothermometer has some advantages over those based on zircon saturation index (Watson, Harrison, 1983; Boehnke et al., 2013) and on Ti in Zrn (Ferry, Watson, 2007), as it does not depend on major oxides composition of the melts and on the correct estimates of the  $\text{SiO}_2$  and  $\text{TiO}_2$  activities. Calculations of the Zr and Hf fractionation trends assuming Rayleigh fractionation allow estimating the temperature at which separation of the more evolved melt portion(s) from the parental magma chamber has occurred.

*This work was supported by RNF grant 18-17-00126*

Boehnke P., Watson E.B., Trail D., et al. Zircon saturation re-visited. // Chem. Geol. 2013. V. 351. P. 324–334.

Ferry J.M., Watson E.B. New thermodynamic models and revised calibrations for the Ti-in-zircon and Zr-in-rutile thermometers // Contrib. Mineral. Petrol. 2007. V. 154. P. 429–437.

Watson E.B., Harrison T.M. Zircon saturation revisited: temperature and composition effects in a variety of crustal magma types // Earth Planet. Sci. Lett. 1983. V. 64. P. 295-304.

### References:

Asdf et al., (2006) Am. Mineral., 91,435440

## Rutile solubility and TiO<sub>2</sub> activity in silicate melts: an experimental study

Leonid Aranovich<sup>1</sup>, Alexander Borisov<sup>1</sup>

<sup>1</sup>Institute of Geology and Ore Deposits, Petrography, Mineralogy and Geochemistry, RAS

Experiments on rutile solubility in synthetic silicate melts of a wide range of compositions have been conducted at ambient pressure at temperature (T) from 1230 - 1500°C. The results support the previous findings, namely: (1) at fixed T addition of silica and alumina results in essential decrease of rutile solubility; (2) at fixed composition increasing T results in essential increase in rutile solubility. New equations describing rutile solubility in silicate melts as a function of T, pressure and melt composition, both empirical and consistent with the thermodynamic model of Melts (Ghiorso and Sack, 1995), are derived based on the new and literature experimental data. The new equations predict  $\log X_{\text{TiO}_2}$  (TiO<sub>2</sub> mole fraction) in melts with a standard error of 0.067, which is equivalent to ca 15% error, in a wide range of melts major element composition and the  $X_{\text{TiO}_2}$  value in the range from 0.0008 to 0.39 covered by the experiments. The new equations are applied to calculate the TiO<sub>2</sub> activity values relative to Rutile saturation ( $a_{\text{TiO}_2}$ , m/rut) in a variety of well documented natural magmatic rocks. The resulting ( $a_{\text{TiO}_2}$ , m/rut) values for different tested samples vary from 0.1 to close to 1. Simultaneously solving the new equations and the equation for Ti-in Zircon geothermometer (Ferry and Watson, 2007) gives much more reliable T estimates than those based on the assumption of constant  $a_{\text{TiO}_2}$ , m/rut = 0.6 or 1.

*This work was supported by RNF 18-17-00126.*

Ghiorso M.S., Sack R.O. (1995). *Contrib Mineral Petrol* 119:197–212  
Ferry J.M., Watson E.B. (2007). *Contrib Mineral Petrol* 154:429–437

## Superheating and cooling rates effects on olivine growth in chondritic liquid: experimental and petrographic approach

Marion Auxerre<sup>1</sup>, François Faure<sup>1</sup>, Delphine Lequin<sup>1</sup>

<sup>1</sup> Université de Lorraine, CNRS, UMR 7358 Centre de Recherches Pétrographiques et Géochimiques, 15 rue Notre-Dame des Pauvres, 54500 Vandœuvre-Lès-Nancy, France

Chondrules - major constituent of chondrites (primitive meteorites) - belong to the first object formed in the solar system. They are millimetre-sized igneous objects resulting from partial to complete fusion and are divided into main families: non-porphyritic and porphyritic (Gooding and Keil, 1981); the latter one is more abundant in chondrites. This study aims to reproduce thermal histories of macro-porphyritic olivine chondrules (PO) and to better constrain (thermal, temporal) the conditions reigning in the early solar system.

In general, PO chondrules are composed of numerous euhedral crystals of olivine and/or pyroxene suggesting an initially melting below their liquidus temperatures. By contrast, in our study, the macro-porphyritic olivine chondrule displays only one large euhedral olivine. The low number of olivine crystals indicates that chondrule suffered an initial step of superheating, limiting nucleation process (Lofgren, 1988; Hewins et al., 1988). Moreover, embayments observed in euhedral olivine show that olivine crystal began to grow rapidly and then the growth-rate decreased during the cooling. Therefore, our petrographic investigation proposes a first high temperature stage ( $\Delta T_{\text{liq}} = +10$  °C) followed by a slow cooling.

To test this thermal history, experiments are performed to determine degree of superheating and cooling rate effect (i) on nucleation rate and (ii) on morphology of olivines formed during cooling. Preliminary results seem to confirm that macro-porphyritic olivine chondrules result from the slow cooling of a superheated initial chondritic liquid (Varela et al., 2006). Then these results allow to precise the beginning of the igneous processes (minimum thermal temperature and cooling rate) and to discuss the complete thermal evolution of the chondrule, by considering all other reaction textures observed in this chondrule: peritectic and oxidation reactions, quench texture and aqueous alteration.

### References:

- Gooding et al., (1981) *Meteoritics*, 16, No. 1
- Hewins et al., (1988) *Meteoritics*, 25, 309-318
- Lofgren, (1988) *Geochim. & Cosmochim. Acta*, 50, 1715-1726
- Varela et al., (2006) *Icarus*, 178 (2), 553–569.

## Experimental dehydration of natural serpentinite

Nathalie Bolfan-Casanova<sup>1</sup>, Paul Chauvigne<sup>1</sup>, Juliette Maurice<sup>1</sup>, Sylvie Demouchy<sup>2</sup>, Federica Schiavi<sup>1</sup>, Baptiste Debret<sup>3</sup>

<sup>1</sup>Laboratoire Magmas et Volcans, Université Clermont Auvergne, CNRS, IRD, OPGC, 63000 Clermont-Ferrand, France

<sup>2</sup>Geosciences Montpellier, France

<sup>3</sup>now at IPGP, France

Antigorite is considered as the most important source of water in subduction zones, playing a key role during arc magma genesis. Although, these magmas seem more oxidized than mid-oceanic ridge basalts (MORB), the possible inherent link between the oxidation state of arc magmas and serpentinite-derived hydrous fluids is still not well established. Here, we have performed dehydration experiments of natural antigorite serpentinite containing 5 wt. % magnetite at 3 GPa and at temperatures from 600 to 900 °C using a multi-anvil apparatus. These experiments aim to reproduce the different stages of H<sub>2</sub>O release, forming secondary antigorite, chlorite, olivine and orthopyroxene and water as observed in nature. Our study aims at characterizing the  $f_{O_2}$  under which the fluids that form upon antigorite dehydration equilibrate.

## Trace element distribution in mantle clinopyroxene by melt-peridotite reaction: experiments up to 2 GPa

Giulio Borghini<sup>1</sup>, Patrizia Fumagalli<sup>1</sup>, Stephan Klemme<sup>2</sup>, Elisabetta Rampone<sup>3</sup>

<sup>1</sup> Dipartimento di Scienze della Terra "Ardito Desio", Università di Milano, Italy

<sup>2</sup> Westfälische Wilhelms Universität Munster, Munster, Germany

<sup>3</sup> Dipartimento di Scienze della Terra, Ambiente e Vita (DISTAV), Università di Genova, Italy

Deep melt infiltration into peridotite induces melt-rock reactions that may strongly affect the mineralogy and chemistry of the upper mantle. The interaction of interstitial melts percolating via reactive porous flow within mantle peridotite modifies the major and trace element composition of clinopyroxene (Borghini et al., 2019). In particular, the chemical exchange can reset the trace element (e.g. REEs) composition of clinopyroxene modifying its chemical and, over time, isotopic signature (Borghini et al., 2013). In order to unravel the efficiency of melt-rock reactions in resetting the composition of mantle clinopyroxene, we carried out piston cylinder experiments at conditions of the lithosphere-asthenosphere boundary. A mixture of natural mantle clinopyroxene and San Carlos olivine (Fo<sub>90</sub>) is used to model the peridotite matrix. Mantle minerals are mixed with a natural tholeiitic glass having a relatively low X<sub>Mg</sub> (X<sub>Mg</sub> = Mg/(Mg+Fe<sub>tot</sub>) = 0.60), high alkali contents (Na<sub>2</sub>O = 3.48 wt%, K<sub>2</sub>O = 0.81 wt%) and enriched-MORB signature (La<sub>N</sub>/Yb<sub>N</sub> = 5.49).

Reaction experiments have been performed at 1300 and 1350°C, 1.5 and 2.0 GPa, on basalt:clinopyroxene:olivine mixtures in proportions 2:1:1 and 1:1:1. All runs produced chemical and textural evidence of reaction glass<sub>1</sub> + cpx<sub>1</sub> + ol<sub>1</sub> = glass<sub>2</sub> + cpx<sub>2</sub> + ol<sub>2</sub>. The new olivine is chemically homogeneous and shows slightly lower X<sub>Mg</sub> and higher Ca content with respect to the starting San Carlos olivine. Clinopyroxene consists of large relicts preserving the composition of the starting material. Newly crystallized clinopyroxenes occur as rather large (80-150 μm) reacted rims or new grains. Modified clinopyroxenes display lower X<sub>Mg</sub>, Cr, Ca and higher Al, Na contents than the unreacted clinopyroxenes. At fixed starting glass amount, at 1300°C, the remaining reacted melt fraction is significantly lower as compared with runs at 1350°C, suggesting melt-consuming reactions.

In-situ laser ablation analyses reveal that clinopyroxene is modified in terms of trace element composition. Few relicts still preserve the original REE spectra, characterized by LREE depletion (La<sub>N</sub>/Sm<sub>N</sub> = 0.55-0.61). Newly crystallized clinopyroxenes show REE patterns with variable LREE enrichment and lower HREE abundances with respect to the starting clinopyroxene. The highest LREE enrichment in clinopyroxene (La<sub>N</sub>/Sm<sub>N</sub> = 0.93) are generated at high crystallization rate in melt-consuming reaction experiment at 1300°C. At higher temperature (1350°C) and using higher proportions of initial glass (2:1:1), reacted melt has higher X<sub>Mg</sub> and lower CaO, Al<sub>2</sub>O<sub>3</sub>, Na<sub>2</sub>O and REE contents than the starting glass suggesting that the reaction mostly results in olivine dissolution. New experimental results indicate that melt-peridotite interaction induces a rapid redistribution of major and trace elements in mantle minerals.

### References:

Borghini et al., (2013) *Geology*, 41, 1055-1058.

Borghini et al., (2019) *Chem. Geol.*, 532, 119252.

## Melting of pargasite-bearing pyroxenites in the presence of apatite at 1.0-2.0 GPa: Implications on the origin of sanukitoids

Antonio Castro<sup>1</sup>, Daniel Gómez-Frutos<sup>1</sup>

<sup>1</sup> Institute of Geosciences (IGEO), Consejo Superior de Investigaciones Científicas—Universidad Complutense de Madrid, Ciudad Universitaria, 28040 Madrid, Spain.

<sup>2</sup> Departamento de Mineralogía y Petrología. Universidad Complutense de Madrid, Ciudad Universitaria, 28040 Madrid, Spain.

Sanukitoids (=vaugnerites) are K-rich, Mg-rich intermediate ( $\text{SiO}_2 > 53$  wt%) magmatic rocks that, although forming small intrusions in the upper crust, are widely represented in post-collisional and cordilleran-type batholiths, with which they are associated in space and time. This association leads to a largely debated topic: The role of a pargasite-bearing metasomatized mantle in the generation of sanukitoids (Fowler and Rollinson, 2012; Castro, 2019). The high enrichment in incompatible elements is not compatible with the sole participation of pargasitic amphibole in the source region. An additional metasomatic agent is required to account for the observed features. We propose that this agent can be found in apatite (Ap). Based on the petrology of Prg-bearing xenoliths in lavas of the Olot (NE Spain) volcanoes, we made mineral compounds that are used as starting materials in our experiments at 1.0 to 2.0 GPa and 1000 to 1200 °C. Two sets of experiments were made: (1) an Ap-doped compound and (2) an Ap-free compound. Prg and Cpx were the essential phases of both compounds. Experiments were performed in a Boyd-England Piston-Cylinder apparatus using a double capsule (Au-Pd in Pt) arrangement to prevent changes in oxidizing conditions and minimize Fe loss towards the capsule. Our study shows that Ap-doped runs are much more fertile compared with the Ap-free runs at the same conditions of pressure and temperature. In the absence of Ap, a Prg-bearing pyroxenite produces traces (<1 wt%) of melt. Whereas in the Ap-bearing runs, the obtained melt fractions are 6.8 wt% at 1.5 GPa and 20.6 wt% at 1.0 GPa. The melts formed at 1.5 GPa are very similar to common sanukitoids. We demonstrate that Ap has a strong control by increasing the melt fraction in the source. It is envisaged that apatite is also involved in the supply of incompatible elements that characterize sanukitoid rocks.

### References:

- Castro, A. (2019), The dual origin of I-type granites: The contribution from laboratory experiments, in *Post-Archean Granitic Rocks: Petrogenetic Processes and Tectonic Environments*, edited by V. Janoušek, B. Bonin, W. J. Collins, F. Farina and P.-. Bowden, Geological Society, London, Special Publications, doi: <https://doi.org/10.1144/SP491-2018-110>.
- Fowler, M., and H. Rollinson (2012), Phanerozoic sanukitoids from Caledonian Scotland: Implications for Archean subduction, *Geology*, *40*, 1079-1082, doi:10.1130/G33371.1

## Dissolution reactions of loparite and eudyalite and the solubility of Nb and Zr in carbonatitic melt

Dmitry Chebotarev<sup>1,2</sup>, Ilya V. Veksler<sup>1,3,4</sup>, Cora Wohlgemuth-Ueberwasser<sup>3</sup>

<sup>1</sup> V.S. Sobolev Institute of Geology and Mineralogy SB RAS, prosp.Akad. Koptyuga, 3, Novosibirsk 630090, Russia

<sup>2</sup> Geological Institute, Kola Science Centre, Russian Academy of Sciences, 14, Fersmana Street, 184209 Apatity, Russia

<sup>3</sup> Helmholtz Centre Potsdam – German Research Centre for Geosciences GFZ, Telegrafenberg, 14473 Potsdam, German

<sup>4</sup> University of Potsdam, Institute of Geosciences, Karl-Liebknecht-Str. 24-25, 14476 Potsdam-Golm, Germany

The largest deposits of REE and Nb, and economically significant Zr mineralization reside in carbonatites. However, experimental studies of silicate-carbonate liquid immiscibility showed that Zr and Nb concentrated in silicate melt and not in the conjugate carbonatite (Martin et al., 2012; Veksler et al., 2012). Mechanisms for the Nb enrichment in carbonatite magmas are further obscured by contradictory experimental data on the solubility of Nb in carbonatitic melt. On one hand, the solubility of Nb in the system  $\text{CaCO}_3\text{--Ca(OH)}_2$  was estimated at 5–7.5 wt.%  $\text{Nb}_2\text{O}_5$  (Jago and Gittins, 1993) and it was about 10 times less in melts with the  $\text{Na}_2\text{CO}_3$  component. On the other hand, much higher concentrations (14 and 48 wt.%  $\text{Nb}_2\text{O}_5$ ) were found in melts of the  $\text{CaCO}_3\text{--CaF}_2\text{--NaNbO}_3$  and  $\text{CaCO}_3\text{--Ca(OH)}_2\text{--NaNbO}_3$  systems by Mitchell and Kjarsgaard (2002, 2004).

In order to get estimations of the Nb and Zr solubility in multicomponent carbonatite which are more realistic for natural magma we studied dissolution reactions of natural loparite  $(\text{Na,Ca,REE})(\text{Ti,Nb})\text{O}_3$  and eudialyte  $\text{Na}_{15}\text{Ca}_6(\text{Fe,Mn})_3\text{Zr}_3[\text{Si}_{25}\text{O}_{73}](\text{OH,Cl})_5$  in synthetic carbonatite melt analogous to the immiscible liquid in equilibrium with nephelinite produced in experiments by Kjarsgaard (1998). Our experiments were carried out at 100 MPa and 850 °C in cold-seal rapid-quench pressure vessels. Run products were analyzed by electron microprobe and LA ICP-MS. Reaction of loparite crystals with the melt resulted in the formation of rims depleted (by half) in REE and Na, enriched in Ca and Ti, and with Nb concentrations practically unchanged. The melt crystallized wollastonite and calcite, and contained 100-150 ppm Nb. Eudialyte partly decomposed to wollastonite and Zr-silicates of Ca (presumably baghdadite) or Na (parakeldyshite). The latter formed in runs with a higher eudialyte to melt mass ratio in the starting charges. Zr concentrations in the melt varied between 86 and 104 ppm. Melts that reacted with both minerals contained about 400-500 ppm Ti. Our results imply very low solubilities of high field strength elements (HFSE) with values for Nb almost an order of magnitude lower than the lowest estimations reported by Jago and Gittins (1993). If it is true that carbonatite melts have no capacity to carry large amounts of HFSE, the formation of Nb and Zr deposits in carbonatites becomes even more enigmatic.

This work was supported by RSF grant No. 19-17-00013.

### References:

- Jago, B. and Gittins, J. (1993) *S. Afr. J. Geol.*, 96(3), 149-159  
 Kjarsgaard, B. (1998) *J. Petrol.*, 39, 2016-2076.  
 Martin, L.H.J. et al. (2012) *Chem. Geol.*, 320-321, 96-112  
 Mitchell, R. and Kjarsgaard, B. (2002) *Contrib. Mineral. Petrol.*, 144, 93–97  
 Mitchell, R. and Kjarsgaard, B. (2004) *Contrib. Mineral. Petrol.*, 148, 281-287  
 Veksler, I.V. et al. (2012) *Geochim. Cosmochim. Acta.*, 79, 20-40

## The solubility of N<sub>2</sub> in silicate melts

Laura Cialdella<sup>1</sup>, Michael Wiedenbeck<sup>2</sup>, Hans Keppler<sup>1</sup>

<sup>1</sup> Bayerisches Geoinstitut, Universität Bayreuth, 95440 Bayreuth, Germany

<sup>2</sup> GFZ German Research Centre for Geosciences, 14473 Potsdam, Germany

Compared to the chondritic abundance pattern, nitrogen appears to be depleted in the bulk Earth by more than one order of magnitude if compared to the other major volatiles<sup>1</sup>. Whether this depletion is real, however, very strongly depends on the estimated bulk nitrogen abundance in the mantle. Some data, particularly from mantle xenoliths, suggest that there may be a deep, nitrogen-rich mantle reservoir. Moreover, the flux of nitrogen into the mantle by subduction has been found to be three times larger than the outgassing flux<sup>2</sup>. This could be consistent with a deep nitrogen reservoir residing within the Earth's interior. Previous experiments carried out at Bayerisches Geoinstitut have shown that mantle minerals may store more than 53 times more nitrogen than presently resides in the atmosphere<sup>3,4</sup>.

Controversies exist about the nitrogen subduction efficiency. The ingassing and outgassing processes are affected by the nitrogen solubility in melts and by the nitrogen partitioning between melts and minerals. We therefore studied the solubility of N<sub>2</sub> at oxygen fugacity conditions realistic for subduction zones ( $fO_2 > Ni-NiO$ ), at 1 – 30 kbar and 1000 – 1550 °C. Starting materials were glasses with a haplogranitic and a MORB composition. Experiments were carried out up to 5 kbar in cold-seal TZM vessel or an internally-heated vessel, up to 30 kbar in a piston-cylinder apparatus. As source of nitrogen Ag<sup>15</sup>N<sub>3</sub> was used. The samples were analysed with the Cameca 1280-HR SIMS at GFZ Potsdam using ion-implanted glasses and crystals as reference material. The results show that nitrogen solubility increases nearly linearly with pressure up to 30 kbar. Increasing temperature decreases solubility, at least at low pressures. The solubility is consistently higher in the haplogranitic melt, as expected from its higher ionic porosity. By slow cooling of the MORB melt from high temperature, crystals of olivine, plagioclase, orthopyroxene, clinopyroxene, and garnet were grown and the partition coefficients of nitrogen between these phases and the residual melt was quantified. Partition coefficients are typically  $< 10^{-3}$ , implying very efficient outgassing of nitrogen under relatively oxidizing conditions. Further experiment under reducing conditions are expected to yield higher solubilities and mineral/melt partition coefficients.

### References:

1. Marty, B. The origins and concentrations of water, carbon, nitrogen and noble gases on Earth. *Earth Planet. Sci. Lett.* (2012). doi:10.1016/j.epsl.2011.10.040
2. Johnson, B. & Goldblatt, C. The nitrogen budget of Earth. *Earth-Science Rev.* **148**, 150–173 (2015).
3. Yoshioka, T., Wiedenbeck, M., Shcheka, S. & Keppler, H. Nitrogen solubility in the deep mantle and the origin of Earth's primordial nitrogen budget. *Earth Planet. Sci. Lett.* **488**, 134–143 (2018).
4. Li, Y., Wiedenbeck, M., Shcheka, S. & Keppler, H. Nitrogen solubility in upper mantle minerals. *Earth Planet. Sci. Lett.* **377–378**, 311–323 (2013).

## Assimilation of Xenocrystic Apatite in Granite Magmas

D. Barrie Clarke<sup>1</sup>, Daniel Harlov<sup>2</sup>, Anne Jähkel<sup>3</sup>, Sarah B. Cichy<sup>4</sup>, Franziska Wilke<sup>5</sup>, Xiang Yang<sup>6</sup>

<sup>1</sup> Department of Earth and Environmental Sciences, Dalhousie University, Halifax, NS, Canada B3H 4R2

<sup>2</sup> Section 3.6, GeoForschungsZentrum GFZ, Telegrafenberg, 14473 Potsdam, Germany

<sup>3</sup> Departments of Hydrogeology / Aquatic Ecosystem Analysis, Helmholtz Centre for Environmental Research – UFZ, Magdeburg, Germany

<sup>4</sup> Institute of Geosciences, University of Potsdam, Germany; now at Bundesgesellschaft f. Endlagerung mbH, Peine, Germany

<sup>5</sup> Section 3.1, GeoForschungsZentrum GFZ, Telegrafenberg, 14473 Potsdam, Germany

<sup>6</sup> Department of Geology, St. Mary's University, Halifax, NS, Canada B3H 3C3

Apatite is a ubiquitous phase in granite plutons and in most adjacent country rocks, thus contamination of a granite magma with wall-rock xenoliths results in two genetic types of apatite in the magma: cognate and foreign. These two textural and chemical varieties of apatite undergo textural and compositional changes to reach physical and chemical equilibrium (perfect assimilation) in the melt. Our experiments replicate the conditions in such contaminated granites.

The starting materials consist of a peraluminous synthetic  $\text{SiO}_2\text{-Al}_2\text{O}_3\text{-Na}_2\text{O-K}_2\text{O}$  (SANK) granite gel with A/NK of 1.3, synthetic F-apatite, synthetic Cl-apatite, and natural Durango apatite. Our initial experiments in cold-seal hydrothermal pressure vessels at realistic temperatures of 750°C and pressures of 200 MPa produced negligible reactions, even after run times of 6 months. Instead, we used an argon-pressurized internally heated pressure vessel with a rapid-quench setup at temperatures of 1200°C, pressures of 200 MPa, and run durations of 8 days. An advantage of this high temperature is that it exceeds the liquidus for quartz and feldspar, and therefore apatite is the only solid phase in the run products. The starting composition of each run was 90 wt.% SANK granite gel and 10 wt.% crushed apatite (consisting of one, two, or three varieties), with and without 4 wt.% added water. Run products were examined by SEM for texture and by EMPA for composition. The synthetic granite composition contains no Ca, F, Cl, or REEs thus, in every run, apatite was initially undersaturated in the melt. In all experiments, most large apatite grains consisted of anhedral shards with rounded corners, most small apatite grains were round, and a small proportion of apatite grains developed one or more crystal faces. In experiments with two or three apatite compositions, the run-product grains had compositions intermediate between those of the starting-material grains, and they were homogeneous with respect to Cl, and probably F, but not with respect to REEs.

The processes to reach textural equilibrium consist of dissolution until the melt is saturated in apatite, followed by Ostwald ripening to eliminate small grains and to develop crystal faces on larger ones. The processes to reach chemical equilibrium consist of dissolution of apatite, diffusion of cations (Ca, P, REE) and anions (F, Cl, OH) through the silicate melt, and solid-state diffusion in the undissolved apatite grains. The halogens approached chemical equilibrium in all experiments, but in the experiments containing Durango apatite, the REEs have not. We conclude that the rate of chemical equilibrium for the halogens is greater than that for the REEs, and is also greater than the rate to achieve textural equilibrium. The hypothetical ultimate equilibrium state of assimilation in all experiments should ideally consist of one homogeneous euhedral apatite grain in a quenched SANK granite glass.

## Partial melting of planetesimals: implications for the formation of primitive achondrites and trachyandesite achondrites

Max Collinet<sup>1,\*</sup> Timothy L. Grove<sup>1</sup>

<sup>1</sup>Massachusetts Institute of Technology, Department of Earth, Atmospheric, and Planetary Sciences, 77 Massachusetts avenue, MA 02139, USA.

\* current affiliation: German Aerospace Center (DLR), Institute of Planetary Research, Rutherfordstraße 2, 12489 Berlin, Germany. E-Mail: max.collinet@dlr.de.

We have performed melting experiments of ordinary and carbonaceous synthetic chondrites (H, LL, CI, CM and CV) in an externally heated Molybdenum Hafnium Carbide pressure vessel at 1060-1300 °C, low pressure (2-13 MPa) and under reducing conditions ( $\log fO_2 = -1$  to  $-2.5 \Delta IW$ ). Those experiments highlight the role of alkali elements on the melting processes of chondritic planetesimals. Alkali-rich compositions (CI, H and LL) start to melt at low temperature (1040 °C) and produce silicate melts with high alkali, SiO<sub>2</sub> and Al<sub>2</sub>O<sub>3</sub> contents, similar in composition to “trachyandesite achondrites” such as GRA 06128 (Shearer et al., 2008) and ALM-A (Bischoff et al., 2014). Alkali-poor compositions (CM and CV) melt at higher temperature (1090-1120 °C) and produce melts that are basaltic to andesitic in composition.

Several groups of meteorites are derived from the mantle of partially differentiated planetesimals and are known in the meteorite record as “primitive achondrites” (brachinites, acapulcoites-lodranites and ureilites). Our experiments show that the parent bodies of primitive achondrites and all planetesimals thought to have accreted in the inner solar system were not depleted in alkali elements relative to the sun’s photosphere. The depletion of alkalis in other parent bodies (e.g. Vesta) resulted from processes that occurred during partial melting rather than from the incomplete condensation of the solar nebula.

Low-degree melts (<15 wt.%) rich in SiO<sub>2</sub>, Al<sub>2</sub>O<sub>3</sub> and alkalis were mobilized and extracted from the mantle of numerous planetesimals. Ureilites, the second most abundant group of achondrites with >550 samples, represent the mantle of such a planetesimal. The Ureilite Parent Body (UPB) was catastrophically disrupted, which enabled rapid cooling of ureilites and quenching of their high-temperature equilibrium state. Our experiments show that the UPB produced a total of 16-24 wt.% melt as small increments (< 5%). The last melts extracted were CaO-rich and alkali-poor. Melting likely stopped due to the near-complete removal of the heat source (<sup>26</sup>Al), quarried away by the melt. The UPB reached high temperatures (up to 1300 °C) but rapid extraction of a silicate melt preserved primordial heterogeneities in O, C and Cr isotopes as well as in intrinsic  $fO_2$ .

### References:

- Bischoff et al., (2014) PNAS, 111, 12689–12692.  
Shearer et al., (2008) Am. Mineral., 93, 1937-1940.

## Diamond dissolution experiments and role of volatiles in kimberlite emplacement

Yana Fedortchouk<sup>1</sup>

<sup>1</sup> Department of Earth and Environmental Sciences, Dalhousie University, Halifax, Canada B3H 4R2

Kimberlites, the deepest mantle magmas reaching the surface of the Earth, are important source of information about the processes in the subcratonic mantle. The origin and composition of kimberlite melt are still poorly understood due to the complex features and significant alteration of kimberlites. Many lines of evidence indicate that high content of volatiles drives the fast ascent of kimberlite magma from the depths > 200 km to the surfaces. However, content, H<sub>2</sub>O:CO<sub>2</sub> ratio and exsolution depth of kimberlitic fluid are poorly constrained due to an ambiguous origin of hydrous and carbonate minerals in kimberlites and volatile loss during the eruption. Diamond xenocrysts transported by kimberlite magmas from their mantle source develop a range of dissolution features due to their reaction with kimberlite magma. This study uses the morphology of dissolution features on diamonds to investigate emplacement conditions of different diamond-bearing kimberlites. Diamond dissolution experiments examined the role of individual factors in the geometry of diamond dissolution features. The results were applied to the natural diamonds selected from different kimberlite lithologies and types as well as different depths within kimberlite pipes in order to reconstruct their emplacement conditions.

Experiments conducted in piston-cylinder apparatus at 1 – 3 GPa and 1150 – 1350°C in a range of synthetic melts and H<sub>2</sub>O-CO<sub>2</sub> fluids demonstrated that diamond dissolution in volatile-undersaturated melts produced dissolution features distinct from those developed in the presence of a free C-O-H fluid. The former features are common on natural diamonds from magmatic (hypabyssal) kimberlites and the latter are typical for diamonds from various volcanoclastic (pyroclastic) facies. Experiments also showed that kimberlitic diamonds undergo dissolution in fluid with at least 10 mol% H<sub>2</sub>O ( $X_{CO_2} = CO_2 / (CO_2 + H_2O)$ , mol% <0.9) and features produced in experiments with fluid containing > 90 mol% CO<sub>2</sub> are absent on natural diamonds. Examination of the geometry of diamond dissolution features with Atomic Force Microscope (AFM) allowed to identify parameters of dissolution features indicative of the fluid with  $X_{CO_2} > 0.5$  and <0.5. Both types occur on natural diamonds and show an association with the presence of hydrous and carbonate magmatic minerals in different kimberlite bodies.

These results demonstrate that dissolution features on diamonds are robust proxy of the presence and composition of magmatic fluid in kimberlite magma. Diamonds from volcanoclastic kimberlite facies in different localities record a range of  $X_{CO_2}$  of kimberlitic fluid indicating different depth of fluid exsolution that may explain the differences in the emplacement mechanism of these kimberlites. Dissolution features on diamonds from hypabyssal facies are different in the three kimberlite classes, which suggests variation in the composition of melt forming the three kimberlite classes. The ongoing experiments examine diamond dissolution morphology in volatile-undersaturated melts to constrain the composition of melt forming different kimberlite types.

## Partial melting of hydrous pyroxenites in the cratonic mantle

Stephen F. Foley

*Dept. of Earth and Environmental Sciences and ARC Centre of Excellence for Core to Crust Fluid Systems, Macquarie University, North Ryde, New South Wales 2109, Australia*

Volatile-rich incipient melts of the upper mantle commonly do not reach the Earth's surface, but solidify within the mantle to form either reacted (metasomatised) rocks or discrete veins and dykes that are rich in hydrous minerals because of the incompatibility of water during melting. In the cratonic lithosphere many form rocks with several minerals of the MARID series (mica, amphibole, rutile, ilmenite, diopside), which are types of hydrous pyroxenite. Second-stage melts of such rocks will form components of magmas seen at the surface, but their compositions are very poorly constrained by experiments. Experiments on the melting of hydrous pyroxenite are rare, as most attention has been directed to dry pyroxenites involved in the deep recycling of ocean crust.

I report here on partial melting experiments at 1.5 and 5 GPa on MARID-like natural mineral mixtures containing a third each of phlogopite (PHL), clinopyroxene (CPX), and potassic richterite (KR), in some cases with 5% of ilmenite, rutile or apatite added. This embodies a re-assessment and partly re-analysis of a full set of >50 experiments for which only a select few have been published previously<sup>1</sup>. Melt compositions were measured in melt traps made up of vitreous carbon spheres, which enabled rigorous and well-constrained melt compositions to be derived. Equilibrium compositions are demonstrated by reversal experiments in which the melt compositions from the traps were run as separate experiments at the same temperature and pressure, producing the same mineral assemblage apart from the identity of titanate minerals.

Temperature series of up to 8 experiments at 1.5 GPa allow progressive melting to be tracked. Low-degree melts of PHL+CPX+KR are broadly lamproitic, with high SiO<sub>2</sub> (53.5-56 wt%) and K<sub>2</sub>O (11-13.5%) and low Al<sub>2</sub>O<sub>3</sub> (<6%) and CaO (<4%) contents. The addition of 5% accessory phases does not greatly affect melting temperatures, but melt compositions are strongly influenced (e.g. 11wt% TiO<sub>2</sub> with rutile; 6-10% TiO<sub>2</sub> with ilmenite; 7-8% P<sub>2</sub>O<sub>5</sub> with apatite). Melts at 5 GPa are richer in MgO (16-18%) and poorer in SiO<sub>2</sub> (<50%) and Na<sub>2</sub>O (<1.8%), resembling olivine lamproites.

Trace element patterns of melts from the 3-mineral mixture are considerably less enriched than natural lamproites (e.g. Sr 1750±70 ppm but La <15ppm). Only with a titanate mineral and apatite also in the source do the trace element patterns resemble those of lamproites, indicating an essential role for accessory phases.

### References:

<sup>1</sup> Foley, S.F., Musselwhite, D.S., van der Laan, S.R. (1999) Proceedings of the Cape Town Kimberlite Conference, Red Roof Publishers, Cape Town, J.B. Dawson volume, pp. 238-246.

## The role of melt/olivine ratio in dissolution and reactive crystallization: an experimental study at 0.5 GPa

Michela Grammatica\*<sup>1</sup>, Patrizia Fumagalli<sup>1</sup>, Giulio Borghini<sup>1</sup>

<sup>1</sup> Dipartimento di Scienze della Terra "Ardito Desio", Università degli Studi di Milano, Italy

Microstructural and geochemical evidence have emphasized that melt-rock reactions play an important role in the origin of gabbroic rocks in the lower oceanic crust. It is widely accepted that olivine-rich rocks might form through dunite infiltration followed by reactive crystallization of interstitial melts. Experiments on the origin of olivine-rich troctolites through basalt-dunite interactions suggested that the melt/olivine ratio plays an important role (Borghini et al., 2018). In this study, we aim to experimentally quantify the effect of the melt/olivine ratio on dissolution and reactive crystallization processes. We performed piston cylinder experiments at 0.5 GPa on San Carlos olivine (Fo<sub>90</sub>) variably mixed to MORB-type glass (10, 25 and 50 wt%). We performed both isothermal runs at 1300°C, lasted 24 hours, and step-cooled runs carried out by lowering the temperature from the isothermal dwell at 1300°C down to 1100°C at 1°C/min.

Run products of isothermal experiments consist of olivine and glass. Texturally we distinguish two generations of olivine: i) large subhedral crystals (~ 50 µm) with both straight and lobate rims and ii) smaller (5-20 µm) rounded grains. At increasing initial melt amount (from 25 to 50 wt%), olivine grain size increases (up to ~ 80 µm) and the amount of smaller rounded grain decreases. Relatively high initial melt/olivine ratio enhanced the reaction promoting olivine crystal growth and dissolution resulting in higher olivine tortuosity. Olivine X<sub>Mg</sub> increases from 0.91 to 0.92 at initial melt amount increasing (from 25 to 50 wt%). NiO content decreases via reaction with initial melt as a function of the melt/olivine ratio. Reacted glass records higher X<sub>Mg</sub> and NiO contents and lower Na<sub>2</sub>O, CaO and Al<sub>2</sub>O<sub>3</sub> abundances. Mass-balance calculations support an increase of olivine dissolution at increasing initial melt fraction.

When a cooling path is followed and the temperature is lowered down to 1100°C, run products, in starting mixture with 25 wt% of melt, consist of olivine, glass and interstitial clinopyroxene. Crystallization of reacted melt leads to the early appearance of clinopyroxene as compared with plagioclase. This results from the decrease of melt MgO (7.6 ± 0.4 wt%) via olivine crystallization promoting early clinopyroxene crystallization. Raman spectroscopy has revealed H<sub>2</sub>O dissolution in experimental glass, suggesting that experimental conditions are not perfectly dry, but nominally anhydrous conditions. This could further inhibit the crystallization of plagioclase (Husen et al., 2016). After cooling, olivine X<sub>Mg</sub> is similar (X<sub>Mg</sub> = 0.91) to its analogue isothermal experiment. Clinopyroxene crystallizing from the reacted melt shows high X<sub>Mg</sub> (0.91) and Al<sub>2</sub>O<sub>3</sub> content (7.5 ± 1.5 wt%). Experimental results provide new insights on the origin of primitive gabbros at the base of the oceanic crust.

### References:

- Borghini et al., (2018) *Lithos*, 323, 44-57.  
Husen et al., (2016) *J. Petrol.* 57, 309-344.

## Experimental study on partial melting of lherzolite + kaersutite-rich metasome at 1-4 GPa

Tobias Grützner<sup>1,2</sup>, Dejan Prelević<sup>3,4</sup>, Yannick Bussweiler<sup>2</sup>, Jasper Berndt<sup>2</sup>

<sup>1</sup>Sorbonne Université– IMPMC, Paris, France.

<sup>2</sup>University of Münster – Institute for Mineralogy, Münster, Germany.

<sup>3</sup>University of Mainz – Institute of Geoscience, Mainz, Germany.

<sup>4</sup>University of Belgrade - Faculty of Mining and Geology, Belgrade, Serbia.

For several decades it was proposed that the high Na/K alkaline basalts from intraplate continental and oceanic settings are produced by a small degree of partial melting of a peridotitic mantle source [1] but more recent data show that the trace element and isotopic signatures of these melts may be derived from a more enriched source than the fertile lherzolitic mantle. Several models are introduced for this enrichment, including recycling of oceanic lithosphere into the Earth's convecting mantle with subsequent transformation into pyroxenitic/eclogitic lithologies, "digestion" of enriched lithospheric mantle via subduction, delamination, or interaction with plumes as well as metasomatic mantle enrichment which may lead to the formation of volatile-rich veins in oceanic and continental mantle lithosphere [2].

In this experimental study, we simulate melting processes within the veined metasomatized mantle at 1-4 GPa. We combine synthetic lherzolite (KLB-1) with a natural kaersutite-rich metasome from Kula Volcanic Region, Western Anatolia [3]. Both rock types make up two halves of each capsule, in order to systematically monitor the effects of the P-T change on the major and trace element compositions of the melt that infiltrates the peridotite. Compositional changes are then analyzed with EPMA and LA-ICPMS.

Below 1250 °C and at 3-4 GPa two distinct melt compositions are produced: the metasome-melt has similar SiO<sub>2</sub>, but much higher K<sub>2</sub>O (9 wt.%) contents compared with the infiltration-melt produced within the peridotitic part by melt-mantle interaction due to the assimilation of opx and ol crystallization. The infiltration melts are silica-rich (up to 50 wt.% SiO<sub>2</sub>), with low Na<sub>2</sub>O/K<sub>2</sub>O (~1) and resemble Alpine-Himalayan orogenic belt high-K calc-alkaline as well as shoshonitic lavas [4].

Infiltration melts produced at 1 GPa strongly resemble Kula intraplate lavas, not only in major elements but also in trace element patterns. With varying temperature, the natural range of erupted Kula lava can be covered by metasome-reaction experiments. Both, major and trace element abundances in experimental melts are in good agreement with analyzed natural samples.

Our experiments illustrate that melting of mixed source regions is not simply a question of producing and mixing two melt types. Instead, they show a melt-rock reaction where the melt produced in the metasome with the lower melting temperature reacts with the mantle peridotite, changes its mineralogy and takes up some of its components. The resulting melts vary strongly with changing P, T.

### References:

- [1] Hart, S.R. (1971) *Phil. Trans. R. Soc. Lond. A*, 268, 573-587. [2] Pilet, S. (2015) in Foulger, G. R., Lustrino, M., and King, S.D. ed. *GSA Special Paper 514 and AGU Special Publication 71*, 281-304. [3] Grützner, T. et al. (2013). *Lithos*, 180-181, 58-73. [4] Conticelli, S., et al., *Lithos*, 2009. 107(1-2): p. 68-92.

## Experimental constraints on the formation of massive Fe-Ti oxide ores in the Panxi region, SW China

Sarah-Lynn Haselbach<sup>1</sup> François Holtz<sup>1</sup> Roman Botcharnikov<sup>2</sup> Tong Hou<sup>3</sup>

<sup>1</sup> Institut für Mineralogie, Leibniz Universität Hannover, Callinstr. 3, 30167 Hannover, Germany

<sup>2</sup> Institut für Geowissenschaften, Johannes Gutenberg-Universität Mainz, J.-J.-Becher-Weg 21, 55128 Mainz, Germany

<sup>3</sup> School of Earth Science and Resources, China University of Geosciences, 29 Xueyuan Road, Haidian District, Beijing 100083, P. R. China

Massive Fe-Ti-V oxide ore deposits are hosted in mafic-ultramafic layered intrusions of the Panxi region (Emeishan Large Igneous Province, SW China, ~260 Ma). The intrusions are associated with high- and low-Ti flood basalts and granitoids, and were emplaced either in Neoproterozoic limestones or in Proterozoic metasedimentary and volcanic rocks. With respect to the ore reserves, Panzhihua is one of the largest intrusion in this region. Howarth et al. (2013) suggested that multiple magma replenishment events, i.e., an H<sub>2</sub>O-enriched parental magma intruded into a 'dry' crystallising magma chamber, resulted in the formation of the massive oxide ore deposits of Panzhihua – mainly consisting of magnetite (Mt), and less ilmenite (Ilm). To test this hypothesis, we investigated the role of magma mixing in the Fe-Ti oxide ore formation, and experimentally simulated these processes to constrain the conditions at which the oxides are the only stable solid phases coexisting with silicate melt. Therefore, two Ti-enriched ferrobaltic glass powders were placed in varying proportions on top of each other in Au<sub>80</sub>Pd<sub>20</sub> capsules, thus, allowing us to analyse possible interactions at the interface between the two compositions. One of the glasses represents a parental magma composition pre-hydrated with 5 wt.% H<sub>2</sub>O (P1, ~13 wt.% FeO\*). The other one (LS, ~18 wt.% FeO\*) is of a more evolved and nominally dry composition. The experiments were performed in internally heated pressure vessels at 200 MPa, at temperatures (*T*) ranging between 1025 °C and 1100 °C, and at different redox conditions.

Experimental results at oxidising conditions (nominal  $\Delta\text{FMQ}+3.3$  and  $\Delta\text{FMQ}+2$  at  $a\text{H}_2\text{O} = 1$ ) show that, with decreasing *T*, different solid phases crystallise, i.e., oxides only (highest *T*), oxides + pyroxene, or oxides + pyroxene + plagioclase (lowest *T*). In contrast, at relatively reducing conditions (nominal  $\Delta\text{FMQ}+1$ ), either pyroxene or no solid phases are observed in the experiments performed so far at 1050 °C. With respect to the oxide minerals, Mt and Hm-Ilm<sub>ss</sub> crystallise in experiments conducted at  $\Delta\text{FMQ}+3.3$ , whereas titano-Mt is the only stable oxide phase observed at  $\Delta\text{FMQ}+2$  – with one exception at 1050 °C and a bulk H<sub>2</sub>O content of 1.25 wt.%, where also Ilm crystallises. Although the oxide proportions are higher in the domains of the capsules where the evolved LS composition was initially placed, the amount of oxides does usually not exceed 10 vol.%. Reactions at the interface between the two end-member compositions (e.g., local crystallisation of phases) were not observed.

The minimum *T* at which 'oxides only' coexist with silicate melt is ~1075 °C, at both  $\Delta\text{FMQ}+3.3$  and  $\Delta\text{FMQ}+2$ . They are, furthermore, only observed in experiments with P1:LS ratios of 1:1, 2:1 and 3:1 – corresponding to bulk H<sub>2</sub>O contents of 2.5, 3.3, and 3.75 wt.%, respectively. Thus, the results obtained so far indicate that the formation of 'monomineralic' oxide layers requires at least a 1:1 ratio of P1 to LS, and redox conditions of the system above  $\Delta\text{FMQ}+1.2$ .

### References:

Howarth, G.H., Prevec, S.A., and Zhou, M.-F. (2013) *Lithos*, 170-171, 73-89.

## Stability field of crystalline silica in felsic magmas

Caroline Martel<sup>1</sup>, Ida Di Carlo<sup>1</sup>, Rémi Champallier, Guillaume Wille<sup>2</sup>, Jonathan M. Castro<sup>3</sup>, Michel Pichavant<sup>1</sup>, Karine Devineau<sup>4</sup>, Vesta O. Davydova<sup>5</sup>, Alexandra R. L. Kushnir<sup>6</sup>

<sup>1</sup> Univ. Orléans, CNRS, BRGM, ISTO, UMR 7327, Orléans, France

<sup>2</sup> Bureau de Recherches Géologiques et Minières, BRGM, Orléans, France

<sup>3</sup> Institute of Geosciences, Johannes Gutenberg, Univ. Mainz, Mainz, Germany

<sup>4</sup> Centre de Recherches Pétrographiques et Géochimiques, CRPG, UMR 7358, CNRS-UL, Nancy, France

<sup>5</sup> Lomonosov Moscow State University, Moscow, Russia

<sup>6</sup> Ecole et Observatoire des Sciences de la Terre, EOST, Univ. Strasbourg, CNRS, Strasbourg, France

Felsic lava domes are often rich in low-pressure silica polymorphs (e.g. quartz, cristobalite, tridymite). Explosions of these domes can release silica microparticles into the air; these microparticles may be particularly hazardous to human health, with cristobalite being a more potent carcinogen than quartz. Evaluating the extent of the hazard posed by these silica polymorphs requires knowledge of the conditions attending their formation.

To date, the pressure-temperature stability fields of silica polymorphs have been determined for pure SiO<sub>2</sub> or SiO<sub>2</sub>-H<sub>2</sub>O melts, which are not representative of the more chemically complex rhyolitic liquids that typically exist in magmatic/volcanic systems. We used phase-equilibrium data to constrain crystalline silica stability for H<sub>2</sub>O-saturated and H<sub>2</sub>O-undersaturated rhyolitic melts at pressures between of 0-200 MPa and temperatures of 700-1100°C. Quartz is the dominant silica polymorph at temperatures of ~700 to 1000°C and pressures between 25 and 200 MPa. The Quartz-appearance curve more or less follows the rhyolitic liquidus curve, with a shift to lower temperatures by about 100°C. Cristobalite is stable at pressures < 25 MPa for a large range of temperatures from ~800 to 1100°C. Tridymite was not identified in the investigated range of conditions. The silica-polymorph phase diagram constructed using hydrated rhyolitic melts is thus drastically different from that created using pure SiO<sub>2</sub> or SiO<sub>2</sub>-H<sub>2</sub>O melts, highlighting the crystalline silica ability to incorporate in their structure other oxides than SiO<sub>2</sub>, such as Al<sub>2</sub>O<sub>3</sub> (up to 3 wt%).

Quartz crystallizes at depth in magmatic reservoirs or volcanic conduits, whereas cristobalite is stable at shallow levels, under lava dome conditions. Cristobalite's propensity to protrude into gas bubbles and to crystallize in large amounts concomitantly with microlites, exacerbates dome instability, which makes dome explosion one of the highest risks for fibrotic disease.

## **Polybaric fractionation - the effect of decompression and oxygen fugacity on the liquid line of descent of calc-alkaline arc magmas – an experimental study**

Felix Marxer<sup>1</sup>, Peter Ulmer<sup>1</sup>

<sup>1</sup> Institute of Geochemistry and Petrology, ETH Zürich, Clausiusstrasse 25, CH-8092 Zürich (felix.marxer@erdw.ethz.ch)

To date, various magmatic processes have been proposed and discussed to explain the wide chemical spread characteristic of calc-alkaline rocks. Among these are, for example, fractional crystallisation, assimilation of crustal lithologies or mixing of liquids of different compositions. However, the relative importance of these processes is still a topic of controversial debate in magmatic petrology.

In this experimental study, we are exploring in detail the case of fractional crystallisation and the impact of decompression and oxygen fugacity on phase equilibria and, consequently, on liquid lines of descent (LLD) of arc magmas. Unlike earlier isobaric experimental fractionation series on calc-alkaline rocks (e.g. Nandedkar et al. 2014; Ulmer et al. 2018) we are simulating polybaric fractionation, meaning the continuous fractional crystallisation of arc magmas during their ascent through the continental crust. Thereby, various pressure-temperature trajectories were explored to cover a wide range of hypothetical magma ascent rates. In addition, experiments were performed at moderately (Ni-NiO buffer, NNO) and strongly oxidising  $fO_2$  conditions (Re-ReO<sub>2</sub> buffer, RRO  $\approx$  NNO + 2) to investigate the influence of oxygen fugacity on arc magma differentiation.

Our experiments result that pressure and oxygen fugacity both have crucial impacts on the differentiation behaviour of arc magmas. Decompression as well as oxidation leads to a shift of the olivine-clinopyroxene cotectic towards more clinopyroxene-rich liquid composition, thereby circumventing a rapid evolution of residual melts towards peraluminous compositions (molar ratio  $Al_2O_3 / (CaO + Na_2O + K_2O) > 1.0$ ).

P-T trajectories simulating rapid magma ascent result in liquid lines of descent overlapping with the (predominantly metaluminous) compositional spread covered by typical arc suites (e.g. Cascades Volcanics or Adamello Batholith in Northern Italy), while differentiation trends established for slow ascent trajectories lie distinctively off and rapidly evolve to peraluminous compositions. One further critical observation is that experiments buffered at RRO reproduce better the natural trend than LLDs established for NNO conditions. In conclusion, our polybaric fractional crystallisation experiments indicate that arc magmas are differentiating under oxidised conditions during their rapid rise through the crust.

### References:

Nandedkar RH, Ulmer P, Muntener O (2014) Fractional crystallization of primitive, hydrous arc magmas: an experimental study at 0.7 GPa. *Contrib Mineral Petrol* 167:1015.

Ulmer P, Kaegi R, Muntener O (2018) Experimentally derived intermediate to silica-rich arc magmas by fractional and equilibrium crystallization at 1.0 GPa: an evaluation of phase relationships, compositions, liquid lines of descent and oxygen fugacity. *J Petrol* 59:11–58.

## Experimental crystallisation of a REE-rich calciocarbonatitic melt: crystallisation sequence and REE behaviour

Valentin Mollé<sup>1</sup>, Fabrice Gaillard<sup>1</sup>, Zineb Naby<sup>1,2</sup>, Johann Tuduri<sup>2</sup>, Giada Iacono-Marziano<sup>1</sup>,  
Ida Di Carlo<sup>1</sup>, Saskia Erdmann<sup>1</sup>

<sup>1</sup> Institut des Sciences de la Terre d'Orléans/Observatoire des Sciences de l'Univers en région Centre, 1A rue de la Férollerie, CS20066 – 45071 Orléans Cedex 2, France

<sup>2</sup> Bureau de Recherches Géologiques et Minières, 3 avenue Claude-Guillemin, BP 36009,45060 Orléans Cedex 2, France

Carbonatites host the principal REE ore deposits, the main REE-bearing mineral being bastnaesite (Ce,La)CO<sub>3</sub>F (Verplanck et al., 2016). The bastnaesite crystallisation process is still debated, with putative magmatic or hydrothermal origins. This study focused on calciocarbonatite crystallisation sequence, in order to evaluate whether bastnaesite may be of magmatic origin, characterize the REE behaviour during crystallization, and also discusses the genetic link between calcio- and natrocarbonatites stated by Weidendorfer et al., 2017.

Experiments have been done using an internally heated pressure vessel (IHPV) under moderately oxidizing conditions (ca. NNO+0.5), from 900 to 600°C by 50°C steps, at 100 MPa, on a REE-rich, primary calciocarbonatitic composition. We calculated the composition of the starting material as a carbonate melt in equilibrium with an immiscible silicate melt, using a compilation of experimental and natural data based on the work of Naby et al. (2020).

Results show that REE-rich calcite (Ca,REE)CO<sub>3</sub> is the main mineral phase. The halogen content of the system lowers the calcite saturation curve, implying crystallisation at a lower temperature than in F-free systems (Jago and Gittins, 1991). Water has a similar though weaker effect. Calcite crystallisation evolves the residual melt composition toward more alkaline compositions. However, neither natrocarbonatitic composition nor natrocarbonatitic mineralogy have been reached, even at temperature as low as 600°C. This suggests that the current genetic link hypothesis is not validated and needs further investigation.

REE are slightly incompatible with respect to calcite, especially light REE. REE incompatibility increases with the temperature decrease, inducing a slight enrichment of the residual melt with crystallisation. No bastnaesite has been observed in crystallisation experiments. A bastnaesite saturation experiment has been done at 600°C and 100 MPa. The equilibrium carbonate melt contains ca. 20 wt% of REE. This value is not realistic in natural carbonatites, suggesting bastnaesite cannot occur as a magmatic phase in carbonatitic REE ore deposits.

A Na- and Cl-rich fluid seems to exist above 700°C and in hydrous conditions, as revealed by halite-bearing Na,K-Ca carbonated deposits formed inside fluid bubbles during sample quenches. These deposits are REE-rich, suggesting the fluid to be REE-rich as well. As chlorine is assumed to be a functional ligand for the stability of REE complexes in fluids (Williams-Jones et al. 2012), this observation argues for REE mobilisation by fluids in carbonatitic systems.

### References:

- Jago and Gittins, (1991) *Nature*, 349, 56-58  
Naby et al., (2020, accepted), *Geochim. Cosmochim. Acta*  
Verplanck et al., (2016) *Rare earth and critical elements in ore deposits* (Chap. 1), 5-32  
Weidendorfer et al., (2017) *Geology*, 45(6), 507-510  
Williams-Jones et al., (2012) *Elements*, 8(5), 355-360

## **An experimental investigation into mixing processes in primitive Icelandic basalts**

David A. Neave<sup>1,2</sup>, Philipp Beckmann<sup>1</sup>, Harald Behrens<sup>1</sup>, François Holtz<sup>1</sup>

<sup>1</sup> Institut für Mineralogie, Leibniz Universität Hannover, Callinstraße 3, 30167 Hannover, Germany

<sup>2</sup> School of Earth and Environmental Sciences, The University of Manchester, Oxford Road, Manchester, M13 9PL, UK

Near-fractional melting of the Earth's geochemically and lithologically heterogeneous mantle produces diverse primary melt compositions. However, these diverse compositions are frequently homogenised by magma mixing during ascent towards the surface. Unravelling disequilibrium within and between crystals and their carrier melts provides one way to evaluate the true complexity of melts fed supplied crustal plumbing systems. However, crystals are not passive tracers of magmatic processes. For example, changes in temperature may trigger growth, resorption or diffusive reequilibration depending on the degree of disequilibrium and interplay between different kinetic processes. Changes in magma chemistry also induce similar responses in crystal cargoes; changing phase relations is essentially equivalent to changing temperature. However, the response of compositionally distinct basaltic magmas (i.e. crystal-melt mixtures) to mixing has yet to be quantified experimentally. To address this, we performed experiments on two primitive Icelandic magma compositions derived from geochemically and lithologically distinct depleted and enriched mantle sources and whose equilibrium phase relations are well understood. Synthesis experiments were performed at 300 MPa and 1190 °C, resulting in different phase assemblages. The depleted composition crystallised ol+plg+cpx (~50% crystals), whereas the enriched composition crystallised only ol+cpx (~20% crystals). Mixing experiments were then performed by placing pairs of quenched magma cylinders into new capsules and performing timeseries experiments for 1, 4, 24 and 96 hours. Transects across experimental products show that melt compositions underwent diffusive reequilibration, with different elements showing responses commensurate with their diffusivities. The reequilibration of melt compositions is largely unaffected by the presence of crystals yet controls crystal stability, with a wave of plagioclase dissolution invading depleted cylinders with increasing time. The ability to crystals to serve as archives of magmatic processes may thus be compromised by mixing-triggered dissolution processes. Chemical disequilibrium between mixing basalts may modify crystal records of magmatic processes in significant and previously underappreciated ways.

## The origin of Alpine-Himalayan orogenic K-rich lavas: an integrated experimental and geochemical approach

Dejan Prelević<sup>1,2</sup>, Stephan Buhre<sup>1</sup>, Fatma Gülmez<sup>1</sup>, Michael W. Förster<sup>3</sup>

<sup>1</sup> Institute für Geowissenschaften, Johannes Gutenberg Universität, 55099 Mainz, Germany

<sup>2</sup> University of Belgrade, Faculty of Mining and Geology, 11000 Belgrade, Serbia

<sup>3</sup> ARC Centre of Excellence of Core to Crust Fluid Systems and Department of Earth and Planetary Sciences, Macquarie University, NSW 2109, Australia

K-rich mantle-derived magmatism occurring within Alpine-Himalayan orogenic belt (AHOB) is characterized by the close association of different petrological members including high-K calc-alkaline, shoshonitic and lamproitic lavas. Rather than homogeneous peridotite, their source is heterogeneously metasomatised with the metasomatic assemblages situated in the veins (metasomes) within peridotitic wall-rock (Prelević, et al., 2013). The metasomes originated through a two-stage process that enriches K<sub>2</sub>O and increases K/Na in intermediary assemblages in the source prior to ultrapotassic magmatism at the plate boundaries during the previous subduction (Förster, et al., 2019; Sokol et al., 2020).

Here, we simulate this two-stage formation of ultrapotassic K-rich mantle-derived magmas by performing two principally different types of high T, P experiments:

i) In our 2GPa experiments at T range 1350-1100°C, we combine phlogopite-clinopyroxenites (metasome) with either harzburgite or lherzolite, in which these rock types make up two halves each capsule, in order to observe the role of wall-rock fertility on major and trace element compositions of the final melt. Two distinctive melt compositions are produced: the metasome-melt has lower SiO<sub>2</sub>, higher MgO and similar K<sub>2</sub>O contents compared with the infiltration-melt produced within peridotitic part by melt-mantle interaction due to the assimilation of Opx and Ol crystallization that increases the Ol/Opx ratio. The infiltration melt from harzburgite compositionally resembles lamproites. When lherzolite is involved, the resulting infiltration-melts are silica-rich, with high Al<sub>2</sub>O<sub>3</sub> and with the lower K<sub>2</sub>O/Na<sub>2</sub>O ~1, resembling AHOB high-K calc-alkaline and shoshonitic lavas. These experiments allow clarification of the role of the mantle fertility on the composition of diverse K-rich melts.

ii) In the second type of experiments at considerably lower temperatures (750-900 °C), we simulate the production of glimmerite by heating of two-layer charges consisting of different crustal lithologies including carbonate-bearing siliciclastic marine sediment, marl, blueschist and gneiss, in combination with harzburgite and lherzolite. In all experiments with high water contents > 10% H<sub>2</sub>O, the thin glimmeritic layer was produced after reaction between the high-K rhyolitic crustal melt and the mantle. In most experiments, melts derived from the sediments will react with the mantle part of the capsules producing dolomitic and ph-cpx rich pockets. Moreover, during this reaction, two conjugate melts will be produced: carbonatitic and extremely K-rich silicic melt.

### References:

Förster, et al., (2019) *Minerals*, 10, 41.

Prelević, et al., (2013) *EPSL*, 362, 187-197.

Sokol et al., (2020) *Lithos*, 354–355, 105268.

## Solubility of wöhlerite in peralkaline silica-undersaturated melt at 750 °C, 200 MPa

Christian Schmidt<sup>1</sup>, Ilya Veklsler<sup>1,2</sup>, Oona Appelt<sup>1</sup>

<sup>1</sup> GFZ German Research Centre for Geosciences, Telegrafenberg, Potsdam 14473, Germany

<sup>2</sup> University of Potsdam, Institute of Geosciences, Karl-Liebknecht-Str. 24, 14476 Potsdam, Germany

Agpaitic and miaskitic feldspathoid syenites and peralkaline granitic rocks are becoming increasingly important as sources of niobium, zirconium, and other high field strength elements (HFSE). Such deposits indicate unusually high solubilities of HFSE in alkali silicate melts, with the most important parameters thought to be peralkalinity and the halogen and water contents of the magma (Andersen et al., 2013). The solubilities of HFSE may also depend on silica activity because the HFSE mineralogy of silica-saturated and silica-undersaturated rocks is quite different (Kynicky et al., 2011; Andersen et al., 2013; Marks and Markl, 2017), and because X-ray absorption spectroscopy shows that Zr dissolves as alkali zircono-silicate complexes in  $\text{H}_2\text{O}+\text{Na}_2\text{Si}_3\text{O}_7\pm\text{Al}_2\text{O}_3$  fluids (Wilke et al., 2012). In comparison to silica-saturated systems, there is so far much less information on the HFSE solubility from experiments on silica-undersaturated peralkaline melts.

Here, we report first experimental results of a study on the dissolution of wöhlerite,  $\text{NaCa}_2(\text{Zr,Nb,Hf,Ta})(\text{Si}_2\text{O}_7)(\text{O,OH,F})_2$ , from the Langesundsfjord, Norway, in a peralkaline silica-undersaturated melt (produced from a glass near the albite-nepheline-sodium disilicate eutectic composition, mass%:  $\text{SiO}_2$  60.6,  $\text{Al}_2\text{O}_3$  12.2,  $\text{Na}_2\text{O}$  24.9). Up to 2.4%  $\text{CaF}_2$  and up to 12%  $\text{H}_2\text{O}$  were added to the charge, which was sealed in Au capsules. The experiments were done at 750 °C, 200 MPa using cold-seal hydrothermal autoclaves and water as pressure medium. After quench, the run products were analysed using an electron microprobe (EMP) and Raman spectroscopy.

Euhedral crystals of parakeldyshite,  $\text{Na}_2\text{ZrSi}_2\text{O}_7$ , lueshite,  $\text{NaNbO}_3$ , and wollastonite were observed in the produced glass in some experiments. Calcium fluoride and water dissolved completely in the melt. The HFSE concentrations in the quenched glass were substantial if the glasses contained water (mass%:  $\text{ZrO}_2$  0.40–0.59,  $\text{Nb}_2\text{O}_5$  0.38–0.60,  $\text{HfO}_2$  0.08–0.18,  $\text{Ta}_2\text{O}_5$  0.02–0.05) irrespective of the fluorine content. Addition of  $\text{CaF}_2$  without addition of  $\text{H}_2\text{O}$  resulted in only a slight increase in the Nb concentration but no significant Zr concentration in the glass (mass%:  $\text{Nb}_2\text{O}_5$  0.02–0.11,  $\text{ZrO}_2$  0.01–0.02). The detection limits of the EMP analyses were (ppm): Zr 860, Nb 1000, Hf 6300, Ta 1950).

In summary, the experiments indicate that the solubility of HFSE from wöhlerite in peralkaline silicate melt is independent of the fluorine activity, whereas water promotes HFSE solubility. Thus, they confirm studies that did not find evidence for Zr–F bonding (e.g. Farges et al., 1996).

### References:

- Andersen, T., et al., (2013) *Mineralogia* 44, 61–98  
Farges, F., (1996) *Chem. Geol.* 127, 253–268  
Kynicky, J., et al., (2011) *Can. Min.* 49, 947–965  
Marks, M.A.W., Markl, G., (2017) *Earth-Sci. Rev.* 173, 229–258  
Wilke, M., et al., (2012) *Earth Planet. Sci. Lett.* 349–350, 15–25

## The oxidation state of tin in silicate melts

Paolo A. Sossi<sup>1,2</sup>, Daniel R. Neuville<sup>2</sup>, Mathieu Roskosz<sup>3</sup>, Raúl O. C. Fonseca<sup>4</sup>, Hugh St. C. O'Neill<sup>5</sup>, Frédéric Moynier<sup>2</sup>, Nicolas Trcera<sup>6</sup>, Delphine Vantelon<sup>6</sup>

<sup>1</sup> Institute for Geochemistry and Petrology, ETH Zürich, 8092, Zürich, Switzerland

<sup>2</sup> Institut de Physique du Globe de Paris, Université de Paris, 75005, Paris, France

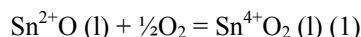
<sup>3</sup> Muséum National d'Histoire Naturelle, 75005, Paris, France

<sup>4</sup> Fakultät für Geowissenschaften, Ruhr-Universität Bochum, 44801, Bochum, Germany

<sup>5</sup> Research School of Earth Sciences, Australian National University, 2601, Canberra, Australia

<sup>6</sup> Synchrotron SOLEIL, 91192 Gif sur Yvette cedex, France

The Group 14 element tin (Sn), typically exists in two oxidation states in natural rocks; stannous (Sn<sup>2+</sup>) or stannic (Sn<sup>4+</sup>), giving rise to distinct geochemical behaviour. Stannous tin is incompatible in igneous minerals, and instead tends to partition into vapours (fluid or gas) to form Cl- or S-bearing species (Heinrich et al. 1990); while Sn<sup>4+</sup> readily substitutes for Ti<sup>4+</sup> in oxide phases (Badullovich et al. 2017). The relationship between the two species in silicate melts is described by the reaction:



The equilibrium constant ( $K$ ) of this reaction is:

$$\log K_{(1)} = \log \left( \frac{X_{\text{SnO}_2}}{X_{\text{SnO}}} + \frac{\gamma_{\text{SnO}_2}}{\gamma_{\text{SnO}}} \right) - \frac{1}{2} \log f_{\text{O}_2} \quad (2)$$

Where  $X$  the mole fraction,  $\gamma$  the activity coefficient and  $f_{\text{O}_2}$  the oxygen fugacity. The value of  $K$  in natural silicate liquids varies with *i*) temperature, pressure, *ii*)  $f_{\text{O}_2}$  and *iii*) silicate melt composition. Here we quantify the effects of these variables on Sn<sup>2+</sup>/Sn<sup>4+</sup> by synthesising glasses at the anorthite-diopside eutectic (An<sub>42</sub>Di<sub>58</sub>) doped with ~4000 ppm Sn, with the addition of FeO<sup>T</sup>, TiO<sub>2</sub>, SiO<sub>2</sub> and Na<sub>2</sub>O at  $f_{\text{O}_2}$ s over 10 orders of magnitude, and recording XANES spectra on quenched glasses at the Sn L<sub>III</sub>-edge (3939 eV) at LUCIA, SOLEIL Synchrotron, France. The L<sub>III</sub>-edge is more sensitive to changes in the Sn<sup>2+</sup>/Sn<sup>4+</sup> ratio than is the K-edge (Farges et al. 2006), due to a  $2p-5s$  transition that occurs in Sn<sup>4+</sup> - but not in Sn<sup>2+</sup> compounds, producing a distinctive pre-edge feature.

Log(Sn<sup>4+</sup>/Sn<sup>2+</sup>) in both AnDi and AnDi+FeO<sup>T</sup> glasses changes gradually with a dependence on  $\log f_{\text{O}_2}$  of  $0.54 \pm 0.05$ ; within uncertainty of the theoretical value (0.5; eq. 1). However, the  $\log K$  value for the Fe-bearing and Fe-free glasses at 1300 °C and 1 bar differs, yielding  $4.10 \pm 0.37$  and  $3.27 \pm 0.23$ , respectively, where higher values denote higher Sn<sup>4+</sup>/Sn<sup>2+</sup> at a given  $f_{\text{O}_2}$ . This relates to the capacity for the melt to provide suitable bonding environments for Sn<sup>2+</sup> and Sn<sup>4+</sup>, hence changing  $\gamma_{\text{SnO}}/\gamma_{\text{SnO}_2}$ . We find a log-linear dependence of  $\gamma_{\text{SnO}}/\gamma_{\text{SnO}_2}$  on the melt optical basicity ( $\Lambda$ ), where Si-, Al-rich glasses with low  $\Lambda$  stabilise stannous tin, whereas basic (Fe-, Na-rich) compositions have Sn<sup>4+</sup>/Sn<sup>2+</sup> identical to that predicted for ideal solution of both species. Because activity coefficients of divalent cations are constant in silicate melts (O'Neill and Eggins, 2002), we argue that changes in  $\gamma_{\text{SnO}}/\gamma_{\text{SnO}_2}$  are caused by an increase of  $\gamma_{\text{SnO}_2}$  in acidic compositions. This reflects a decrease in the abundance of cations (Na, Ca, Mg, Fe) that are able to charge balance SnO<sub>6</sub>-SiO<sub>4</sub> units in the silicate melt network.

### References:

Heinrich et al. (1990), *Econ. Geol.* 85, 457-481; Badullovich et al. (2017), *GPL*, 5, 24-28; Farges et al. (2006) *Can. Min.* 44, 795-810; O'Neill, Eggins (2002) *Chem. Geol.* 186, 151-181

## Origin of chromitite layers in the Bushveld complex, South Africa, by hydration melting: an experimental study

Ilya V. Veksler<sup>1,2</sup>, Cora C. Wohlgemuth-Ueberwasser<sup>1</sup> and Tong Hou<sup>3,4</sup>

<sup>1</sup> GFZ German Research Centre for Geosciences, Telegrafenberg, 14473 Potsdam, Germany

<sup>2</sup> Institute of Geosciences, University of Potsdam, Potsdam-Golm, Germany

<sup>3</sup> State Key Laboratory of Geological Process and Mineral Resources, China University of Geosciences, Beijing, China

<sup>4</sup> Institute for Mineralogy, Leibniz Universität Hannover, Germany

The formation of chromitite layers, also known as stratiform chromite deposits, in mafic-ultramafic layered intrusions has been one of the most difficult and persistent scientific problems in igneous petrology. The Early Proterozoic Bushveld Complex in South Africa presents the most spectacular and best-preserved examples of chromitite layers constituting the world's greatest reserve of metallurgical chromium and platinum group elements. Layered sequence of mafic-ultramafic silicate rocks that hosts chromitite layers is believed to have formed from a parental magma with the initial SiO<sub>2</sub> content at 55 wt.%, MgO at about 12 wt.% and Cr<sub>2</sub>O<sub>3</sub> at 0.15 wt.%. Previous experimental study at 300 MPa and nominally dry conditions (Cawthron and Davis, 1983) showed that this composition had orthopyroxene on liquidus between 1250 and 1300 °C, and the mineral was joined by plagioclase and clinopyroxene at and below 1166 °C. The objective of this study was to investigate the effects of variable additions of water (2, 4 and 6 wt.% H<sub>2</sub>O in starting compositions) on liquidus and sub-liquidus phase equilibria. Main attention was given to the solubility of Cr-spinel and Cr distribution between melt and crystalline phases. Six experiments were carried out in the internally heated pressure vessel (IHPV) at 300 MPa and in the temperature interval 1100-1300 °C. Redox conditions were not controlled and thermal dissociation of the H<sub>2</sub>O component followed by hydrogen diffusion through container walls resulted in a noticeable oxidation of run products. The effective values of fO<sub>2</sub> in experiments were calculated using SPINMELT 2.0 software bases on the regression of experimental data on the spinel-melt equilibrium (Nikolaev et al., 2018). According to the calculations, H<sub>2</sub>O additions in isothermal series of experiments increased fO<sub>2</sub> by 0.8-1.6 log-units from the level in a nominally dry run. Overall, the experiments showed that H<sub>2</sub>O additions suppressed crystallization of silicates, shifted olivine-orthopyroxene peritectic equilibrium towards higher olivine stability (olivine first appears in H<sub>2</sub>O-bearing compositions at 1175 °C) and increased the proportion of magnetite component in spinel solid solution. The addition of 4 wt.% H<sub>2</sub>O to the starting composition at 1200 °C resulted in complete melting of orthopyroxene, which left Cr-spinel as the only liquidus phase. Equal amount of H<sub>2</sub>O at 1125 °C leads to complete melting of plagioclase, orthopyroxene and clinopyroxene, which leaves only olivine and spinel stable and increases the liquid mass fraction from 0.62 in the nominally dry compositions to 0.9. The results of this study appear to support the idea that chromitite layers in the Bushveld Complex may have been formed by episodes of hydration melting of silicate cumulates.

### References:

- Cawthron RG and Davies G (1983) *Contrib. Mineral. Petrol.*, 83,128-135  
Nikolaev et al., (2018) *Geochem. Internat.* 56, 24–45

## Experimental constraints of magma storage prior to the 1257 trachydacite eruption of Mt Samalas

Annika Voigt<sup>1\*</sup> Michael Cassidy<sup>1</sup> David Pyle<sup>1</sup> Tamsin Mather<sup>1</sup> Jonathan Castro<sup>2</sup> Christoph Helo<sup>2</sup>

<sup>1</sup>Dept. of Earth Sciences, University of Oxford, South Parks Road, Oxford OX1 3AN, UK; \*annika.voigt@earth.ox.ac.uk

<sup>2</sup>Institute of Geosciences, Johannes Gutenberg-University Mainz, J.-J.-Becher-Weg 21, 55128 Mainz, Germany

The caldera-forming eruption of the Samalas volcano on Lombok island, Indonesia in 1257, ranks as one of the most explosive (VEI 7) and sulphur-rich ( $158 \pm 12$  Tg SO<sub>2</sub>) eruptions of the Holocene (Vidal et al., 2015; 2016). To improve surveillance data interpretation and systems monitoring such potentially life-threatening volcanoes, it is therefore vital to investigate the magmatic processes leading up to such eruptions.

The aim of this project is to develop a better understanding of the pre-eruptive magma reservoir conditions, as well as volatile storage and exsolution processes during magma ascent in the volcanic conduit for intermediate alkaline systems. Partial-equilibrium experiments at potential magma reservoir conditions are performed to investigate changes in the chemical and textural state of the magma at different P-T conditions. The experiments were run at water-saturated conditions using natural trachydacite pumice from the 1257 Samalas eruption as starting material. Likely conditions of the magma chamber were constrained from experimental matrix glass data matching that of the natural pumice. In addition, the reproduction of the natural mineral assemblage in mineral rims grown during the experiments provided further indication of the pre-eruptive storage conditions. Systematic experiments at various pressures (25-200 MPa) and temperatures (850°C-1000°C) point towards pre-eruptive magma chamber conditions being most likely between 875 and 950°C and above 100 MPa for an oxygen fugacity  $f_{O_2}$  of about 1 log unit above the NNO buffer. Preliminary FTIR measurements of hydrous experiments show that the solubility of H<sub>2</sub>O in trachydacite magma under equilibrium conditions can be relatively high (about 3.73 wt.%) at pressures as low as 50 MPa.

### References:

Vidal et al., (2015): Abstracts of Volcanoes, Climate, and Society, Bicentenary of the great Tambora eruption Conference, 7–11 April 2015, Bern, Switzerland.

Vidal et al., (2016): Scientific reports, 6, 34868.

## Experimental liquid lines of descent for low-Ti and high-Ti basalts of the Emeishan Large Igneous Province, SW China

Yi-shen Zhang<sup>1</sup>, Olivier Namur<sup>1</sup>, Bernard Charlier<sup>2</sup>

<sup>1</sup> Department of Earth and Environmental Sciences, KU Leuven, 3000 Leuven, Belgium

<sup>2</sup> Department of Geology, University of Liège, 4000 Sart Tilman, Belgium

We present a full investigation of the liquid lines of descent of high-Ti and low-Ti magma series of the Emeishan large igneous province (Emeishan LIP). A stepwise experimental approach was used to reproduce fractional crystallization with the objective to understand the effect of starting compositions, crystallization sequences, and  $fO_2$  on the formation of Fe-Ti-V and/or Ni-Cu-(PGE) ore deposits in the Emeishan LIP.

Synthetic high-Ti and low-Ti picritic starting compositions were selected from a compiled database of Emeishan lavas. Experiments were carried out in one-atmosphere gas-mixing furnace (CO-CO<sub>2</sub> gas mixtures) from 1330 to 1120 °C under the QFM buffer (quartz-fayalite-magnetite) and QFM+2. The crystallization sequences of high-Ti magmas in step-1 (1330–1160 °C) are olivine + spinel ± augite at both two  $fO_2$ , whereas those of low-Ti magmas are olivine + spinel ± augite ± plagioclase. The occurrence of plagioclase quickly increased the crystallinity in low-Ti magmas with cooling. The step-2 (1200–1120 °C) experiments were carried out using starting materials synthesized from residual melt composition produced at 1170 °C of step-1. The crystallization sequences of high-Ti and low-Ti magmas are augite + pigeonite + plagioclase ± Fe-Ti-oxides.

Overall, the results of the experiments are in good agreement with the mineralogy of natural rocks and minerals compositions observed in Emeishan LIP. Differentiation of high-Ti picritic magmas produces compositions that are comparable with the proposed parental magma compositions of the Fe-Ti oxides bearing intrusions (liquidus at ~1200 °C with Mg-number ~ 52; Pang et al., 2008). More oxidizing conditions of the parental magmas may contribute to the early saturation of Fe-Ti oxides.

### References:

Pang et al., (2008) *Contrib Mineral Petrol.*, 156(3): 307–321.

## Ti-in-quartz thermobarometry and TiO<sub>2</sub> solubility in rhyolitic melts: new experiments and parametrization

Chao Zhang<sup>1,2</sup>, Xiaoyan Li<sup>1,2</sup>, Renat R. Almeev<sup>1</sup>, Harald Behrens<sup>1</sup>, Francois Holtz<sup>1</sup>

<sup>1</sup> Institute of Mineralogy, Leibniz University Hannover, Callinstr. 3, 30167 Hannover, Germany

<sup>2</sup> State Key Laboratory of Continental Dynamics, Department of Geology, Northwest University, 710069 Xi'an, China

The Ti-in-quartz thermobarometer has a wide potential for constraining crystallization conditions of quartz in natural geological systems. However, there is a long-lasting debate on the applicability of two models that were proposed previously, based on the equilibration of quartz with Ti-bearing aqueous fluids. In this study, the Ti-in-quartz thermobarometer was calibrated based on partitioning data of Ti between quartz and aluminosilicate melt in the pressure and temperature range of 0.5–4 kbar and 700–900 °C. For seventeen experiments, in which quartz, rutile and high-silica glass are present as experimental products (i.e., activity of TiO<sub>2</sub> is unity), the Ti concentrations in quartz can be predicted with the following equation:

$$\log C_{\text{Ti}}^{\text{Qtz}} = 5.3226 - 1948.4/T - 981.4 * P^{0.2}/T,$$

in which  $C_{\text{Ti}}^{\text{Qtz}}$  is the Ti concentration (ppm) in quartz,  $T$  is temperature in kelvin and  $P$  is pressure in kbar. Based on the available data (literature and this study) we modelled the dependence of rutile solubility in silicic melt on temperature, pressure and melt composition, which can be expressed as

$$\log(S_{\text{Ti}}^{\text{liq}}) = 6.5189 - 3006.5/T - 461.0 * P^{0.2}/T + 0.1155 * \text{FM},$$

in which  $S_{\text{Ti}}^{\text{liq}}$  is Ti solubility (ppm) at rutile saturation and FM is a parameter accounting for melt compositional effect, computed as

$$\text{FM} = (\text{Na} + \text{K} + 2\text{Ca} + 2\text{Mg} + 2\text{Fe})/(\text{Si} * \text{Al}),$$

in which the chemical symbols denote molar fractions of each cation. Combining the two models presented above as well as some additional experimental data at activity of TiO<sub>2</sub> <1, and assuming an ideal behaviour for the activity of TiO<sub>2</sub>, the following Ti-in-quartz thermobarometer is proposed:

$$\log(C_{\text{Ti}}^{\text{Qtz}}/C_{\text{Ti}}^{\text{liq}}) = -1.1963 + (1058.1 - 520.4 * P^{0.2})/T - 0.1155 * \text{FM},$$

in which  $C_{\text{Ti}}^{\text{liq}}$  is Ti concentration (ppm) in melt. Assuming an uncertainty of input temperature of ±25 °C, the corresponding pressure can be determined within ±0.2 kbar. However, the Ti concentrations in quartz and glass need to be determined with a high precision. Typical values of the ratio  $C_{\text{Ti}}^{\text{Qtz}}/C_{\text{Ti}}^{\text{liq}}$  in natural systems vary in the range from ~0.09 to ~0.13, corresponding to a change of pressure from ~5 to ~1 kbar assuming a temperature of ~800 °C.

The model above was applied to natural datasets obtained for several silicic eruptions (i.e. Oruanui Rhyolite, Early Bishop Tuff, Toba Tuff, Upper Bandelier Tuff). The analyses of quartz and glass inclusions in quartz indicate that the pre-eruptive magma storage pressures are mainly in the range 2–4 kbar. These pressures are consistent to or slightly higher than the maximum value estimated previously from the analysis of H<sub>2</sub>O-CO<sub>2</sub> in glass inclusions, indicating a possible post-entrapment loss of hydrogen from melt inclusions and that gas saturation provides a minimum estimation of pressure.

## **EMPG – XVII**

### **17th International Symposium on Experimental Mineralogy, Petrology and Geochemistry**

#### Abstracts

#### Theme 6 “Applied and environmental mineralogy”

(sorted alphabetically by first author)

## The decisive role of cracks for weathering of inscribed marble: application to epigraphy

Stylianos Aspiotis<sup>1</sup>, Jochen Schlüter<sup>2</sup>, Kaja Harter-Uibopuu<sup>3</sup>, Boriانا Mihailova<sup>1</sup>

<sup>1</sup> Department of Earth Sciences, Universität Hamburg, Grindelallee 48, 20146 Hamburg, Germany, email: stylianos.aspiotis@uni-hamburg.de, email: boriana.mihailova@uni-hamburg.de

<sup>2</sup> CeNak, Mineralogisches Museum, Universität Hamburg, Grindelallee 48, 20146 Hamburg, Germany, email: jochen.schlueter@uni-hamburg.de

<sup>3</sup> Department of History, Universität Hamburg, Überseering 35 #5, 22297 Hamburg, Germany, email: kaja.harter@uni-hamburg.de

The interpretation of written artefacts has a substantial meaning in understanding thoroughly the roots of human civilization. However, material sciences have to face the challenge that rock-base inscriptions, as any other rock types, are subjected to weathering processes. Considerable efforts have been made to decipher vanished or hardly readable written artefacts on marble headstones and sculptures by applying preferably non-destructive methods such as X-ray fluorescence (XRF) [1], [2], based on the trace elements introduced during the inscription. The obtained results were unsatisfactory. Thus, alternative non-invasive methods such as Raman spectroscopy are highly desired. Rock-base written artefacts are expected to have more extended cracks and structural defects beneath inscribed areas than away of them, which promote the development of weathering products like various oxalates, carbonate hydrates and calcium sulphates or the growth of biological organisms such as lichens and fungi. Such weathering products or microorganisms can non-invasively be mapped by Raman spectroscopy through the lateral distribution of the guest secondary phase or molecular inclusions in the host matrix via the guest-to-host peak intensity ratio. Besides, the nature of the weathering products as well as the weathering rate depend on the environmental conditions; temperature, humidity, air pollution, exposure to rain and sun and on the exact location and altitude of the weathered object (e.g. [3], [4]). In this study, ~ 2000-year-old inscribed marble fragments from an excavation site in Asia Minor (W Turkey) and ~ 70-year-old engraved marble gravestones of different grain size from the cemetery of Ohlsdorf (Hamburg, Germany) are going to be analyzed with Raman spectroscopy to investigate the potential of this analytical technique for visualization of inscriptions on rock-base epigraphic objects. The results from line profiling on cross-sections clearly imply that a higher abundance of lichens or amorphous carbon (a-C) does exist beneath engraved letters than beneath non-inscribed areas of the headstones of Ohlsdorf and marble fragments of Asia Minor, respectively. Such evidence can be monitored by the intensity ratio of the peaks near  $1522\text{ cm}^{-1}$  (typical of the stretching mode of C=C in lichens) and  $1594\text{ cm}^{-1}$  (typical of the stretching mode of C-C in a-C) against the major peak of the carbonate group near  $1087\text{ cm}^{-1}$  or  $1085\text{ cm}^{-1}$ , which is attributed to the symmetric C-O stretching mode of calcite or aragonite respectively. Finally, results focusing on the factors, like color and grain size, that influence the type and penetration depth of the weathering products / molecular inclusions will be also presented.

### References:

- [1] Powers et al., (2005) *Z. Papyr. Epigr.*, 152, 221-227
- [2] Pinna et al., (2015) *Heritage Science*, 3, 1-13
- [3] Frost and Weier, (2003) *Thermochimica Acta*, 406 (1-2), 221-232
- [4] Moropoulou et al., (1998) *Atmospheric Environment*, 32, 967-982

## Rare Earth Elements (REEs) in mine waste: a way to solve the rising worldwide REEs demand?

Fiorenza Deon<sup>1</sup> Oona Appelt<sup>2</sup>, Franziska Wilke<sup>2</sup>, Caroline Lievens<sup>1</sup>, Arjan Dijkstra<sup>1</sup>, Harald van der Werff<sup>1</sup>, Imam Purwadi<sup>1</sup>

<sup>1</sup>University of Twente Faculty of Geo-Information Science and Earth Observation (ITC), Hengelosestraat 99, 7500 AE Enschede The Netherlands

<sup>2</sup>Electron microprobe laboratory, Deutsches GeoForschungsZentrum GFZ Telegrafenberg, 14473 Potsdam, Germany

The increasing demand of Rare Earth Elements (REE) in the industry and their economic importance plays a crucial role in the mining exploration. More knowledge on unconventional deposits such as dumps and tailings should be gathered to recover REEs.

Purwadi et al. (2018) studied the concentration and visible and near-infrared reflectance spectroscopy of REEs-bearing tailings of a closed tin mine located on the Bangka Island (Indonesia) but detected no REEs bearing minerals due to their low abundance (<1wt.%).

Our study investigates quartz rich tailings from this tin mine by means of Electron Microprobe (EMP). The measurements on 12 samples have shown the occurrence of zircon  $ZrSiO_4$  and abundant REE bearing minerals such as monazite  $(Ce,La)PO_4$ , xenotime  $YPO_4$ , thorite  $(Th,U)SiO_4$ , and uranite  $UO_2$ . REEs bearing phases occur in quartz or at the grain boundaries, are approximately 5 to 50  $\mu$  large, and form relatively fresh (poorly altered) un-to subhedral grains suitable for EMP point analyses.

Plotting the concentration of the monazite and xenotime REEs in the chondrite normalized diagram they show the typical monazite decreasing and xenotime increasing pattern with no obvious anomaly. Chemically monazites are characterized by high thorium (up to 18% ThO - mainly as huttonite component) and very high yttrium and xenotime component (up to 3.5 wt. %  $Y_2O_3$ ) indicating a high monazite formation temperature. Additional ICP-OES analyses, elemental mappings and in situ dating on monazite, will show the REEs distribution, e.g. depleting and or enrichment triggered by fluids, and the geochemical signature of these tailings.

### References:

Purwadi, I., van der Werff H., and Lievens, C. (2018) Reflectance spectroscopy and geochemical analysis of rare earth element-bearing tailings: A case study of two abandoned tin mine sites in Bangka Island, Indonesia. *Int J Appl Earth Obs Geoinformation* 74 (2019) 239–247

## Multicolor tourmalines from pockets of the Befisiotra pegmatite Fianarantsoa Province, Madagascar: Indication of two different crystallization stages

Andreas Ertl<sup>1</sup>, Federico Pezzotta<sup>2</sup>, Dan Topa<sup>3</sup>, Gerald Giester<sup>1</sup>

<sup>1</sup> Institut für Mineralogie und Kristallographie, Geozentrum, Universität Wien, Althastrasse 14, 1090 Wien, Austria

<sup>2</sup> Natural History Museum, Corso Venezia 55, 20121 Milano, Italy

<sup>3</sup> Zentrale Forschungslaboratorien, Naturhistorisches Museum, Burgring 7, 1010 Wien, Austria

Different multicolor tourmalines from the large gem bearing pegmatite of Befisiotra (about 50 meters thick and one kilometer long), Fianarantsoa Province, central Madagascar, were chemically and structurally characterized. A set of tourmaline samples (pink, green, yellowish, brown, black) from 4 different pockets found in this pegmatite, were investigated. Single-crystal structure refinements show that the pale colored tourmalines contain significant amounts of Li and <sup>14</sup>B up to ~0.23 apfu. The observed lattice parameters are in the range  $a = 15.804\text{-}15.817$ ,  $c = 7.090\text{-}7.097$  Å. The crystal chemical formula of each sample was established by a combination of microprobe and structural X-ray data. The highest observed component of each tourmaline endmember is as follows: elbaite: 40 mol%, fluor-elbaite: 42 mol%, fluor-liddicoatite: 67 mol%, foitite: 70 mol%, olenite: 28 mol%, rossmanite: 26 mol%, schorl: 35 mol%, tsilaisite: 28 mol%. By plotting the fluorine content against the *X*-site charge (the *X* site can be occupied by Na, Ca, K or can be vacant), we observed that almost all tourmaline samples plotted in two different positive correlations with  $r^2 = 0.991$  (10 samples) and  $r^2 = 0.992$  (8 samples). By doing such a plot, we can't assign tourmaline samples to individual pockets, but these two different correlations seem to indicate at least two different stages of crystallization within each pocket. This is not surprising, because this relatively thick dike is probably composed by multiple intrusions and a complex history of pocket crystallization, resulting in a complex compositional zoning of tourmaline crystals and, possibly, a multistage process of pocket evolution.

A high correlation ( $r^2 = 0.998$ ) between the fluorine content and the *X*-site charge were also found by investigating tourmalines from a Li-pegmatite from the Himalaya mine, San Diego co., California, USA (Ertl et al., 2010). However, this linear function plots in a different field than the functions of the tourmaline samples from Befisiotra, and further it has a lower slope. Therefore, this is an indication that in future we will probably be able to use this method to characterize the different production localities of gem tourmalines. If such correlations can be established for other localities, the analysis (major and minor elements; boron, Li and H<sub>2</sub>O can be calculated) of cut and rough tourmaline could give an indication about the provenance of the stones.

We conclude that, very likely, plots of the fluorine content against the *X*-site charge will be a useful tool for the future characterization of tourmalines found in different gem bearing pegmatites and other tourmaline occurrences.

This work was supported in part by Austrian Science Fund (FWF) project no. P31049-N29 to AE.

### References:

Ertl et al., (2010) Am. Mineral., 95, 24-40

## Nature of the color and opalescence of jewelry rare-earth glass-ceramics

Vladimir M. Khomenko<sup>1</sup>, Arkadiy M. Tarashchan<sup>1</sup>, Olexij A. Vyshnevskiy<sup>1</sup>, Olexander O. Kosorukov<sup>1</sup>

<sup>1</sup> M.P. Semenenko Institute of Geochemistry, Mineralogy and Ore Formation  
Acad. Palladin Ave. 34, Kyiv, Ukraine

A series of 34 differently colored samples of rare-earth jewelry glass-ceramics (REJGS) was studied using a complex of physical methods focusing on their structure and nature of coloration and opalescence. To study the electronic structure of the optically active centers of transition metal ions with incomplete *d*- and *f*-shells, methods of optical and IR spectroscopy, X-ray and photoluminescence were used. Composition and phase structure of REJGS were studied by means of X-ray fluorescence analysis, X-ray diffraction and SEM.

According to the chemical composition, REJGS samples can be divided into 4 groups: Y-Al-Si (YAS), La-Al-Si (LaAS), Y-Ti-Al-Si (YTAS) and Mg-Zr-Al-Si (MZAS), the majority of samples being of the YAS type. The ratio between the three main groups of atoms: Si (Si), Al (Al + Ti + Zr + Sn) and REE (Y + Ln + Ba), remains practically unchanged in all samples and is about 2:3:1 (Khomenko e.a., 2017). Aluminum along with silicon predominantly acts as a glass-forming element and occupies tetrahedral positions, whereas lanthanoid ions are modifiers and enter the large positions in the glass matrix.

Spectra of electronic *ff*- transitions of Nd<sup>3+</sup>, Pr<sup>3+</sup>, Er<sup>3+</sup> and Ho<sup>3+</sup> ions in aluminosilicate glass, which composition is close to allanite, were obtained in the range 28000-1000 cm<sup>-1</sup>. It was found that the colors of the REJGS are originated due to (a) impurities of single trivalent lanthanide ions: Nd<sup>3+</sup>, Pr<sup>3+</sup>, Er<sup>3+</sup>, Ho<sup>3+</sup>; (b) their combinations: Nd<sup>3+</sup>+Er<sup>3+</sup>, Nd<sup>3+</sup>+Pr<sup>3+</sup>, Nd<sup>3+</sup>+Er<sup>3+</sup>+Ho<sup>3+</sup>; (c) combinations of lanthanide ions with ions of transition metals of the iron group: Pr<sup>3+</sup>+Cu<sup>2+</sup>, Pr<sup>3+</sup>+Fe<sup>3+</sup>, Nd<sup>3+</sup>+Ni<sup>2+</sup>, Ti<sup>4+</sup>+Er<sup>3+</sup>; and (d) separate ions of the iron group: Ti<sup>4+</sup>, Cu<sup>2+</sup>. Positions of the maxima and the character of splitting of Ln<sup>3+</sup> ions' bands in the absorption spectra depend on the composition of the glass matrix, although the corresponding shifts are very small (10-30 cm<sup>-1</sup>). The main distinctive feature of the absorption and luminescence spectra of Nd<sup>3+</sup> ions in glass-ceramics in comparison with their spectra in britholite crystals is the weakly resolved thin structure of the bands. This suggests that the bulk of the chromophoric Ln<sup>3+</sup> ions in REJGS do not enter the nanocrystalline phases, but remains in the glass matrix. The above conclusion is confirmed by the significant width, invariability of positions and the intensities' ratios of the emission bands of Nd<sup>3+</sup>, Pr<sup>3+</sup>, and Er<sup>3+</sup> in the REJGS luminescence spectra.

X-ray diffraction study of transparent and opalescent samples before and after two-step heating experiments at temperature 600-1000 °C reveals that the opalescence phenomenon observed in the samples of the MZAS REJGS is related to crystallization of the nanoparticles of the tetragonal modification of ZrO<sub>2</sub>. The main part of the Ln<sup>3+</sup> ions in this case remains in the glass matrix. In LaAS REJGS with admixture of Zr and Er<sup>3+</sup> at temperature above 900 °C small (<2 μm) skeletal crystals of Al<sub>2</sub>O<sub>3</sub> appear. At higher temperature large skeletal crystals of unidentified strongly enriched in Er phase crystallize near the surface of the sample forming semitransparent opalescent layer.

### References:

V.M. Khomenko et al., (2017) Mineral. Journ. (Ukraine), 39, No 4, 24-41

## Heterogeneous nucleation of calcium carbonate on smectite substrate - the effects of magnesium and phosphorus

Zsombor Molnár<sup>1</sup>, Péter Pekker<sup>1</sup>, Mihály Pósfai<sup>1</sup>

<sup>1</sup> University of Pannonia, Research Institute of Biomolecular and Chemical Engineering, Nanolab

The heterogeneous nucleation of minerals is a ubiquitous process in nature and thermodynamically the most favourable way to form a crystal nucleus. Despite their known or assumed importance, the effects of pre-existing minerals on the nucleation and crystal growth of carbonates are relatively poorly understood. Previous observations suggested that the presence of a sheet silicate substrate could not just decrease the free energy barrier of nucleation, but template the structure of the newly formed CaCO<sub>3</sub> phase and affect its chemical composition (Xu et al., 2018). Here, we study the effects of smectite clay minerals on the nucleation of pure CaCO<sub>3</sub> and Mg-bearing CaCO<sub>3</sub> phases in an environmentally relevant experimental setting.

In order to observe the evolution of the mother solution and the nucleation and phase transitions of carbonates, we titrated continuously stirred Na<sub>2</sub>CO<sub>3</sub> buffer solutions at constant pH with CaCl<sub>2</sub> or Mg-bearing CaCl<sub>2</sub> solutions, both in the presence and absence of smectite. We monitored the solutions with pH and Ca ion selective electrodes and sampled the solution at different Ca:CO<sub>3</sub> ratios for transmission electron microscopy (TEM) analysis.

In the Mg-free homogeneous nucleation experiments we observed the well-known Ostwald step rule, as the most soluble crystalline solid CaCO<sub>3</sub> phase (vaterite) transformed into the less soluble one (calcite). In contrast, the presence of smectite enhanced the direct formation of rhombohedral calcite crystals. In the Mg-rich solutions aragonite formed first in both types of experiments. However, after aging the precipitated materials in their mother solutions aragonite persisted in the clay-free system, while Mg-bearing CaCO<sub>3</sub> phases developed in the presence of smectite. According to TEM tomographic analysis of the morphologies of peculiar associations of two Mg-bearing CaCO<sub>3</sub> phases, fibrous protodolomite enveloped a low-magnesian calcite core. These observations provide insights into the formation mechanisms of Mg-bearing calcite and protodolomite in freshwater environments.

Currently we are performing experiments using the system described above in order to understand (1) the role of phosphate on carbonate nucleation and (2) the binding of phosphorus on carbonates and its release from the sediments of a freshwater lake. Preliminary results of these experiments will be also reported.

### References:

Xu H., Zhou M., Fang Y., Teng H. H. (2018) Effect of mica and hematite (001) surfaces on the precipitation of calcite. *Minerals*, **8**, 17.

## Synthesis and study of Ga- and Ge-rich analogues minerals

Tatiana Setkova<sup>1</sup>, Vladimir Balitsky<sup>1</sup>, Dmitry Pushcharovsky<sup>2</sup>, Ludmila Balitskaya<sup>1</sup>, Tatiana Bublikova<sup>1</sup>, Valentina Nesterova<sup>1,2</sup>, Pavel Kvas<sup>1,2</sup>

<sup>1</sup> D.S. Korzhinskii Institute of Experimental Mineralogy of Russian Academy of Sciences, Chernogolovka, Russia

<sup>2</sup> Department of Geology, Lomonosov Moscow State University, Moscow, Russia

The synthesis of Ga- and Ge-substituted minerals is of particular interest both from the point of view of modeling changes of the mineral structure at high pressure, geochemistry of gallium and germanium, and with the aim of improving physical properties of minerals. Crystals of Ga-, Ge-, and Ga-Ge-rich tourmaline and topaz were grown at a temperature of 600–650° C and a pressure of 100 MPa using a hydrothermal thermogradient method in Gr-Ni autoclaves [1, 2]. Tourmaline has a maximum thickness of grown layer up to 1 mm (Fig.1a), and the gallium and germanium content is from 2 to 20 wt. % Ga<sub>2</sub>O<sub>3</sub> and from 2 to 32 wt. % GeO<sub>2</sub>. An increased content of iron and titanium and a lower content of silicon and aluminum in comparison with the seed crystal are observed.

Ge,Ga-rich topaz single crystals of bluish-green color has a thickness of up to 4 mm on one side of the seed (Fig.1b). The external morphology of the as grown crystals is determined by crystallographic orientation of seeds, their form and sizes. Grown layer characterized by a clear zoning and sectorial structure. EMPA shows a sharply uneven distribution of gallium and germanium in topaz. The maximum replacement of silicon and aluminum by the indicated elements occurs at the boundary of the seed crystal and the grown layer, reaching 25 wt.% GeO<sub>2</sub> and 10 wt.% Ga<sub>2</sub>O<sub>3</sub>, respectively.

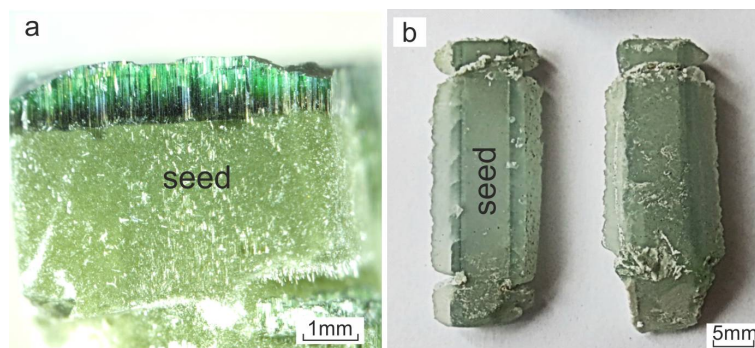


Fig. 1 Overgrown layer of Ga, Ge-rich tourmaline (a); Crystals of Ga, Ge-rich topaz (b)

### References:

Setkova et al., (2019) *Geochemistry Int.*, 57(10), 1082-1094

Balitsky et al., (2002) *J.Crystal Growth*, 237(1), 833–836

## Temperature-induced order-to-disorder transition in bulk kesterite-type $\text{Cu}_2\text{ZnSnS}_4$

Nicole Yvonne Suss<sup>1,2</sup>, Ilias Efthimiopoulos<sup>1</sup>, Anna Ritscher<sup>2</sup>, Martin Lerch<sup>2</sup>

<sup>1</sup> Section 3.6. Chemistry and Physics of Earth Materials, Deutsches GeoForschungsZentrum (GFZ), Potsdam, 14473, Germany

<sup>2</sup> Institute of Chemistry, Technische Universität Berlin (TUB), Berlin, 10623, Germany

$\text{Cu}_2\text{ZnSnS}_4$  gained increasing interest as a potential absorber material in solar cells, partly due to its earth-abundant non-toxic constituents. It crystallizes in the tetragonal layered kesterite phase (SG *I4*,  $Z = 2$ ). Several types of disorder in the cationic sublattice are known, such as the random distribution of equisized  $\text{Zn}^{2+}$  and  $\text{Cu}^+$ . This random distribution results in the adoption of a disordered kesterite phase (Schorr et al., 2007) with concomitant changes in the electronic bandgap, i.e. the photovoltaic properties of the material (Scragg et al., 2016). Consequently, the exploration of the order-to-disorder transition in  $\text{Cu}_2\text{ZnSnS}_4$  is important.

We have examined the aforementioned order-disorder transition in a bulk  $\text{Cu}_2\text{ZnSnS}_4$  sample up to 400°C by *in-situ* Raman spectroscopy. The phase transition in this sample was expected at 275°C, according to previous works (Ritscher et al., 2016). At 225°C, however, the Raman spectra indicate the appearance of the disordered kesterite phase signal. This high-temperature disordered  $\text{Cu}_2\text{ZnSnS}_4$  modification becomes the dominating phase above 275°C. Considering former ex-situ neutron diffraction study by Ritscher et al. (2016) on the sample, a direct connection between the Raman spectroscopic results and the structural transition can be made for the first time in this important system.

### References:

- Schorr et al., (2007) *Eur. J. Mineral.*, 19(1), 65  
Scragg et al. (2016) *Phys. Status Solidi B*, 253(2), 247  
Ritscher et al. (2016) *J. Solid State Chem.*, 238, 68

## Solubility of glasses at the molecular scale: insight from Raman spectroscopy

Mariona Tarrago<sup>1</sup>, Charles Le Losq<sup>1</sup>, Eric van Hullebusch<sup>1</sup>, Daniel R. Neuville<sup>1</sup>

<sup>1</sup> Université de Paris, Institut de physique du globe de Paris, CNRS, F-75005 Paris, France

Glass is commonly considered a durable material. Natural glasses and glass-containing rocks such as obsidian and basalt may be millions of years old. Glass is also used as a container for liquids to either hold (tableware, bottles) or cook (kitchenware) food. In both cases, it is often exposed to both relatively high temperatures and acidic media. Glasses often contain potentially toxic elements (PTE) such as Co, Cr, Cu, Pb, Sb, Zn, and Zr, either those naturally present in rocks or to improve their esthetics (coloring, increasing the refractive index).

Glass solubility is interesting from both a geological and an industrial point of view. From a geological perspective, the dissolution of the glassy fraction of basalt is a major contributor to the chemical mass balance of seafloor alteration. Industrial producers are increasingly responsible for the safety of their products (i.e. European REACH and Food Contact Materials regulations). However, the relationship between the role of the elements inside glass and how these elements leach during alteration is not fully understood.

The present study focuses on the alteration process of a set of industrial and natural (obsidian and MORB) glasses in an acidic aqueous medium (4 vol% acetic acid, initial pH 2.3) at both 22 °C and 70 °C. The effects of glass dissolution include an increase in pH (specially at 70 °C), the leaching of the glass components into the liquid medium (analyzed by ICP-MS) and surficial structural modifications that can be tracked by Raman spectroscopy. The main changes are due to the interaction of  $\text{H}_3\text{O}^+$  and  $\text{OH}^-$  with the silicate network. Alteration changes both the speciation of silicate  $\text{Q}^n$ -groups and the polymerization of the network and, in consequence, the bonds to the network-modifying elements. The presence of cations of large ionic radius such as  $\text{Pb}^{2+}$  seems to favor the alteration.

**EMPG – XVII****17th International Symposium on  
Experimental Mineralogy,  
Petrology and Geochemistry**

## Abstracts

## Theme 7 “Element and isotope partitioning”

(sorted alphabetically by first author)

## Trace element partitioning between clinopyroxene, wollastonite & alkaline evolved melts: comparison between natural and experimental studies

Céline Baudouin<sup>1</sup>, Lydéric France<sup>1</sup>, Marine Boulanger<sup>1</sup>, Celia Dalou<sup>1</sup>, Jean-Luc Devidal<sup>2</sup>

<sup>1</sup> CRPG/CNRS, Nancy, France

<sup>2</sup> LMV, Clermont-Fd, France

In the case of alkaline magmas, few partition coefficient data are available. Natural and experimental studies should be considered to apply relevant D values for different alkaline-rich compositions and PT conditions. We calculated partition coefficients from Oldoinyo Lengai samples (East African Rift, Northern Tanzania) which is a carbonatite-phonolite volcano and a natural laboratory to study the REE concentration processes along the liquid line of descent. We have quantified element partitioning between alkali-rich phonolite melt and clinopyroxene (Cpx) and wollastonite (Woll).

Clinopyroxenes are widespread in alkaline systems and their crystallisation clearly govern the enrichment of associated residual melts. In alkaline rocks and carbonatites, Cpx display sinusoidal REE pattern with unusual enrichments in heavy REE (HREE) and in Zr-Hf. Based on our new results we show that the specific DREE partitioning of Cpx in some alkaline systems (DL<sub>a</sub>: 0.01, DH<sub>o</sub>: 0.06, DL<sub>u</sub>: 0.4) is not consistent with the standard models assuming incorporation of all REE in the M2 site; rather HREE substitutes both in M1 and M2 sites. HREE incorporation in M1 site is strongly dependant of Cpx geochemistry (Fe<sup>3+</sup>, Mn, Mg, Al<sup>IV</sup>). A parametrized model based on Cpx major element composition is also provided and compared to Mollo et al. 2016 (D derived from natural samples) and Beard et al. 2019 (experimental study).

Although rare in igneous systems, wollastonite is eventually common in silica-undersaturated and carbonatite systems, and is likely to play a role in magma differentiation. Previously, Law et al. (2000) proposed experimental derived partition coefficient at 3 GPa for silicate-carbonate melt, which have a small range of applications. We propose the first partition coefficients between Woll and silicate melts (Baudouin and France 2019). We highlight the strong incompatibility of Zr and Nb in Woll ( $D < 0.01$ ), and various behaviour for REE partition coefficients increasing from  $D_{La} = 0.2$  to  $D_{Lu} = 3$ . The crystallization of Woll strongly influences REE fractionation during magmatic differentiation of alkali-rich melts and should therefore be considered if we are to fully understand trace element evolution and partitioning in alkaline magma series.

### References:

- Beard, C. D., van Hinsberg, V. J., Stix, J., & Wilke, M. (2019). Clinopyroxene/melt trace element partitioning in sodic alkaline magmas. *J. Pet.*
- Mollo, S., Forni, F., Bachmann, O., Blundy, J. D., De Astis, G., & Scarlato, P. (2016). Trace element partitioning between clinopyroxene and trachy-phonolitic melts: A case study from the Campanian Ignimbrite (Campi Flegrei, Italy). *Lithos*, 252, 160-172.
- Law, K. M., Blundy, J. D., Wood, B. J., & Ragnarsdottir, K. V. (2000). Trace element partitioning between wollastonite and silicate-carbonate melt. *Min. Mag.*, 64(4), 651-661.
- Baudouin, C., & France, L. (2019). Trace element partitioning between wollastonite and alkaline silicate magmas. *Chem. Geol.*, 523, 88-94.

## Fate of carbon during the formation of Earth's core

I. Blanchard<sup>1</sup>, E. S. Jennings<sup>2</sup>, I. A. Franchi<sup>3</sup>, X. Zhao<sup>3</sup>, S. Petitgirard<sup>1</sup>, N. Miyajima<sup>1</sup>, S. A. Jacobson<sup>4</sup>, D.C. Rubie<sup>1</sup>

<sup>1</sup>Bayerisches Geoinstitut, Universität Bayreuth, 95440 Bayreuth, Germany

<sup>2</sup>Department of Earth and Planetary Sciences, Birkbeck, University of London, Malet Street, London WC1E77HX, United Kingdom

<sup>3</sup>School Physical Sciences, Open University, Milton Keynes MK7 6AA, UK

<sup>4</sup>Department of Earth and Environmental Sciences, Michigan State University, East Lansing, MI 48824, USA

Carbon is an element of great importance in the Earth, because it is intimately linked to the presence of life at the surface, and, as a light element, it may contribute to the density deficit of the Earth's iron-rich core. Carbon is strongly siderophile at low pressures and temperatures (1), hence it should be stored mainly in the Earth's core. Nevertheless, we still observe the existence of carbon at the Earth's surface, stored in crustal rocks, and in the mantle, as shown by the exhumation of diamonds. The presence of carbon in the crust and mantle could be the result of the arrival of carbon during late accretion after the process of core formation ceased or because of a change in its metal–silicate partitioning behavior at the high pressures and temperatures of core formation ( $P > 40$  GPa,  $T > 3500$  K). Previous studies reported metal–silicate partitioning of carbon based on experiments using large volume presses up to 8 GPa and 2200°C (2). We performed laser-heated diamond anvil cell experiments in order to quantify carbon partitioning behavior between liquid metal and silicate at the extreme conditions (49–71 GPa and 3600–4000 K) of Earth's core–mantle differentiation. We recovered our samples using the Focused Ion Beam technique and welded a 3  $\mu\text{m}$  thick slice of each sample onto a TEM grid. Major elements were analyzed by electron microprobe, whereas the concentrations of carbon in the silicate were analyzed by nanoSIMS. We thus have obtained metal–silicate partitioning results for carbon at  $PT$  conditions relevant to planetary core formation. While C remains siderophile in all experiments, its partition coefficient is up to two orders of magnitude lower than in low  $PT$  experiments. We derive a new parameterization of the pressure–temperature dependence of the metal–silicate partitioning of carbon and apply this in a state-of-the-art model of planet formation and differentiation (3,4) that is based on astrophysical N-body accretion simulations. Results show that BSE carbon concentration increases strongly starting at a very early stage of Earth's accretion and, depending on the concentration of carbon in accreted bodies, can easily reach or exceed estimated BSE values without requiring additional carbon delivery by late accretion events.

### References:

- (1) Dasgupta et al., 2013. *Geochimica et Cosmochimica Acta* 102, 191–212
- (2) Li et al., 2016. *Nature Geoscience* 9, 781–785
- (3) Rubie et al., 2015. *Icarus* 248, 89–108
- (4) Rubie et al., 2016. *Science* 353, 1141–1144

**The role of the crystallization kinetics on trace element partitioning between clinopyroxene and K-basaltic melts: investigation on a primitive composition from the Campi Flegrei Volcanic district (Italy)**

Barbara Bonechi<sup>1\*</sup>, Cristina Perinelli<sup>1</sup>, Mario Gaeta<sup>1</sup>, Alessandro Fabrizio<sup>2</sup>, Maurizio Petrelli<sup>3</sup>, Ladislav Strnad<sup>4</sup>

<sup>1</sup> Dipartimento di Scienze della Terra, Sapienza Università di Roma, P.le Aldo Moro 5, 00185, Rome, Italy

<sup>2</sup> Institute of Petrology and Structural Geology, Faculty of Science, Charles University, Albertov 6, 12843 Prague, Czech Republic

<sup>3</sup> Department of Physics and Geology, University of Perugia, Piazza Università, Perugia 06100, Italy

<sup>4</sup> Laboratories of the Geological Institutes, Charles University, Albertov 6, Prague 2, CZ-12843, Czech Republic

The role of the crystallization kinetics on trace elements partitioning behaviour between clinopyroxene and alkaline silicate glass have been investigated experimentally. Time-series experiments were conducted on a hydrous (~1 - 4 wt% of H<sub>2</sub>O) K-basalt from Procida Island (Campi Flegrei Volcanic District, south Italy) at temperatures of 1080-1250 °C and at 0.8 GPa of pressure, conditions relevant for deep magmatic reservoirs. In general, crystallization products show that large ion lithophile elements (LILE) are incompatible (e.g.,  $D_{Sr} \leq 0.15$ , where  $D$  is partition coefficients between clinopyroxene and melt), light rare elements (LREE; e.g.,  $D_{La} \leq 0.20$ ) are always more incompatible than heavy rare elements (HREE), which in some cases result to be compatible with clinopyroxene (e.g.,  $D_{Dy} = 1.40$ ); high field strength elements (HFSE) are generally incompatible ( $D_{HFSE} \leq 0.8$ ), while transition elements (TE) range from slightly incompatible (e.g.,  $D_V = 0.6$ ) to highly compatible (e.g.,  $D_{Cr} = 63$ ). Growth rate manifests a clear influence on the REE element partition coefficients as denoted by the highest  $D_{REE}$  values calculated in the runs with the highest growth rate ( $\sim 10^{-7}$  cm s<sup>-1</sup>). This is due to the less efficient rejection of incompatible elements during rapid crystal growth. Since growth rates are fast at the beginning of the crystallization process and then decrease with increasing time,  $D_i$  values should decrease with increasing time. Therefore, the apparent increase in  $D_{REE}$  values with time noticed in some runs is not ascribable to a change in time but rather to the dissimilar degrees of polymerization, expressed as the ratios NBO/T of these melts, strictly linked to a loss of Fe arisen during the experiments, and thus to a different melt viscosity. Indeed, the low NBO/T ratio calculated in the run with longer duration (9 hours) is associated to its higher loss of Fe with respect to the other run at 3 and 6 hours, pointing out the strong influence of melt structure and thus of melt viscosity on the partitioning behaviour of trace elements between clinopyroxene and basaltic melt. Finally, we used the calculated experimental clinopyroxene/melt partition coefficients to model the deepest step of the magmatic differentiation from a basaltic to a trachybasaltic composition in the Campi Flegrei Volcanic District, that results to be well reproduced by the fractionation of about 20-30% of a clinopyroxene >> olivine mineral assemblage from a basaltic parental magma.

## Oxygen fugacity and melt composition effect on nitrogen solubility in silicate melts: implications for Earth's magma ocean

Julien Boulliang<sup>1</sup>, Evelyn Füre<sup>1</sup>, Célia Dalou<sup>1</sup>, Laurent Tissandier<sup>1</sup>, Laurent Zimmermann<sup>1</sup>, Yves Marrocchi<sup>1</sup>

<sup>1</sup> Université de Lorraine, CNRS, CRPG, F-54000 Nancy, France.

During its accretion and earliest evolution, Earth experienced partial or perhaps complete melting as a result of the heat provided by radioactive decay, energetic impacts, and core formation. Magma ocean (MO) in- or outgassing thus controlled the abundance and distribution of nitrogen (N) at the surface of the young Earth. In this study, we investigate the influence of the oxygen fugacity ( $fO_2$ ) and melt composition on the N solubility in silicate melts through N equilibration experiments at atmospheric pressure and high temperature (1425°C). The oxygen fugacity (expressed with respect to the Fe-FeO (IW) buffer) was varied from IW -8 to IW +4.1, and the melt composition covered a wide range of polymerization degrees, defined by the NBO/T ratio (i.e., the number of non-bridging oxygen atoms per tetrahedrally-coordinated cations), which ranged from 0 to 2.0. The nitrogen content of the quenched run products (i.e., silicate glasses) was analyzed by both *in-situ* SIMS (1280-HR2) and bulk CO<sub>2</sub>-laser extraction-static mass spectrometry (VG-5400 and Noblesse HR). The results from the two methods are in good agreement even for nitrogen concentrations at the (sub-)ppm level. Furthermore, SIMS analyses demonstrate that the nitrogen concentration is homogenous across the glass spherules, confirming that equilibrium is reached between the gas and the melt during the 24-hour experiments.

The data obtained here highlight a fundamental control of both the  $fO_2$  and the polymerization degree of the silicate melt on the nitrogen solubility. Under highly reduced conditions ( $fO_2 = IW -8$ ), the nitrogen solubility increased with increasing NBO/T from  $17.4 \pm 0.4 \text{ ppm.atm}^{-1/2}$  in highly polymerized melts (NBO/T = 0) to  $6710 \pm 102 \text{ ppm.atm}^{-1/2}$  in depolymerized melts (NBO/T = 2). In contrast, under less reducing conditions ( $fO_2 > IW -3.4$ ), nitrogen solubility is very low ( $\leq 2 \text{ ppm.atm}^{-1/2}$ ), irrespective of the NBO/T value.

A key finding of this study is that nitrogen solubility under reducing conditions is governed by melt composition (i.e., melt structure), more particularly by the proportion of non-bridging oxygen (NBO) atoms in the melt. This confirms that interactions between nitrogen and oxygen of the silicate network control the chemical nitrogen dissolution in nominally anhydrous melts, likely by the substitution of O<sup>2-</sup> by N<sup>3-</sup>. However, for more oxidized conditions (i.e.,  $fO_2 \geq IW -3.4$ ), where nitrogen is expected to be incorporated into silicate melts in the form of N<sub>2</sub>, no significant N solubility variations were observed over a wide range of NBO/T values.

The new N solubility results provide constraints on the behavior of nitrogen in the shallow part of a MO. Mafic to ultra-mafic melts can incorporate 0.3 ppm to 35 ppm N under  $fO_2$  conditions inferred for the young Earth (i.e., IW -5 to IW). The nitrogen storage capacity of a reduced magma ocean (i.e., IW -3.4 to IW) in equilibrium with a nitrogen-rich atmosphere is  $\leq 1 \text{ ppm}$ , comparable to the nitrogen content of the present-day mantle. However under more reducing conditions (i.e., IW -5 to IW -4), the nitrogen storage capacity is significantly higher (35 ppm); in this case, Earth would have lost nitrogen to the atmosphere and/or nitrogen would have been transported into and stored within its deep interior (i.e., deep mantle, core).

## Calcium isotopes in alkaline rocks track metasomatism and melt types during progressive continental rifting

Chunfei Chen<sup>1,2</sup>, Stephen Foley<sup>1</sup>, Yongsheng Liu<sup>2</sup>, Ming Li<sup>2</sup>, Zaicong Wang<sup>2</sup>, Zsanett Pintér<sup>3</sup>

<sup>1</sup>Dept. of Earth and Environmental Sciences and ARC Centre of Excellence for Core to Crust Fluid Systems, Macquarie University, North Ryde, New South Wales 2109, Australia

<sup>2</sup>State Key Laboratory of Geological Processes and Mineral Resources, School of Sciences, China University of Geosciences, Wuhan 430074, China

<sup>3</sup>School of Earth, Atmosphere and Environment, Monash University, Clayton, Victoria, Australia.

Three generations of alkaline rocks comprising lamproites (1374 Ma), ultramafic lamprophyres (590–555 Ma), and nephelinites (141 Ma) occur at one location at Aillik Bay on the western margin of the Labrador Sea rift. These have been explained as products of gradual, episodic thinning of the lithosphere during rifting that passed through the North Atlantic craton, separating Archean crust in Labrador and western Greenland. We present new Ca isotope data for these alkaline intrusives to investigate the behaviour of calcium isotopes in magmas with a range of compositions that lie between silicate and carbonate melts.

Olivine phenocryst compositions in the Mesoproterozoic lamproites have high Ni but low Ca contents. These correlate with low whole-rock  $\delta^{44/40}\text{Ca}$  values (mostly 0.57 to 0.67‰), which are consistent with a metasomatic lithosphere source in which phlogopite pyroxenite veins are present. These were formed by injection of silicate melt itself derived from melting of materials including ancient sediments, into the base of lithosphere mantle.

In the second attempted rifting event, the  $\delta^{44/40}\text{Ca}$  values of the Late Neoproterozoic ultramafic lamprophyres are highly variable (0.46 to 0.80‰) and correlate positively with  $\text{SiO}_2$  content. This range results from enrichment of heavy Ca isotopes in differentiated carbonates during decarbonation, and light Ca isotopes in the residual silicate fraction (damtjernite) during liquid immiscibility. Primary aillikites have MORB-like  $\delta^{44/40}\text{Ca}$  values (0.74 to 0.80‰) consistent with melting of asthenosphere-derived phlogopite-carbonate veins at the base of the lithospheric mantle at depths of 120-150 km. New experiments on melting of peridotite with  $\text{H}_2\text{O}$  and  $\text{CO}_2$  at 4-7 GPa produce melts that range from carbonatite to ultramafic lamprophyre in composition and could result in phlogopite-carbonate-dominated veins when they crystallise in the lower lithosphere at these depths.

Olivine phenocrysts in the Cretaceous nephelinite-melilitite suite (the third stage, which was closely followed by successful rifting to produce ocean crust) have low Ni and high Ca contents implying that their source consisted of orthopyroxene-poor wehrlite. Positive correlation between  $\delta^{44/40}\text{Ca}$  values and  $\text{SiO}_2$  content indicate mixing of asthenosphere and enriched lithospheric mantle with low  $\delta^{44/40}\text{Ca}$ , which is explained as resulting from metasomatism by damtjernitic magma during the Late Neoproterozoic second stage.

These results highlight that episodic metasomatism weakens the lithosphere, and this is essential for inducing lithospheric melting and thinning to drive continental rifting. Our results also indicate that magmatic differentiation in carbonate-bearing systems may be the cause of the considerable variation of previously reported  $\delta^{44/40}\text{Ca}$  values in mantle-derived igneous rocks.

## Eu partitioning as a function of oxygen fugacity ( $fO_2$ ): Proposal for a Eu-in-pyroxene oxybarometer

Alessandro Fabbrizio <sup>1</sup>, Max W Schmidt <sup>2</sup>, Maurizio Petrelli <sup>3</sup>

<sup>1</sup> Institute of Petrology and Structural Geology, Faculty of Science, Charles University, Albertov 6, 12843 Prague, Czech Republic

<sup>2</sup> Institute of Geochemistry and Petrology, ETH Zürich, 8092 Zürich, Switzerland

<sup>3</sup> Department of Physics and Geology, University of Perugia, Piazza Università, Perugia 06100, Italy

The quantification of the mineral-melt partitioning behavior of elements that are heterovalent at geological conditions, as well as the relative abundances of oxidized and reduced species have the potential to constitute excellent proxies for the oxidation state of magma and may shed light on the influence of changing redox conditions on the chemical and physical properties of the magma such as volatile solubility, phase equilibria, and viscosity, which in turn influence the eruptive style of a volcano (Fabbrizio et al., 2021). Pyroxene is a common magmatic rock-forming mineral found in plutonic, effusive and metamorphic rocks that can host many different cations in its M1 and M2 sites. Eu is of particular interest as i) it is an abundant trace element in pyroxene, ii) it is a heterovalent element, and iii) the change from dominant  $Eu^{2+}$  to dominant  $Eu^{3+}$  falls within the range of redox conditions characterizing terrestrial magma (Carmichael, 1991). This implies that the relative proportions of  $Eu^{2+}$  and  $Eu^{3+}$  in a silicate melt will be a function of oxygen fugacity ( $fO_2$ ) and the magnitude of the resultant Eu anomaly in minerals resulting from different partition coefficients of  $Eu^{2+}$  ( $D_{Eu^{2+}}$ ) and  $Eu^{3+}$  ( $D_{Eu^{3+}}$ ) could then record the prevailing redox conditions (Fabbrizio et al. 2021). In this study, we report a series of experiments performed at high-temperature (1275-1300 °C), high-pressure (1.5 GPa) and varying  $fO_2$  ( $\sim -11 \leq fO_{2s} \leq \sim -1$ ) using a synthetic Fe-free basaltic starting material to better understand how Eu is fractionated between clinopyroxene (cpx), orthopyroxene (opx) and basaltic melt. A series of observations strongly suggest that  $fO_2$  influences  $D_{Eu}$  in pyroxene, these are: i) presence of europium anomaly in pyroxene, ii) the Onuma diagrams for di- and tri-valent cations of runs at reduced conditions do not include, respectively,  $Eu^{2+}$  and  $Eu^{3+}$ , whereas iii) those for trivalent cations of runs at oxidized conditions include  $Eu^{3+}$ , and  $Eu^{2+}$  is again out of the fit for divalent cations, iv) the calculated proportion of  $Eu^{2+}$  in the melt shows a variation with  $fO_2$ , and v) in runs with two pyroxenes the amount of  $Eu^{2+}$  in the melt calculated with  $D_{Eu}$  data for cpx and opx are comparable. The new experimental results for Eu are combined with previously reported data to parameterize a model for cpx-melt and for opx-melt Eu partitioning as a function of oxygen fugacity based on the expression  $D_{Eu} = [K \cdot D_{Eu^{2+}} + D_{Eu^{3+}}(fO_2)^{0.25}] / [K + (fO_2)^{0.25}]$ . By nonlinear least-square regression we obtained  $K = 29.8(5.6) \times 10^{-4}$  for cpx and  $K = 4.7(1.7) \times 10^{-3}$  for opx. The reported models reproduce measured Eu partition coefficients within a factor of two. Europium partitioning in pyroxene seems to be a promising tool for estimating the redox conditions in natural magmatic systems. However, additional experimental data are needed to expand the dataset, to explore the effect of other parameters such as bulk composition and the mutual interaction with other heterovalent elements (e.g. Fe).

### References:

Carmichael, (1991) Contrib. Mineral. Petrol., 106, 129-141

Fabbrizio et al., (2021) Chem. Geol., 559, 119967

## Bromine and Iodine Behaviour in Alkaline Magmas

C.F. Faranda<sup>1</sup>, G. Prouteau<sup>1,2,3</sup>, B. Scaillet<sup>1,2,3</sup>, J. Andujar<sup>1,2,3</sup>, I. Di Carlo<sup>1,2,3</sup>

<sup>1</sup> Université d'Orléans, ISTO, UMR 7327  
45071 Orléans, France

<sup>2</sup> CNRS/INSU, ISTO, UMR 7327  
45071 Orléans, France

<sup>3</sup> B.R.G.M., ISTO, UMR 7327  
P.O. Box 36009, 45060 Orléans, France

Volcanic eruptions can release huge amounts of climate sensitive species into the atmosphere, among which CO<sub>2</sub> and SO<sub>2</sub> figure prominently. Minor species such as the halogens also play a key role, in particular as destructive agents of the ozone layer. So far however, no extensive assessments of the impact of volcanic halogens on atmospheric composition and climate have been carried out. Such assessments require to characterize the deep cycling of halogens in order to constrain halogen emissions processes and ultimately construct emission fluxes datasets. Whilst the degassing behaviour of Cl and F has been experimentally well constrained, there is no such detailed knowledge for the heavy halogens Br and I. Especially, little is known about iodine behaviour in natural volcanic context, probably due to its concentration, several orders of magnitude lower than that of bromine. Previous studies in iron-free synthetic system showed that the distribution of Cl, Br and I between fluids and melts increasingly favors the fluid as the ionic radii of the halogenide ions increases<sup>1</sup>. These results suggest that the bromine and iodine flux to the atmosphere is probably underestimated and highlight the need to constrain their behavior in natural magma compositions. In this context, the behavior of Br and I in coexisting fluids and natural silicate melts has been investigated experimentally as a function of pressure, temperature, oxygen fugacity fluid and melt composition. Compositions investigated and corresponding geodynamic settings are representative of alkaline/ hyperalkaline magma degassing worldwide. The fluid/melt partitioning experiments were performed in rapid-quench internally heated pressure vessels (IHPV) under controlled oxygen fugacity. Br and I abundances in the experimental glasses were determined by  $\mu$ -XRF, LA-ICP-MS or SIMS, while fluid composition was estimated by mass balance calculations. The results show that bromine partitioning in the fluid-melt system is dependent on all investigated parameters and in agreement with previous studies performed using metaluminous composition<sup>2</sup>, bromine strongly favours fluid to silicate melts and  $D_{Br}^{f/m}$  increases drastically with melt silica content. The study of the behaviour of iodine is currently in progress and we are developing analytical methods allowing the analysis of this element (LA-ICP MS, neutron irradiation noble gas mass spectrometric technique). As a complement to conventional experiments, we will also perform in the near future gas sampling experiments that allow to extract and measure directly online the high pressure high temperature degassed fluids. We can therefore determine the gas composition in equilibrium with the melt at any fixed P-T and also during decompression down to atmospheric pressure. Data gathered in this study constitute part of the essential basis to develop the very first physically-based quantitative framework for volcanic heavy halogen emissions as a function of magma characteristics.

### References

- <sup>1</sup> Bureau et al., (2000), *Volcanic Degassing Of Bromine And Iodine: Experimental Fluid/Melt Partitioning Data And Applications To Stratospheric Chemistry*. Earth And Planetary Science Letters 183, 51-60.
- <sup>2</sup> Cadoux et al., (2018), *The Role Of Melt Composition On Aqueous Fluid Vs. Silicate Melt Partitioning Of Bromine In Magmas*, Earth And Planetary Science Letters 498, 450-463.

## Trace elements in the Lunar Magma Ocean: High-precision insights into partitioning behavior

Cordula Haupt<sup>1</sup> Stephan Klemme<sup>1</sup> Andreas Stracke<sup>1</sup> Christian Renggli<sup>1</sup> Arno Rohrbach<sup>1</sup>  
Jasper Berndt<sup>1</sup> Mischa Böhnke<sup>1</sup> Sabrina Schwinger<sup>2</sup>

<sup>1</sup> Institut für Mineralogie, WWU Münster, Corrensstraße 24, 48149 Münster

<sup>2</sup> Institut für Planetenforschung, Deutsches Zentrum für Luft- und Raumfahrt (DLR), Rutherfordstraße 2, 12489 Berlin

Recent models of Lunar Magma Ocean (LMO) chemical evolution (Elardo et al. 2011, Maurice et al. 2020) rely on modeled or experimentally defined partitioning information (c.f. Sun and Liang 2012, Dygert et al. 2020, Klemme et al. 2006). Specifically, modeling of the fractionation and crystallization history of the LMO (Snyder et al. 1992, Elardo et al. 2011) requires well-known partition coefficients of trace elements between minerals and coexisting melts. To check which thermo-chemical evolution scenarios and estimates of the bulk LMO composition are consistent with lunar rock analyses we need to know such partition coefficients. Partition coefficients are not constant values but depend on temperature, pressure, the redox conditions and on the chemical composition of the melt (Blundy and Wood 1998, Dygert et al. 2020). In the LMO fractionation history, clinopyroxene (Cpx) is the first Ca-bearing mineral to crystallize (Rapp and Draper, 2018), prone to incorporate the vast majority of trace elements, such as the REE (Lundstrom et al. 1998). Hence, Cpx is an important carrier of according trace elements and our main research interest.

In order to better constrain the solidification history and thermo-chemical evolution of the Moon and to parameterize the partitioning behavior of trace elements, we conducted 1-atm vertical tube furnace experiments with lunar compositions, based on estimates of the bulk silicate moon and fractionation experiments run by Rapp and Draper (2018). Starting mixtures are doped with a variety of trace elements incl. REE, transition metals, large ion lithophile and high field strength elements. The prepared powders are attached to Pt and Re-wire loops and hung into the furnace, where they are molten and cooled down until Cpx crystallizes. Different redox conditions are imposed by a mixture of CO and CO<sub>2</sub> and cover a wide range of conditions relevant for the Moon (IW to IW-2). Run products are characterized with SEM and analyzed by EPMA. Subsequently, Cpx and glass are separated mechanically by drilling using a Micro-Mill (New Wave Research). Mineral separates and glasses are analyzed using isotope dilution ICP-MS (Stracke et al. 2014). Uncertainties on the hereby measured trace element concentrations are usually one magnitude smaller than that of commonly employed in-situ microanalytical techniques. Refined information and reduced analytical uncertainties on the partitioning behavior of key elements in the LMO will improve models of the evolution of the lunar magma ocean.

### References:

Blundy and Wood (1998) *Earth Planet. Sc. Lett.*, 160:493-504; Dygert et al., (2020) *Geochim. Cosmochim. Acta* 279:258-280; Elardo et al., (2011) *Geochim. Cosmochim. Acta* 75, 11:3024-3045; Klemme et al., (2006) *Chem. Geol.* 234,251-263; Lundstrom et al., (1998) *Geochim. Cosmochim. Acta* 62,16:2849-2863; Maurice et al., (2020) *Science advances*, 6,28, eaba8949; Rapp and Draper (2018) *Meteorit Planet Sci*, 53,7:1432-1455; Sun and Liang (2012) *Contrib Mineral Petrol* 163:807-823 ; Snyder et al., (1992) *Geochim. Cosmochim. Acta* 56:3809-3823; Stracke et al., (2014) *Treatise on Geochemistry (Second Edition)*, 15:71-86

## Element partitioning into sulphides: implications for planetary core compositions

Ekaterina S. Kiseeva<sup>1</sup>, Bernard J. Wood<sup>2</sup>

<sup>1</sup> School of Biological, Earth and Environmental Sciences, UCC, Cork, T23 N73K, Ireland,

<sup>2</sup> Department of Earth Sciences, University of Oxford, South Parks Road, Oxford OX1 3AN, UK

Kiseeva and Wood (2013) showed that partitioning of most metals between sulphide and silicate melts is a strong function of the FeO content of the silicate melt and of the oxygen content of the sulphide. The relationship follows the equation  $D_i \approx A + n/2 \log(\text{FeO})$  where  $D_i$  is the partition coefficient of an element  $i$  between sulphide and silicate liquid,  $A$  is a constant related to the free energy of Fe-M exchange,  $n$  is a constant related to the valence of the element and  $[\text{FeO}]$  is the FeO content of the silicate melt in mole fraction or weight %. In a subsequent study (Kiseeva and Wood, 2015) we parameterised the effect of temperature, along with the Ni, Cu and oxygen contents of sulphide, expanding the model to more realistic sulphide compositions.

In this study, we compile a dataset of ~90 experiments (both published and new data) in order to expand the model to low FeO contents of the silicate liquid and to a wide range of silicate melt compositions, varying between dacitic and nephelinitic to boninitic and komatiitic compositions.

We show that at low FeO contents (<1 wt%) of the silicate liquid, strongly chalcophile elements, like Cu and Ag show a concave downward curve on a plot of  $\log D$  versus  $\log [\text{wt}\% \text{FeO}]$ . In contrast, a number of lithophile and weakly chalcophile elements, like Ce, Ti and Ga, respectively, show concave upward behaviour. Our results suggest:

1. The effect of S concentration in the silicate melt (at low FeO concentrations) and the effect of oxygen concentration in sulphides (at high FeO concentrations) are the most significant parameters affecting  $D_i$ .

2. Tl and In show the strongest dependences on silicate melt composition with  $D_{\text{Tl}}$  higher in high-Mg and low-Si melts, and  $D_{\text{In}}$  correlating negatively with both Si and Mg contents of the silicate melt.

3. Segregation of hadean matte is a plausible way to reproduce the pattern of chalcophile element abundances in the mantles of both Earth and Mars.

4. Partition coefficients of moderately chalcophile and lithophile elements into sulphide on Mercury are substantially higher than on Earth and on Mars, which means that Mercury's surface is likely enriched in moderately chalcophile elements (In, Pb, etc) (Fig. 1).

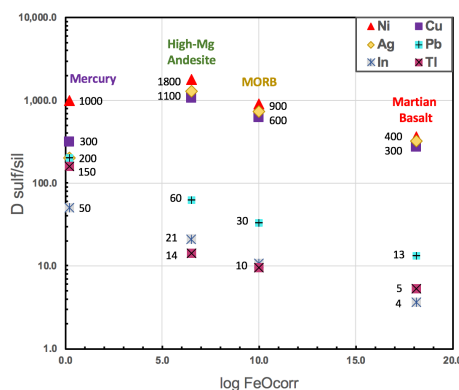


Figure 1. Calculated partition coefficients for chalcophile and lithophile elements between sulphide and basaltic melt on Earth, Mars and Mercury.

Kiseeva E.S., Wood B. J. (2013). *EPSL* 383, p. 68-81.

Kiseeva E.S., Wood B. J. (2015). *EPSL* 424, p. 280-294.

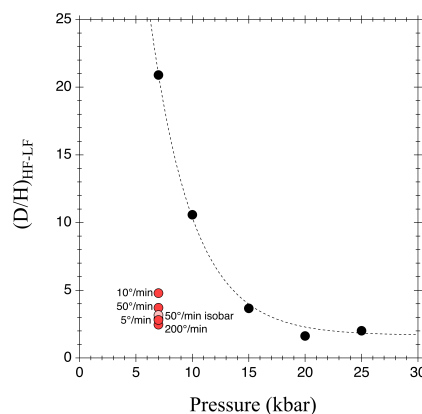
## Tracing D/H fractionation inside sodium silicate melts via $^1\text{H}$ and $^2\text{H}$ MAS NMR spectroscopy

Nico Kueter<sup>1\*</sup>, George D. Cody<sup>1\*</sup>, Dionysis I. Foustoukos<sup>1</sup>, Bjorn Mysen<sup>1</sup>

<sup>1</sup> Carnegie Science Earth and Planets Laboratory, 5251 Broad Branch Road, NW, 20015 – Washington D.C., U.S.A.

\*corresponding authors: [nkueter@carnegiescience.edu](mailto:nkueter@carnegiescience.edu), [gcody@carnegiescience.edu](mailto:gcody@carnegiescience.edu)

Hydrogen isotopes are important tracers for unravelling the deep water cycle on Earth. However, in contrast to the temperature-dependent isotope fractionation of higher-mass elements, the fractionation of hydrogen isotopes is also controlled by molar volume and pressure changes [1]. Hydrogen isotope fractionation in magmatic/hydrothermal systems is not well understood, especially regarding the unusual deuterium-enrichment in the fluid phase and the surprisingly large fractionation factors of several 100 ‰ [2-4]. Recent experimental studies recognized a preferential deuterium enrichment in the vicinity of alkali cations dissolved in the silicate melt (“*cation site*”) relative to the silicate network itself (“*network site*”), giving rise to a little known isotope effect *inside* the silicate melt [2,4]. To constrain this isotope effect, we performed pressure (7-25 kbar), temperature (900-1400 °C) and quench-rate (5-4100 °/min) experiments in the hydrous sodium-silicate system (NS4, 1:4 Na<sub>2</sub>O - SiO<sub>2</sub> + 2 to 8 wt% 1:1 H<sub>2</sub>O-D<sub>2</sub>O), by using a solid-media, high-pressure apparatus. Run products were analysed by  $^1\text{H}$  and  $^2\text{H}$  magic angle spinning nuclear magnetic resonance spectroscopy (MAS NMR) to reveal the site partitioning of hydrogen isotopes, dissolved in form of molecular X<sub>2</sub>O and Si-OX (silanol; X= D or H) in the quenched silicate melt. Our results confirm a deuterium enrichment in the cation site. Protonated species are preferentially partitioned into the silicate network and are less abundant at the cation site. The resulting D/H fractionation between the sites appears to be less sensitive to temperature, but is highly dependent on pressure (Fig. 1). Data suggest that D/H site fractionation is decreased when the system undergoes fluid phase separation induced by slow-quenching. A strongly deuterated cation site paired with a high partition ratio of Na into the fluid phase [5] could explain the large (D/H)<sub>fluid-melt</sub> fractionation factors observed in in-situ hydrothermal diamond anvil experiments [3].



shown equilibrated at 1400°C for 2 hours. Black symbols: rapid quench, red symbols: quench-rate

### References:

- (1) Horita et al., (2002) GCA 66:3769-3788
- (2) Wang et al., (2015) Am. Mineral., 100:1182-1189
- (3) Dalou et al., (2015) EPSL, 426:158-166
- (4) Le Losq et al., (2016) Geochim. Perspect. Lett. 2:87-94
- (5) Zajacz et al., (2008) GCA 72:2169-2197

## Trace element partitioning between aqueous fluids and hydrothermal pyrite

Christof Kusebauch<sup>1</sup>, Sarah A. Gleeson<sup>1,2</sup>, Marcus Oelze<sup>1</sup>

<sup>1</sup> GFZ Potsdam, Telegrafenberg, 14473 Potsdam

<sup>2</sup> FU Berlin, Malteserstr. 74-100,

Pyrite is the most abundant sulfide on Earth and can host a large variety of trace elements including Au, Co, Mo, Cu, Pb, As, Se, Te, Bi and Sb. Trace element variations in pyrite have been used to study various processes during ore formation, to reconstruct paleo-seawater composition and to understand hydrothermal systems. Furthermore, element enrichment in pyrite can reach high enough concentrations that pyrite itself becomes an ore mineral and can be mined. For example, the enrichment of Au in As-bearing pyrite can reach up to several thousand ppm in the giant Au deposits of the Carlin trend (Nevada, USA). In this case the coupled partitioning of Au and As is considered to be an ore forming process<sup>1</sup>. The high variability of trace elements in pyrite makes it potentially a powerful tool for the reconstruction of fluid compositions in hydrothermal settings. Nevertheless, the lack of partition coefficients (D values) of trace elements between hydrothermal fluids and coexisting/newly forming pyrite hinders a wider use of pyrite as a fluid proxy. Also, the underlying processes controlling the incorporation into the crystal structure and the interplay of different trace elements during partitioning are not well understood.

Here, we present first results of hydrothermal batch experiments done at 200°C studying the partitioning of Co, Cu, Pb, Se, Bi, As and Sb between aqueous solutions and newly formed pyrite. We grew euhedral pyrites large enough to be measured by LA-ICPMS for their trace element content by coupled dissolution-precipitation reaction of siderite with an H<sub>2</sub>S-rich fluid<sup>2</sup>. The initial trace element concentration in the experimental fluid varied from 0.1 to 10 ppm. To study the influence of As in pyrite on the partition coefficients, As concentration in the experiments was varied independently, whereas all other tracers had a constant ratio.

Concentrations of trace elements in hydrothermal pyrite range between 10 ppm and 1200 ppm, and depend strongly on the initial fluid composition. Partition coefficients for Sb and Se are in the range of 20-300. Co, Cu, Pb, Bi have lower but more variable D values ranging from 0.1 up to 50. Almost all studied elements show a high compatibility in the pyrite structure, replacing most likely either S (i.e., Se, Sb) or Fe (i.e., Co, Cu, Bi, Pb) in the crystal structure. Unlike Au, partitioning of studied trace metals is not coupled to the As concentration of newly formed pyrite. Nevertheless, D values of Co, Cu, Se and Sb from experiments with a high concentration of trace elements (i.e., 10 ppm) decrease compared to D values from experiments done at lower concentrations (i.e. 0.1 and 1 ppm). This behavior indicates either a solubility limit of the particular element in the pyrite structure or results from an over-occupation of the potential crystal sites by other trace elements. The partition data from our experiments will help to unlock the potential to use the pyrite composition as a proxy for hydrothermal fluids.

### References:

<sup>1</sup> Kusebauch et al., (2019) *SciAdvances*, 5:eaav5891

<sup>2</sup> Kusebauch et al., (2018) *Chemical Geology*, 500, 136-147

## The influence of intensive parameters (P-T) on the partitioning of trace element between basaltic melt and olivine, clinopyroxene, orthopyroxene and hornblende

Elena Melekhova<sup>1</sup>, Jon Blundy<sup>1</sup>, Barbara Kunz<sup>2</sup>

<sup>1</sup> School of Earth Sciences, University of Bristol, Wills memorial Building, Queens Road, Bristol, BS8 1RJ

<sup>2</sup> School of Environment, Earth and Ecosystem Sciences, The Open University, Gass building, Walton Hall, Milton Keynes, MK7 6AA

To be able to quantify petrological processes we need to have accurate partition coefficients between minerals and melts. Partition coefficients ( $D_0$ ) are controlled by pressure, temperature and composition. In this study we obtained consistent data set of partition coefficients for olivine/melt, clinopyroxene/melt, orthopyroxene/melt, and hornblende/melt. A total of 29 equilibrium piston cylinder experiments have been carried out at 0.4, 0.7, 1.0 and 1.3 GPa, temperature range, 1350 to 1050 °C and three different initial H<sub>2</sub>O content, 0.6, 2.3 and 4.5 wt%. Starting composition of high-Mg basalt (RSV49, Melekhova et al., 2015) was doped with trace elements at ppm level. The total amount of trace elements added was ~ 4000ppm. Forty minor and trace elements in minerals and glasses were analysed with combination of laser ablation inductively coupled plasma mass spectrometry (Open University) and ion micro-probe (University of Edinburgh). Melt composition in experimental run products changes systematically from high-MgO basalt to andesite. The coexisting minerals also change their composition systematically with P-T-H<sub>2</sub>O (Melekhova et al., 2015).

$D_{\text{REE}}$  for all four minerals show parabolic patterns when plotted against ionic radius, following closely lattice strain model of Blundy & Wood (1994). We did not find any effect of H<sub>2</sub>O on  $D_{\text{ol/melt}}$  but there is an increase of  $D_{\text{Li}}$  with pressure, and  $D_{\text{Be}}$  and  $D_{\text{Y}}$  with temperature.

Comparison of clinopyroxene and hornblende  $D_i$ , at the same initial H<sub>2</sub>O content, reveals very little change with temperature and pressure. The  $D_i$  is almost constant throughout the explored parameters. The effect of H<sub>2</sub>O on clinopyroxene-melt  $D_i$  is minor at our experimental conditions and result only in increase of Rb with increasing H<sub>2</sub>O<sub>melt</sub>. We do not have enough data to explore effect of H<sub>2</sub>O on hornblende-melt  $D_i$ . This data suggests that single set of  $D_i$  for olivine, clinopyroxene, hornblende and orthopyroxene is sufficient for modelling trace element evolution of hydrous basalt differentiation in mid- to lower-crustal pressures.

### References:

Melekhova et al., (2015) J. Petrol., 56, 161-192

## Trace element partitioning in hyperalkaline magmatic systems: an experimental study

Sander M. Molendijk<sup>1</sup>, Olivier Namur<sup>1</sup>, Paul R. D. Mason<sup>2</sup>, Benoît Dubacq<sup>3</sup>, Benoît Smets<sup>4</sup>, Bernard Charlier<sup>5</sup>

<sup>1</sup> Department of Earth and Environmental Sciences, KU Leuven, Celestijnenlaan 200E, 3001 Leuven, Belgium

<sup>2</sup> Department of Earth Sciences, Utrecht University, Budapestlaan 4, 3584 CD Utrecht, The Netherlands

<sup>3</sup> Sorbonne Université, CNRS-INSU, Institut des Sciences de la Terre Paris, IStEP, UMR 7193, F-75005 Paris, France

<sup>4</sup> Department of Earth Sciences, Royal Museum for Central Africa, Leuvensesteenweg 13, B-3080 Tervuren, Belgium

<sup>5</sup> Département de Géologie, Université de Liège, B-4000 Liège, Belgium

The partitioning of trace elements between alkaline melts and their dominant mineral phases remains poorly constrained. Feldspathoids in particular have received only limited attention with regards to their trace element uptake, limiting our ability to interpret geochemical trends for alkaline magmatic systems. Here we investigate the influence of the melt-, and crystal-composition on partitioning for feldspathoids, Ca-rich pyroxene, and olivine. We have performed a series of 1 atm gas-mixing experiments using a variety of highly alkaline ( $\text{Na}_2\text{O} + \text{K}_2\text{O} = 4.15\text{-}14.97$  wt.%), silica undersaturated ( $\text{SiO}_2 = 36.73\text{-}45.96$  wt.%) lava compositions from Nyiragongo, DR Congo ( $\text{Mg\#} = 31\text{-}79$ ). Experimental runs were performed at a variety of temperatures with  $f\text{O}_2$  buffered at both QFM (quartz-fayalite-magnetite) and QFM+1 in order to measure the partition coefficients along the entire series of naturally occurring phases (leucite, nepheline, melilite, rhönite ( $\text{Ca}_2[\text{Mg,Fe,Ti}]_6[\text{Si,Al}]_6\text{O}_{20}$ ), clinopyroxene, and olivine). Samples were cooled down from super-liquidus ( $1180 - 1500$  °C) to final temperature at a rate of 2-3 °C/h and were left to equilibrate for 2 to 5 days depending on temperature. Glass-crystal pairs in quenched products were analysed by EPMA and LA-ICP-MS in order to constrain partition coefficients for the rare earth elements (REEs), large-ion lithophile elements (LILEs), and high-field-strength elements (HFSEs). Leucite and aluminian melilite are respectively reported to be preferential carriers of LILEs (e.g.  $D_{Cs}^{Lc} = 10 - 24$ ) and Sr ( $D_{Sr}^{Mel} = 0.9 - 2.5$ ). The partitioning behaviour of rhönite is shown to be analogous to clinopyroxene, incorporating significant amounts of transition metals (e.g.  $D_{Sc}^{Rh} = 7 - 11$ ,  $D_V^{Rh} = 1.7 - 2.1$ ), and having a strong preference for heavy over light rare earths ( $\frac{D_{La}^{Rh}}{D_{Yb}^{Rh}} \approx 0.25$ ). Incorporation of trace elements in clinopyroxene (Cpx) is indicated to be primarily crystallographically controlled, positively correlating with the fraction of aegirine in the crystal. REEs are more compatible in these cpx as compared to tholeiitic systems, and a slight enlargement of the M2 site results in more favourable incorporation of light and middle rare earths ( $\frac{D_{La}^{Cpx}}{D_{Yb}^{Cpx}} = 0.37 \pm 0.03$  vs  $0.15 \pm 0.1$ <sup>[1]</sup>). The reported partitioning behaviours indicate that whole-rock trends at Nyiragongo cannot solely be explained through fractional crystallization, but also require an effect of crystal accumulation processes.

### References:

[1] Bédard, J. H., (2014) *Geochem Geophys.*, 15, 303-336

## S-gas-silicate reaction experiments at highly reducing conditions

Christian J. Renggli<sup>1</sup> Stephan Klemme<sup>1</sup> Jasper Berndt<sup>1</sup>

<sup>1</sup> Institut für Mineralogie, Uni Münster, Corrensstr. 32, 48149 Münster, renggli@uni-muenster.de

Gas-solid reactions between S-rich gases and silicates at high temperatures are ubiquitous on terrestrial planetary bodies (King et al. 2018). At oxidizing conditions on the Earth or on Mars, the reaction between SO<sub>2</sub>-rich gas and silicate glasses and minerals results in the formation of sulfates (Renggli & King 2018, Renggli et al. 2019). These reactions occur in explosive volcanic eruptions, where volcanic ash particles scavenge SO<sub>2</sub> from the eruption plume (Ayriss et al. 2013, Delmelle et al. 2018), or in the subvolcanic environment where sulfates and sulfides form large porphyry copper deposits (Henley et al. 2015). Similar gas-solid reactions are also inferred at reducing conditions. For example, sulfidation of silicate minerals is observed in lunar Apollo samples (Norman et al. 1991) and in enstatite chondrites (Fleet & MacRae 1987, Lehner et al. 2013). We propose, that sulfidation reactions between reducing C-O-S-gas and silicate minerals, melts and glasses are responsible for the enrichment of S on the surface of Mercury, where up to 4 wt.% of S have been detected by the NASA MESSENGER mission (Weider et al. 2015).

We conduct experiments in evacuated silica glass tubes at temperatures from 800-1200 °C. The experimental load consists of two graphite crucibles, placed above each other in the silica glass tube, separated by silica glass wool (Fig. 1). The lower graphite crucible contains elemental S, which forms a gas at high temperatures. This gas reacts with the silicate samples placed in the upper graphite crucible, resulting in the formation of sulfides. One aliquot of the reacted samples was embedded in epoxy resin, cut, and polished for electron microprobe analysis. A second aliquot of samples was used to image the reacted surfaces by electron microscopy.

Here we present observations of the sulfidation of the minerals anorthite, diopside and Fo-rich olivine. We observe sulfides in all experiments, increasing in abundance with temperature. On the reacted anorthite we identify CaS (oldhamite), on the diopside CaS and (Mg,Ca)S, and on the olivine (Mg,Fe)S and (Fe,Cr,Ti)S. The sulfides are associated with a depletion of the sulfide-forming cations (Ca, Mg, Fe, Ti) in the silicate, including the nucleation of SiO<sub>2</sub> where the reaction resulted in a complete consumption of Ca, Mg and Fe by the sulfides.

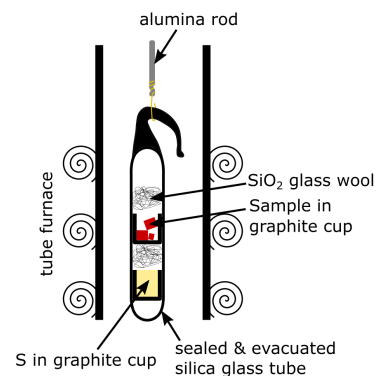


Fig. 1: Experimental setup of silicate sulfidation experiments in a sealed silica glass tube.

### References:

- King et al., (2018) *Rev. Mineral. Geochem.* 84, 1-56. Renggli & King, (2018) *Rev. Mineral. Geochem.* 84, 229-255. Delmelle et al., (2018) *Rev. Mineral. Geochem.* 84, 285-308. Renggli et al., (2019) *J. Geophys. Res. Planet.* 124, 2563-2582. Ayriss et al., (2013) *Geochim. Cosmochim. Ac.* 110, 58-69. Henley et al., (2015) *Nat. Geosci.* 8, 210-215. Norman et al., (1991) *Geophys. Res. Lett.* 18, 2018-2084. Fleet & MacRae, (1987) *Geochim. Cosmochim. Ac.* 51, 1511-1521. Lehner et al., (2013) *Geochim. Cosmochim. Ac.* 101, 34-56. Weider et al., (2015) *Earth. Plan. Sc. Lett.* 416, 109-120.

## Ni and Sr uptake during serpentine formation and implications for redox conditions in altered peridotite and element transfer *via* subduction

A.D. Rosa<sup>1</sup>, M. Louvel<sup>2</sup>, A-L. Auzende<sup>3</sup>, L. Truche<sup>3</sup>, E. Nielsen<sup>4</sup>, M. Krstulovic<sup>5</sup>,  
F. Rodriguez<sup>6</sup>, T. Irifune<sup>7</sup>, M. Munoz<sup>8</sup>, E. Schwarzenbach<sup>9</sup>, M. Wilke<sup>5</sup>

<sup>1</sup> European Synchrotron Radiation Facility, Grenoble, France

<sup>2</sup> Institute for Mineralogy, University of Muenster, Germany

<sup>3</sup> Institut des Sciences de la Terre, Université Grenoble Alpes, France

<sup>4</sup> Department of Chemistry, University of Copenhagen, Denmark

<sup>5</sup> Institute for Geosciences, University of Potsdam, Germany

<sup>6</sup> Department of Earth Sciences and Condensed Matter Physics, University of Cantabria, Spain

<sup>7</sup> Geodynamics research centre, Matsuyama, Japan

<sup>8</sup> Géosciences Montpellier, University of Montpellier, France

<sup>9</sup> Mineralogy-Petrology, Freie Universitaet Berlin, Germany

It is well established that serpentines form in the mantle wedge by hydration of olivine (the major mantle constituent) with aqueous slab-derived fluids. These slab-derived fluids are enriched in fluid mobile elements (FMEs) such as Ba, Sr, Sb, Pb [1]. Recent field observations have shown that mantle-wedge serpentines may be important hosts for FMEs and volatiles and could constitute important tracers for chemical mass transfers in subduction zones. [2, 3, 4]. The interpretation of elemental concentration patterns in obducted serpentinites in terms of fluid generation and chemical mass transfer requires precise knowledge on the elemental uptake capacity of newly formed serpentine. Such data are presently limited due to the experimental difficulties. Serpentines play also a key role in controlling the redox conditions of the coexisting fluid phases [5]. While iron has been widely studied, the role of Ni, an element highly compatible in serpentine [6] and also potentially mobile in the fluid [7] has been so far little investigated.

In this contribution, we will present the geochemical behavior of strontium and nickel during serpentinization and the role of serpentinization in the global cycling of these elements. We have combined micro X-ray fluorescence emission and absorption spectroscopy ( $\mu$ XRF and  $\mu$ XAS) techniques with a resistively heated diamond anvil cell (RH-DAC), which allows operating *in situ* during stable high *P/T* conditions. This approach permitted to investigate quantitatively the uptake of strontium and nickel during serpentine formation from olivine and slab-derived fluids at the shallow mantle-wedge conditions (0.3 GPa and 300°C). The incorporation mechanism of Ni and Sr in serpentine was derived from the analysis of the XAS data and full multiple scattering calculations. Recovered samples were characterized for elemental compositions using SEM and for structural characteristics using XRD. Our *in-situ* observations on Ni were further complemented with *ex-situ* autoclave experiments and measurements on natural serpentinized harzburgite from the Santa Elena Ophiolite in Costa Rica.

### References:

- [1] Van Keken, et al., (2011) *J. Geophys. Res.*, B1, 116, 2156-2202.
- [2] Deschamps et al., (2011), *Terra Nova*, 23, 171-178.
- [3] Deschamps et al., (2012), *Chem. Geol.*, 312-313, 93-117.
- [4] Lafay et al., (2013), *Chem. Geol.*, 343, 38-54.
- [5] Schwarzenbach et al., (2016), *Contrib. Mineral. Petrol.*, 171:5
- [6] Munoz et al., (2019), *J. Geochem. Expl.*, 198, 82-99
- [7] Scholten et al., (2018), *Geochem. Cosmochem. A.*, 224

## Titanium isotope fractionation in synthetic Ti-rich lunar melts

Laura Jennifer, Anabel Rzehak<sup>1,2</sup>, Sebastian Kommescher<sup>2</sup>, Raúl O.C. Fonseca<sup>1</sup>

<sup>1</sup> Institut für Geologie, Mineralogie und Geophysik, Universitätsstraße 150, 44780 Bochum

<sup>2</sup> Institut für Geologie und Mineralogie, Zùlpicher Straße 49b, 50674 Köln

Fractional crystallisation of a lunar magma ocean (LMO) culminated in a sequence of ilmenite-bearing mafic cumulates (IBC) and a residual component enriched in incompatible trace elements (i.e. KREEP). After complete LMO crystallisation, the lunar mantle overturned, which generated large volumes of magma that filled impact craters with what are now lunar mare basalts. Mare basalt petrogenesis likely involved partial melting or assimilation of IBC. Mare basalts, which can be divided into low- and high-Ti varieties, are well suited to investigate Ti stable isotope fractionation since they can contain up to 16 wt.% TiO<sub>2</sub><sup>[1]</sup>. Low-Ti mare basalts resemble unfractionated terrestrial basalts with respect to their Ti isotope composition. Conversely, high-Ti mare basalts have elevated  $\delta^{49}\text{Ti}$  (+0.011 to +0.033 ‰), coupled with Ta/W and Hf/W fractionation associated with TiO<sub>2</sub> enrichment, which indicates the involvement of Fe-Ti-oxides in their petrogenesis<sup>[2,3]</sup>. The presence of Ti-rich oxides like ilmenite and rutile during basalt petrogenesis leads to Ti isotope fractionation in both lunar and terrestrial samples<sup>[2,4,5]</sup> where Ti-oxides are isotopically light and coexisting melt is isotopically heavy, which likely explains the range in  $\delta^{49}\text{Ti}$  of lunar mare basalts. However, at  $f\text{O}_2$  relevant to lunar magmatism ( $\sim$  IW-1) 10% of the overall Ti is Ti<sup>3+</sup><sup>[6]</sup>, which might influence Ti stable isotope fractionation during petrogenesis of lunar basalts to an unknown extent.

In order to determine the effect of Fe-Ti-oxides and  $f\text{O}_2$  on Ti stable isotope fractionation during mare basalt petrogenesis, experiments with variable TiO<sub>2</sub>-rich compositions were carried out at different  $f\text{O}_2$  using gas mixing furnaces at the University of Cologne. Two identical bulk compositions were equilibrated simultaneously during each experiment to guarantee reproducibility. One experiment was investigated with the EPMA to characterise experimental run products, whereas the second experiment was crushed, and phases (i.e. oxides, silicates and glass) were handpicked, separated and digested. Subsequently, an aliquot of each sample was mixed with a Ti double-spike, and then processed in a highly modified HFSE chemistry<sup>[7,8]</sup> to separate Ti from matrix and interfering elements. The long-term reproducibility of the applied <sup>47</sup>Ti-<sup>49</sup>Ti double spike technique is better than 0.076‰ (2 s.d.) after  $n = 196$  measurements, which corresponds to a 95% confidence interval of 0.005‰ at 95% confidence on  $\delta^{49}\text{Ti}$ . All  $\delta^{49}\text{Ti}$  values are given relative to OL-Ti<sup>[9]</sup>.

First results show that from oxidised to reduced conditions, armalcolite displays light Ti isotope compositions ( $\delta^{49}\text{Ti}$  relative to OL-Ti<sup>[9]</sup> of -0.056‰ after equilibration in air, to -0.003‰ at IW-1). Coexisting orthopyroxenes have higher  $\delta^{49}\text{Ti}$  (+0.033‰ to +0.247‰ over the same  $f\text{O}_2$  range). Silicate melt in the same experiments shows intermediate values of  $\delta^{49}\text{Ti}$  (+0.035‰ to +0.197‰). Our results show that Ti isotope fractionation during mare basalt petrogenesis is likely to be redox dependent and mineral-melt fractionation factors as determined at terrestrial  $f\text{O}_2$  may not be directly applied in the case of lunar basalt petrogenesis.

[1] Marvin and Walker, (1978) *Am. Mineral.*, 63, 924-929; [2] Millet et al., (2016) *EPSL*, 449, 197-205; [3] Münker, (2010) *GCA*, 74, 7340-7361; [4] Schauble et al., (2004) *Rev. Mineral. Geochem.*, 55, 65-111; [5] Deng et al., (2019) *PNAS*, 116 (4), 1132-1135; [6] Leitzke et al., (2018) *Contrib. to Mineral. Petrol.*, 173, 103; [7] Tusch et al., (2019) *GCA*, 257, 284-310; [8] Kommescher et al., (2020) *GPL*, 13, 13-18; [9] Millet and Dauphas, (2014) *JAAS*, 29, 1444

## Lithium and Boron mobility in degassing magma: an experimental study

Roberta Spallanzani<sup>1</sup>, Sarah B. Cichy<sup>1,2</sup>, Ken Koga<sup>3</sup>, Marcus Oelze<sup>2</sup>, Max Wilke<sup>1</sup>, Sara Fanara<sup>4</sup>, Michael Wiedenbeck<sup>2</sup>

<sup>1</sup>Institute for Geosciences, University of Potsdam, Germany (spallanzani@uni-potsdam.de)

<sup>2</sup>Helmholtz Centre Potsdam, GFZ German Research Centre for Geosciences, Germany

<sup>3</sup>Laboratoire Magmas et Volcans, Université Clermont Auvergne, France

<sup>4</sup>Institute of Mineralogy, Georg-August University Göttingen, Germany

It is well established that the concentration and behaviour of major volatile elements affect volcanic characteristics such as eruption style and dynamics. Among the minor volatile species, Lithium and Boron are light elements with comparable properties. Because of their fluid-mobility, they have been largely used in the past decades to track fluid-related processes in subduction zones; this property can also be applicable to volcanic systems. Therefore, the main goal of this study is to trace elemental diffusion and isotopic fractionation of Li and B as a function of decompression-driven magma degassing. First, we performed sets of diffusion-couple experiments, in order to better characterize the mobility of Li and B in highly silicic and water-bearing melts. Pressure was kept constant at 300 MPa, while we investigated the temperature between 700 and 1250 °C with run durations in the range of 0 seconds to 24 hours. Subsequently, isothermal decompression experiments were performed from 300 MPa to 75 MPa (at 900 and 1000 °C), varying decompression rates between 0.125 and 0.004 MPa/s. All experiments were done in an internally heated pressure vessel, while elemental concentrations of the end-products were measured by LA-ICP-MS and isotopic ratios will be quantified by SIMS analysis. Preliminary diffusion data show that the two elements are substantially different in terms of diffusion rate. For instance, the 0 seconds experiment at 1000 °C shows no elemental diffusivity for Boron, whereas Lithium results in almost complete homogenisation. This agrees with other studies that present Lithium as a very fast-diffusing element in hydrated melts<sup>[1,2]</sup>. Our decompression experimental results indicate an enrichment of Lithium towards the bubble meniscus, even at the highest decompression rate. On the contrary, Boron needs slower decompression (i.e. longer run durations) to show notable variations in concentration over the measured diffusion profile length. We expect to confirm findings from previous studies, showing that for both elements the heavy isotope (<sup>7</sup>Li, <sup>11</sup>B) is more concentrated in the fluid phase than the light isotope (<sup>6</sup>Li, <sup>10</sup>B)<sup>[1,3]</sup>. However, their diffusive behaviour is opposed, where the lighter <sup>6</sup>Li and the heavier <sup>11</sup>B are the fast-diffusing isotopes<sup>[2,3]</sup>. We will correlate these results with the decompression-induced bubble formation processes, in order to identify possible links between Li and B mobility and the decompression rate, creating a useful proxy to trace magmatic ascent rates.

### References:

- [1] Richter FM, Davis AM, DePaolo DJ, Watson EB (2003) Isotope fractionation by chemical diffusion between molten basalt and rhyolite *GCA* 67, 20, 3905-3923
- [2] Holycross M.E, Watson EB, Richter FM, Villeneuve J (2018) Diffusive fractionation of Li isotopes in wet, highly silicic melts. *GPL* 6, 39-42
- [3] Hervig RL, Moore GM, Williams LB, Peacock SM, Holloway JR, Roggensack K (2002) Isotopic and elemental partitioning of boron between hydrous fluid and silicate melt. *AmMin* 87, 769-774

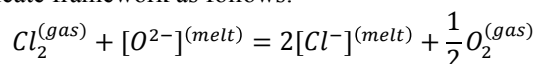
## The chemical behaviour of chlorine in silicate melts

Richard W Thomas<sup>1\*</sup>, Bernard J Wood<sup>1</sup>

<sup>1</sup> Department of Earth Sciences, University of Oxford, UK  
\* richard.thomas@earth.ox.ac.uk

The Halogens (F, Cl, Br and I) are typically found as minor components in many magmatic and hydrothermal systems. Despite their relatively low abundances, they are thought to strongly affect the chemical and physical properties of melts [1], the genesis and evolution of magmas, and their eruptive processes [2]. Understanding these effects requires knowledge of the thermodynamic properties of halogens in silicate melts, which is the principal aim of our study. In order to measure halogen activities, we added halogen buffers such as Ag/AgCl, Ag/AgI and Ag/AgBr in which the metal (as oxide) is virtually insoluble in silicate melt under the conditions of the experiment. The buffer controls the fugacity of the halogen of interest. Experiments were performed at 5-20 Kbar and temperatures of 1200-1500°C in a piston-cylinder apparatus. The effect of oxygen fugacity on Cl solubility was also tested using Pt-PtO<sub>2</sub>, Re-ReO<sub>2</sub> and C-CO<sub>2</sub> oxygen buffers.

Our experiments show (1) that chlorine solubility in haplobasalt at 1.5GPa/1400°C can reach 5 weight %, even at Cl<sub>2</sub> fugacities as low as 0.0035 bar; thus, Cl has the potential to dissolve into silicate melts at concentrations much higher than is typically seen in nature. (2) Cl concentration increases linearly with the square root of chlorine fugacity at fixed  $f(O_2)$ , obeying Henry's law, up to ~3% Cl in the melt. An additional series of experiments were conducted at various  $f(Cl_2)$  using an Icelandic basalt. This also obeyed a Henrian relationship with increasing  $\sqrt{f(Cl_2)}$ , but with lower Cl solubility at fixed Cl fugacity than the haplobasalt. The data indicate that chlorine dissolves in the melt as Cl<sup>-</sup>. (3) Cl solubility increases linearly with the fourth root of oxygen fugacity at fixed  $\sqrt{f(Cl_2)}$ . Therefore, Cl<sup>-</sup> replaces O<sup>2-</sup> in the silicate framework as follows:



(4) At fixed  $f(Cl_2)$  and  $f(O_2)$ , Cl solubility increases with temperature. (5) Cl concentration decreases with pressure between 5 and 20 Kbar. This study demonstrates the importance of considering the influence of  $f(Cl_2)$  and  $f(O_2)$  in exploring the solubility of halogens in silicate melts.

Preliminary additional measurements indicate (1) that Br is significantly less soluble than Cl when Br<sub>2</sub> and Cl<sub>2</sub> have similar fugacities and (2) I solubility is extremely low in both compositions we have investigated

[1] Filiberto, & Treiman., (2009). The effect of chlorine on the liquidus of basalt: First results and implications for basalt genesis on Mars and Earth. *Chemical Geology*, 263, 60–68. [2] Aiuppa, et al., (2009). Halogens in volcanic systems. *Chemical Geology*, 263(1–4), 1–18.

**EMPG – XVII**

**17th International Symposium on  
Experimental Mineralogy,  
Petrology and Geochemistry**

Abstracts

Theme 8 “Metamorphic petrology”

(sorted alphabetically by first author)

## Synthetic NH<sub>4</sub>-phengite: *In situ* micro-FTIR spectroscopic study under pressure and temperature

Nada Abdel-Hak<sup>1,2</sup>, Bernd Wunder<sup>1</sup>, Ilias Efthimiopoulos<sup>1</sup>, Monika Koch-Müller<sup>1,2</sup>

<sup>1</sup>Section 3.6. Chemistry and Physics of Earth Materials, Deutsches GeoForschungsZentrum (GFZ), Potsdam, 14473, Germany

<sup>2</sup>Institute of Applied Geosciences, Technische Universität Berlin (TUB), Berlin, 10623, Germany

Phengite is a key mineral in the transport of alkalis and water into the lowermost parts of the Earth's upper mantle through subduction of metasedimentary and basaltic rocks (Poli and Schmidt, 1995; 2002). Since ammonium (NH<sub>4</sub><sup>+</sup>) can substitute for the isovalent K<sup>+</sup> in K-bearing minerals (e.g. Wunder et al., 2015), phengite is thus a potential host to transport nitrogen into the mantle and contribute to the deep-Earth reservoir of nitrogen and hydrogen. However, the temperature and pressure conditions at which such ammonium-bearing phengite loses its volatile content (i.e. devolatilization) are not well-constrained.

NH<sub>4</sub>-phengite endmember (NH<sub>4</sub>)(Mg<sub>0.5</sub>Al<sub>1.5</sub>)(Al<sub>0.5</sub>Si<sub>3.5</sub>)O<sub>10</sub>(OH)<sub>2</sub> was synthesized in piston-cylinder experiments at 700°C and 4.0 GPa following the method described in Watenphul et al. (2009). Its devolatilization (ammonium-loss and dehydration) behavior was studied by means of *in situ* micro-FTIR spectroscopy under low and high temperatures from -180°C up to 600°C at ambient pressure using a Linkam cooling-heating stage, and pressures up to 42 GPa at ambient temperature in diamond-anvil-cell (DAC) experiments. In addition to these short-time *in situ* experiments, quench experiments were also performed; samples were annealed for 24 hours at certain temperatures, quenched back to room conditions and then analyzed by micro-FTIR spectroscopy. These data are compared with recent studies on the devolatilization of natural phengite containing trace-amounts of NH<sub>4</sub><sup>+</sup> (Liu et al., 2019; Yang et al., 2017) and with own experimental results (on samples from Melzer and Wunder, 2000; Chopin and Maluski, 1980) as well as with existing data (Goryainov et al., 2017; Zhang et al., 2010) on the dehydration of synthetic and natural ammonium-free phengite.

Our results can be summarized as follows: (1) an order-disorder process of the NH<sub>4</sub><sup>+</sup> group is taking place with temperature variation at ambient pressure, (2) NH<sub>4</sub><sup>+</sup> is still retained in the phengite structure up to 600°C and the expansion of the NH<sub>4</sub><sup>+</sup> molecule with heating is reversible for short-time experiments, (3) kinetic effects partly control the destabilization of NH<sub>4</sub><sup>+</sup> in phengite, (4) devolatilization occurs at temperatures near dehydration, and (5) a structural distortion of NH<sub>4</sub><sup>+</sup> in phengite is apparently occurring above 8.6 GPa at ambient temperature.

### References:

- Chopin and Maluski, (1980) *Contrib. Mineral. Petrol.*, 74, 109-122.  
 Goryainov et al., (2017) *J. Raman Spectrosc.*, 48, 1431-1437.  
 Liu et al., (2019) *EPSL*, 513, 95-102.  
 Melzer and Wunder, (2000) *Geology*, 28, 583-586.  
 Poli and Schmidt, (1995) *J Geophys. Res.*, 100, 22299-22314.  
 Poli and Schmidt, (2002) *Ann. Rev. Earth. Planet. Sci.*, 30, 207-235.  
 Watenphul et al., (2009) *Am. Mineral.*, 94, 283-292.  
 Wunder et al., (2015) *Am. Mineral.*, 100, 250-256.  
 Yang et al., (2017) *Am. Mineral.*, 102, 2244-2253.  
 Zhang et al., (2010) *Am. Mineral.*, 95, 1444-1457.

## Experimental study of some mantle metasomatism reactions at 3-5 GPa

Valentina Butvina<sup>1</sup> Oleg Safonov<sup>1,2</sup> Evgenii Limanov<sup>1</sup> Sofia Vorobey<sup>2,3</sup>

<sup>1</sup> *Korzhinskii Institute of Experimental Mineralogy RAS, st. Akademika Osipiana, 4, Chernogolovka, Moscow region, 142432 Russia*

<sup>2</sup> *Lomonosov Moscow State University, Geological Faculty, Leninskie Gory, 119991 Moscow, Russia*

<sup>3</sup> *Institute of Geochemistry and Analytical Chemistry RAS, st. Kosygin, 19 Moscow, 119991 Russia*

This work summarizes previous and new experimental data on the study of the reactions forming phlogopite and chromium-bearing potassium titanates of the crichtonite, magnetoplumbite and hollandite groups, which are indicative minerals characterizing various stages of the modal metasomatism in the upper mantle. The reactions of the phlogopite formation in the orthopyroxene-garnet system in presence of H<sub>2</sub>O-KCl fluid at 3 and 5 GPa and 900-1000 ° C simulate the processes of phlogopite formation in garnet peridotites and pyroxenites. The experiments demonstrated regular changes in the Ca and Cr content in garnet, Al in pyroxenes, as well as the composition of newly formed phlogopite, in dependence on the concentration of the potassium component in the fluid. Experiments on the formation of potassium titanates (imengite, matiasite, and priderite) in the chromite - rutile / ilmenite - K<sub>2</sub>CO<sub>3</sub> - H<sub>2</sub>O-CO<sub>2</sub> system at 3.5 and 5 GPa proved the possibility of the formation of these minerals during the reactions of chromite with a potassium water-carbonate fluid. However, the formation of titanates does not occur directly after chromite, but requires additional sources of Ti and Fe, which are rutile and ilmenite. Thus, the experiments confirmed the conclusion that the formation of titanates characterizes the most advanced stages of metasomatism in mantle peridotites. The formation of assemblages of these titanates with phlogopite characterizes higher concentrations of the potassium component in the fluid than the formation of phlogopite alone. The relationship between the various titanates is also a function of the activity of the potassium component in the fluid. The regularities revealed in the experiments illustrate well the features of mineral assemblages and compositional variations of minerals in metasomatized peridotites of the lithospheric mantle.

## The effect of fluorine on reaction rim growth dynamics in the ternary CaO-MgO-SiO<sub>2</sub> system

M.G. Franke<sup>1</sup>, B. Joachim-Mrosko<sup>1</sup>

<sup>1</sup>Institute of Mineralogy and Petrography, University of Innsbruck, Austria

Growth of metamorphic corona and reaction rim structures in rocks indicates a change of physical parameters such as pressure and temperature, and/or a change in the chemical composition of a system. Therefore, gaining understanding and quantifying the effect of changing physical and chemical factors on phase stability, reaction mechanisms and internal microstructures in reaction rims may provide insight into the dynamics of complex geological systems.

We investigated the effect of fluorine on reaction rim growth dynamics in the ternary CaO-MgO-SiO<sub>2</sub> system. Experiments were conducted using a conventional piston-cylinder apparatus at upper mantle P-T conditions (1000-1200°C and 1.5 GPa). Reaction rims are grown in a platinum capsule setup using natural quartz and wollastonite grains in a MgO powder matrix with or without addition of up to 5 wt% fluorine. The composition of crystal phases were determined using electron microprobe analysis.

Preliminary results show a rim sequence around wollastonite and quartz crystals of wo | mer + di | mtc | fo | per and qtz | en | fo | per respectively in fluorine-free systems. In fluorine-rich systems, F-clinohumite is stabilised to higher temperatures [1], thus leading to the replacement of forsterite by clinohumite, which affects the overall phase succession in both rim sequences. Compared to fluorine-poor systems, overall rim thickness significantly increases in fluorine-rich systems where symplectite microstructures consisting of alternating merwinite + diopside phases oriented perpendicular to the original periclase-wollastonite interface start to become more pronounced. Our preliminary data imply that fluorine, and possibly other volatiles, play an important role in phase stabilities, component mobilities and the kinetics of metamorphic reactions at crustal and upper mantle conditions.

### References:

- [1] Grützner et al., (2017) *Geology*, 45(5), 443-446

## REE redistribution during the fluid-induced alteration of chevkinite-(Ce): an experimental approach

Daniel E. Harlov<sup>1</sup>, Bogusław Bagiński<sup>2</sup>, Witold Matyszczyk<sup>2</sup>, Petras Jokubauskas<sup>2</sup>,  
Jakub B. Kotowski<sup>2</sup>, Ray Macdonald<sup>2,3</sup>

<sup>1</sup> Section 3.6, GeoForschungsZentrum, Telegrafenberg, 14473 Potsdam, Germany

<sup>2</sup> Institute of Geochemistry, Mineralogy and Petrology, University of Warsaw, 02-089 Warszawa, Poland

<sup>3</sup> Environment Centre, University of Lancaster, Lancaster LA1 4YQ, UK

The partial alteration of chevkinite-(Ce) in the presence of quartz, albite, and a Ca(OH)<sub>2</sub>-bearing fluid (sealed Pt capsule) has been experimentally achieved at 600 °C and 400 MPa with a duration of 21 days in a standard cold seal autoclave on a high pressure hydrothermal line. After quench, the capsule was opened, dried, and the experimental charge evaluated using BSE imaging and EMP analysis. The chevkinite-(Ce) reacted readily, but variably, the main products being britholite-(Ce) and titanite, with lesser amounts of hedenbergite, wollastonite, and allanite-(Ce) (Fig. 1). Alteration had proceeded along grain rims and along a complex network of cracks in the chevkinite-(Ce) primarily via a coupled dissolution – reprecipitation process. The variable degrees of alteration, the formation of compositionally anomalous rims, and variations in the alteration assemblages are taken to be evidences of local disequilibrium during the reaction between the chevkinite-(Ce) and the fluid. This perhaps was also a product variable metamictization in the original chevkinite, i.e. areas of high metamictization would be more prone to reaction than areas of low metamictization. The somewhat localized formation of allanite-(Ce) appear to reflect regions of high Ca activity in the fluid.

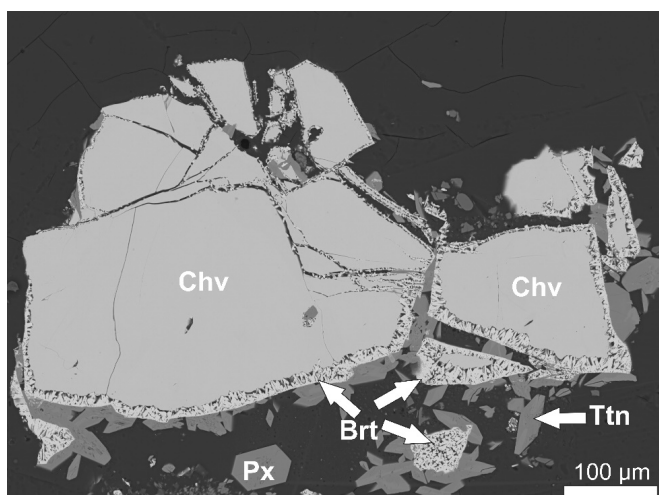


Fig. 1. BSE image of altered pieces of chevkinite-(Ce) (Chv) with pronounced rim of britholite-(Ce)(Brt) followed by titanite (Ttn). Note the unevenness in the alteration of the chevkinite grains.

We gratefully acknowledge funding by NCN Harmonia no. 2017/26/M/ST10/00407.

## Experimental investigations on Pb loss in uraninite

Daniel Harlov<sup>1</sup>, Fritz Finger<sup>2</sup>, David Schiller<sup>2</sup>, Michael Waitzinger<sup>2</sup>

<sup>1</sup> Section 3.6, GeoForschungsZentrum GFZ, Telegraphenberg, 14473 Potsdam, Germany

<sup>2</sup> Department Chemistry and Physics of Materials, University of Salzburg, Jakob Haringer Straße 2a, 5020 Salzburg, Austria

Electron-microprobe dating of accessory uraninite crystals by means of the U-total Pb method (Bowles 1990) is about to become an increasingly popular geochronological tool (Finger et al. 2017, Timón-Sánchez et al. 2018). To fully exploit the potential of uraninite as a geochronometer, it is necessary to learn more about the factors that trigger Pb loss in this mineral. There are, for instance, reports that uraninite is prone to fluid-induced in-situ dissolution-precipitation at low temperature (i.e., greenschist facies) conditions and that this process can cause total Pb loss (Waitzinger and Finger 2017).

In order to better understand the alteration behavior of uraninite in the presence of fluids, two sets of 5 experiments (200 MPa, 600 °C, 21 days; 200 MPa, 450 °C, 66 days) were carried out using natural uraninite from Příbram, CZ with a mean Pb content of 3-4 wt.%. The fluids used for each set of experiments were NaF + H<sub>2</sub>O; CaF<sub>2</sub> + H<sub>2</sub>O; Ca(OH)<sub>2</sub> + H<sub>2</sub>O; 2M NaOH; and Na<sub>2</sub>Si<sub>2</sub>O<sub>5</sub> + H<sub>2</sub>O. In the 450 °C experiments a small amount of elemental S was also added to the capsule. All the experiments were loaded into 1 cm long, 3 mm wide Au capsules, which were arc-welded shut. The 5 Au capsules were loaded together into a cold seal autoclave with rod fillers (buffered NiO-O) and taken up to pressure (Heise gauge) and temperature on a hydrothermal line. The thermocouple tip (+/- 5°C) was located at the end of the autoclave within 5 mm of the 5 Au capsules. After isobaric quench using compressed air, the capsules were extracted, cleaned, weighed, and punctured. After drying in a 100 °C oven, the contents were extracted, mounted in an epoxy grain mount, and then polished. The experimental run products were then evaluated in an SEM at the University of Salzburg.

In both experiments with **NaF**, the uraninite grains lost their Pb almost completely, although primary zoning textures remain fully visible. In the 450 °C experiment with sulphur added, many new grains of PbS<sub>2</sub> formed, while in the S-free experiment at 600 °C no newly grown Pb-phase was encountered. In the experiments with **CaF<sub>2</sub>** no changes occurred to the uraninite. Likewise, **Ca(OH)<sub>2</sub>** did not substantially alter the uraninite. In the 450 °C experiment with S, a few PbS<sub>2</sub> (10-20 µm) crystals did form inside porous parts of uraninite, but no significant lead loss was measured. In both experiments with **NaOH**, a clear loss of Pb is recorded in the uraninite grains (contents are 0-2 wt.% PbO, vs. 3-4 wt. % in the starting material). Again, no newly grown Pb-phase was detected in the S-free 600 °C experiment. In the S-containing experiment (450 °C) newly formed PbS<sub>2</sub> is present. In the **Na<sub>2</sub>Si<sub>2</sub>O<sub>5</sub>** experiments there was considerable Pb loss from the uraninite (50-80%) at 600 °C though no new Pb-mineral appeared. In the 450°C experiment a few PbS<sub>2</sub> (10-20 µm) inclusions appeared, but only small domains in the uraninite around the PbS<sub>2</sub> suffered Pb loss.

The experiments demonstrate that active F-bearing, alkali-bearing fluids followed by high pH, alkali-bearing fluids have the capability to reset the U-Pb system of uraninite via a coupled dissolution-precipitation reaction such that the mineral itself is not changed with regard to its form and internal texture (primary zoning).

Bowles 1990: *Chem. Geol.* 83, 1–2, 47–53.

Finger et al. 2017: *Geology* 45, 991–994.

Timón-Sánchez et al., 2019: *Geologica Acta*, 17,

Waitzinger and Finger, 2017: *Geol. Carpath.*, 69, 6, 558–572

## Heterotype solid solution in the system $\text{CaCO}_3\text{-SrCO}_3\text{-H}_2\text{O}$ at 0.5–5 kbar and 600°C re-examined

Ferry Schiperski<sup>1</sup>, Gerhard Franz<sup>1</sup>, Axel Liebscher<sup>2,\*</sup>, Matthias Gottschalk<sup>2</sup>

<sup>1</sup> Technische Universität Berlin, Dept. of Applied Geosciences, Applied Geochemistry, 10587 Berlin, Germany

<sup>2</sup> Helmholtz Centre Potsdam, GFZ German Research Centre for Geosciences, Telegrafenberg, D-14473 Potsdam, Germany

\* now: Federal Office for the Safety of Nuclear Waste Management, 10117 Berlin, Germany

To shed light on the topology of the two-phase field between calcite-type and aragonite-type  $(\text{Ca,Sr})\text{CO}_3$  solid solutions as function of P, we performed an experimental study in the system  $\text{CaCO}_3\text{-SrCO}_3\text{-H}_2\text{O}$ ; run conditions were  $T = 600\text{ °C}$  and 0.5 to 5 kbar, using conventional and rapid quench hydrothermal synthesis techniques. Fluid compositions were analyzed to calculate distribution coefficients ( $K_d$ ) of Sr and Ca between fluid and solid phases. Starting materials were (I) synthetic pure calcite and strontianite (+ $\text{H}_2\text{O}$ ), (II) synthetic strontianite and natural aragonite (+ $\text{H}_2\text{O}$ ), and (III) metastable aragonite-type  $(\text{Sr,Ca})\text{CO}_3$  solid solutions (+ $\text{H}_2\text{O}$ ), all with bulk compositions being within the postulated two-phase field of calcite-type and aragonite-type  $(\text{Ca,Sr})\text{CO}_3$  solid solutions. Run products were analyzed by scanning electron microscopy, electron microprobe analysis, and powder X-ray diffraction. On the calcite-type limb the results show a smaller miscibility gap than previously assumed. Compositions of the aragonite-type solid solution were identical to literature data. Fluid data suggests that the  $K_d$  values of Sr in both aragonite-type and calcite-type phases are generally decreasing at higher P meaning that Sr tends to prefer the fluid phase over the solid phases. An order-disorder phase transition that was previously postulated for the trigonal  $(\text{Ca,Sr})\text{CO}_3$  solid solution to explain some observed compositional trends in this system is not supported by our data, in line with recent other studies on phase transitions of  $\text{CaCO}_3$ . Based on the collected data a phase diagram P-x (Sr) at 600 °C for the system  $\text{CaCO}_3\text{-SrCO}_3$  was calculated (Fig. 1).

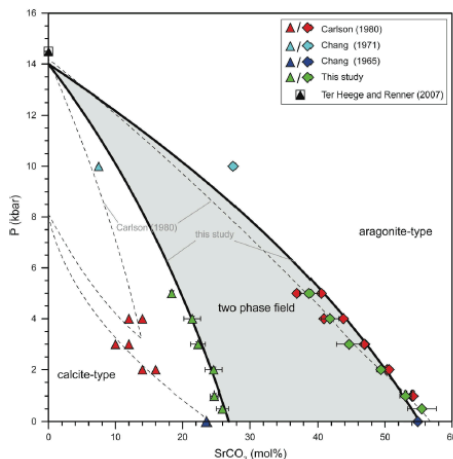


Fig. 1: Calculated isothermal ( $T = 600\text{ °C}$ ) P-x<sub>Sr</sub>-diagram of solid solution between calcite- and aragonite-type  $(\text{Ca,Sr})\text{-carbonate}$  and experimental data

### References:

Carlson (1980) *Amer Mineral* 65, 1252; Chang (1965) *J Geol*, 73, 346; Chang (1971) *Amer Mineral* 56, 1660; Ter Heege & Renner (2007) *Phys Chem Mineral*, 34, 445

## The persistence of memory: experimental *P-T* loop simulation of orogenic metamorphism in a piston cylinder apparatus

Peter Tropper<sup>1</sup> Philipp Mair<sup>1</sup> Philip Schantl<sup>2</sup>

<sup>1</sup> Institute of Mineralogy and Petrography, University of Innsbruck, A-6020 Innsbruck, Austria ([peter.tropper@uibk.ac.at](mailto:peter.tropper@uibk.ac.at))

<sup>2</sup> Department of Earth Sciences, University of Graz, A-8010 Graz, Austria

Metamorphic rocks are recorders of geodynamic processes. But how much memory, e.g. which part of the *P-T* path is actually recorded in the observed mineral assemblages remains often still a mystery. Experimental investigations using natural rocks are a forward modelling technique and allow putting additional constraints on the mineralogical evolution of a rock under defined *P* and *T* conditions. For this purpose, simple experiments using natural rocks as starting materials can easily be conducted. The disadvantage of this method lies in the complex chemical compositions of natural rocks and the deviation from chemical end-member systems. Therefore these experiments need to be evaluated in their ability to be reproduced by thermodynamic modelling using pseudosections. In this study experimental investigations of collision-related metamorphism of a natural muscovite-rich quartzphyllite sample (Grt + Ms + Chl + Bt + Rt + Qz) was investigated using a piston cylinder apparatus with an automated *P-T* control.

For the *P-T* loop experiments four different *P-T* conditions were chosen and run subsequently representing a clockwise *P-T* loop from a collisional setting. The *P-T* conditions were: 400°C, 0.8 GPa, 600°C, 1.2 GPa, 700°C, 0.8 GPa representing the prograde *P-T* path and 500°C, 0.4 GPa representing the retrograde part of the *P-T* path. In the first 16 days *P-T* loop experiment each *P-T* condition was run for 4 days before the *P-T* conditions were changed to the next *P-T* condition using the automated *P-T* control. In addition to this experiment, two similar experiments (one with 10% and one with 20% water added) with a duration of 32 days were conducted, where all four *P-T* conditions were run subsequently for 8 days each. All three *P-T* loop experiments yielded the same mineral assemblage: Grt<sub>2,3</sub> + Sta + Ms<sub>2</sub> + Bt<sub>2</sub> + Chl<sub>2</sub> + Ilm + Qz. In addition to the *P-T* loop experiments four separate single *P-T* experiments at the *P-T* conditions mentioned above were conducted. Each of these experiments was run for 4 days in accordance with the 16 day *P-T* loop experiment. These single *P-T* experiments were conducted to provide means to attribute the observed mineral assemblages to each of the four stages of mineral growth in the *P-T* loop experiments. Due to kinetic reasons these experiments yielded some slightly different results since metastable chloritoid grew instead of staurolite in the 700°C and 0.8 GPa experiment. Nonetheless, combining the observations from the single *P-T*- and *P-T* loop experiments allowed the attribution of characteristic mineral assemblages to specific *P-T* conditions. Pseudosection modelling using DOMINO-THERIAK also yields overall a good agreement between calculated and observed assemblages except that calculated aluminium silicates and melt were not observed in the experiments and staurolite persists longer in the experiments.

This study shows that experimental forward modelling using whole-rock experiments does indeed provide clues about the mineralogical memory of a given rock composition that can be attributed to different *P-T* stages. On the other hand thermodynamic testing is still slightly hampered somewhat by kinetics and the complex nature of the bulk compositions of the starting materials.

## Raman microspectroscopy of experimentally altered monazite and xenotime

Fabian Tramm<sup>1</sup>, Grzegorz Rzepa<sup>2</sup>, Bartosz Budzyń<sup>1</sup>, Gabriela A. Kozub-Budzyń<sup>2</sup>,  
Jakub Dybaś<sup>3</sup>, Jiří Sláma<sup>4</sup>

<sup>1</sup> Institute of Geological Sciences, Polish Academy of Sciences, Kraków, Poland; ndtramm@cyf-kr.edu.pl

<sup>2</sup> AGH Univ. of Science and Technology, Faculty of Geology, Geophysics and Environmental Protection, Kraków, Poland

<sup>3</sup> Jagiellonian Centre for Experimental Therapeutics (JCET) Raman Imaging Group, Kraków, Poland

<sup>4</sup> The Czech Academy of Sciences, Institute of Geology, Prague, Czech Republic

Monazite and xenotime are well known U-(Th)-Pb geochronometers used for dating igneous and metamorphic processes. However, both minerals can be chemically altered by fluid-mineral reactions. These processes may result in replacement by other phases, which affect the age record. In order to analyse the structural changes caused by alteration, Raman microspectroscopy provides compositional and structural information possibly supplementing common methods such as EPMA and LA-ICP-MS microanalytical techniques. However, the potential of Raman microspectroscopy strongly depends on detailed and resourceful reference material. Because the availability of monazite and xenotime spectra is limited, there is need to evaluate all possible features of full range Raman spectra to create a vast database for references of future works.

In the current study, altered monazite and xenotime from experiments of Budzyń et al. (2017) were evaluated with Raman microspectroscopy, EPMA and LA-ICP-MS measurements. The two latter methods provided compositional data to constrain the features of known Raman bands together with possible artefacts, which are attributed to experimental alteration of monazite and xenotime. The P-T conditions of the experiments are representative for greenschist to granulite facies metamorphism.

Preliminary data have shown good quality Raman spectra of monazite and xenotime within consistent variation in unaltered monazite and xenotime. Spectra of altered domains, however, show significant differences compared to those for Gd-orthophosphates (Clavier et al., 2018) regarding REE bending modes (0–700 cm<sup>-1</sup>) and close to the PO<sub>4</sub>-symmetric stretching bands (850–1000 cm<sup>-1</sup>). Furthermore, unknown features in the shape of three broad peaks (1500–2500 cm<sup>-1</sup>) have been documented for monazite within unaltered and altered domains. The intensity of these unknown Raman features correlates within altered domains and secondary fluorcalciobriholite overgrowth broadening further (1500–2800 cm<sup>-1</sup>). The project is in progress and future Raman analysis using a variation of laser wavelength, together with major and trace element compositions within unaltered and altered domains of monazite and xenotime are expected to provide more detailed insight in the altered structure. The resulting database will serve as a reference for future geochronological studies on monazite and xenotime, supported by Raman microspectroscopy.

**Acknowledgements.** The project was funded by the National Science Centre of Poland, grant no. 2017/27/B/ST10/00813.

### References:

Budzyń et al. (2017) *Mineralogy and Petrology*, 111, 183–217.

Clavier et al. (2018) *Spectrochimica Acta Part A: Molecular and Bio-molecular Spectroscopy*, 205, 85–94.

**EMPG – XVII****17th International Symposium on  
Experimental Mineralogy,  
Petrology and Geochemistry**

Abstracts

Theme 9 “Diffusion and kinetics”

(sorted alphabetically by first author)

## Nitrogen diffusion in silicate melts: an experimental challenge

Julien Boulliung<sup>1</sup>, Evelyn Füre<sup>1</sup>, Célia Dalou<sup>1</sup>, Laurent Tissandier<sup>1</sup>, Cécile Deligny<sup>1</sup>, Yves Marrocchi<sup>1</sup>

<sup>1</sup> Université de Lorraine, CNRS, CRPG, F-54000 Nancy, France.

Understanding the diffusion of volatile elements like nitrogen (N) or noble gases is fundamental for investigating the origin and evolution of volatiles on Earth. Indeed, volatiles diffusion coefficients are important parameters for constraining their kinetic fractionation during high temperature processes (e.g., Earth magma ocean stage or magmatic processes). Only few data are currently available for noble gases diffusion in silicate melts under different pressure and temperature conditions (e.g., He and Ar), but no N diffusion coefficient in silicate melts has been reported so far. The N solubility strongly depends on the redox conditions, and increases when  $fO_2$  decreases. Under oxidizing conditions (i.e.,  $fO_2 > IW - 1.5$ , expressed with respect to the Fe-FeO (IW) buffer) N is molecularly incorporated in silicate melts as  $N_2$  form. Miyazaki et al. (1995 and 2003) proposed that  $N_2$  is as incompatible as noble gases and its behavior is comparable to that of Ar. However, under more reducing conditions (i.e.,  $fO_2 < IW - 1.5$ ), N is chemically incorporated in the silicate melt by substituting  $O^{2-}$  for  $N^{3-}$ . This difference between molecular and chemical incorporation mechanisms of N should imply different diffusion coefficients. In order to investigate the diffusion of N in silicate melts, we performed multi-axial and uniaxial diffusion experiments at atmospheric pressure and under different reducing conditions (ranging from  $IW - 8$  to  $IW - 5.1$ ). Considering the equilibration duration determined for N solubility in silicates melts (i.e., 24h), we performed diffusion experiments between 1 and 6 hours to obtain N content gradients. Different types of melt support were used for this study (i.e., graphite capsules, graphite tubes, vitreous graphite tubes, platinum tubes). The N contents of the quenched run products (silicate glasses) were analyzed by *in-situ* secondary ion mass spectrometry (SIMS) in order to determine N diffusion coefficients ( $D_N$ ).

Depending on the melt support used, intriguing results have been obtained with:

- Platinum tube experiments (uniaxial) showing too low N contents (i.e.,  $> 5$  ppm).
- Vitreous graphite tube experiments characterized by homogeneous N contents.
- C-graphite crucible experiments (multi-axial) present N content gradients but for a given sample, different diffusion coefficients are obtained (i.e.,  $D_N$  varied from  $1.0 \times 10^{-6}$  to  $1.2 \times 10^{-5} \text{ m.s}^{-1}$ ).
- C-graphite tube experiments expected to present uniaxial diffusion profiles show instead multi-axial N diffusion with  $D_N = 4.3$  and  $4.9 \times 10^{-6} \text{ m.s}^{-1}$ .

For the first time, this study reports N diffusion coefficients in silicate melts. The estimations of  $D_N$  in silicate melts with C-graphite support, shows that when N is chemically incorporated in silicate melts, the diffusion seems to be faster than noble gases (e.g.,  $D_{Ar} = 9.3 \pm 1.3 \cdot 10^{-7} \text{ m.s}^{-1}$  in basaltic like composition under 1 atm; Amalberti et al., 2017). Despite the different experimental methods used in this study, the N diffusion in silicate melts remains a real experimental challenge.

### References:

- Amalberti et al., (2018) Chem. Geol., 480, 35-43  
Miyazaki et al., (1995) AIP Conference Proceedings., 341, 276-283  
Miyazaki et al., (2003) Geochim. Cosmochim. Acta, 68, 387-401

## **Kelyphite textures experimentally reproduced through garnet breakdown and the implications for the subsolidus breakdown of garnet bearing lherzolite**

Isra S Ezad<sup>1</sup>, David P Dobson<sup>2</sup>, Andrew R Thomson<sup>2</sup>, Simon A Hunt<sup>2</sup>, John P Brodholt<sup>2</sup>

<sup>1</sup> Earth and Environmental Sciences, Macquarie University, Balaclava Road, Macquarie Park, NSW, 2109, Australia

<sup>2</sup> Department of Earth Sciences, University College London, Gower Street, WC1E 6BT, UK

Mantle xenoliths provide insight into the behaviour of the deeper parts of Earth that would be otherwise inaccessible, however their scarcity leads to challenges in interpreting their tectonic histories. Xenoliths often undergo breakdown reactions during exhumation that leave behind textural relics from their journey, such as kelyphitic coronae that form from retrogressed garnet in peridotite. Such coronae have been used to estimate uplift rates, however, the lack of kinetic data and understanding of breakdown mechanisms has limited PTt pathway estimations and the understanding of emplacement mechanisms.

We present results from new high pressure, high temperature experiments on the breakdown of pyropic garnets in the presence of olivine, representative of a garnet bearing mantle peridotite. Natural pyropic garnets were surrounded in San Carlos olivine and equilibrated in the spinel stability field at pressures and temperatures of 1.0 – 2.0 GPa and 1000 – 1400 °C, for 1 to 120 hours. The resulting reaction rim textures were found to be representative of natural kelyphite (Obata, 2011; Špaček et al., 2013), we also successfully reproduce kelyphite assemblages resulting from isochemical breakdown of garnet.

We performed mass balance calculations on our kelyphite products; spinel, orthopyroxene and transient melt, to model appropriate phase equilibria with Perple\_X. We find garnet does not require olivine to initiate breakdown, and rather the involvement of olivine occurs at later stages to fulfil equilibrium breakdown to a spinel lherzolite assemblage.

We therefore propose a new reaction sequence of garnet breakdown, initiated first by isochemical breakdown of garnet then, a reaction of garnet and olivine to completion resulting in a spinel lherzolite.

Each progressive reaction can be modelled by phase equilibria calculations, and progression throughout our time series experiments. We demonstrate as garnet breakdown progresses, an initial assemblage of Sp + Opx + An, will equilibrate rapidly at high temperatures (above 1100 °C) to Sp + Opx ± Cpx. At low temperatures, equilibration to the final assemblage may be infinite resulting in assemblages of Sp + Opx + An in some mantle peridotites exhumed to the surface.

The breakdown of garnet in mantle peridotites has now been shown, to be geologically fast. Requiring rapid uplift rates to preserve both garnet and kelyphitic textures in natural mantle peridotites. The assemblage range seen in kelyphitic minerals can be explained through a sequence of garnet breakdown reactions, beginning with the decomposition of garnet alone.

### References:

- Obata, M. (2011). Kelyphite and symplectite: textural and mineralogical diversities and universality, and a new dynamic view of their structural formation. In *New Frontiers in Tectonic Research - General Problems, Sedimentary Basins and Island Arcs: Vol. i* (p. 13). InTech
- Špaček, P., Ackerman, L., Habler, G., Abart, R., & Ulrych, J. (2013). Garnet breakdown, symplectite formation and melting in basanite-hosted peridotite xenoliths from zinst (bavaria, bohemian massif). *Journal of Petrology*, 54(8), 1691–1723.

## Halogen diffusion in silicic melts

Yves Feisel<sup>1</sup>, Jonathan M. Castro<sup>1</sup>, Christoph Helo<sup>1</sup>, Donald B. Dingwell<sup>2,3</sup>

<sup>1</sup> Institute of Geosciences, Johannes Gutenberg-Universität Mainz, 55128 Mainz, Germany

<sup>2</sup> Department für Geo- und Umweltwissenschaften, Ludwig Maximilians Universität München, 80333 München, Germany

<sup>3</sup> Gutenberg Research Center, Johannes Gutenberg-Universität Mainz, 55128 Mainz, Germany

The diffusion of halogens (F, Cl, Br, I) in halogen-enriched, rhyodacitic melts (~70 wt.% SiO<sub>2</sub>) was studied experimentally using the diffusion couple technique. Two experimental series were performed: 1) nominally anhydrous experiments conducted in a vertical tube furnace at 1 bar and 750 – 1000 °C, and 2) water-bearing experiments (~3.5 wt.% H<sub>2</sub>O) carried out at pressurized conditions (100 – 160 MPa) and elevated temperatures using TZM-autoclaves in a vertical tube furnace with a rapid-quench assemblage. Concentration profiles of F and Cl in dry and water-bearing samples were measured with an Electron Microprobe, while some additional analyses of all four halogens including Br and I were undertaken using a Secondary Ion Mass Spectrometer.

Results on both dry- and water-bearing melts indicate that the halogens exhibit Arrhenian behaviour during diffusion. In general, diffusion in dry melts is slower and the variability of diffusivity among the different halogens is more pronounced compared to the water-bearing equivalents. In dry melts, Fluorine exhibits diffusion coefficients on the order of 10<sup>-15</sup> to 10<sup>-13</sup> m<sup>2</sup>/s, which is on average about 2 orders of magnitude greater than the magnitude of Chlorine's diffusivity. In the wet melts, initial results indicate that Fluorine diffusivity is increased by about 1 order of magnitude over the dry-melt case. Chlorine diffusion is even more enhanced in wet melts, resulting in diffusivities less than 1 order of magnitude slower than Fluorine.

Preliminary data on the diffusion of Bromine and Iodine was obtained for the dry melts only and indicate that these elements diffuse even slower than Chlorine. These observations suggest that halogen diffusivity correlates with the ionic radius of the diffusant, with Fluorine being the fastest and Iodine being the slowest.

Our results are the first halogen diffusion data in natural rhyodacitic melts obtained by the diffusion couple technique and, to our knowledge, the very first to investigate Iodine diffusion in volcanic melts. The pronounced differences in diffusivity among the halogens in dry melts—also apparent in the wet equivalents—could indicate that diffusive fractionation may be possible under certain eruptive regimes. For example, under conditions of magma ascent, bubble growth, driven by mass addition from the decompressing melt, would lead to partitioning of the relatively fast-diffusing halogens into the vapour phase. Consequently, halogen species ratios monitored in actively degassing vents could in turn be used as a proxy for volcanic unrest.

The dependence of diffusivity on the ionic radius seen in our SiO<sub>2</sub>-rich melts is stronger than that generally seen in mafic melts. This suggests that the halogen diffusion mechanism is dependent on the melt structure and pronounced fractionation by diffusion should be expected in differentiated magmas only.

Further work in this project will involve the investigation of halogen diffusion in higher silica natural melts and expanding the dataset of water-bearing experiments with regard to all four halogens.

## Alkali trace element (Li, Cs, Rb) diffusion in water-bearing silicic melts

Juliana Troch<sup>1,2</sup>, Chris Huber<sup>1</sup>, Mac Rutherford<sup>1</sup>, Nico Kueter<sup>3</sup>, Nicholas Tailby<sup>4</sup>, Keiji Hammond<sup>4</sup>, Steve Parman<sup>1</sup>, Olivier Bachmann<sup>2</sup>

<sup>1</sup> Department of Earth, Environmental and Planetary Sciences, Brown University, 324 Brook St, Providence RI 02912, USA

<sup>2</sup> Institute of Geochemistry and Petrology, ETH Zurich, Clausiusstrasse 25, 8092 Zurich, Switzerland

<sup>3</sup> Carnegie Science Earth and Planets Laboratory, 5251 Broad Branch Rd, Washington DC 20015, USA

<sup>4</sup> Department of Earth and Planetary Sciences, American Museum of Natural History, 200 Central Park West, New York NY 10024, USA

Trace element diffusion in silicic melts is a critical tool to track the timescales of magmatic processes, such as magma recharge and fluid or gas exsolution. Recently, lithium has become the focus of attention due to its extreme mobility and large isotopic fractionation during magmatic processes (e.g. Ellis et al. 2018, Holycross and Watson 2019, Neukampf et al. 2019, Rubin et al. 2017). However, the diffusivities of other alkali trace elements remain fairly unconstrained, or have only been determined in water-free melts unrealistic for most natural magmatic settings (Jambon 1982, Jambon and Semet 1978). In this project, we investigate diffusion of trace amounts of the alkali elements Li, Cs, and Rb in rhyodacitic melt as a function of temperature and water content.

Small amounts of Li-, Rb-, and Cs-carbonate are added to a powdered sample of well-characterized natural Avlaki rhyodacite lava (Nisyros, Greece) to increase original alkali trace element contents (ca. 45 ppm Li, 4 ppm Cs, 140 ppm Rb) by a factor of 10-20. This powder is fused in a 1-atm box furnace at 1300 °C to remove all carbonate, prior to a last grinding step. Homogenous, crystal- and bubble-free glass cylinders are produced by melting the powdered glass product in the presence of selected amounts of water in sealed AuPd-capsules in vertical externally heated pressure vessels (TZM; conditions 1050 °C, 1 kbar, 48 h). For the diffusion experiments, doped and undoped glass cylinders are polished on one end and loaded into sealed AuPd-capsules so that polished surfaces are in contact, prior to melting at 900-1100 °C and 1 kbar in the TZM-externally heated pressure vessel. Trace element diffusion profiles are measured via a 193-nm excimer (ArF) laser ablation system coupled to an X-series-2 quadrupole ICP-MS using an ablation slit of 10 µm width. Li, Rb, and Cs diffusivities are then derived by fitting the concentration profiles with the time-dependent solution for diffusion in an infinite diffusion couple, and temperature series allow to extract diffusion constant from the expected Arrhenius relationship.

We present first data of our experimental setup and preliminary results. Coupled to fluid-melt partition coefficients, the differential diffusion of alkali trace elements provides a powerful tool to track the exsolution of fluids from magma stored in long-lived shallow mushy magma reservoirs in the Earth's crust (e.g. Huber et al. 2012).

### References:

- Ellis et al. (2018). *Nature communications*, 9(1), 1-9.  
Holycross and Watson (2018). *Geochemical Perspectives Letters*, 6, 39-42.  
Huber et al. (2012). *Geochemistry, Geophysics, Geosystems*, 13, Q08003.  
Jambon (1982). *Journal of Geophysical Research: Solid Earth*, 87(B13), 10797-10810.  
Jambon and Semet (1978). *Earth and Planetary Science Letters*, 37(3), 445-450.  
Neukampf et al. (2019). *Chemical Geology*, 506, 175-186.  
Rubin et al., (2017). *Science* 356, 1154-1156.

## Experimental Simulations on Underplating Using Chaotic Mixing: the Paraná-Etendeka LIP-case for Major and Minor Elements

Caio M. Vicentini<sup>1,2</sup>, Cristina P. de Campos<sup>1</sup>, Werner Ertel-Ingrisch<sup>1</sup>,  
Leila S. Marques<sup>2</sup>, Diego Perugini<sup>3</sup>, Donald B. Dingwell<sup>1</sup>

<sup>1</sup> Dept. of Earth and Environmental Sciences, University of Munich – DEGEO /LMU, Germany

<sup>2</sup> Instituto de Astronomia, Geofísica e Ciências Atmosféricas – IAG/USP, São Paulo, Brazil

<sup>3</sup> Dept. of Physics and Geology, University of Perugia, Italy

E-mail: caio.vicentini@usp.br

The Paraná-Etendeka Magmatic Province (PEMP) is the second largest igneous province on the Earth (*approx.* 10<sup>6</sup> km<sup>2</sup>; *approx.* 133 Ma old). Basaltic rocks (SiO<sub>2</sub> ≈ 50%) predominate over other chemically more evolved lithologies (dacites and rhyolites: SiO<sub>2</sub> > 63%). Low- and high-titanium groups are distinguished in PEMP and, apparently, followed different evolutionary paths. This work is a first attempt to experimentally reproduce one of the most accepted models for the high-Ti acidic member (Chapecó-type) generation, *i.e.*, the impact of underplating basaltic melt (high-Ti Pitanga-type of PEMP) into a pre-existing continental crust. Isotopic geochemistry supports such a formation/contamination mechanism and guided the contaminants selection. Our goal is to study the role of chaotic mixing dynamics in this process. Two experiments (Exp1 and Exp2) were performed at 1,350°C using independent and non-simultaneous movements of two cylinders (Journal Bearing System [1]): (i) two clockwise rotations of an outer cylinder (35 min); (ii) six anticlockwise rotations of an inner cylinder (18 min). The procedure was repeated twice (212 min in total) and a chaotic flow has been generated. Homogenized glasses were used as the starting end-member compositions before each experiment, *i.e.*, KS-700 basalt (20%; high-Ti Pitanga-type;  $\eta_{1350} = 8.78$  Pa.s;  $\rho_{1350} = 2.469$  g/cm<sup>3</sup>) and LMC-027 granite (80%; syenogranite from Capão Bonito Stock;  $\eta_{1350} = 1.22 \cdot 10^5$  Pa.s;  $\rho_{1350} = 2.292$  g/cm<sup>3</sup>) for Exp1. For Exp2 the contaminant was another granite (LMC-020; 20%; monzogranite from Cunhaporanga batholith;  $\eta_{1350} = 1.73 \cdot 10^4$  Pa.s;  $\rho_{1350} = 2.317$  g/cm<sup>3</sup>). The chaotic dynamics created vortex structures, filaments, stretched and folded arms involving regions of well-preserved end-member compositions and transitional intermediary areas. Representative sections of Exp1 were analysed using an electron microprobe. Major and minor oxide variations show diffusion patterns similar to those from previous experiments with melts from natural samples. Transects for the main oxides crossing the structures present two compositional plateaux: (i) one close (but not the same) to the original basaltic composition and; (ii) one corresponding to the rhyolitic glass. Exceptionally, the K<sub>2</sub>O-plateau in the rhyolitic region is systematically lower than expected. Between the plateaux “S” shaped curves are observed, typical for diffusive patterns. SiO<sub>2</sub> and MgO show a smoother behaviour in comparison with TiO<sub>2</sub> and CaO, which represent inflexion-changing points. Na<sub>2</sub>O and Al<sub>2</sub>O<sub>3</sub> contents are similar in both end-members, therefore the points are more disperse. Besides, some uphill diffusion (*i.e.*, opposite to the gradient) has been detected. The results confirm that basaltic areas change faster in composition (*e.g.* they are faster contaminated) than the rhyolitic ones. Further experiments varying the end-members are on their way. Laser ablation-ICP-MS investigations will be performed for the chemical behaviour of trace elements, which should be crosschecked by numerical simulations.

[1] Swanson & Ottino (1990), J. Fluid Mech., 213: 227-249.

**EMPG – XVII****17th International Symposium on  
Experimental Mineralogy,  
Petrology and Geochemistry**

Abstracts

Theme 10 “Mineral physics”

(sorted alphabetically by first author)

## New Thermal Pressure Equations of State in EoSFit

Ross Angel<sup>1</sup>, Matteo Alvaro<sup>2</sup>, Francesca Miozzi<sup>3</sup>, Herbert Kroll<sup>4</sup>, Peter Schmid-Beurmann<sup>4</sup>

<sup>1</sup> Istituto di Geoscienze e Georisorse, CNR, Via Giovanni Gradenigo, 6, I-35131 Padova, Italy

<sup>2</sup> Department of Earth and Environmental Sciences, University of Pavia, Via A. Ferrata 1, I-27100, Pavia, Italy.

<sup>3</sup> Sorbonne Université, UMR CNRS 7590, Muséum National d'Histoire Naturelle, Institut de Minéralogie, de Physique des Matériaux et de Cosmochimie, IMPMC, 75005 Paris, France

<sup>4</sup> Institut für Mineralogie, Universität Münster, Corrensstr. 24, D-48149 Münster, Germany

The determination of accurate parameters for P-V-T Equations of State (EoS) of minerals from experimental data remains challenging, in part because of correlation between the parameters; different combinations of parameter values can predict very similar values for the volume over the experimental range of data. One approach to reduce this correlation is to use EoS with constraints imposed from physical theories.

The Mie-Grüneisen-Debye (MGD) is one such widely-used EoS. It is based on the quasi-harmonic approximation in which the thermal pressure is derived from a simplified phonon density of states (the Debye model) characterised by the Debye temperature  $\theta_D = \theta_{D0} \exp\left(\frac{\gamma_0 - \gamma(V)}{q}\right)$  in which  $q$  is a constant parameter that defines the volume variation of the thermal Grüneisen parameter  $\gamma = \gamma_0 \left(\frac{V}{V_0}\right)^q$ . Nonetheless, in least-squares fits to PVT data the values of the parameters  $\theta_{D0}$  and  $\gamma_0$  are strongly correlated with the value of  $V_0$  and, as a consequence, they are also sensitive to the weighting schemes applied to the experimental data, especially those close to room conditions. Kroll et al. (2019a,b) noted that the values of both  $\theta_D$  and  $\frac{\gamma(V)}{V}$  of minerals vary very weakly with  $T$  and  $P$  and proposed a modification of the MGD EoS in which they are both kept constant. Because constant  $\theta_D$  corresponds to a value of  $q = 0$ , and constant  $\frac{\gamma(V)}{V}$  to a value of  $q = 1$ , we name this the ‘ $q$ -compromise’ thermal-pressure model. The removal of the parameter  $q$  greatly reduces the correlation between the remaining parameters, whose refined values change very little compared to the full refinement of the MGD EoS, and it typically results in a marginally better quality of fit to the data ( $\chi_w^2$ ) with one less parameter.

The  $q$ -compromise model has been added to the EoSFit suite of programs ([www.rossangel.net](http://www.rossangel.net)) for determining EoS parameters from experimental data. Further reduction of the correlation between parameters can be achieved in EoSFit by simultaneously fitting measurements of both the volume and bulk modulus of the mineral (Milani et al., 2017). And stability of refinements of the parameters of thermal-pressure EoS is improved in EoSFit by restricting parameter values to those that correspond to significantly positive bulk moduli (Angel et al., 2019).

*This work was supported by ERC-StG TRUE DEPTHS grant (number 714936) to M. Alvaro.*

### References:

- Angel et al., (2019) *Minerals*, 9, 562.  
 Kroll et al., (2019a,b) *Euro. J. Mineral.*, 31, 313, and 31, 813.  
 Milani et al., (2017) *Am. Mineral.*, 102, 851.

## High-Pressure behavior of 3.65 Å Hydrous Phase

Abhisek Basu<sup>1</sup>, Christelle Bucag<sup>1</sup>, Mainak Mookherjee<sup>1</sup>, and Bernd Wunder<sup>2</sup>

<sup>1</sup> Earth, Ocean & Atmospheric Science, Florida State University - Tallahassee, Florida 32306

<sup>2</sup> Deutsches GeoForschungsZentrum GFZ, Section 3.3, Telegrafenberg, 14473 Potsdam, Germany

**Abstract:** Water has a significant influence on the solid Earth processes. In the deep Earth, trace quantities of water dissolved in the mineral as hydrogen influence rheological properties, thus enabling mantle convection. Hydrous mineral phases play a vital role in transporting water into the deep interior. The 3.65 Å [MgSi(OH)<sub>6</sub>] is one such hydrous phase that is likely to be stable in MgO-SiO<sub>2</sub>-H<sub>2</sub>O ternary system at pressures of 9–10 GPa. The 3.65 Å has limited thermal stability and could only transport water effectively along colder subduction geotherm. The crystal structure of 3.65 Å phase consists of corner sharing MgO<sub>6</sub> and SiO<sub>6</sub> octahedral units that are also held together by hydrogen bonded O-H...O units. Although, the 3.65 Å phase consists of SiO<sub>6</sub> octahedral units, its density is lowest among dense hydrous magnesium silicate phases such as phase-D. The 3.65 Å may contain up to ~35 wt% of structurally bound water. It is well known that physical properties such as elasticity of hydrous phases are often influenced by pressure induced strengthening and eventual symmetrization of hydrogen bonding. Hence in this study, we have undertaken Raman scattering measurements in diamond anvil cell up to pressures of ~20 GPa. At ambient conditions, in the lattice region we find the presence of 23 modes, while in the hydroxyl stretching region, we observe 7 modes. We find that all the vibrational modes in the lattice region (100-1200 cm<sup>-1</sup>) increases with pressure i.e.,  $\frac{dv_{lattice}}{dP} > 0$ . The pressure dependence of lattice modes,  $v_{lattice}$  do not show any anomalous behavior. The hydroxyl stretching modes shows a pressure induced softening i.e.,  $\frac{dv_{OH}}{dP} < 0$ . This implies that in the O-H...O units, the  $d_{O...O}$  distances decrease, whereas the  $d_{OH}$  distances increases upon compression, i.e., hydrogen bonding is strengthened. However, within the pressure ranges explored in this study, i.e., 20 GPa, we do not find evidence of hydrogen bond symmetrization.

## Vibrational anisotropy of $\delta$ -(Al,Fe)OOH: a nuclear resonant inelastic X-ray scattering study on single crystals

Johannes Buchen<sup>1</sup> Wolfgang Sturhahn<sup>1</sup> Takayuki Ishii<sup>2</sup> Jennifer M. Jackson<sup>1</sup>

<sup>1</sup> Seismological Laboratory, California Institute of Technology, Pasadena, CA, USA

<sup>2</sup> Bayerisches Geoinstitut, Universität Bayreuth, Bayreuth, Germany

The vibrational properties of minerals influence their thermodynamic behavior and thus play an important role in geophysical and geochemical processes. The anisotropy of vibrational properties, however, is less well understood in particular for vibrational modes that are not accessible by common light spectroscopies. We studied the vibrational anisotropy of  $\delta$ -(Al,Fe)OOH single crystals using nuclear resonant inelastic X-ray scattering (NRIXS). High-pressure experiments suggest that the isostructural oxyhydroxide phases  $\delta$ -AlOOH ( $\delta$ -phase; Sano et al., 2008) and  $\text{MgSiO}_2(\text{OH})_2$  (phase H; Nishi et al., 2014) as well as their solid solutions (Ohira et al., 2014; Walter et al., 2015) may act as carriers of water in the form of hydroxyl groups and retain hydrogen in Earth's lower mantle. Replacing a small fraction of aluminum in  $\delta$ -phase with ferric iron allows one to probe lattice vibrations that displace  $^{57}\text{Fe}$  atoms using NRIXS and to study the vibrational anisotropy of high-pressure oxyhydroxide phases.

Single crystals of  $\delta$ -(Al,Fe)OOH with  $\text{Al}/(\text{Fe}+\text{Al}) = 0.87$  and 96 %  $^{57}\text{Fe}$  of the iron atoms were synthesized at the Bayerisches Geoinstitut, Bayreuth, Germany. We recorded NRIXS spectra for six different crystallographic orientations and over an energy range from  $-100$  meV to  $+180$  meV at beamline 3-ID-B of the Advanced Photon Source (APS) at Argonne National Laboratory, Lemont, IL, USA. After calculating the projected partial phonon density of states (PDOS) from each single-crystal NRIXS spectrum, we determined the Lamb-Mössbauer factor, the mean kinetic energy per vibrational mode, and the mean force constant of  $^{57}\text{Fe}$  atoms from the PDOS. We found substantial anisotropy for all of these properties and propose a tensor description that captures the observed anisotropy. Our results show how NRIXS experiments on single crystals can be applied to study anisotropic vibrational properties of Fe-bearing materials and to explore the anisotropy of the bonding environment of  $^{57}\text{Fe}$  atoms in crystal structures (Buchen et al., 2020, under review). The detailed picture of the vibrational anisotropy of  $^{57}\text{Fe}$  atoms in  $\delta$ -(Al,Fe)OOH at ambient conditions will further serve as a basis to understand changes in the vibrational properties that arise from compression, for example across the recently detected spin transition of ferric iron in this compound (Ohira et al., 2019).

### References:

- Nishi et al. (2014) *Nat. Geosci.*, 7, 224-227
- Ohira et al. (2014) *Earth Planet. Sci. Lett.*, 401, 12-17
- Ohira et al. (2019) *Am. Mineral.*, 104, 1273-1284
- Sano et al. (2008) *Geophys. Res. Lett.*, 35, L03303
- Walter et al. (2015) *Chem. Geol.*, 418, 16-29

## High-pressure behavior of layered silicates: insights from Raman Spectroscopy

Stephen Clapp, Abhisek Basu, Mainak Mookherjee

Department of Earth, Ocean, and Atmospheric Science, Florida State University, 1011 Academic Way, Tallahassee, FL, 32306

Layered hydrous silicates play an important role in transporting water into the Earth's interior. However, these layered hydrous silicates have limited thermal stability and upon subduction they tend to dehydrate and release aqueous fluids. Recent studies have suggested that some of these layered hydrous silicates such as talc and kaolinite may intercalate water molecules in the interlayer region thus expanding the (001) layers. It is speculated that such intercalation is often initiated by polytypic transitions in the layered hydrous silicate minerals. To examine pressure induced polytypic transitions, we investigated the high pressure behavior of talc ( $\text{Mg}_3\text{Si}_4\text{O}_{10}(\text{OH})_2$ ) and kaolinite ( $\text{Al}_2\text{Si}_2\text{O}_5(\text{OH})_4$ ) using in-situ Raman spectroscopy using a diamond anvil cell. The powdered samples of kaolinite and talc were compressed up to pressures  $\sim 10$  GPa. Structural changes in talc and kaolinite were traced by analysis of Raman mode shifts in both the lattice-stretching ( $100\text{-}1250\text{ cm}^{-1}$ ) and hydroxyl-stretching ( $3000\text{-}4000\text{ cm}^{-1}$ ) regions. A possible polytypic transformation of talc is identified in the lattice-stretching region between 3-4 GPa. This confirms recent X-ray diffraction studies. However, the hydroxyl-stretching modes of talc do not exhibit any anomalous pressure dependence. In contrast, both the lattice region and the hydroxyl region indicates anomalous pressure dependence suggesting polytypic transitions in kaolinite.

## Phase Change of Pyrolitic Material: In-situ Transformation of Ringwoodite to Bridgmanite at 660 km Conditions

Jeff Gay<sup>1</sup>, Estelle Ledoux<sup>1</sup>, Matthias Krug<sup>2</sup>, Anna Pakhomova<sup>3</sup>, Julien Chantel<sup>1</sup>, Carmen Sanchez-Valle<sup>2</sup>, and Sébastien Merkel<sup>1</sup>

<sup>1</sup>Univ. Lille, CNRS, INRA, ENSCL, UMR 8207 - UMET - Unité Matériaux et Transformations, F-59000 Lille, France

<sup>2</sup>Institut für Mineralogie, Westfälische Wilhelms-Universität Münster, Münster, Germany

<sup>3</sup>Deutsches Elektronen-Synchrotron DESY, Hamburg, Germany

It has long been known that phase transitions have contributed to seismic reflections in the mantle (Ringwood, 1969; Cobden et al, 2015; Saki, 2018; Tauzen, 2018). More specifically, at the 660 km discontinuity, phase transitions from ringwoodite to bridgmanite in pyrolitic composition samples have been experimentally observed (Nishiyama et al, 2011; Ishii et al 2011; Ishii et al 2018). These two minerals transform from a cubic to orthorhombic crystal structure and result in crystallographic preferred orientations (Wenk et al, 2004, Miyagi & Wenk 2016). Determining whether or not and why these textures are preserved throughout the transformation at 660 km conditions will lead to better understanding of associated microstructures within the mantle and sources of observed seismic reflections. By implementing a high energy x-ray source at PETRA Beamline P02.2, we are able to track individual grains, their phase transformations, and later compression in-situ at pressures ranging from 24-55 GPa and temperatures of 1800K. We use a diamond anvil cell to deform our pyrolitic sample and collect 3D multigrain XRD images, which allow us to extract information including grain orientation, grain size, and bulk texture. Before transformation at 18 GPa, ringwoodite grains form a texture with (100) perpendicular to the compression axis. After transformation, bridgmanite grains show strong texture with (001) planes oriented parallel to compression (when indexed in a Pnma crystal setting). Further investigations of the origin and evolution of these bridgmanite crystal orientations is under way and will be presented during the meeting.

### References:

- Cobden L, Thomas C, Trampert J. *The Earth's Heterogeneous Mantle: A Geophysical, Geodynamical, and Geochemical Perspective*. Springer International Publishing Switzerland; 2015. doi:10.1007/978-3-319-15627-9
- Ishii T, Kojitani H, Akaogi M. Post-spinel transitions in pyrolite and Mg<sub>2</sub>SiO<sub>4</sub> and akimotoite-perovskite transition in MgSiO<sub>3</sub>: Precise comparison by high-pressure high-temperature experiments with multi-sample cell technique. *Earth Planet Sci Lett*. 2011;309(3-4):185-197. doi:10.1016/j.epsl.2011.06.023
- Ishii T, Kojitani H, Akaogi M. Phase relations and mineral chemistry in pyrolitic mantle at 1600–2200 °C under pressures up to the uppermost lower mantle: Phase transitions around the 660-km discontinuity and dynamics of upwelling hot plumes. *Phys Earth Planet Inter*. 2018;274(April 2017):127-137. doi:10.1016/j.pepi.2017.10.005
- Miyagi L, Wenk HR. Texture development and slip systems in bridgmanite and bridgmanite + ferropericlasite aggregates. *Phys Chem Miner*. 2016;43(8):597-613. doi:10.1007/s00269-016-0820-y
- Nishiyama N, Irifune T, Inoue T, Ando J ichi, Funakoshi K ichi. Precise determination of phase relations in pyrolite across the 660 km seismic discontinuity by in situ X-ray diffraction and quench experiments. *Phys Earth Planet Inter*. 2004;143(1-2):185-199. doi:10.1016/j.pepi.2003.08.010
- Ringwood AE. Composition of the crust and upper mantle. *Earth's crust Up Mantle, Geophys Monogr Ser Vol 13*. 1969;13:1-17.
- Saki M, Thomas C, Merkel S, Wookey J. Detecting seismic anisotropy above the 410 km discontinuity using reflection coefficients of underside reflections. *Phys Earth Planet Inter*. 2018;274(August 2017):170-183. doi:10.1016/j.pepi.2017.12.001
- Tauzin, B., Kim, S., & Afonso, J. C. (2018). Multiple phase changes in the mantle transition zone beneath northeast Asia: Constraints from teleseismic reflected and converted body waves. *Journal of Geophysical Research: Solid Earth*, 123.
- Wenk HR, Lonardelli I, Pehl J, et al. In situ observation of texture development in olivine, ringwoodite, magnesio-wüstite and silicate perovskite at high pressure. *Earth Planet Sci Lett*. 2004;226(3-4):507-519. doi:10.1016/j.epsl.2004.07.033

## **In-situ studies of olivine-wadsleyite transformation and related microstructures at 18-22 GPa and 1400-1700 K**

Estelle Ledoux<sup>1</sup>, Julien Chantel<sup>1</sup>, Nadège Hilairet<sup>1</sup>, Volodymyr Svitlyk<sup>2</sup>, Maxim Bykov<sup>4</sup>, Elena Bykova<sup>3</sup>, Georgios Aprilis<sup>5</sup>, Alexandre Fadel<sup>1</sup>, Sébastien Merkel<sup>1</sup>

1. Univ. Lille, CNRS, INRA, ENSCL, UMR 8207 – UMET – Unité Matériaux et Transformation, F-59000, Lille, France.
2. European Synchrotron Radiation Facility, 38043 Grenoble, France.
3. PETRA III, Deutsches Elektronen Synchrotron, 22607 Hamburg, Germany.
4. Bayerisches Geoinstitut, Universität Bayreuth, D-95440 Bayreuth, Germany.
5. Materials Physics and Technology at Extreme Conditions, Laboratory of Crystallography, Universität Bayreuth, D-95440 Bayreuth, Germany.

The 410 km depth seismic discontinuity in the Earth is attributed to the transformation from olivine to its high pressure polymorph, wadsleyite (Ringwood, 1969). This phase transformation can be martensitic-like, i.e. with a crystallographic orientation relationship between the parent crystal and the transformed crystal, but not in all cases (Smyth et al., 2012). In a martensitic-like phase transformation wadsleyite inherits a lattice preferred orientation (LPO) from the starting olivine. Hence, an LPO in olivine will be inherited by the wadsleyite and give rise to seismic anisotropy in the mantle transition zone. However, in the case of a non-martensitic-like transformation, no trace of the upper mantle olivine LPO will be preserved by the newly-formed wadsleyite.

In order to determine which scenario applies at the conditions of the 410 km depth discontinuity, we reproduce the transformation in the laboratory. We use polycrystalline samples of pure San Carlos olivine loaded inside a pressure medium in diamond anvil cells and apply combined pressure and temperature to induce the phase transformation. The evolution of the sample's microstructure is followed using in-situ synchrotron X-rays diffraction at the ID27 beamline of the ESRF and the P02 beamline of PETRA III at DESY. Key steps of the transformation are documented by 3D-XRD data collection. Data processing of these 3D-XRD collections with the multigrain crystallography method gives us crucial information about orientations and positions of individual grains in the samples during the whole experiment. Based on the orientations of these grains, we track the texture evolution during the experiments and search for evidences of a crystallographic orientation relationships between the two phases. This characterization will allow us to determine the transformation mechanism occurring at the conditions of the 410 km discontinuity and the effect of the transformation on the seismic anisotropy in the Earth's mantle.

### References:

- Ringwood, (1969) *EPSL*, 5, 401-412.  
Smyth et al., (2012) *PEPI*, 200-201, 85-91.

## Investigation of nanominerals and nanostructures using synchrotron diffraction, pair distribution function, and transmission electron microscopy

Seungyeol Lee<sup>1,2</sup>

<sup>1</sup> USRA Lunar and Planetary Institute, 3600 Bay Area Boulevard, Houston, TX 77058, USA (slee2@usra.edu)

<sup>2</sup> ARES, NASA Johnson Space Center, 2101 NASA Parkway, Houston, TX 77058, USA

Nanominerals are common and widely distributed in various geological environments such as soils, sediments, waters, rocks, atmosphere as well as in living organisms. The nanominerals play essential roles in many geochemical processes involving the adsorption and transport of ions, redox processes, metabolism, and global element cycling. However, it is challenging to measure and describe their structure, especially when structures include the short-range ordering, defects, and local domains. I have applied multiple/complementary methods integrating synchrotron X-ray diffraction (XRD), X-ray/Neutron pair distribution function (PDF), High-resolution transmission electron microscope (TEM), Z-contrast image, and ab-initio calculations to better understand the nanominerals including crystal structure, interface, and surface behaviors.

First, the new nanominerals of luogufengite (IMA 2016-005; Xu et al., 2017), valleyite (IMA 2017-026; Lee et al., 2019a) and were discovered in basaltic scoria and characterized by using the synchrotron XRD and High-resolution TEM. The new nanominerals may be important magnetic phases for paleomagnetism of volcanic rocks due to their magnetic coercivity. The unique magnetic property may explain the observed unusually high-remanent magnetization in some igneous and metamorphic rocks, lodestones (natural magnet), and even Martian surfaces.

Next, the nanostructures and nano-domains in lodestone (natural permanent magnets) and Fe-Ti oxide rocks have been described to understand their strong remanent magnetization and magnetic coercivity (Lee and Xu, 2018). The nanoscale multilayers parallel to the magnetic easy axis, plays an important role in enhancing the remanent magnetization and coercivity. The nanoscale exsolution lamellae of titanohematite and ferric ilmenite enhance their magnetic remanence and coercivity. The nanostructures and nano-domains extend our knowledge of magnetism and help us to understand the magnetic anomalies on Earth and other planetary bodies.

Finally, the combined method applied to determine the short-range ordered nanominerals such as vernadite, 6-line ferrihydrite, and opal-A (Lee, et al. 2019b). The synchrotron radiation XRD/PDF, high-resolution TEM, and Z-contrast imaging is a powerful tool to determine the nanostructure and crystal chemistry. The direct images of TEM and Z-contrast image provide the domain and interface structures. The detailed structure was refined by the method of synchrotron total scattering and PDF analysis. The combined methods will be useful for determining other crystal structures of poorly crystallized nanominerals.

References: Xu, H., Lee, S., & Xu, H. (2017) *Am. Mineral.*, 102(4), 711-719

Lee, et al., (2019a) *Am. Mineral.*, 104(9), 1238-1245.

Lee, S., and Xu, H. (2018).. *Minerals*, 8(3), 97.

Lee, et al. (2019b). *cta Crystallogr. B Struct. Sci. Cryst.* 75(4), 591-598.

## Phase stability and Elasticity of Al-bearing Superhydrous Phase B at High Pressure and Temperature

Xinyang Li<sup>1,2</sup>, Sergio Speziale<sup>2</sup>, Konstantin Glazyrin<sup>1</sup>Hanns-Peter Liermann<sup>1</sup>, Monika Koch-Müller<sup>2</sup>

<sup>1</sup> Photon Science, DESY, Notkestrasse 85, 22607 Hamburg, Germany

<sup>2</sup> GFZ German Research Center for Geosciences, Potsdam, Germany

Recent studies have discovered Ice-VII [1] and hydrous ringwoodite [2] in diamond inclusions from Earth's transition zone, indicating that the transition zone could be locally hydrated. Water could be transported into the Earth's mantle via various hydrous minerals in the sinking subduction slabs [3]. High pressure-temperature experiments have shown that a number of hydrous dense magnesium silicates (DHMS) with several weight percent H<sub>2</sub>O content could be stable in the cold subduction slabs at pressures corresponding to the depth of the Earth's lower mantle [3,4]. These DHMSs are among the most important carriers of H<sub>2</sub>O to the Earth's deep interior. Of particular interest is superhydrous phase B (Shy-B), which crystallizes in the orthorhombic symmetry with an ideal composition of Mg<sub>10</sub>Si<sub>3</sub>H<sub>4</sub>O<sub>12</sub> [5]. Recent studies show that Al-bearing shy-B (Al-Shy-B) could remain stable to 2300 K between 20 and 24 GPa indicating that the Al-Shy-B might be stable at pressure and temperature conditions relevant for the bulk mantle [6]. In this study, we investigated the phase stability and elasticity of shy-B with different Al contents in a series of high pressure experiments. Using a rotating multi-anvil press, Shy-B with 4.4 and 12.2 wt. % Al<sub>2</sub>O<sub>3</sub> were synthesized at 19 GPa and 1500 K. The H<sub>2</sub>O content, Al content and substitution of Al were characterized by Fourier-transform infrared spectroscopy (FTIR), electron microprobe analyses and single-crystal X-ray diffraction, respectively. Powder X-ray diffraction of Al-Shy-B has been measured at the Extreme Condition Beamline (ECB) P02.2 at PETRA III in Hamburg up to 50 GPa and 2200 K in laser and resistive heated diamond anvil cells. Our results indicate that Al-bearing Shy-B remains stable at the conditions of slab geotherms and decompose at the conditions of the average mantle geotherm. We observe that Al-bearing Shy-B thermally decomposes to periclase, hydrous ringwoodite and majorite, Al-bearing-akimotoite, -phase D and -bridgmanite depending on pressure between 18 and 50 GPa.. The pressure dependence of dehydration temperature is complex and depends on the different decomposition products and dehydration reactions taking place at different pressures. Brillouin scattering measurements of Al-bearing shy-B also show that Al incorporation causes higher anisotropy and lower sound velocity with respect to the Al-free end member. Our results play a key role in understanding the water recycling in the deep Earth's interior.

### References:

- [1] Tschauer, O., Huang, S., Greenberg, E., Prakapenka, V. B., Ma, C., Rossman, G. R., and Tait, K. (2018). Ice-VII inclusions in diamonds: Evidence for aqueous fluid in Earth's deep mantle. *Science*, 359(6380), 1136-1139.
- [2] Pearson, D. G., Brenker, F. E., Nestola, F., McNeill, J., Nasdala, L., Hutchison, M. T. and Vekemans, B. (2014). Hydrous mantle transition zone indicated by ringwoodite included within diamond. *Nature*, 507(7491), 221.
- [3] Ohtani, E., 2005. Water in the mantle. *Elements* 1, 25-30.
- [4] Ohtani, E., Toma, M., Kubo, T., Kondo, T. and Kikegawa, T., 2003. In situ X-ray observation of decomposition of superhydrous phase B at high pressure and temperature. *Geophys. Res. Lett.* 30, DOI: 10.1029/2002gl015549.
- [5] Koch-Müller, M., Dera, P., Fei, Y., Hellwig, H., Liu, Z., van Orman, J., Wirth, R. (2005) Polymorphic phase transition in superhydrous phase B. *Phys. Chem. Miner.*, 32, 349 - 361.
- [6] Kakizawa, S., Inoue, T., Nakano, H., Kuroda, M., Sakamoto, N., and Yurimoto, H. (2018). Stability of Al-bearing superhydrous phase B at the mantle transition zone and the uppermost lower mantle. *Am. Miner.*, 103(8), 1221-1227.

## Optical probing of solid and molten silicates at extreme pressure-temperature conditions

Sergey S. Lobanov<sup>1</sup>, Lukas Schifferle<sup>1</sup>, Reiner Schulz<sup>1</sup>

<sup>1</sup> GFZ German Research Centre for Geosciences, Section 3.6, Telegrafenberg, 14473 Potsdam, Germany

Optical properties of silicates at high pressure-temperature (P-T) conditions provide insights into the electrical and radiative conductivities of planetary mantles, which are among the key parameters that govern planetary evolution. The temperature range of previous optical studies of silicates at high pressure has been limited to below  $\sim 1000$  K due to the increasingly bright thermal background that impedes optical probing. This temperature range is not sufficient as planetary mantles are generally much hotter (e.g. Earth's mantle is at  $T \sim 1000$ - $4000$  K). Here we report on a system to perform optical absorption experiments in a laser-heated diamond anvil cell at  $T$  up to at least  $4000$  K. This setup is based on a pulsed supercontinuum (broadband) light probe and a gated CCD detector. Precise and tight synchronization of the detector gates ( $3$  ns) to the bright probe pulses ( $1$  ns) diminishes the recorded thermal background and preserves an excellent probe signal at high temperature. We demonstrate the efficiency of this spectroscopic setup by measuring the optical absorbance of solid and molten (Mg,Fe)SiO<sub>3</sub>, an important constituent of planetary mantles, at  $P \sim 30$  GPa and  $T \sim 1200$ - $4150$  K. Optical absorbance of hot solid (Mg,Fe)SiO<sub>3</sub> is moderately sensitive to temperature but increases abruptly upon melting and acquires a strong temperature-dependence. Our results enable quantitative estimates of the opacity of planetary mantles with implications to their thermal and electrical conductivity, all of which have never been constrained at representative P-T conditions, and call for an optical detection of melting in silicate-bearing systems to resolve the extant ambiguity in their high-pressure melting curves.

## Elastic softening of $(\text{Mg}_{0.8}\text{Fe}_{0.2})\text{O}$ ferropericlase across the iron spin crossover measured by time-resolved x-ray diffraction in a dynamic diamond-anvil cell

Hauke Marquardt<sup>1</sup>, Alba San José Méndez<sup>2,3</sup>, Rachel Husband<sup>3</sup>, Hanns-Peter Liermann<sup>3</sup>

<sup>1</sup>Department of Earth Sciences, University of Oxford, Oxford OX1 3AN, United Kingdom

<sup>2</sup>Bayerisches Geoinstitut BGI, University of Bayreuth, 95440 Bayreuth, Germany;

<sup>3</sup>Deutsches Elektronen-Synchrotron (DESY), 22607 Hamburg, Germany.

The elastic bulk modulus softening of  $(\text{Mg,Fe})\text{O}$  ferropericlase across the iron spin crossover is expected to affect seismic wave velocities in Earth's lower mantle. Direct measurements of the bulk modulus of  $(\text{Mg,Fe})\text{O}$  as well as computations suggest largely different pressure ranges over which the elastic softening occurs. Here, we performed compression on polycrystalline  $(\text{Mg}_{0.8}\text{Fe}_{0.2})\text{O}$  employing a piezo-driven dynamic Diamond Anvil Cell (dDAC) and monitored the compression behavior of the sample using time-resolved x-ray diffraction measurements. The bulk modulus of ferropericlase was derived from our high-resolution data directly by differentiation of the compression data (pressure/volume), without the need to assume a specific functional form to describe the elastic behavior in the spin crossover region. Experimental runs have been performed at different average compression rates ranging from 1 GPa/s to 1TPa/s to study the dependence of the elastic softening on the stress state in the sample. At all compression rates, our results show a broad and asymmetric softening of the bulk modulus at pressures between about 40 and 80 GPa. We observed a slight lowering of the spin crossover onset pressure with increasing compression rate that we attribute to changes of the stress conditions in the sample with changing compression rate. Our experimental data suggest that the elastic softening occurs over a significantly larger pressure (depth) range than inferred based on previous x-ray diffraction data and most computations. We will also present first results of the bulk modulus softening of ferropericlase across the spin crossover measured at high temperatures in a resistive-heated dDAC. We will discuss implications of our findings for the seismic signature of the spin crossover in the lower mantle.

## Pressure induced phase transitions in CaCO<sub>3</sub>-SrCO<sub>3</sub> solid solution

Martirosyan N.S.<sup>1,2</sup>, Pennacchioni L.<sup>1,3</sup>, Efthimiopoulos I.<sup>1</sup>, Jahn S.<sup>2</sup>, Koch-Müller M.<sup>1</sup>

<sup>1</sup> GFZ German Research Centre for Geosciences, Telegrafenberg, 14473 Potsdam, Germany

<sup>2</sup> Institute of Geology and Mineralogy, University of Cologne, Zùlpicher Str. 49b, 50674 Cologne, Germany

<sup>3</sup> Institute of Geosciences, Goethe University, Altenhòferallee 1, D-60438 Frankfurt am Main, Germany

Inclusions in diamonds reflect rich mineralogy of carbonates at the Earth's mantle conditions [1]. These inclusions contain mainly Ca- and Mg-carbonates, as well as carbonates of alkaline (Na<sup>+</sup>, K<sup>+</sup>) and incompatible elements (Ba<sup>2+</sup> and Sr<sup>2+</sup>) [1]. Given the variety of compositions found in natural carbonate samples, studies of multicomponent phase diagrams at mantle pressures and temperatures ( $P - T$ ) are of great importance.

Here we investigated the  $P$ -induced phase transitions in the CaCO<sub>3</sub>-SrCO<sub>3</sub> solid solution with 18 mol.% of Sr<sup>2+</sup> at  $P$  and  $T$  up to 55 GPa and 1300 K using *in situ* Raman spectroscopy and X-ray diffraction. The results of this work show deviations in the high- $P$  phase behavior of the solid solution compared to that of the CaCO<sub>3</sub> and SrCO<sub>3</sub> end members. In a nutshell, our results can be epitomized as follows: i) crystallization of the CaCO<sub>3</sub>-II – type structure (Sr-calcite-II) at 1300 K and 2 GPa; ii) formation of a new high-pressure modification, Sr-calcite-IIIc at 7-14 GPa at ambient temperature; iii) formation of Sr-aragonite and Sr-calcite-VII at lower  $P$ - $T$  conditions compared to pristine CaCO<sub>3</sub>. CaCO<sub>3</sub>-II in pure Ca-carbonate system is a metastable phase which forms only on cold compression within a narrow stability field – 1.7 to 2.5 GPa [2]. Our study shows that incorporation of Sr<sup>2+</sup> stabilizes the CaCO<sub>3</sub>-II structure in a larger temperature and pressure range. Additionally, the present data indicate that substitution of Ca<sup>2+</sup> with Sr<sup>2+</sup> in Ca-carbonate promotes the formation of structures with larger cation coordination numbers such as aragonite, CaCO<sub>3</sub>-VII, and post-aragonite at lower  $P - T$  conditions compared to pure CaCO<sub>3</sub>.

### References:

[1] Logvinova et al., (2018). EJM 20(3): 317-331.

[2] Pippinger et al., (2015). Phys Chem Min.. 42(1), 29-43.

## Magnetic transitions in iron-nickel alloy at high pressure

Catherine McCammon<sup>1</sup>, Qingguo Wei<sup>2</sup>, Stuart Gilder<sup>2</sup>

<sup>1</sup> Universität Bayreuth, Bayerisches Geoinstitut, Bayreuth, Germany

<sup>2</sup> Ludwig-Maximilians-Universität München, Department für Geo- und Umweltwissenschaften, München, Germany

Iron-nickel alloy is a major constituent of iron meteorites that have been used to infer planetary core compositions. Many aspects of its magnetic properties are controversial, particularly near the Invar (“invariable”) composition around 36 at% nickel. Open questions include the conditions under which magnetism is lost, so to address this particular controversy, we undertook a combined magnetic remanence and Mössbauer study of synthetic taenite at high pressure. We synthesised polycrystalline iron-nickel alloy with 38 at% nickel, loaded the sample into a diamond anvil cell and collected Mössbauer spectra during decompression from 20 GPa. Our results show a clear loss of magnetism, but at pressures that differ considerably depending on the fitting model. The pressure obtained using the traditional approach involving a magnetic field distribution conflicts with results obtained from other methods, while a simple model based on magnetic field fluctuations gives results that are consistent with other data. Comparison of data from all methods provides insight that can be applied to planetary magnetism.

## Sound velocities of FeSi at high P-T conditions and implications for the structure of the Core-Mantle-Boundary

V. Mergner<sup>1</sup>, I. Kuppenko<sup>1</sup>, G. Spiekermann<sup>2</sup>, S. Petitgirard<sup>3</sup>, L. Libon<sup>2</sup>, S. Chariton<sup>4</sup>, I. Sergeev<sup>5</sup>, R. Steinbrügge<sup>5</sup>, M. Krug<sup>1</sup>, C. Sanchez-Valle<sup>1</sup>

<sup>1</sup> Institut für Mineralogie, Universität Münster, 48149 Münster, Germany

<sup>2</sup> Institut für Geowissenschaften, Universität Potsdam, 14476 Potsdam, Germany

<sup>3</sup> Institut für Geochemie und Petrologie, ETH Zürich, 8092 Zürich, Switzerland

<sup>4</sup> Bayerisches Geoinstitut (BGI), 95440 Bayreuth, Germany

<sup>5</sup> Deutsches Elektronen-Synchrotron DESY, 22607 Hamburg, Germany

Investigating the elastic and thermodynamic properties and, thus, identifying the seismic signature of candidate materials of the Earth's interior, is vital to attain a thorough understanding of the structure of the deep Earth. Silicon has frequently been proposed as a likely alloying element in the core based on geochemical and cosmochemical arguments [e.g. 1,2]. Additionally, the reaction between iron and mantle silicates could be a source for iron-silicon alloying at the core-mantle boundary (CMB) [3]. Silicon-rich Fe-Si alloy decomposes into a silicon-poor hexagonal-iron phase (hcp) and stoichiometric FeSi at CMB conditions [3,4]. Therefore, studying the lattice dynamics in FeSi under relevant high pressure-temperature conditions and, thus, deriving the seismic signature of FeSi is key in order to refine the core and lowermost-mantle compositional models. So far, sound velocities have been measured in the low-pressure phase of FeSi at room temperature up to 90 GPa [2]. However, studies on the combined effect of high pressure and temperature on the lattice dynamics of the high-pressure B2-phase of FeSi is absent as yet.

Here we report investigations of the dynamics and sound velocities of B2-FeSi at pressures up to 110(3) GPa and 1600(200) K by means of nuclear inelastic scattering of synchrotron X-rays in laser-heated diamond anvil cells. The experiments were conducted at PETRA III beamline P01.

The results provide a comprehensive characterization of the elastic and thermodynamic properties of B2-FeSi at P-T conditions of the CMB and further allow to extrapolate these data to inner core conditions. Implications of these findings for the composition and structure of the CMB and inner core will be discussed.

### References:

[1] Alfè, D., Gillan, M. J. & Price, G. D., (2002) *Earth Planet. Sci. Lett.* 195, 91–98.

[2] Badro, J. *et al.*, (2007) *Earth Planet. Sci. Lett.* 195, 91–98.

[3] Dubrovinsky, L. *et al.*, (2003) *Nature* 422, 58–61.

[4] Tateno, S. *et al.*, (2015) *Earth Planet. Sci. Lett.* 418, 11–19.

## Seismic signature of isolated iron-sulfur melt pockets: experimental acoustic wave velocity measurements

Adrien Néri, Dan J. Frost

Bayerisches Geoinstitut, University of Bayreuth, Germany

The lithospheric mantle can show evidence for long-term low seismic wave-speeds associated with plumes or hot spots (Ekström and Dziewonski, 1998; Lodge and Helffrich, 2006; Schimmel et al., 2003; Wolfe et al., 1997). In some instances, however, low seismic velocity regions are located in old tectonic environments, where there has been no hot spot activity for more than 60 Myr. The normal explanation for velocity anomalies near plumes or hotspots is the presence of melt or raised temperatures. Remnant thermal anomalies can be ruled out in old settings, however, as they have much shorter lifetimes (Carslaw and Jaeger, 1959). Silicate and carbonate melts also provide a poor explanation for these anomalies as they are highly mobile due to their buoyancy and low dihedral angles (Minarik and Watson, 1995; Laporte and Provost, 2000 and references therein) and are, therefore, not expected to remain trapped for long timescales. However, the high dihedral angles (Laporte and Provost, 2000) and high interconnection thresholds (Bagdassarov et al., 2009) of iron-sulfur melts make them more plausible candidates.

Based on geometrical relations and assuming an interconnected sulfide network, Helffrich et al. (2011) calculated the effect of a small fraction of iron-sulfur melt on seismic velocity reduction. Results indicate an upper limit of 5 vol% of iron-sulfur melt to explain velocity reductions of up to 4%.

Although acoustic velocity experimental data exist for partially molten silicates, none are reported for metal-silicate aggregates. The present study aims at investigating the effect of an isolated iron-sulfur melt on the acoustic properties of an aggregate. Experiments are currently being run at 6 GPa and 1400°C in a 25/15 multi-anvil apparatus, which are conditions relevant to the context of the above-mentioned persistent seismic anomalies. Acoustic velocities will be measured using the phase comparison method and results will be compared with existing literature data and models based on a statistical mechanical approach (e.g. Takei 1998, 2000), which do not make simplified geometric assumptions.

### References:

- Bagdassarov et al., (2009) PEPI 177
- Carslaw and Jaeger, (1959) Conduction of heat in solids
- Ekström and Dziewonski, (1998) Nature 394
- Helffrich et al., (2011) GRL 38
- Laporte and Provost, (2000) Physics and Chemistry of Partially Molten Rocks
- Lodge and Helffrich, (2006) Geology 34
- Minarik and Watson, (1995) EPSL 133
- Schimmel et al., (2003) JGR Solid Earth 108
- Takei, (1998) JGR Solid Earth 103
- Takei, (2000) JGR Solid Earth 105
- Wolfe et al., (1997) Nature 385

## Insights into the formation mechanism of stishovite from rapid compression experiments of quartz in diamond anvil cells

Christoph Otzen<sup>1,2</sup>, Hanns-Peter Liermann<sup>2</sup>, Falko Langenhorst<sup>1</sup>

<sup>1</sup> Friedrich-Schiller-Universität Jena, Institut für Geowissenschaften, Carl-Zeiss-Promenade 10, 07745 Jena

<sup>2</sup> Extreme Conditions Beamline P02.2, Deutsches Elektronen-Synchrotron DESY, Notkestraße 85, 22607 Hamburg

The mineral stishovite is seldomly found in nature and only appears in trace amounts [De Carli and Milton (1965)], but it is of high geological importance, providing evidence of shock events in extraterrestrial rock samples and meteorite impacts on Earth. The majority is found in melt veins, i.e. pseudotachylites, which are formed by frictional melting during shock compression. Suggested by the randomly oriented, defect-free crystals found inside pseudotachylites, stishovite is likely to be formed by homogeneous nucleation and growth in the undercooled, high-pressure melt of these veins [Mansfeld et al. (2017)]. Besides this melt-associated occurrence, stishovite has also been found in the interstices between planar deformation features [Stähle et al. (2008)], where amorphization of quartz is the dominant process, but melting does not seem to take place. Furthermore, numerous experiments indicate a solid-state transition, for which various mechanisms have been suggested. For example, shear-mediated and displacive transitions seem to be possible by the observation of an almost instantaneous appearance of diffraction reflexes during shock compression experiments [Stolper and Ahrens (1987), Tracy et al., (2020)]. Despite the rapidity of the transformation process, ruling out time-consuming diffusion-mediated mechanisms, homogenous nucleation followed by coalescence grain growth has also been proposed by shock experiments using amorphous SiO<sub>2</sub> as starting material [Gleason et al. (2015), Tracy et al. (2018)]. Latest experimental results, however, even question the formation of stishovite, favoring the formation of a defective niccolite structure [Tracy et al., (2020)]. In summary, the mechanisms leading to the polymorphic phase transition of quartz at high pressures are still unclear.

Using single crystals of quartz, we have conducted rapid compression experiments in membrane-driven diamond anvil cells and investigated the recovered samples using transmission electron microscopy. We find nanometer-sized stishovite crystals spatially associated with amorphous lamellae and conclude that these crystals are formed by nucleation and growth in amorphized quartz. Although our compression conditions are very different from natural shock compression, we provide insights into the formation mechanism of stishovite at high pressures transferable to the natural case of stishovite formation during shock compression.

### References:

- De Carli and Milton, (1965) *Sci.*, 147, 144–145
- Mansfeld et al., (2017) *Meteorit. Planet. Sci.*, 52, 1449–1464
- Stähle et al., (2008) *Contrib. Mineral. Petrol.*, 155, 457–472
- Stolper and Ahrens, (1987) *Geophys. Res. Lett.*, 14, 1231–1233
- Tracy et al., (2020) *Sci. Adv.*, 6, eabb3913
- Tracy et al., (2018) *Phys. Rev. Lett.*, 120, 135702
- Gleason et al. (2015) *Nat. Commun.*, 6, 1–7

## High-pressure Raman spectroscopic study of amphiboles

Ye Peng<sup>1</sup> Abhisek Basu<sup>1</sup> Mainak Mookherjee<sup>1</sup> Geeth Manthilake<sup>2</sup>

<sup>1</sup> Earth Materials Laboratory, Department of Earth, Ocean and Atmospheric Sciences, Florida State University, Tallahassee, FL, 32306, USA.

<sup>2</sup> Laboratoire Magmas et Volcans CNRS, IRD, OPGC, Université Clermont Auvergne, 63000 Clermont-Ferrand, France.

Amphiboles are hydrous minerals that could store up to 2 wt.% water in their crystal structure as hydroxyl units, and are often found in xenoliths from the upper mantle. They play a vital role in transporting water into the deep Earth via the subduction zone. More recently, the presence of amphiboles in the metasomatized lithosphere has been invoked to explain anomalously low seismic velocities (Rader et al., 2015; Selway et al., 2015; Peng and Mookherjee, 2020; Saha et al., 2021).

Clearly, an in-depth understanding of the structure and properties of amphibole at high-pressure is crucial for a better understanding of the deep Earth processes and their geophysical signatures. Hence, in this study, to understand the pressure dependence of the crystal structure of amphibole, we investigate two natural amphibole samples: tremolite [(Na<sub>0.38</sub>K<sub>0.05</sub>)(Ca<sub>1.73</sub>Na<sub>0.27</sub>)(Mg<sub>4.69</sub>Al<sub>0.17</sub>Ti<sub>0.06</sub>Fe<sub>0.03</sub>Mn<sub>0.02</sub>)(Si<sub>7.61</sub>Al<sub>0.39</sub>)O<sub>22</sub>((OH)<sub>1.90</sub>F<sub>0.10</sub>)] and actinolite [(Ca<sub>1.70</sub>Na<sub>0.20</sub>K<sub>0.01</sub>)(Mg<sub>4.30</sub>Fe<sub>0.57</sub>Mn<sub>0.03</sub>Al<sub>0.01</sub>)(Si<sub>7.82</sub>Al<sub>0.18</sub>)O<sub>22</sub>((OH)<sub>1.29</sub>F<sub>0.10</sub>)]. We use Raman spectroscopy to characterize amphiboles at pressures up to ~10 GPa using a diamond anvil cell. Our preliminary results show that at ambient conditions, tremolite (tr) has a single hydroxyl mode  $\nu_{OH1}^{tr}$  at ~3673 cm<sup>-1</sup>, while actinolite (act) has two hydroxyl modes  $\nu_{OH1}^{act}$  at ~3673 cm<sup>-1</sup> and  $\nu_{OH2}^{act}$  at ~3659 cm<sup>-1</sup>. Upon compression, the  $\nu_{OH1}^{tr}$  increases with a pressure derivative  $\nu_{OH1}^{tr}/dP$  of ~2.17 cm<sup>-1</sup>/GPa. This is in good agreement with a recently reported high-pressure Raman study with 1.73 cm<sup>-1</sup>/GPa (Ott and Williams, 2020). Results from the infrared spectroscopic study vary between 1.43 and 1.69 cm<sup>-1</sup>/GPa (Thompson et al., 2016). Upon compression, the  $\nu_{OH1}^{act}$  and  $\nu_{OH2}^{act}$  also increase with the  $\nu_{OH1}^{act}/dP$  and  $\nu_{OH2}^{act}/dP$  being 1.65 and 1.94 cm<sup>-1</sup>/GPa, respectively. Our results are in overall agreement with the prior infrared spectroscopic study which reported the  $\nu_{OH1}^{act}$  of 1.43-1.63 cm<sup>-1</sup>/GPa and  $\nu_{OH2}^{act}$  of 1.01-1.03 cm<sup>-1</sup>/GPa (Thompson et al., 2016). We will also explore and discuss the pressure dependence of the lattice regions of tremolite and actinolite.

Acknowledgement: We acknowledge support from the U.S. National Science Foundation grants EAR 1763215 and EAR 1753125.

### References:

- Ott and Williams, (2020) Phys. Chem. Mineral., 47  
 Peng and Mookherjee, (2020) Am. Mineral., 105, 904-916  
 Rader et al., (2015) Geochim. Geophys. Geosyst., 16, 3484-3504  
 Saha et al., (2021) Earth Planet. Sci. Lett., 553, 116602  
 Selway et al., (2015) Earth Planet. Sci. Lett., 414, 45-57  
 Thompson et al., (2016) Am. Mineral., 101, 706-712

## Sound velocities of amorphous calcium carbonate across the polyamorphic transition

L. Pennacchioni<sup>1,2</sup> S. Speziale<sup>2</sup> L. Bayarjargal<sup>1</sup> B. Winkler<sup>1</sup>

<sup>1</sup> Goethe Universität, Institut für Geowissenschaft, Frankfurt am Main, Germany

<sup>2</sup> GFZ, German Research Centre for Geosciences, Telegrafenberg, 14474 Potsdam, Germany

Calcium carbonate  $\text{CaCO}_3$  is one of the most abundant crustal carbonates and calcite is the thermodynamically stable polymorph. Two further crystalline polymorphs are observed at ambient conditions: vaterite and aragonite. Amorphous calcium carbonate (ACC) is an important precursor in the biological synthesis of calcium carbonate crystalline polymorphs[1]. In addition, a recent study has shown that the high pressure calcium carbonate polymorph, aragonite, amorphizes at high pressures and temperatures and this amorphous phase is stable at depths of 70 - 400 km (3.9-7.5 GPa) in the subducting slabs[2]. Previous studies have shown the existence of an irreversible pressure-induced polyamorphic transition from vaterite-like ACC to an aragonite-like ACC around 10 GPa[3][4]. Here we present a Brillouin spectroscopy study on synthetic ACC compressed in a diamond anvil cell (DAC) in the pressures range between 2 to 20 GPa. Two samples were synthesized according to the methods reported by Faatz et al.[5] and Koga et al.[6]. The first sample was studied by Brillouin spectroscopy directly after its loading in the DAC. The second sample was studied after it had already been subjected to a cycle of compression up to 10 GPa and decompression to 2 GPa. A dense dataset of Brillouin scattering spectra was collected for the two samples both in compression and decompression. Despite the differences in synthesis, hydration state and compression history, the two samples show an indistinguishable (within the experimental resolution) smooth pressure dependence of both  $v_p$  and  $v_s$  in both compression and decompression.

The experiments performed on the first sample, during compression, show a broad central peak around 10 GPa, the pressure of the previously reported polyamorphic transition[3]. Synchrotron X-ray diffraction experiments performed on the first sample confirmed that the material was still amorphous after the whole compression-decompression cycle.

The acoustic velocities determined by Brillouin scattering, combined with the densities calculated by Fernandez-Martinez et al.[3], allowed us to obtain the bulk modulus  $K_s = 44 \pm 1$  GPa and the shear modulus  $G_s = 17.3 \pm 0.4$  GPa for ACC at ambient conditions.

The elastic moduli's dependence on pressure is similar to the crystalline aragonite's[7], but the ACC appears to be more compressible and less rigid than the crystalline phase.

This work is within the scope of the DFG funded "CarboPaT" research group (FOR 2125), Projects Wi1232 and SP1216/7-1. We are grateful for the financial support.

### References:

- [1] Weiner et al.(2005) *Science*. 309 1027
- [2] Hou et al. (2019) *Nat. Comm.* 10:1963
- [3] Fernandez-Martinez et al. (2013) *Angew. Chem. Int. Ed.* 52:8354-8357
- [4] Fruhner et al. (2018) *Eur. J. Mineral.* 30, 711-720
- [5] Faatz et al. (2004) *Adv. Mat.* 16 (12), 996-1000
- [6] Koga et al. (1998) *Thermochim. Acta.* 318 (1-2), 239-244
- [7] Huang et al. (2017) *Chin. Phys. B.* 26 (8) 089101

## Time-resolved x-ray diffraction measurements of the ice VII – ice X transition in a dynamic diamond-anvil cell

Alba San José Méndez<sup>1,2</sup>, Florian Trybel<sup>2</sup>, Rachel Husband<sup>1</sup>, Gerd Steinle-Neumann<sup>2</sup>, Hanns-Peter Liermann<sup>1</sup> and Hauke Marquardt<sup>3</sup>

<sup>1</sup>Deutsches Elektronen-Synchrotron (DESY), 22607 Hamburg, Germany;

<sup>2</sup>Bayerisches Geoinstitut BGI, University of Bayreuth, 95440 Bayreuth, Germany;

<sup>3</sup>Department of Earth Sciences, University of Oxford, Oxford OX1 3AN, United Kingdom

Ice VII and ice X are predominant phases in the high pressure phase diagram of H<sub>2</sub>O where high temperatures activate fast proton diffusion, leading to the rise of a superionic behaviour that may have important implications for the geophysics of the Ice Giant planets Uranus and Neptune, as well as mini-Neptune exoplanets. Ice VII undergoes a sequence of proton order-disorder transitions through which H<sub>2</sub>O loses its molecular character to form the atomic ice X phase. Proton order-disorder transitions are not evident in the x-ray diffraction signature of ice, hampering an accurate identification of boundaries in the phase diagram. Previous x-ray diffraction studies have reported a shallow decrease of the unit cell volume of ice VII at pressures from 40-60 GPa, likely associated with the formation of the intermediate dynamically disordered phases ice VII' and ice X'. Here, we collected continuous compression data up to Mbar pressures at room temperature employing a dynamic Diamond Anvil Cell (dDAC) in combination with very fast x-ray diffraction detectors at the Extreme Conditions Beamline (P02.2) at PETRA III. Our data show a practically continuous pressure-resolution that allows us to directly observe changes in the bulk modulus of ice by differentiating pressure-volume data. We find that the bulk modulus of ice VII shows two pronounced changes at 40 and 60 GPa that we associate to the formation of ice VII' and ice X'. Our experimental data suggest that the ice VII - ice X phase transition has a stronger effect on the elasticity of H<sub>2</sub>O ice than observed in previous Brillouin scattering measurements. In addition, we present first time-resolved x-ray diffraction results collected during compression of H<sub>2</sub>O ice to >100 GPa at high-temperature employing a newly designed resistive-heated dDAC (RHdDAC).

## High pressure single-crystal elasticity of $\delta$ -(Al<sub>0.97</sub>Fe<sub>0.03</sub>)OOH

Niccolò Satta<sup>1,2</sup>, Giacomo Criniti<sup>1</sup>, Alexander Kurnosov<sup>1</sup>, Tiziana Boffa Ballaran<sup>1</sup>, Takayuki Ishii<sup>1</sup>, and Hauke Marquardt<sup>2</sup>

<sup>1</sup> Bayerisches Geoinstitut, Universität Bayreuth, 95440 Bayreuth, Germany

<sup>2</sup> Department of Earth Sciences, University of Oxford, Oxford OX1 3AN, United Kingdom

Water strongly influences the physical properties and geochemical behavior of the Earth's mantle. Its presence is pivotal to a variety of geological processes that control the dynamics of the Earth's interior. Water can be efficiently stored in the crystal structure of hydrous phases present in Earth's mantle. At lower mantle conditions, a solid solution between  $\delta$ -(Al,Fe)OOH and phase H, MgSiO<sub>2</sub>(OH)<sub>2</sub> has been suggested to be the most important carrier of water, possibly up to the core-mantle boundary. Under compression,  $\delta$ -AlOOH undergoes a phase transition at approximately 8 GPa which is associated with a change in compression mechanism. While the effect of this phase transition on the bulk modulus has been quantified by X-ray diffraction, the influence on the shear modulus or the elastic tensor has never been explored experimentally. The lack of experimental data on the elastic properties of  $\delta$ -(Al,Fe)OOH does not allow an accurate determination of its seismic signature, and hence hampers the quantification of possible water reservoirs present in the lower mantle.

In this study, we provide the first experimental determination of the single-crystal elastic properties of a member of the  $\delta$ -(Al,Fe)OOH solid solution and present the elastic tensor ( $C_{ij}$ ) before, during, and after the  $P2_1nm - Pnm$  transition.

The  $\delta$ -(Al,Fe)OOH crystals were synthesized in a multi-anvil apparatus at 21 GPa and 1150 °C at the Bayerisches Geoinstitut, University of Bayreuth (Germany). The major element concentration and ferric iron content were quantified using electron microprobe and Mössbauer spectroscopy, respectively. Chemically homogenous samples were selected based on their size and crystalline quality. Selected crystals were then oriented and double-side polished to obtain platelets with a final thickness of 13  $\mu$ m. The high-pressure single-crystal elastic properties were quantified by combining single-crystal X-ray diffraction and Brillouin scattering measurements in the diamond anvil cell. High-pressure measurements were performed by following a multi-sample loading approach in the diamond-anvil cell.

## Crystal field bands in siderite as a function of iron content

Lukas Schifferle<sup>1,2</sup>, Lea Pennacchioni<sup>1,3</sup>, Andrey V. Vishnevskii<sup>4</sup>, Sergey S. Lobanov<sup>1,2</sup>

<sup>1</sup> German Research Centre for Geosciences- GFZ, Section 3.6, Telegrafenberg, 14473 Potsdam, Germany

<sup>2</sup> University of Potsdam, Institute for Geosciences, Karl-Liebknecht-Str. 24-25, 14476 Potsdam, Germany

<sup>3</sup> Goethe University, Department of Geosciences, Altenhöferallee 1, 60438 Frankfurt, Germany

<sup>4</sup> Siberian Branch of the RAS, Sobolev Institute of Geology and Mineralogy, Koptyuga ave. 3, 630090 Novosibirsk, Russia

To shed light on the effects of the Fe-Mg solid solution on crystal field bands in (Fe,Mg)-carbonates we have studied their absorption spectra at ambient conditions on a variety of natural siderite samples ( $X_{\text{Fe}}$  between 0.55 and 0.96). Measurements were performed using FTIR on freestanding crystals. Main features of the spectra are two broad, partly overlapping absorption bands with peak positions around 7800 and 9500 wavenumbers. These can be assigned to electron transitions of octahedrally coordinated  $\text{Fe}^{2+}$  from ground state to excited state. Furthermore, sharp OH-bands around  $3200 \text{ cm}^{-1}$  occur, resulting from minor hydrogen content in these normally anhydrous minerals. By fitting and plotting the position of the Fe absorption bands we observe a linear trend in position, which could be linked to the Fe concentration in the minerals: the higher the Fe content, the lower the frequency of the band position. We interpret this trend as being caused by a changing Me-O bonding length on the octahedral site, resulting in a different splitting of the d-shell electron levels for  $\text{Fe}^{2+}$ . Greater bonding length results in lower crystal field splitting. As the typical bonding length of Mg-O is shorter than for Fe-O, a higher Mg content shortens the overall Me-O bond length and explains why at higher Fe-content a lower frequency of the band is observed. Because we deal with natural samples, impurities e.g. Mn might be responsible for deviations from the trend line as they increase the frequency of Fe crystal field bands by enlarging the Me-O bonding length for the octahedral site. In conclusion, the position of Fe crystal field bands depends on chemical composition and its interplay with the bonding environment.

## Equations of state and phase diagram of the CaO-SiO<sub>2</sub> system

Tatiana Sokolova<sup>1</sup>, Peter Dorogokupets<sup>1</sup>

<sup>1</sup> Institute of the Earth's Crust SB RAS, Irkutsk 664033, Russia

The phase equilibria in the CaO-SiO<sub>2</sub> system are important for modern researches of deep mineralogy. The detecting of high-pressure CaSiO<sub>3</sub> phases (walstromite, larnite, titanite-structure CaSi<sub>2</sub>O<sub>5</sub>) as inclusions in natural diamonds (Joswing et al., 1999; Anzolini et al., 2016; Nestola et al., 2018; Woodland et al., 2020; etc.) has contributed to great interest in investigation of the CaO-SiO<sub>2</sub> system because it's probably indicates to deep nature of genesis of diamonds (transition zone or the lower mantle). Calcium metasilicate CaSiO<sub>3</sub> occurs in a number of structural modifications and its more often identified as wollastonite and walstromite structures under relevant *P-T* conditions (up to 8 GPa and 1600 K). The mineral assemblage larnite (Ca<sub>2</sub>SiO<sub>4</sub>) with titanite-structure CaSi<sub>2</sub>O<sub>5</sub> is stable at higher pressure 10–13 GPa. The phase diagram of the CaSiO<sub>3</sub> system is extensively studied (see review in Woodland et al., 2020). We constructed thermal equations of state of different phases in the CaO-SiO<sub>2</sub> system (wollastonite, pseudowollastonite, walstromite (breyite), calcio-olivine, larnite, titanite-structured CaSi<sub>2</sub>O<sub>5</sub> and CaSiO<sub>3</sub> perovskite) based on the thermodynamic formalism from our previous studies (Dorogokupets et al., 2015; Sokolova et al., 2018), using known experimental measurements of heat capacity and enthalpy at zero pressure and volume measurements at different *P-T* parameters. The fitting parameters of proposed equations of state are derived by least squares method in the Excel spreadsheets. The Gibbs energy of different CaSiO<sub>3</sub> phases is calibrated by using enthalpy formation from (Holland et al., 2011). We will discuss details of our calculations and constructed phase diagram of the CaO-SiO<sub>2</sub> system in comparison with experimental measurements and other calculations in the report.

### References:

- Anzolini et al., (2016) *Lithos*, 265,138–47
- Dorogokupets et al., (2015) *Rus. Geol. Geophys.*, 56,172–189
- Dörsam et al., (2009) *Eur. J. Mineral.*, 21,205–714
- Essene (1974) *Contr. Mineral. Petrol.*, 45,247–250
- Holland et al., (2011) *J. Metamor. Geol.*, 29,333–383
- Joswing et al., (1999) *Earth Planet. Sc. Lett.*, 173,1–6
- Joswing et al., (2003) *Z. Kristallogr.*, 218,811–818
- Nestola et al., (2018) *Nature*, 55,237–42
- Sokolova et al., (2018) *High Pres. Res.*, 38,198–211
- Woodland et al., (2020) *Eur. J. Mineral.*, 32,171–185

## Metastable phase transition of fayalite at high pressure: A single crystal X-ray diffraction study

Sergio Speziale<sup>1</sup>, Konstantin Glazyrin<sup>2</sup>, Elena Bykova<sup>2,3</sup>, Ilias Efthymiopoulos<sup>1</sup>

<sup>1</sup> GFZ Helmholtz-Zentrum, Potsdam

<sup>2</sup> Deutsches Elektronen Synchrotron DESY, Hamburg

<sup>3</sup> Geophysical Laboratory, Carnegie Institution for Science, Washington (U.S.A.)

Fayalite ( $\text{Fe}_2\text{SiO}_4$ ) is the iron end member of the olivine solid solution series. Its high-pressure behavior has been considered prototypical of pressure-induced amorphization [1,2]. We present experimental proof that it actually transforms at high pressures into a metastable polymorph when compressed above 30 GPa at ambient temperature. We have performed synchrotron X-ray diffraction measurements on a single-crystal natural fayalite sample compressed in a diamond anvil cell between 3 GPa and 45 GPa. At  $30 \pm 1$  GPa a new set of diffraction spots appear, and the transformation is completed at  $34 \pm 1$  GPa. We have determined the structure of the metastable polymorph which is triclinic (space group  $\bar{P}1$ ). The diffraction quality deteriorates upon further compression without any indications of subsequent structural transitions. We present a description of the transition, and propose an interpretation of its mechanism. The transition takes place at a pressure compatible with the expected structural instability of fayalite, based on the high-pressure extrapolation of experimental elasticity data [3]. However, our observations indicate that the transition is controlled by the vanishing of the  $C_{55}$  stiffness coefficient, contradicting the prediction from low-pressure elasticity.

### References:

- Williams et al., (1990) J. Geophys. Res., 95, 21549  
Andrault et al., (1995) Phys. Chem. Minerals, 22, 99  
Speziale et al., (2004) J. Geophys. Res., 109, B12202

**EMPG – XVII**

**17th International Symposium on  
Experimental Mineralogy,  
Petrology and Geochemistry**

Abstracts

Theme 11 “Methodological developments”

(sorted alphabetically by first author)

## Rapid-quench multi-anvil technique

Bondar Dmitry<sup>1</sup>, Hongzhan Fei<sup>1</sup>, Anthony C. Withers<sup>1</sup>, Tomoo Katsura<sup>1</sup>

<sup>1</sup> Bayerisches Geoinstitut, University of Bayreuth, Germany

The multi-anvil press (MAP) is widely used in the field of solid Earth science. An important application of MAP is to provide materials synthesized at high pressures and temperatures for various kinds of *ex situ* analyses. In many silicates, it can preserve their high-temperature states upon instantaneous cooling, which is referred to as quenching. Quenching is especially important for silicate melts, which play an important role in igneous petrology, in order to investigate melt structure and volatile partitioning.

Quenching of melt to glass, however, becomes increasingly difficult with increasing pressure, increasing volatile concentrations, and decreasing non-bridging oxygen, which is an obstacle to progress in igneous petrology. The unquenchability is owing to too high diffusion rates relative to cooling rate. High cooling rates are therefore desired to quench more varied materials under broader conditions.

A new rapid-quench technique for Kawai-type MAP was therefore developed in this study. It includes a low thermal-inertia assembly and an external cooling system. In contrast to a regular MAP assembly, which is designed for high heating efficiency, the heat flow from the furnace to the outside is maximized in the low thermal-inertia assembly. The outstanding feature of this assembly is the presence of the tungsten sleeve surrounding the furnace together with rods connecting the sleeve and inner anvils. This design provides fast corridors for heat flow from the furnace to the inner anvils. The external cooling system consists of an acrylic box with low-temperature hoses, a chiller, and pumps. A coolant, which is a mixture of water and ethylene-glycol, is cooled to -25°C by a recirculating chiller. The coolant is pumped into the acrylic box by the pump of the chiller, and then returned back to the chiller with assistance of additional pump. The tops of the outer anvils and the whole Kawai assembly are placed in the acrylic box, where they are cooled by the coolant.

The new rapid-cooling technique allows very high quenching rates of 6000-7000°C/sec, which are more than 1 order of magnitude higher than regular piston cylinder (130°C/sec) and multi-anvil apparatus (650°C/sec). Using the rapid-quench technique, completely transparent hydrous glass (2 wt.% H<sub>2</sub>O by FTIR) with highly magnesian composition (43.5 wt.% MgO; 50 wt.% SiO<sub>2</sub>) was successfully quenched at a pressure of 4 GPa. Melts with garnet and with olivine at 5 GPa were also quenched into glass.

The low thermal-inertia assembly produces a very high cooling rate (5350°C/sec) even without external cooling, and it can be easily implemented in other laboratories.

## News from high pressure technologies

Agnès Dewaele<sup>1</sup>

<sup>1</sup> CEA, DAM, DIF, 91297 Arpajon Cedex, France

High pressure devices coupled with intense X-ray sources disclose the behavior of matter under extreme conditions, from the atomic (density, phase) to the mesoscopic scale (microstructures). I will describe a few recent achievements with these techniques. Developments in static diamond anvil cell tool have drastically expanded the range of compression produced, with pressures approaching 10 Megabars (Dubrovinsky 2015, Dewaele 2018). Dynamic compression techniques allow now generating various pressure-temperature conditions with direct relevance to the planet's interiors, at short timescales (Wicks 2018, Gleason 2015). X-ray diffraction and spectroscopic tools are being adapted to these new devices. To finish, X-ray imaging techniques allow now accessing to chemical/phases heterogeneities under extreme (Boulard 2020), with numerous applications in Earth sciences.

### References:

- Dubrovinsky et al., (2015) *Nature* 525, 226
- Dewaele et al., (2018) *Nat. Comm.* 9, 2913
- Wicks et al., (2018) *Sci. Adv.* 4, 5864
- Gleason et al., (2015) *Nat. Comm.* 6, 8191
- Boulard et al., (2020) in press

## High-pressure geoscience research at the Large Volume Press beamline P61B, PETRA III

Robert Farla<sup>1</sup>, Shuailing Ma<sup>1,2</sup>, Artem Chanyshev<sup>1,3</sup>, Stefan Sonntag<sup>1</sup>,  
Takayuki Ishii<sup>3</sup>, Tomo Katsura<sup>3</sup>

<sup>1</sup> Deutsches Elektronen-Synchrotron (DESY), Hamburg

<sup>2</sup> Jilin University, Changchun, China

<sup>3</sup> Bayerisches Geoinstitut, University of Bayreuth, Bayreuth

A large number of experimental studies in geosciences require the simulation of pressure and temperature conditions in the interior of the Earth. Using multi anvil, high-pressure devices, extreme conditions can now be routinely generated on candidate rock compositions in solid and molten states to study for instance, phase relations, rheology and diffusion. However, typically the experimental conditions have to be decided before the experiment to avoid misinterpretation of the composition and microstructure of the quenched rock sample. While in many cases this approach works, it is neither efficient nor fully reliable. Beamline P61B at PETRA III, currently in commissioning and starting operation with 50% user beam time from summer 2020, offers an alternative approach to conducting high-pressure experiments in the geosciences. Using *in situ* Energy-Dispersive X-ray Diffraction (ED-XRD) and imaging (radiography) techniques (Fig. 1), the sample properties, composition and structure, as well as the precise pressure and temperature environment can be observed and recorded in real-time. Particularly, an experiment can be directed towards a particular outcome (e.g. a phase boundary crossing). Hitherto unknown kinetic and thermodynamic reaction pathways of phase transitions and nucleation of new phases can be observed, which in addition may not be quenchable. Furthermore, the high-pressure rheology of Earth materials (stress and strain history) can be quantified, and melt viscosity directly imaged. The 6-ram LVP at P61B accepts any user assembly with WC anvils to generate pressures up to extreme targets of over 30 GPa. AC and DC power supplies are available for heating up to routine temperatures of 2400 K, or higher. The beamline offers versatile set ups using 1 or 2 Ge-detectors, which can be positioned at a desired diffraction angle (typically between 4° and 10°). The dual objective X-ray microscope is equipped with a fast, high-resolution camera for image acquisition at high frame rates (> 1000 fps). At this meeting, I will present an overview of the beamline, commissioning progress, its future development at PETRA III and PETRA IV, as well as a few in-house geoscience research projects.

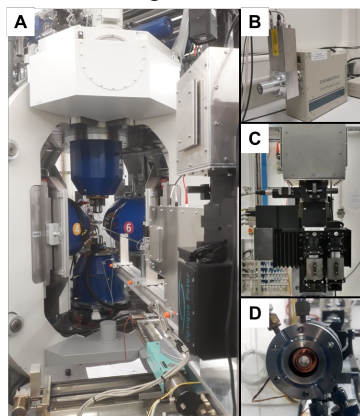


**Figure 1.** Instrumentation in the experimental hutch at P61B.

**A.** The 6-ram LVP, a collimator-slit system and Ge-detector.

**B.** A second Ge detector with an electronic cryostat (cold tip at -190 °C) currently not in use.

**C.** The dual objective (5x, 10x magnification) X-ray microscope equipped with a fast sCMOS camera and GGG:Eu scintillators (20, 40 μm thickness).

**D.** The diamond exit window (water-cooled) from which intense synchrotron ‘white’ X-rays pass through with usable flux between energies of 30 – 200 keV.

## A new approach for the rheometric characterization of visco-elastic materials and phase transitions at high temperatures

Christopher Giehl<sup>1</sup>, Peter Brandes<sup>2</sup>, Daniela Ehgartner<sup>2</sup>

<sup>1</sup> Business Area Rheometry, Anton Paar Germany GmbH, Ostfildern-Scharnhausen, Germany

<sup>2</sup> Business Area Rheometry, Anton Paar GmbH, Graz, Austria

Oscillatory shear rheometry is well-established for various materials and commonly used to characterize the visco-elastic behavior and to determine the glass transition of polymers (e. g. Mezger 2014). In combination with a high temperature furnace, this type of thermo-mechanical analysis enables visco-elasticity measurements at high temperatures relevant for e. g. silicate melts, metal melts and salt melts.

The measurements were performed with a furnace rheometer system (FRS 1800) combined with an air-bearing DSR 502 measuring head (Anton Paar). The measuring system used is a Pt<sub>90</sub>Rh<sub>10</sub> concentric cylinder with 24 mm cup inner diameter and 14 mm bob outer diameter. The combination of a highly torque-sensitive air-bearing measuring head with a concentric cylinder measuring system enables viscosity measurements from very low viscosities in the lower mPas range up to 10<sup>8</sup> Pas. This enables sample characterization over a large temperature interval and bridges the gap between different measurement approaches, thus canceling problems with comparability. This measuring geometry allows to measure absolute values according to DIN 53018-1, confirming reference viscosities of standard glass DGG1.

Visco-elasticity measurements provide the viscous ( $G''$ ) and the elastic ( $G'$ ) modulus via the phase shift between deformation preset and torque response. Reference values of the visco-elasticity standard polydimethylsiloxane (PDMS; Wacker AK 1000000) were confirmed at 25 °C with no calibration needed. In addition, the visco-elasticity of DGG1 was determined between 1200 and 650 °C, showing a continuous increase of  $G'$  with decreasing temperature, with the rheometric glass transition ( $T_g$ ) at 778 °C (10 rad s<sup>-1</sup>,  $G''_{max}$  and  $G''=G'$ ). This value is frequency-dependent and thus higher compared to  $T_g$  determined with differential scanning calorimetry (538 °C). Isothermal variation of oscillatory frequency (frequency sweep) provides relaxation times and mastercurves by time-temperature superposition analysis (Williams et al. 1955) and might shed light on the fragility concept (Angell et al. 2000).

In conclusion, this study demonstrates that oscillatory rheometry serves as a powerful toolbox for high-temperature characterization of non-Newtonian substances. The specification of viscous ( $G''$ ) and elastic ( $G'$ ) contributions (1) rivals viscosity data ( $\eta$ ) owing to the capability of crossing the liquid-solid transition, (2) has the potential to derive relaxation time spectra from isothermal frequency-dependent measurements and (3) offers a strong definition of  $T_g$  beyond the 10<sup>12</sup> Pas concept. In addition to glass transitions, crystallization processes can be monitored with the same approach. Here, the non-Newtonian behavior of suspension can be quantified excluding effects like shear-induced crystallization.

### References:

Mezger (2014) *The Rheology Handbook*. Vincentz, Hanover, 2014 (4<sup>th</sup> edition)

Williams et al. (1955) *J. Am. Chem. Soc.*, 77, 3701

Angell et al. (2000) *J. Appl. Phys.*, 88, 3113

## Development of an in-situ method to determine the hydrolysis constant of adenosine triphosphate (ATP) by application of Raman spectroscopy in a hydrothermal anvil cell

Christoph Moeller<sup>1</sup>, Christian Schmidt<sup>2</sup>, Francois Guyot<sup>3</sup>, Max Wilke<sup>1</sup>

<sup>1</sup> Institut für Geowissenschaften, Universität Potsdam, Potsdam, Germany

<sup>2</sup> Helmholtz-Zentrum Potsdam Deutsches GeoForschungsZentrum – GFZ, Potsdam, Germany

<sup>3</sup> IMPMC Muséum National d'Histoire Naturelle, Paris, France

Life can be found all over our planet and even in extreme environments, e.g. near black smokers on the ocean floor. In order to survive in such temperature, pressure and utmost pH conditions organisms usually interact with the surrounding geochemical system to obtain essential components. The basis of any biochemical mechanism is limited to the synthesis and stability of molecules. The stability of adenosine triphosphate (ATP) and adenosine diphosphate (ADP), however, is limited by the non-enzymatic hydrolysis reaction with water, which is kinetically enhanced at high temperatures. Better understanding of this fundamental reaction for the metabolism of any known organism will provide us insights of life at extreme conditions and may even give us further information about the origin of life.

Leibrock et al. (1994) determined kinetic reaction constants of the hydrolysis for several pH values, temperatures and pressures using quench experiments and subsequent NMR analysis. So far, it was not tested whether quench artefacts might have affected those results. Therefore, the current study was performed to develop a method to follow the reaction in-situ at high temperatures.

We used a con-focal micro Raman spectrometer with a laser of 532 nm wavelength combined with a hydrothermal diamond anvil cell (HDAC). Spectra were measured in the range of 660 to 1157  $\text{cm}^{-1}$  as a function of time. Integration time of a single spectrum was 100 sec. The measurements were made in unbuffered solutions of 0.1  $\text{mol} \cdot \text{L}^{-1}$  ATP and ADP in ultra-pure water at temperatures between 353.15 and 393.15 K and at pH values of 3, 5 and 8 at vapour pressure.

The first findings are consistent with the results of Leibrock et al. (1994) and show that with decreasing pH value the hydrolysis rate increases. The data indicate hydrolysis constants in the magnitude of  $10^{-3} \text{ s}^{-1}$  by 393.15 K,  $10^{-4} \text{ s}^{-1}$  by 373.15 K and  $10^{-5} \text{ s}^{-1}$  by 353.15 K. These initial observations show that this technique produces reliable kinetic data on this reaction. It also provides much better sampling statistics than quench experiments.

The high reaction rates suggest that organisms must have developed a mechanism to regulate this automatic reaction at higher temperatures, which is necessary to maintain the biochemical engine under extreme conditions. Moreover, it is commonly known that ATP interacts with various metal ions with different effects on the reaction rate. An application of this method would be the quantification of the hydrolysis constant in chemically more complex systems to better understand the survival of life in extreme environments.

### References:

Leibrock E., Bayer P., Lüdemann H. -D., Nonenzymatic hydrolysis of adenosinetriphosphate (ATP) at high temperature and high pressures, (1994) *Biophysical Chemistry* 54 (1995) 175-180

## NanoExtreme: Nano-focus end-station with laser heating at ID27@ESRF

Wolfgang Morgenroth<sup>1,2</sup>, Mohamed Mezouar<sup>2</sup>, Gaston Garbarino<sup>2</sup>, Stany Bauchau<sup>2</sup>, Keith Martel<sup>2</sup>, Markus Herrmann<sup>3</sup>, Sandro Jahn<sup>3</sup>, Max Wilke<sup>1</sup>

<sup>1</sup> Institut für Geowissenschaften, Universität Potsdam, Germany

<sup>2</sup> ESRF – The European Synchrotron, Grenoble, France

<sup>3</sup> Institut für Geologie und Mineralogie, Universität Köln, Germany

The ESRF is constructing a new high pressure beamline for X-ray diffraction, fluorescence and imaging at the newly upgraded extremely brilliant source EBS. We plan to build a NanoExtreme end-station with CO<sub>2</sub> laser heating which is fully integrated in this project.

Here, we will present the current status and plans for the modified beamline ID27:

- 120 m long beamline for micro- to nano-focusing X-ray diffraction (XRD) to achieve pressures >500 GPa
- 15 – 60 keV in monochromatic mode with increased photon flux; additional ‘pink’ beam mode, for instance for fast nano X-ray fluorescence (XRF) detection
- fast down to 1 microsecond timescale XRD detection using Eiger 2 CdTe detector
- new experiments exploiting coherence of the beam and providing X-ray imaging (XRI) capabilities
- separate sample stages for nano-focusing, YAG and CO<sub>2</sub> laser heating or heavy duty experiments.

Commissioning and start of user operation is foreseen for spring and autumn of 2021.

This ‘high-flux nano-XRD’ beamline is optimized for the needs of the geo- and materials-science community for *in situ* XRD and XRF studies at extreme conditions. With this setup, it will be possible to study materials relevant to processes of the deep Earth or other planetary bodies in an unprecedented manner. Interested groups are invited to contact the beamline responsible.

We acknowledge support by D. Andrault, Laboratoire Magmas et Volcans, Université Clermont Auvergne in preparing the upgrade project, many divisions within the ESRF for construction and the German BMBF for financial support (BMBF project ‘NanoExtreme’ 05K2019 with projects 05K19IP2 (Potsdam) and 05K19PK2 (Köln)).

## On the reliability of the diamond trap method for determining high-pressure fluid compositions

Greta Rustioni<sup>1</sup>, Andreas Audetat<sup>1</sup>, Hans Keppler<sup>1</sup>

<sup>1</sup> Bayerisches Geoinstitut, Universität Bayreuth, 95440 Bayreuth, Germany

Aqueous fluids play a key role in Earth's crust and mantle for many processes, such as mass transport, melting and crystallization. One of the most popular experimental techniques used to study the composition of fluids in equilibrium with mineral phases at high pressure and temperature is the diamond trap method. In this technique, a layer of diamond powder is placed into the capsule to provide a network of pores preserved at high pressure. As only the fluid should be able to circulate in the diamond trap, Laser-Ablation Inductively-Coupled-Plasma Mass-Spectrometry (LA-ICP-MS) analyses performed on this layer allow to determine the fluid composition in terms of major and trace elements.

We assessed the reliability of the analytical method by loading several capsules with a fluid of known composition and analysing the diamond trap by LA-ICP-MS either (a) after evaporation of the fluid at ambient condition, (b) after freeze-drying the sample, or (c) after opening the capsule in frozen state to directly analyse the fluid in solid state. Among these methods, the latter approach turned out to be most accurate.

We also carried out mineral solubility tests in simple and well-studied systems as well as trace element partitioning experiments in the eclogite-water  $\pm$  NaCl system. All experiments were conducted in a piston cylinder apparatus at conditions ranging between 1-4 GPa and 700-1000 °C. There is generally a good agreement between literature data and our results for silica solubility in both the quartz-water and the forsterite-enstatite-water systems, as well as for experiments conducted on albite-water supercritical fluids. On the other hand, the diamond trap method significantly overestimates mineral solubilities in systems such as rutile-water and corundum-water, which are subject to dissolution and re-precipitation of material during the experiment due to thermal gradients that develop along the capsule. In the eclogite-fluid system, we obtained a very good agreement between trace element partition coefficients measured in "forward" and "reversed" experiments, as well as in experiments containing different initial concentrations of trace elements.

In general, our results suggest that in most cases it is possible to reliably determine fluid compositions at high pressure and temperature using the diamond trap method combined with laser-ablation ICP-MS measurement performed on the sample in frozen state. The typical accuracy of data obtained with this method is within a factor of two. However, major contamination of the diamond trap, resulting in a considerable overestimation of solute concentrations in the fluid, may be encountered in systems where solubilities are highly sensitive to thermal gradients.

## XPS and XES spectra of germanates and titanates

Georg Spiekermann<sup>1,2</sup>

<sup>1</sup> University of Potsdam, 14476 Potsdam, Germany,

<sup>2</sup> now at ETH Zürich, 8092 Zürich, Switzerland

The binding energy of oxygen 1s and 2s electrons in oxide crystals and glasses is very sensitive to local structural aspects and therefore reflects the cation coordination, the polymerization of germanium tetrahedra in glasses, and the type of cations present in crystalline oxides.

X-ray photoelectron spectroscopy (XPS) is the standard technique to access those oxygen binding energies. Unfortunately, XPS requires ultra-high vacuum and is mostly surface-sensitive.

X-ray emission spectroscopy (XES) is, under some conditions, capable of accessing the same chemical shift of oxygen 2s electrons. One advantage of XES over XPS is that no vacuum is needed, the probe is bulk-sensitive and the sample can even be in a confined environment like diamond-anvil cells. The potential of XES has recently been demonstrated for the question of germanium coordination in compressed amorphous GeO<sub>2</sub> (Spiekermann et al. 2019).

We present and compare XPS and XES data on chemically complex germanates and titanates as part of a study that explores the potential of XES to achieve XPS-like information on the chemical shift of oxygen 2s electrons.

### References:

Spiekermann et al., (2019) Phys. Rev. X, 9, 011025

## Nano- vs crystalline materials as starting materials: the case of NiO in the Ni–NiO oxygen buffer

Simone Tumiati<sup>1</sup> and Francesca Miozzi<sup>1</sup>

<sup>1</sup> Dipartimento di Scienze della Terra, Università degli Studi di Milano, via Botticelli 23, Milano (Italy)

The assemblage nickel-nickel oxide (NNO), whose equilibrium in the P-T- $fO_2$  field depends on the thermodynamic properties of the Ni and NiO, is commonly used in experimental petrology as a buffer to constrain the oxygen fugacity. However, commercial NiO is nanocrystalline and, as such, characterized by slightly different thermodynamic properties compared to crystalline NiO. Therefore, several authors recommended a heat treatment before usage in order to promote sintering processes and to increase grain size. In this study, we measured the CO<sub>2</sub> content of aqueous fluids in equilibrium with glass-like carbon, externally buffering the system with NNO and employing both the double-capsule and the triple-capsule techniques to avoid the direct contact of the fluids with the NNO buffer. Fluids were equilibrated at 1 GPa and 800 °C for 24 hours in an end-load piston cylinder. After the experiments, quenched capsules were pierced in a gas tight vessel and the gases conveyed to a quadrupole mass spectrometer (QMS) for the analysis of volatiles. As the ratio CO<sub>2</sub>/H<sub>2</sub>O is highly sensitive to small variations in  $fO_2$ , we used it to retrieve, with reference to ideal crystalline NiO, the thermodynamic properties of different NiO precursors employed to build up the buffering assemblage. Reagent-grade Ni metal powder was mixed with: (i) two commercial nickel oxide nanopowder, green and black, with an average crystallites size of 100 and 10 nm respectively; (ii) sintered nickel oxide, produced by heating green nanopowder for three days at 1300°C and (iii) nickel hydroxide (Ni(OH)<sub>2</sub>), which decomposes to NiO at T > 230°C. As source of carbon glass-like C, a NIST standard material, was preferred to graphite in order to avoid impurities often present in natural samples and to have a material with well characterized thermodynamic properties (cf. Tumiati et al. 2020). Compared to the NNO reference, the minimum variation in  $\Delta G_f^0$  detected, is 0.7 kJ mol<sup>-1</sup> for a 0.07 log  $fO_2$  variation. The  $fO_2$  imposed by the different precursors have a consistent evolution in the investigated T range. While the assemblages with black NiO, sintered NiO and Ni(OH)<sub>2</sub> plot closer to the NNO reference, green NiO plot even below the FMQ equilibrium. The use of triple instead of double capsules slightly increases the  $fO_2$  but not enough to reach the reference. Accordingly, NiO sintering before the experiments is needed in order to impose an  $fO_2$  close to the NNO reference. For black nickel oxide, the high temperature of the experiments coupled with the long duration likely induced the sintering of this disordered material during the experimental run, hence the imposed  $fO_2$  closely reproduce the NNO reference. As such, its usage for experiments at low T or of short duration is discouraged without previous sintering. Sintering during the experimental run is not easily achieved for NiO green nanopowder, due to its relatively ordered (and therefore stable) state with large crystallite sizes and well-shaped crystals.

### References:

- Miozzi & Tumiati (2020) *Geochemical Perspectives Letters*, in press.  
Tumiati et al. (2020) *Geochimica et Cosmochimica Acta* 273, 383-402.



**EMPG – XVII****17th International Symposium on  
Experimental Mineralogy,  
Petrology and Geochemistry**

Authors

## Index

### A

Abdel-Hak, N., 99  
 Achorner, M., 9  
 Albers, C., 10  
 Almeev, R.R., 69  
 Alvaro, M., 114  
 Andujar, J., 86  
 Angel, R., 114  
 Appel, K., 10  
 Appelt, O., 7, 64, 72  
 Aprilis, G., 2, 119  
 Aranovich, L., 44, 45  
 Arbaret, L., 37  
 Aspiotis, S., 71  
 Audétat, A., 143  
 Auxerre, M., 46  
 Auzende, A.-L., 94

### B

Böhnke, M., 87  
 Bachmann, O., 111  
 Bagiński, B., 102  
 Balitskaya, L., 76  
 Balitsky, V., 76  
 Baron, A.Q.R., 4  
 Basu, A., 115, 117, 129  
 Bauchau, S., 142  
 Baudouin, C., 80  
 Bayarjargal, L., 130  
 Bazarkina, E., 27  
 Beckmann, P., 62  
 Behrens, H., 62, 69  
 Belmonte, D., 3  
 Bernadou, F., 13  
 Berndt, J., 57, 87, 93  
 Biedermann, N., 10  
 Bischof, L., 14  
 Blanchard, I., 81  
 Blundy, J., 91  
 Bobrov, A., 6  
 Boffa Ballaran, T., 132  
 Bolfan-Casanova, N., 47  
 Bondar, D., 137  
 Bonechi, B., 82  
 Borghini, G., 23, 48, 56  
 Borisov, A., 45  
 Borisova, A.Y., 31

Botcharnikov, R., 58  
 Boulanger, M., 80  
 Boulliung, J., 83, 108  
 Brandes, P., 140  
 Brodholt, J.P., 109  
 Bublikova, T., 76  
 Bucag, C., 115  
 Buchen, J., 116  
 Budzyn, B., 106  
 Buhre, S., 63  
 Bussweiler, Y., 57  
 Butvina, V.G., 39, 100  
 Bykov, M., 2, 119  
 Bykova, E., 2, 119, 135

### C

Cámara, F., 3  
 Carroll, M.R., 42  
 Casaus, J., 25  
 Cassidy, M., 67  
 Castro, A., 49  
 Castro, J.M., 59, 67, 110  
 Champallier, R., 37, 59  
 Chantel, J., 8, 9, 38, 40, 118, 119  
 Chanyshhev, A.D., 139  
 Chariton, S., 2, 126  
 Charlier, B., 68, 92  
 Chauvigne, P., 47  
 Chebotarev, D., 50  
 Chen, C., 84  
 Chumakov, A.I., 2  
 Cialdella, L., 51  
 Cichy, S.B., 52, 96  
 Clapp, S., 117  
 Clarke, D.B., 52  
 Cody, G.D., 89  
 Colin, A., 31  
 Collinet, M., 53  
 CPakhomova, A., 8  
 Crichton, W., 38  
 Criniti, G., 4, 132

### D

Daffos, C., 37  
 Dalou, C., 80, 83, 108  
 Davydova, V.O., 59  
 de Campos, C.P., 112

Debret, B., 47  
 Deligny, C., 108  
 Demouchy, S., 47  
 Deon, F., 72  
 Derrey, I., 28  
 Desmaele, E., 27, 31  
 Deubener, J., 42  
 Devidal, J.-L., 80  
 Devineau, K., 59  
 Dewaele, A., 138  
 Di Carlo, I., 13, 59, 61, 86  
 Di Genova, D., 42  
 Dijkstra, A., 72  
 Dingwell, D.B., 110, 112  
 Dobson, D.P., 109  
 Dominijanni, S., 4, 10  
 Dorogokupets, P., 134  
 Dubacq, B., 92  
 Dubrovinskaia, N., 2  
 Dubrovinsky, L., 2, 4, 6  
 Dybas, J., 106

**E**

Efthimiopoulos, I., 77, 99, 124, 135  
 Ehgartner, D., 140  
 Erdmann, S., 61  
 Eremin, N., 6  
 Ertel-Ingrisch, W., 112  
 Ertl, A., 73  
 Ezad, I.S., 109

**F**

Förster, M.W., 63  
 Füre, E., 13, 83, 108  
 Fabbrizio, A., 82, 85  
 Fadel, A., 119  
 Fanara, S., 18, 96  
 Faranda, C.F., 86  
 Farla, R., 139  
 Farmer, N., 15  
 Faure, F., 46  
 Fedortchouk, Y., 54  
 Fedotenko, T., 2, 4  
 Fei, H., 137  
 Feisel, Y., 110  
 Finger, F., 103  
 Foley, S.F., 55, 84  
 Fonseca, R.O.C., 65, 95  
 Foustoukos, D.I., 26, 89  
 France, L., 80

Franchi, I.A., 81  
 Franke, M.G., 101  
 Franz, G., 104  
 Frost, D.J., 127  
 Fukui, H., 4  
 Fumagalli, P., 23, 48, 56

**G**

Gülmez, F., 63  
 Gómez-Frutos, D., 49  
 Gaeta, M., 82  
 Gaillard, F., 13, 16, 61  
 Garbarino, G., 142  
 Gardés, E., 16  
 Gay, G.P., 8  
 Gay, J., 118  
 Giehl, C., 140  
 Giester, G., 73  
 Gilder, S., 125  
 Giuli, G., 42  
 Glazyrin, K., 4, 121, 135  
 Gleeson, S.A., 90  
 Gottschalk, M., 104  
 Grützner, T., 57  
 Grammatica, M., 56  
 Grove, T.L., 53  
 Guignard, J., 38  
 Guignot, N., 40  
 Guyot, F., 141

**H**

Hammond, K., 111  
 Hanfland, M., 2  
 Harlov, D.E., 25, 52, 102, 103  
 Harter-Uibopuu, K., 71  
 Haselbach, S.-L., 58  
 Haupt, C., 87  
 Hazemann, J.-L., 27, 31  
 Helo, C., 67, 110  
 Hennet, L., 10  
 Hermann, J., 32  
 Herrmann, M.G., 17, 142  
 Hilairet, N., 38, 40, 119  
 Hofmeister, A.M., 5  
 Holtz, F., 28, 58, 62, 69  
 Horn, I., 28  
 Hou, T., 58, 66  
 Huber, C., 111  
 Hunt, S.A., 109  
 Husband, R., 8, 123, 131

**I**

Iacono-Marziano, G., 61  
 Ikuta, D., 4  
 Irifune, T., 94  
 Ishii, T., 4, 116, 132, 139  
 Iskrina, A., 6

**J**

Jähkel, A., 52  
 Jackson, J.M., 116  
 Jacobson, S.A., 81  
 Jahn, S., 17, 124, 142  
 Jennings, E.S., 81  
 Joachim-Mrosko, B., 11, 101  
 John, T., 30  
 Jokubauskas, P., 102

**K**

Kaa, J., 10  
 Katsura, T., 137, 139  
 Keppler, H., 34, 51, 143  
 Khandarkhaeva, S., 2, 4  
 Khomenko, V.M., 74  
 King, A., 40  
 Kiseeva, E.S., 88  
 Kleest, C., 18  
 Klemme, S., 30, 48, 87, 93  
 Koch-Müller, M., 7, 99, 121, 124  
 Koemets, E., 2  
 Koga, K., 96  
 Kokh, M., 27, 31  
 Kommescher, S., 95  
 Konzett, J., 11  
 Kosorukov, O.O., 74  
 Kotowski, J.B., 102  
 Kozub-Budzyn, G.A., 106  
 Kroll, H., 114  
 Krstulovic, M., 94  
 Krug, M., 8, 9, 118, 126  
 Kueter, N., 89, 111  
 Kunz, B., 91  
 Kupenko, I., 9, 126  
 Kurnosov, A., 132  
 Kusebauch, C., 90  
 Kushnir, A.R.L., 59  
 Kvas, P., 76

**L**

La Fortezza, M., 3  
 Langenhorst, F., 128

Laskar, C., 27, 31  
 Laumonier, M., 16  
 Le Godec, Y., 38, 40  
 Le Losq, C., 22, 78  
 Ledoux, E., 8, 9, 118, 119  
 Lee, S., 120  
 Lequin, D., 46  
 Lerch, M., 77  
 Li, M., 84  
 Li, N., 28  
 Li, W.-C., 35  
 Li, X., 69, 121  
 Libon, L., 10, 126  
 Liebscher, A., 104  
 Liermann, H.-P., 8, 9, 121, 123, 128, 131  
 Lievens, C., 72  
 Limanov, E., 39, 100  
 Liu, K., 29  
 Liu, Y., 84  
 Lobanov, S.S., 122, 133  
 Loges, A., 30  
 Lotti, P., 3  
 Louvel, M., 30, 94

**M**

Ma, S., 139  
 Macdonald, R., 102  
 Mair, P., 105  
 Mandolini, T., 38, 40  
 Manthilake, G., 129  
 Marchenko, E., 6  
 Marquardt, H., 123, 131, 132  
 Marques, L.S., 112  
 Marrocchi, Y., 13, 83, 108  
 Martel, C., 37, 59  
 Martel, K., 142  
 Martirosyan, N.S., 124  
 Marxer, F., 60  
 Mason, P.R.D., 92  
 Massuyeau, M., 16, 19  
 Mather, T., 67  
 Matyszczyk, W., 102  
 Maurice, J., 47  
 McCammon, C., 2, 4, 10, 125  
 Melai, C., 2  
 Melekhova, E., 91  
 Mergner, V., 126  
 Merkel, S., 8, 9, 38, 40, 118, 119  
 Merlini, M., 3  
 Mezouar, M., 142

Michaud, J. A.-S., 20  
 Mihailova, B., 71  
 Miozzi, F., 114, 145  
 Miyajima, N., 41, 81  
 Moeller, C., 141  
 Molendijk, S.M., 92  
 Mollé, V., 61  
 Molnár, Z., 75  
 Mookherjee, M., 115, 117, 129  
 Moretti, R., 22  
 Morgenroth, W., 10, 142  
 Moynier, F., 65  
 Muñoz, M., 94  
 Mueller, M., 14  
 Mysen, B.O., 26, 89

**N**

Néri, A., 127  
 Nabyl, Z., 61  
 Namur, O., 68, 92  
 Neave, D.A., 62  
 Nesterova, V., 76  
 Neuville, D.R., 21, 22, 65, 78  
 Ni, H., 29, 35  
 Nielsen, E., 94

**O**

O'Neill, H.S.C., 65  
 Oelze, M., 90, 96  
 Ohtani, E., 4  
 Otzen, C., 128

**P**

Pósfai, M., 75  
 Pakhomova, A., 2, 118  
 Pannefieu, S., 22  
 Paris, E., 42  
 Parman, S., 111  
 Pausch, T., 11  
 Pekker, P., 75  
 Peng, Y., 129  
 Pennacchioni, L., 124, 130, 133  
 Perinelli, C., 82  
 Perugini, D., 112  
 Petitgirard, S., 81, 126  
 Petrelli, M., 82, 85  
 Pezzotta, F., 73  
 Pichavant, M., 20, 59  
 Pintér, Z., 84  
 Pokrovski, G.S., 27, 31

Poli, S., 23  
 Précigout, J., 37  
 Prelević, D., 57, 63  
 Prouteau, G., 86  
 Purwadi, I., 72  
 Pushcharovsky, D., 76  
 Pyle, D., 67

**Q**

Qiao, S., 30

**R**

Rampone, E., 48  
 Renggli, C.J., 87, 93  
 Rigoni, A., 9  
 Ritscher, A., 77  
 Ritter, X., 9, 19  
 Roddatis, V., 10  
 Rodriguez, F., 94  
 Rohrbach, A., 87  
 Rosa, A.D., 94  
 Roskosz, M., 65  
 Rubie, D.C., 81  
 Rushmer, T., 15  
 Rustioni, G., 143  
 Rutherford, M., 111  
 Rzehak, L.J.A., 95  
 Rzepa, G., 106

**S**

Safonov, O.G., 39, 100  
 Sakamaki, T., 4  
 San José Méndez, A., 123, 131  
 Sanchez-Valle, C., 8, 9, 19, 33, 118, 126  
 Satta, N., 132  
 Scaillet, B., 86  
 Schantl, P., 105  
 Schiavi, F., 47  
 Schifferle, L., 122, 133  
 Schiller, D., 103  
 Schiperski, F., 104  
 Schlüter, J., 71  
 Schmid-Beurmann, P., 114  
 Schmidt, C., 31, 64, 141  
 Schmidt, M.W., 14, 85  
 Schulz, R., 122  
 Schwarzenbach, E., 94  
 Schwinger, S., 87  
 Sergeev, D., 14  
 Sergeev, I., 126

- Setkova, T., 76  
 Sicola, S., 42  
 Sieber, M.J., 10, 32  
 Simon, A., 25  
 Sláma, J., 106  
 Slodczyk, A., 13  
 Smets, B., 92  
 Sokolova, T., 134  
 Sonntag, S., 139  
 Sossi, P.A., 14, 65  
 Spallanzani, R., 96  
 Spartà, D., 23  
 Speziale, S., 8, 121, 130, 135  
 Spiekermann, G., 10, 126, 144  
 Spivak, A., 6  
 Stabile, P., 42  
 Steinbrügge, R., 126  
 Stracke, A., 87  
 Strnad, L., 82  
 Sturhahn, W., 116  
 Suss, N.Y., 77  
 Svitlyk, V., 119
- T**  
 Tailby, N., 111  
 Tarashchan, A.M., 74  
 Tarrago, M., 78  
 Testemale, D., 31  
 Thomas, R.W., 97  
 Thomson, A.R., 109  
 Tiraboschi, C., 33  
 Tissandier, L., 83, 108  
 Tomé, C., 38  
 Topa, D., 73  
 Tramm, F., 106  
 Trcera, N., 65  
 Troch, J., 111  
 Tropper, P., 105  
 Truche, L., 94  
 Tuduri, J., 61  
 Tumiati, S., 145
- U**  
 Uchiyama, H., 4  
 Ulmer, P., 60
- V**  
 van der Werff, H., 72  
 van Hullebusch, E., 78  
 Van, K.V., 39  
 Vantelon, D., 65  
 Vazhakuttiyakam, J., 11  
 Veksler, I.V., 50, 64, 66  
 Vicentini, C.M., 112  
 Villaros, A., 20  
 Vishnevskii, A.V., 133  
 Vlasov, K., 34  
 Voigt, A., 67  
 Vorobey, S., 100  
 Vuilleumier, R., 27, 31  
 Vyshnevskiy, O.A., 74
- W**  
 Waitzinger, M., 103  
 Wang, H., 38  
 Wang, Q., 35  
 Wang, Z., 84  
 Webb, S.L., 18  
 Wei, Q., 125  
 Weyer, S., 28  
 Wiedenbeck, M., 51, 96  
 Wilke, F., 52, 72  
 Wilke, M., 10, 30, 31, 94, 96, 141, 142  
 Wille, G., 59  
 Winkler, B., 130  
 Wirth, R., 7  
 Withers, A.C., 11, 137  
 Wohlgemuth-Ueberwasser, C.C., 50, 66  
 Wood, B.J., 88, 97  
 Wunder, B., 7, 99, 115  
 Wykes, J., 15
- X**  
 Xi, W., 28
- Y**  
 Yang, X., 52  
 Yaxley, G.M., 32
- Z**  
 Zhang, C., 69  
 Zhang, Y., 68  
 Zhao, X., 81  
 Zhou D., 35  
 Zimmermann, L., 83